A combined *in vivo* and *in vitro* approach to assess supraspinatus activation and tissue responses to arm elevation demands

by

Alan Christian Cudlip

A thesis
presented to the University of Waterloo
in partial fulfillment of the
thesis requirements for the degree of
Doctor of Philosophy
in
Kinesiology

Waterloo, Ontario, Canada 2020

Examining Committee Membership

The following individuals served on the Examining Committee for this thesis. The decision of the Examining Committee is by majority vote.

Supervisor	Dr. Clark Dickerson Professor Department of Kinesiology University of Waterloo
Internal Members	Dr. Jack Callaghan Professor Department of Kinesiology University of Waterloo
	Dr. Andrew Laing Associate Professor Department of Kinesiology University of Waterloo
Internal-External member	Dr. Thomas Willett Assistant Professor Systems Design Engineering University of Waterloo
External member	Dr. Mickael Begon Associate Professor School of Kinesiology and Physical Activity Sciences Université de Montréal

Author's Declaration

This thesis consists of material all of which I authored or co-authored. This is a true copy of the thesis, including any required final revisions, as accepted by my examiners. I understand that my thesis may be made electronically available to the public.

Alan Christian Cudlip

Abstract

Rotator cuff degeneration affects a large portion of the human population, yet knowledge surrounding which loading scenarios allow transition from healthy to diseased states remains largely unresolved. Mechanistic progression of rotator cuff pathology often originates in the supraspinatus before cascading to other tissues, leading to substantial degeneration. Posture, loading and repetitive motions are known risk factors that exacerbate shoulder injury progression. This suggests a causal relationship between specific upper extremity task scenarios and degenerative rotator cuff loading. This thesis intentionally explored regional activations of the supraspinatus and accompanying tendon loading across a range of postures. The global objective was to evaluate how postural and task intensity differences alter tissue-level mechanical parameters in both *in vivo* muscular activation and *in vitro* tangent stiffness, hysteresis and optical stretch ratios. These findings combine *in vivo* muscular activation and physiologically relevant *in vitro* mechanical testing results through novel methods to better understand supraspinatus loading. Three experimental studies provided the means to achieve this global objective.

***In Vivo* Examination of Supraspinatus Activation:** The purposes of this study were 1) to document the interplay of anterior and posterior supraspinatus activations and 2) to describe the influences of posture and hand loads on anterior and posterior supraspinatus activations. Forty participants completed arm elevations in seven planes of elevation with three hand loads that were normalized to the individual's maximal elevation force. Indwelling electromyography was collected from the anterior and posterior regions of supraspinatus. Hand load and elevation angle interacted to affect the anterior region activation in most planes of elevation by up to 41% of maximal activation, but these changes were less influential for the posterior portion. Activation patterns between the two regions suggest different functional roles of the supraspinatus portions;

consistent levels of activation in the posterior supraspinatus may indicate this region is primarily a glenohumeral stabilizer, while the larger anterior region acts to achieve glenohumeral motion. This work represents the most comprehensive concurrent evaluation of these supraspinatus regions over a large set of planes of elevation, hand loads and humeral elevations, providing more holistic descriptions of supraspinatus activation in a critical arm movement.

Comparing Surface Electromyography of Supraspinatus to Anterior and Posterior Indwelling Recordings: The purpose of this study was to compare anterior and posterior supraspinatus indwelling electromyography responses to a surface supraspinatus signal across a range of arm postures in order to develop relationships between these two recording methods. Forty participants completed arm elevations with altering hand loads and planes of elevation at a fixed cadence. Indwelling electromyography of the anterior and posterior supraspinatus as well as a surface recording of supraspinatus were collected. Bivariate regressions of anterior and posterior indwelling electrodes relative to the bipolar surface electrodes were used to determine relationships between these signals throughout the range of these humeral elevations. Differences between these predictions were modulated by plane of elevation, elevation angle, load intensity and sex of the participant, but no interactions existed. Surface signals underestimated indwelling activation recordings at low elevation angles, then overestimated as humeral elevation angle increased. Surface recordings underestimated indwelling signals by up to 15% in unloaded conditions, while overestimating the posterior region by up to 17% at the highest hand load intensity. In addition, surface signals overestimated posterior supraspinatus indwelling activity by 21%. This work greatly expands current knowledge surrounding relationships between these indwelling and surface signals, both in the inclusion of the indwelling posterior supraspinatus recordings and the expansion of arm postures examined. These findings indicate that relationships

between the surface and indwelling signals are altered by plane of elevation, load and elevation angle, and the surface signal more closely predicts anterior region activity.

Examining Changes of *In Vitro* Supraspinatus Mechanical Properties in a Rat Model: The purposes of this study were 1) to complete *in vitro* mechanical tissue testing in scenarios emulative of empirical muscular activation and postural conditions in an animal model, and 2) to determine the relative influences of arm posture and external loading levels on tissue responses. Forty-eight shoulders harvested from Sprague-Dawley rats were affixed into custom 3D printed mounting pots and placed into one of eight testing groups combining glenohumeral posture and load magnitude. Orientations represented four different postures observed *in vivo,* and applied tensile load within the animal model was scaled from human activation of the two supraspinatus regions collected from *in vivo* research for 1500 cycles. A three-way interaction between elevation angle, load magnitude and cycle number occurred for tangent stiffness within specific cycles, with increasing angles, loads and cycles increasing stiffness by up to 49% in some scenarios; differences in maximum and minimum displacement indicated elevated tissue responses in higher elevation angles. Interactions between elevation angle, load intensity and cycle number altered stretch ratio characteristics, with increased elevation angles, loads and cycles increasing stretch ratios, as well as differentiating articular and bursal side responses. Complex interactions between angle, load and cycle number suggest higher abduction angles, increased load magnitude and subsequent cycles generated increased tendon response characteristics.

Novel thesis contributions: Multiple novel findings and contributions originated from this work. This dissertation has combined *in vivo* and *in vitro* methodologies to advance understanding of rotator cuff mechanics. This dissertation supports the notion that supraspinatus loading varies throughout the range of motion, and postural and external load variations alter tissue-level

supraspinatus responses. Activations of the anterior and posterior regions of the supraspinatus were collected from the largest collection of postures to date and described activation differences between these regions. These EMG activations were used to assist in determining applied force load levels for mechanical testing, representing the first known attempt to generate force-controlled tensile loading using physiologically derived exposure levels for the supraspinatus. This work is also the first to maintain a functional glenohumeral unit to complete mechanical testing using postures representative of those observed *in vivo* to examine supraspinatus responses.

General conclusions: Posture and load magnitude have distinct and noteworthy effects on supraspinatus, both in muscular activation and tendon responses. This research combined *in vivo* muscular activation with *in vitro* mechanical tissue testing to generate novel findings for rotator cuff loading; further work should continue to pair *in vivo* responses with mechanical tendon loading to generate physiologically relevant research scenarios throughout the range of humeral postures. This work has established that the supraspinatus is sensitive to scenario conditions, but continued expansion of our understanding of exposure aspects would help diagnose or anticipate overexposure.

Acknowledgements

I'd like to thank my family and friends for all the support that I've received through this thesis; most importantly my wife Erin and my family. Your continuous support throughout this process was invaluable, and I'm incredibly grateful to have such a strong support system.

Special thanks go to my supervisor, Dr. Clark Dickerson for his exceptional mentorship. Upon completion of this degree we have worked together for over a decade, and your support has been critical to my success. It was never in doubt that you were in my corner, and I'm proud to complete this stage with an excellent mentor and friend. I would also like to thank my committee members Dr. Jack Callaghan, Dr. Andrew Laing and Dr. Thomas Willett for their expertise and guidance, particularly for your assistance with the *in vitro* aspects of this thesis.

I would like to thank my colleagues and friends who have contributed to various aspects of this process. It has been such a privilege to work with the members of DIESEL, and I am so appreciative of your support. I appreciate the support of Dr. Soo Kim for her expertise in rotator cuff anatomy and to Jeff Barrett, Kayla Fewster and Mamiko Noguchi for sharing their proficiency in tissue mechanics. Special thanks to Dr. David Kingston – your support has been incalculable, and I'm grateful to have a friend like you.

I will fondly remember my time at the University of Waterloo. Words cannot express my gratitude to all those who shared their skills, technical training, experiences and companionship during my thesis work. I feel fortunate to have been your colleague and friend.

Erin –

You're my sunshine. Thanks for your unconditional love and support.

Mom and Dad –

Without you, these words wouldn't be here. Thanks for everything.

TABLE OF CONTENTS

LIST OF FIGURES

LIST OF TABLES

CHAPTER I – INTRODUCTION

1.1 Motivation

The human shoulder is highly mobile, with a wide range of opportunities to generate pain or injury. Shoulder problems are common in activities of daily living, work, recreation, or high-level athletics. Rotator cuff injuries are highly prevalent in the human population, with increasing occurrences in aging populations (Lehman, Cuomo, Kummer, & Zuckerman, 1995). With >50% of individuals in their 70s and >80% of individuals in their 80s suffering from rotator cuff tears, improved understanding of the scenarios that lead to shoulder injury is paramount.

Rotator cuff degeneration leaves large sections of the population in discomfort or pain, particularly workers in jobs requiring shoulder intensive tasks. Prevalence of shoulder pain in the general population is 7-27%, with one month and one year prevalence of 19-31% and 5-47%, respectively (Pope, Croft, Pritchard, & Silman, 1997). Shoulder pain in the general population across occupations and lifestyles is approximately 30%, with ranges of 22.6-37.8% depending on occupation (Makela et al., 1999). More specifically, sedentary lifestyles had the lowest observed rates (22.6%), agriculture work had the highest (37.8%), and industrial, housework or miscellaneous work prevalence rates ranged between 29.1-30.6% (Makela et al., 1999). Partial- or full-thickness rotator cuff defects were observed in individuals between 30 to 90 years using ultrasound with drastic increases in rotator cuff tear prevalence after 50 years, with over 50% of shoulders in individuals over 70 and 80% of subjects over 80, yet all of these individuals were symptom free and without a history of trauma (Milgrom, Schaffler, Gilbert, & van Holsbeeck, 1995). Shoulder injuries occur in 21% of older populations, yet only 40% of these affected individuals sought medical attention for their symptoms (Chard, Hazelman, Hazelman, King, &

Reiss, 1991). While certain workplaces may exacerbate shoulder dysfunction, the problem of shoulder injuries is pervasive across the population.

Many epidemiologic studies have examined workplace factors and their relationship to shoulder musculoskeletal disorders. Significant positive relationships exist between repetitive motion and shoulder injury, regardless of measurement method (Bernard, 1997; Bjelle, Hagberg, & Michaelson, 1981; Chiang, Chen, Yu, & Ko, 1990; Hagberg, 1981; Ohlsson et al., 1995). The epidemiologic literature has been described as "most convincing" regarding work tasks and shoulder tendinitis, especially for repetitive and overhead work (Kuorinka & Forcier, 1995). Direct evidence for positive associations between applied manual force and shoulder MSDs are scarce, primarily due to the considerable diversity of exposure assessment approaches, including epidemiological (Bernard, 1997), cross-sectional (Chiang et al., 1993; Herberts, Kadefors, Högfors, & Sigholm, 1984; J. Wells, Zipp, Schuette, & McEleney, 1983) and basic science approaches (Jonsson, 1988; Stenlund, Goldie, Hagberg, Hogstedt, & Marions, 1992). This diversity makes comparisons between these studies difficult and obscures relationships between these external task requirements and musculoskeletal injury risk.

The mechanistic progression of rotator cuff degeneration from an initial tear to complete rotator cuff destruction has received attention, but uncertainty remains. The sequence typically begins in the supraspinatus tendon, with a partial-thickness defect on the deep surface near the attachment of the supraspinatus to the greater tuberosity (Davidson, Elattrache, Jobe, & Jobe, 1995; Edelson & Teitz, 2000). This is where loads are believed to be highest, and failure of some fibers increases loading on adjacent ones, exacerbating injury progression (Fukuda, Mikasa, & Yamanaka, 1987; Yamanaka, Fukuda, Hamada, & Mikasa, 1983). This cascade eventually includes other rotator cuff tissues, often leading to complete degeneration and glenohumeral

instability. A critical knowledge gap exists regarding the how these exposures in daily conditions affect the supraspinatus tendon, and if specific scenarios are more likely to provoke changes from healthy to diseased states. Current research often divides into two major foci: study of healthy individuals without consideration of degeneration, or changes in muscular activation or body kinematics in injured populations. Use of young, healthy populations without age-related degeneration provides critical information for prevention strategies and baseline function. While many studies, including several performed at Waterloo (Cudlip, Callaghan, & Dickerson, 2015; Cudlip, Meszaros, & Dickerson, 2016; Nadon, Vidt, Chow, & Dickerson, 2016) have provided foundational knowledge, little interrelationship exists between these studies and the mechanistic responses of the supraspinatus tendon that could lead to future injury. Conversely, robust conclusions based on examination of injured populations is difficult in human populations due to the multifactorial causes of rotator cuff pathology. Research has largely focused on alterations in kinematics (Reuther et al., 2014; Soslowsky et al., 2000; Struyf, Nijs, Baeyens, Mottram, & Meeusen, 2011), mechanical properties of injured tissue (Dunkman et al., 2014; Fang & Lake, 2016; Lujan, Underwood, Jacobs, & Weiss, 2009), or propagation of partial-thickness rotator cuff tears (Engelhardt et al., 2016; Thunes et al., 2015).

Evaluation of rotator cuff muscular activation during specific arm elevation tasks, paired with *in vitro* mechanical testing designed to replicate that loading, can provide novel information to link external demands to responsive behaviours and point toward potential future damage pathways. There are presently no rotator cuff loading assessments achieved through combined *in vivo* muscular activation informing *in vitro* mechanical testing examinations. Determining the relative influences of arm posture and external loading levels on tissue responses has substantial rehabilitative and ergonomic implications. The initial data generated with regard to these

phenomena instigates targeted research surrounding shoulder and injury mechanics. Detailed examination of muscular activation and tissue responses at postures within the shoulder range of motion will allow for inspection of scenarios that could alter risk of future degeneration and prompt specific task avoidance.

1.2 Global Scope & Aim of Research

The global aim of this research was to evaluate how postural differences and tendon load magnitudes alter tissue-level responses. This was achieved through a dual methodological approach including quantification of *in vivo* motion and muscular strategies in humans and tendon mechanics using *in vitro* methods in an animal model. Both studies employed novel techniques to assist in determination of supraspinatus loading across a spectrum of potential exposure scenarios. Postures or scenarios that increase localized loading may raise future injury risk, and prevention of these provocative combinations in work or activities of daily living could prevent rotator cuff pathology. Overall, it was hypothesized that increasing arm elevations and hand load intensities would result in increased muscular activations *in vivo* and increased changes in supraspinatus mechanical properties *in vivo*.

1.3 Outline

Three symbiotic research projects form this dissertation. Collectively, this work aimed to identify scenarios that result in increased loading on the supraspinatus and its tendon, informed by experimental data derived in Stages I (Chapters III and IV) and II (Chapter V) (Figure 1). Stage I consisted of *in vivo* quantification of supraspinatus activation across a range of postures and loading scenarios to define supraspinatus muscular activation. Stage II used *in vitro* testing of supraspinatus tendon in an animal model to quantify tissue responses from repetitive loading in

postures described in Stage I. Collectively, these studies expanded the frontiers of rotator cuff research, produced novel quantification of rotator cuff responses to physiologically relevant loads, and combined *in vivo* and *in vitro* methods in an unprecedented manner. Further, the individual studies independently provided important disciplinary advances, specifically through the application of new experimental methods and exposure techniques. The use of indwelling electromyography in both regions of supraspinatus has never been used to record muscular activation on such a wide range of arm postures and load intensities (Chapter III), and comparing these recordings to those obtained with bipolar surface electrodes (Chapter IV) provides great utility to researchers, including comparisons to the posterior supraspinatus that have never before been completed. Finally, completion of supraspinatus tendon mechanical supraspinatus tendon testing in postures and exposure scenarios emulative of those seen *in vivo* (Chapter V) provides foundational information of supraspinatus tendon responses to plausible exposure levels.

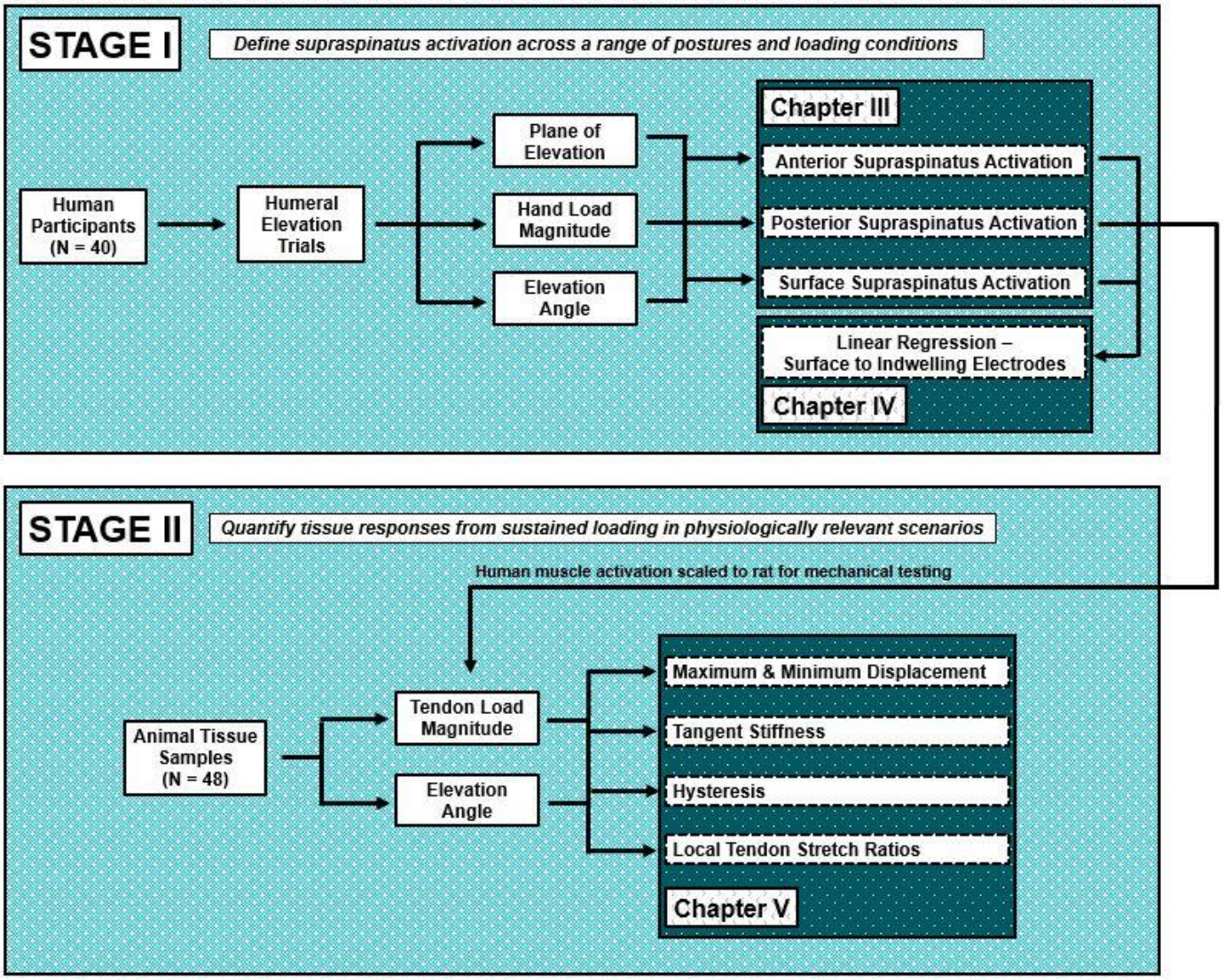

Figure 1. An outline of the specific goals and outcome measures which comprise this thesis. Italicized text indicate general stage purposes; specific study contributions are outlined in dark shaded boxes. The studies outlined in Chapter III and Chapter IV had simultaneous data collections. Methodology for Stage II was partially determined using the results from Stage I.

CHAPTER II – LITERATURE REVIEW

This chapter provides a review of literature regarding primary shoulder and rotator cuff function, rotator cuff injury mechanisms, and measurement and modeling of tendon mechanics, with a primary focus on the role of the supraspinatus. This chapter begins with a definition of the anatomy and motion of the shoulder, followed by description of the supraspinatus muscle and its tendon (Section 2.1). Subsequent focus shifts to rotator cuff pathology and glenohumeral kinematics preceding and succeeding pathology (Section 2.2). The final sections review tendon mechanics (Section 2.3) and experimental techniques for evaluating tendon responses to loads (Section 2.4).

2.1 Shoulder Anatomy & Motion

The shoulder contains architecture and motion characteristics unlike anything else in the rest of the human body. The shoulder includes three bones: the humerus, scapula and clavicle. Motion at the shoulder occurs through four joints: the acromioclavicular joint, between the acromion process of the scapula and the clavicle; the sternoclavicular joint, between the sternum and clavicle; the glenohumeral joint, between the glenoid cavity of the scapula and the humeral head; and the scapulothoracic joint, a gliding surface between the scapula and the thorax. Collectively, this motion is controlled by the concerted interaction of nearly 30 muscles (Holzbaur, Murray, & Delp, 2005). The relationships between glenohumeral and scapulothoracic orientations for healthy shoulders in a resting arm posture of 0º elevation and 0º axial rotation are well known (Basmajian & Bazant, 1959). In this posture, the scapula faces 30º anteriorly to the chest wall, tilts 3º upward relative to the transverse plane and 20º forward relative to the sagittal plane (Inman, Saunders, & Abbott, 1944). Humeral motion through elevation generates predictable position

changes in the other bones of the shoulder, resulting in scapulothoracic relationships or "rhythms" (Codman, 1934; Inman et al., 1944; Poppen & Walker, 1976). The relationship of humeral elevation to scapular upward rotation is reported as approximately 4:1 for the first 30º of humeral elevation, then 5:4 for the remainder of elevation (Poppen & Walker, 1976). Other assumptions of scapular rhythm between the glenohumeral and scapulothoracic joints use ratios of 2:1 below 90º and 1:1 above 90º (Itoi, Hsu, & An, 1996). Understanding the relationships between the scapula, humerus and torso during arm elevation informs logistical considerations in the current research. During *in vitro* testing (Chapter V), the specimen consists of the humerus and scapula, but disarticulated from the torso. Deriving glenohumeral postures from arm elevations relative to the torso allows inferences for positioning the specimens that reflect whole body postures. Scapulohumeral rhythm can be affected by various pathologic conditions, and varies by person and by sex (Doody, Freedman, & Waterland, 1970; Freedman & Munro, 1966; Lin, Lim, & Yang, 2006; Matias & Pascoal, 2006; Walker, 1977). Although these joints can act independently, they act in unison to enable healthy movement of the upper extremity (Inman et al., 1944).

The central theme surrounding the shoulder is a balance between mobility and stability. The amount of motion available at the shoulder separates it from other joints in the human body, and this range of flexibility comes at the cost of stability. This stability is obtained through the coordinated movement of multiple mechanisms while continuing to provide mobility. Anatomic stability control of the glenohumeral joint may be divided into static and dynamic categories (Van der Helm, 1994). Static contributors can be divided into articular and capsuloligamentous components, while dynamic contributions include the deltoid, biceps and rotator cuff muscles (Turkel, Panio, Marshall, & Girgis, 1981; Van der Helm, 1994). Extensive investigation of the static and dynamic components of shoulder stability has been underway since the 1940s, with most

efforts focused on one or the other. Early research emphasized the articular contribution to glenohumeral stability, with focus on the glenoid (Das, Ray, & Saka, 1966; Saha, 1971). The glenoid articulation has a small posterior (retroverted) orientation of ~7° with regard to the body of the scapula, providing increased stability to the glenohumeral joint compared to anteverted glenoid components, leading to increased anterior translation of the humeral head and placing the shoulder at risk for future complications (Das et al., 1966; Nyffeler et al., 2006). Other research has examined the role of the labrum in stability; some found that removing the labrum through a posterior approach could not generate anterior dislocation until the anterior capsule was resected (Townley, 1950), while others concluded that the labrum provided little stability to the joint, as it flattened in external rotation and thus only served as an attachment point for the inferior glenohumeral ligament (Moseley & Overgaard, 1962). However, other researchers have placed increased importance on the labrum. Measurement of glenoid depth observed that the labrum effectively doubled the depth of the glenoid (Howell & Galinat, 1989). As the humeral head needs to override the rim of the glenoid to dislocate, it can be considered that midrange stability depends on the depth of the glenoid to some extent. Static and dynamic stabilizers can work independently or in concert, but tend to work primarily in different ranges of humeral head displacement. Dynamic stabilizers (such as the rotator cuff or biceps) are more important when the displacement of the humeral head is small, where as static stabilizers (including the glenohumeral and coracohumeral ligaments) play a more important role in large displacements of the humeral head (Bost & Inman, 1942; DePalma, Cooke, & Probhaker, 1969; Howell & Kraft, 1991). This distinction is understandable, as for small displacements, the capsuloligamentous components are lax and thus cannot act as stabilizers (Malicky, Soslowsky, & Blasier, 1996).

2.1.1 Anatomy of the Rotator Cuff

The rotator cuff consists of four muscles that originate from the scapula, and whose tendons blend and terminate on the humeral tuberosities. The supraspinatus originates from the supraspinous fossa on the posterior aspect of the scapula, attaches to the posterolateral aspect of the greater tuberosity, and is innervated by the suprascapular nerve (Hermenegildo, Roberts, & Kim, 2014). The subscapularis covers much of the anterior scapular face, attaches to the lesser humeral tuberosity, and is innervated by the upper and lower subscapular nerves (Tubbs et al., 2007). The infraspinatus originates in the infraspinatus fossa on the posterior scapula, attaches at the posterolateral greater tuberosity, and is innervated by the suprascapular nerve. Finally, teres minor arises from the lower lateral aspect of the scapula, attaches to the lower part of the greater humeral tuberosity, and is innervated by a branch of the axillary nerve (Bickelhaupt, Eckmann, Brennick, & Rahimi, 2019).

The complex muscle architecture of supraspinatus contains two distinct regions. It divides into anterior and posterior regions, based on the attachment of muscle fibers onto the tendon (Kim et al., 2007; Roh et al., 2000; Vahlensieck, an Haack, & Schmidt, 1994; Ward et al., 2006). The anterior region accounts for ~75-85% of the muscle volume, and attaches laterally to a thick and narrow section of the supraspinatus tendon (Kim et al., 2007; Roh et al., 2000), while the smaller posterior region attaches to a wider and broader part of the tendon (Kim et al., 2007; Roh et al., 2000). The anterior region is pennate, while the posterior region has parallel fiber bundles (Kim et al., 2007). Each region has three functionally distinct parts based on fiber bundle orientation, and are separated into superficial, middle and deep subregions (Kim et al., 2010, 2007). These regions experience divergent changes in pennation angle with shoulder movement (Kim et al., 2010). Further, each subregion has unique fibre type distributions, with the middle part of the anterior

region possessing significantly more Type I fibers compared to the middle part of the posterior region, and the superficial anterior region having a larger percentage of Type II fibers compared to the other anterior subregions (Kim et al., 2013). The anatomy of these two regions may indicate that functional differences exist between these two regions. The larger anterior region with its fusiform structure and intramuscular tendinous core may be responsible for the bulk of the supraspinatus contractile force (Roh et al., 2000), while the posterior region has been described as "straplike", and is a smaller, unipennate muscle with no intramuscular tendon, and thus its architecture does not appear to be suited for generating large contractile loads (Vahlensieck et al., 1994) (Figure 2).

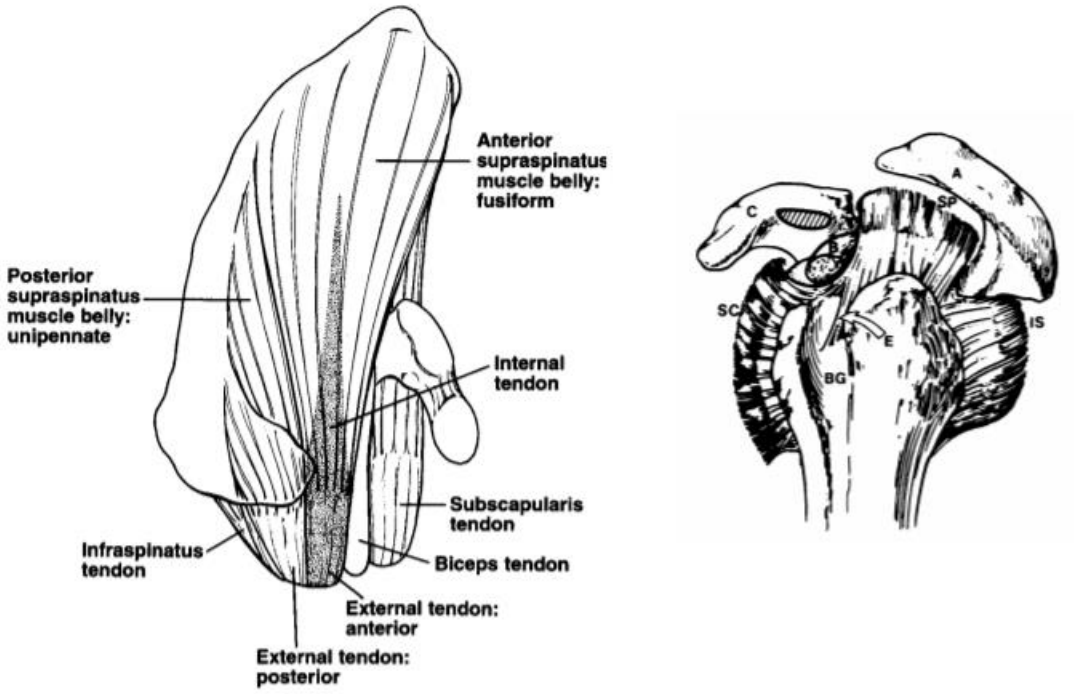

Figure 2. Representative anatomy of the supraspinatus. The supraspinatus has anterior and posterior regions (left), and inserts onto the humerus (labelled SP, right). Adapted from Roh et al., 2000 and Clark & Harryman II, 1992.

The shoulder musculature, particularly the rotator cuff, enhances dynamic shoulder stability during activity; the scapula assists by providing a foundation for the muscles of the rotator

cuff to generate normal shoulder movement. Cuff contributions to joint stability arise from multiple causes, including passive muscle tension, active contraction causing compression of the articular surfaces, resulting joint motion that results in ligament stretch, or a checkrein effect generated by the contracted muscles (Browne, Hoffmeyer, Tanaka, An, & Morrey, 1990; Kumar & Balasubramaniam, 1985; Motzkin, Itoi, Morrey, & An, 1998; Terry, Hammon, France, & Norwood, 1991). Activation of shoulder musculature acts to stabilize the humeral head in the centre of the horizontal plane of the glenoid (Howell & Kraft, 1991), with the rotator cuff working together to act as "steerers" to maintain humeral head position (Saha, 1971) (Figure 3).

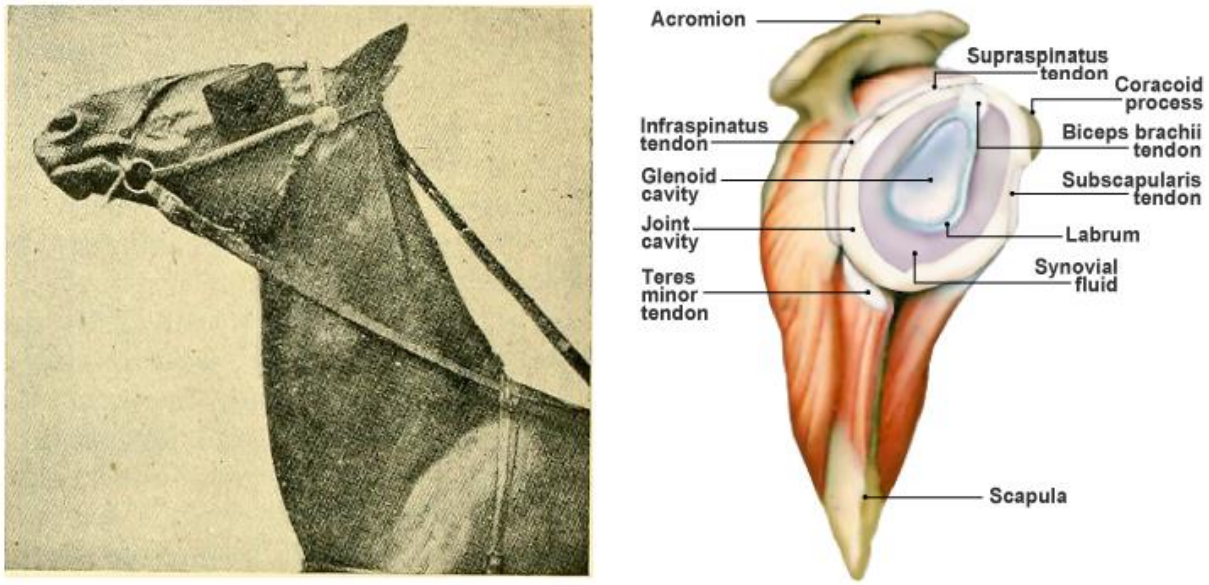

Figure 3. A checkrein for horses (located behind the head) prevents certain head motions such as neck flexion by preventing the horse from lowering its head beyond a certain point; rotator cuff architecture performs similar mechanics at the glenohumeral joint. Adapted from Matsen III & Lippitt (2004).

While the muscles of the rotator cuff have individual functions, they act in concert to maintain glenohumeral stability. These muscles have three primary functions: rotating the humerus with respect to the scapula; compressing the humeral head into the glenoid fossa, and collectively

working to generate proper timing and magnitude of muscle activation to avoid unwanted humeral motion. Although the supraspinatus and subscapularis were once identified as important humeral head inferior or superior stabilizers (Basmajian & Bazant, 1959; DePalma et al., 1969), these components of cuff muscle force have since been shown to be small; instead of stabilizing superiorly or inferiorly, the primarily stabilizing function is through humeral head compression into the glenoid (Sharkey, Marder, & Hanson, 1994; Wuelker, Roetman, Plitz, & Knop, 1994). As the rotator cuff acts collectively to keep the humeral head centred in the glenoid (Howell & Kraft, 1991), unbalanced activation may allow undesirable humeral head migration. Several *in vivo* studies quantified individual stabilizing functions of the individual rotator cuff muscles. The supraspinatus, infraspinatus and teres minor all contribute to anterior stability of the abducted shoulder (Blasier, Guldberg, & Rothman, 1992). Individual muscle contributions to motion differentiate by action. Individual cuff contributions have been evaluated through the use of selective nerve blocks, which found that the supraspinatus and infraspinatus combined represent 45% of abduction strength and 90% of external rotation strength (Colachis Jr & Strohm, 1971; Colachis Jr, Strohm, & Brechner, 1969). Collectively, the insertion of these tendons as a continuous cuff around the humeral head permits an infinite variety of moments to rotate the humerus and assist or oppose components of deltoid and pectoralis force (Holzbaur et al., 2005).

2.1.2 Shoulder Anatomical Axis Systems

This section describes the anatomical axis systems of the thorax, humerus and scapula, as well as scapulothoracic and humerothoracic translations. These joint coordinate systems exist throughout this document, and reflect recommendations of the International Society of Biomechanics (Wu et al., 2005).

2.1.2.1 Thorax

The definition of joint displacements is most useful when it is with respect to a proximal segment or segments. Joint or segment rotations at the shoulder are typically represented relative to the thorax. The torso rotation sequence is Z-Y-X, with positive Z_t rotation representing extension, positive Y_t rotation representing axial rotation to the left, and positive X_t rotation representing lateral flexion to the right (Figure 4). The thorax coordinate system is as follows:

$+Y_t$ is a line connecting the midpoint of the xiphoid process and T8 and the midpoint between the suprasternal notch and C7, pointing upward.

$+Z_t$ is the line perpendicular to the plane formed by the xiphoid process, T8, suprasternal notch and C7, pointing to the right.

$+X_t$ is a line commonly perpendicular to Y and Z, pointing forwards.

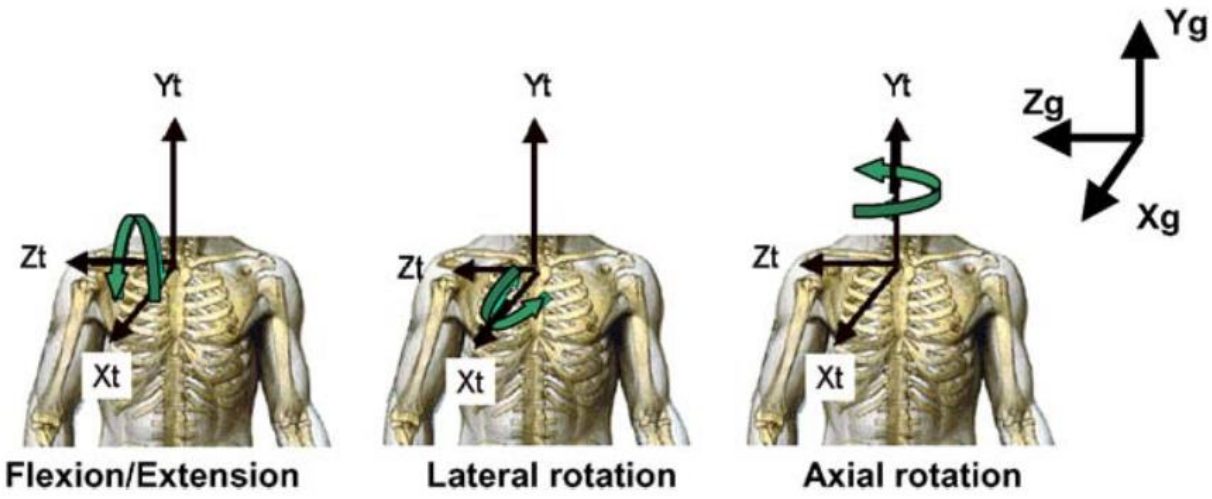

Figure 4. Thorax coordinate system and definition of motions (from Wu et al., 2005).

2.1.2.2 Humerus

The humerus coordinate system combined with the torso system quantifies humeral angle of elevation, plane of elevation and axial rotation relative to the torso. The glenohumeral joint rotation centre is not a bony landmark, but can be can be estimated by regression analysis or instantaneous helical axes (Meskers, Fraterman, Van der Helm, Vermeulen, & Rozing, 1998; Veeger, Yu, & An, 1996). The rotation sequence for the humerus is with respect to the torso, and is a Y-X-Y' rotation. Rotating around the Y_h axis determines plane of elevation, and rotation about the X_h axis determines angle of elevation. Rotation about the X_h axis with preceding 0º, +30º and +90º rotations around the Y_h axis generates elevation in the coronal, scapular and sagittal (forward flexion) planes, respectively (Figure 5). The humerus coordinate system is as follows (Figure 6):

+Y_h is a line connecting the midpoints of the epicondyles, pointing superiorly to the glenohumeral rotation center, estimated by regression or motion recordings;

+X_h is a line perpendicular to the plane formed by Y_h, pointing forwards;

+Z_h is a line commonly perpendicular to Y and X, pointing to the right.

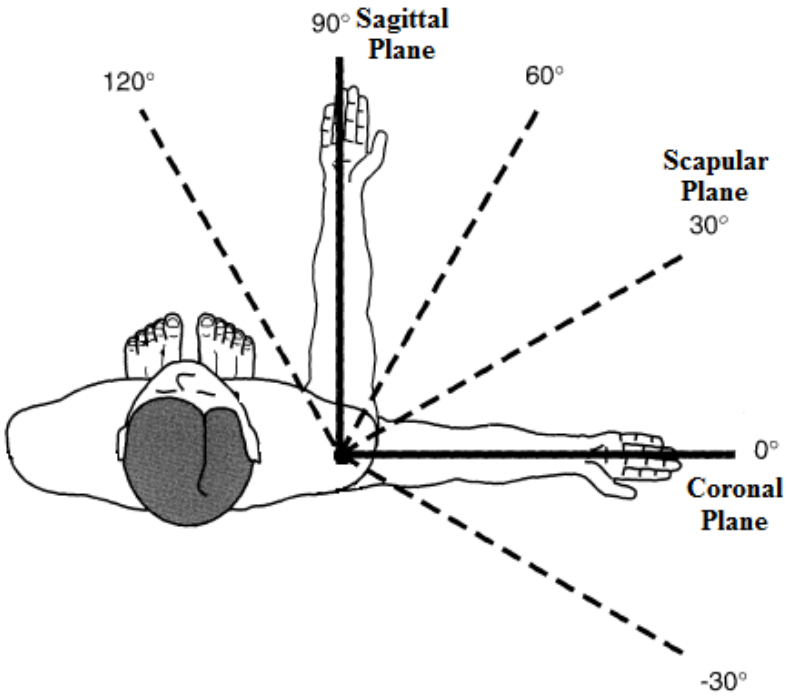

Figure 5. Planes of humeral elevation.

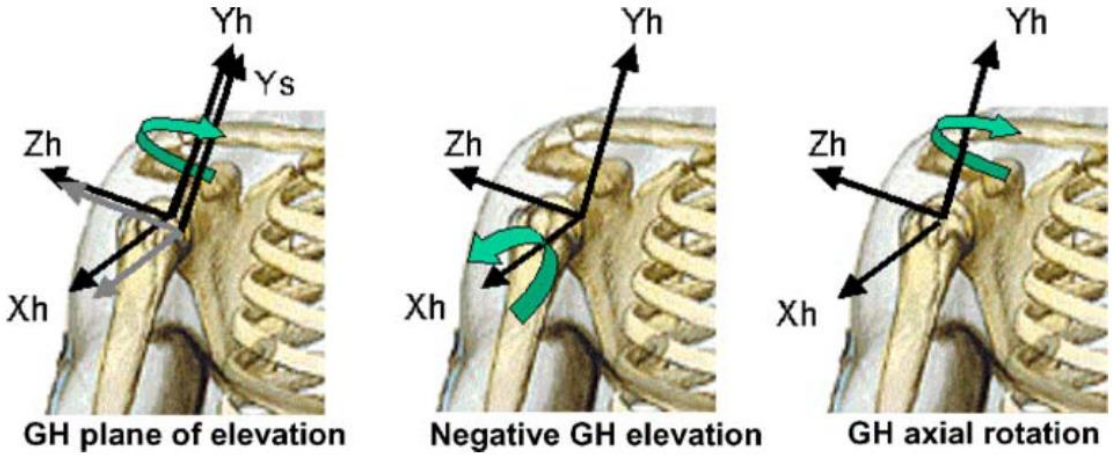

Figure 6. Coordinate system of the humerus relative to the thorax and definition of motions (from Wu et al., 2005).

2.1.2.3 Scapula

The scapular coordinate system is used in conjunction with the torso to quantify scapular rotation, anterior/posterior tilt, and protraction/retraction with respect to the torso. The origin of the scapular coordinate system is located on the acromial angle, the most laterodorsal point of the

scapula (Wu et al., 2005). In a right shoulder, the coordinate system is defined as follows (Figure 7):

+Z_s is the line connecting the root of the scapular spine and the acromion angle, pointing to the acromion angle;

+X_s is the line perpendicular to the plane formed by the inferior angle of the scapula, the acromion angle and the root of the scapular spine, pointing anteriorly;

+Y_s is a line commonly perpendicular to X and Z, pointing upward.

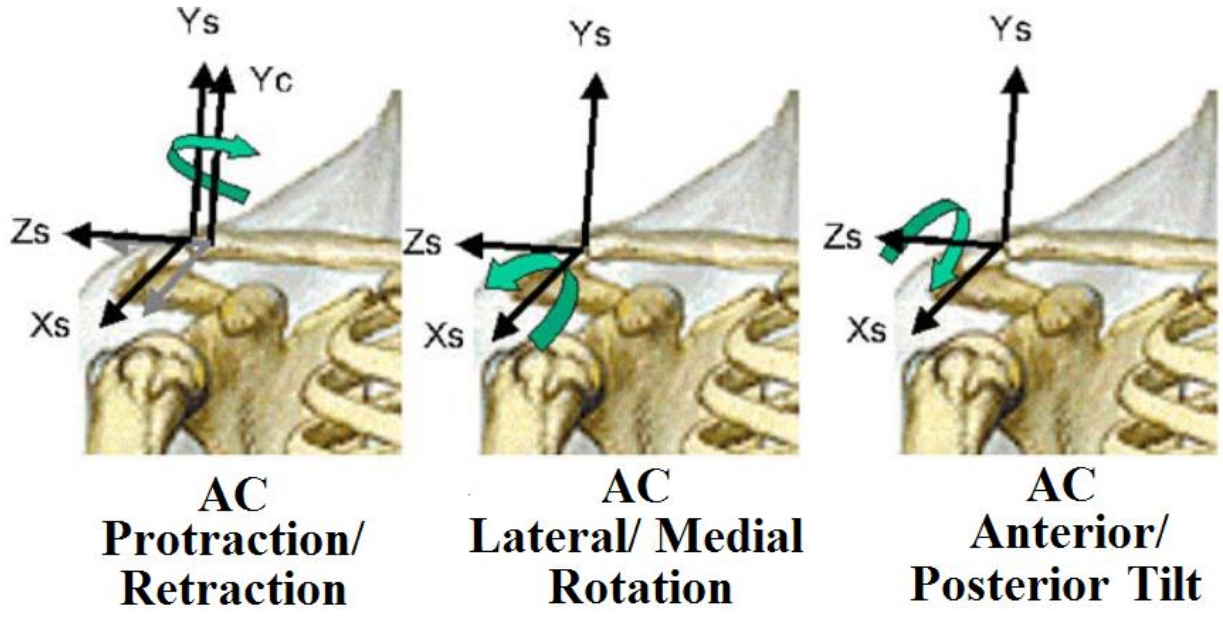

Figure 7. Scapular coordinate system and definition of acromioclavicular (AC) motions (from Wu et al., 2005).

The rotation sequence for the scapula is with respect to the torso, and is Y-X-Z. Rotation about the Y_s axis generates protraction/retraction, rotation about the X_s axis produces

upward/downward rotation, and rotation about the Z_s axis produces anterior/posterior tilt (Figure 8).

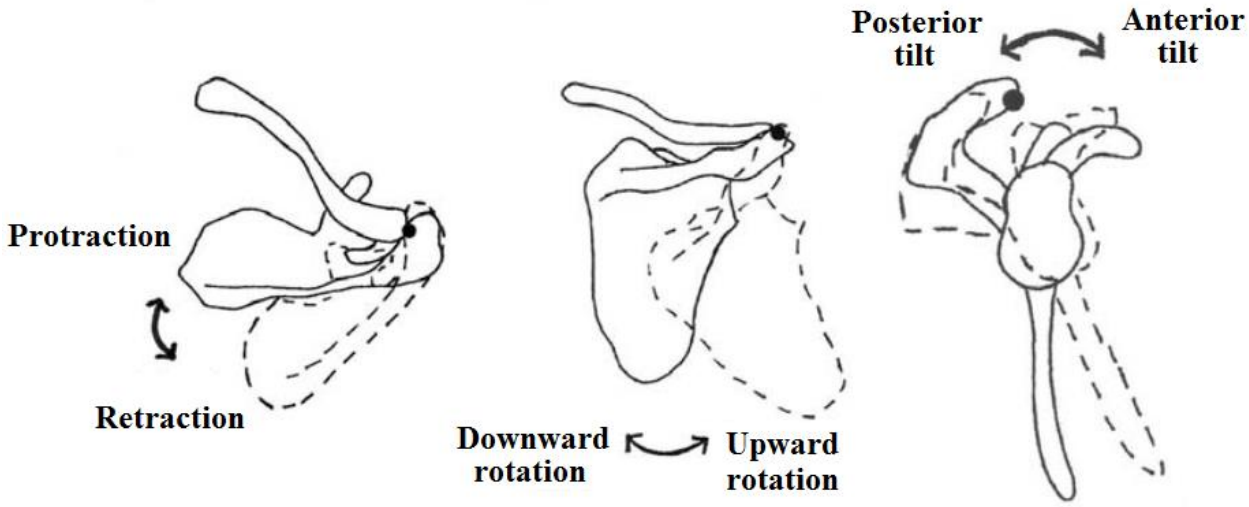

Figure 8. 3 dimensional scapular rotations: protraction/retraction (left), upward/down rotation (centre), anterior/posterior tilt (right).

2.1.2.4 Glenohumeral Translations

The glenohumeral joint rotation center is not a bony landmark, but is regularly used to define the longitudinal axis of the humerus and to calculate three-dimensional movement of the humeral head with respect to the glenoid cavity. Glenohumeral joint translations are typically described by comparing the relative positions of the centre of the humeral head contact area and the centre of the glenoid cavity on the scapula (Bey et al., 2007; Poppen & Walker, 1976). The origin of the glenoid system is located at the centre of the glenoid cavity, with the coordinate system as follows (Figure 9):

$+Y_g$ is a line from the inferior to the superior border of the glenoid cavity (termed the 'glenoid axis');

$+X_g$ is a line perpendicular to Y, directed anteriorly from the posterior border to the

anterior border of the glenoid cavity;

$+Z_g$ is a line commonly perpendicular to X and Y, pointing right.

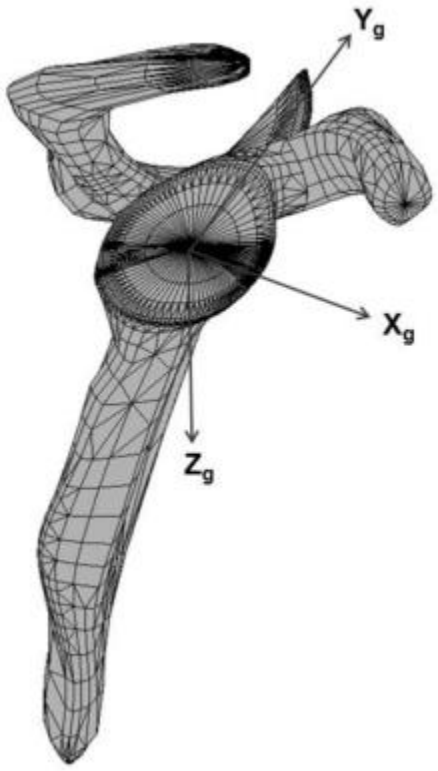

Figure 9. Glenoid translations coordinate system. Adapted from Chopp-Hurley (2015).

In this coordinate system, a $+Y_g$ translation represents upward translation of the humeral head towards the inferior aspect of the acromion, a $+X_g$ translation represents anterior movement of the humeral head towards the anterior border of the glenoid, and a $+Z_g$ translation indicates a separation of the humeral head away from the glenoid cavity (where $-Z_g$ translations would be compression of the humeral head into the cavity).

2.2 Rotator Cuff Pathology

Shoulder injuries are highly prevalent, with chronic injuries increasingly common in older populations. Rotator cuff injuries are particularly frequent, and include impingements (either subacromial or internal), partial cuff tears, or complete tendon ruptures (Reuther, Thomas, Tucker, Yannascoli, et al., 2014). Scarce analogous data exists for living subjects, as only symptomatic patients are often studied. Research examining a community of 644 persons older than 70 years identified shoulder symptoms in 21% of the population, yet only 40% of these affected individuals had sought medical attention for their symptoms (Chard et al., 1991). Chronic shoulder injury rates increase markedly after 50 years of age. For example, more than half of subjects in their 70s and 80% of persons in their 80s had rotator cuff tears, leading the authors to conclude that "rotator-cuff lesions are a natural correlate of aging, and are often present with no clinical symptoms" (Milgrom et al., 1995). Cuff defects become increasingly common after 40 years of age, and many occur without substantial clinical manifestations. Continued research on rotator cuff pathology has largely been derived from cadaveric findings. Incidence of rotator cuff tendon defects in cadaver dissections range from 7% to 26.5% (Fukuda et al., 1987; Keyes, 1952; Wilson & Duff, 1943). Across 500 cadaveric shoulders, the incidence of complete rotator cuff tears was less than 5% (Neer, 1983). However, other research indicated a 17% incidence of full-thickness rotator cuff tears in 235 male and female cadavers ranging from 27 to 102 years (average age 64.7 years) (Lehman et al., 1995). The authors also noted that the incidence of full thickness rotator cuff tears was 6% in individuals under 60, and 30% for those over 60 (Lehman et al., 1995). These discrepancies in incidence rate may relate to population sample differences, as the number of cadavers examined ranged from nine to 500. Partial thickness tears appear to be about twice as common as full thickness tears (Yamanaka et al., 1983). Contributing sources of rotator cuff

injuries include trauma (Codman, 1911, 1937), degenerative abrasion in the subacromial space (Ellman & Kay, 1991; Keyes, 1952; Meyer, 1924; Moseley, 1952), ischemia (Lindblom & Palmer, 1939; Moseley & Goldie, 1963; Rathbun & Macnab, 1970; Rothman & Parke, 1965), or subacromial abrasion (Neer, 1972, 1983; Watson-Jones, 1960).

Rotator cuff pathologies arise from intrinsic and extrinsic factors. Intrinsic factors are generally described as a process where gradual or acute tissue loading or age-related degeneration causes pathology, leading to kinematic changes and secondary pathologies. Alternatively, extrinsic factors are exposure-related processes, in which environmental conditions (such as workplace parameters) lead to tissue changes. Rotator cuff pathologies arising from intrinsic sources are not easily preventable. Associations between acromion morphology and rotator cuff tear rates have been observed through cadaveric research (Bigliani, Morrison, & April, 1986), with increased rotator cuff tear incidence rates appearing in individuals with a hooked acromion compared to flat or curved acromial morphologies. These mechanics can affect the subacromial space, resulting in impingement, which accounts for approximately half of all shoulder complaints (van der Windt, Koes, de Jong, & Bouter, 1995). Aging is a major intrinsic factor surrounding degeneration. Although young healthy tendons seem capable of handling complex loading such as that which occurs in the rotator cuff, structurally inferior tissue or tissue with reduced repair potential is prone to degeneration (Dalton, Cawston, Riley, Bayley, & Hazleman, 1995; Hamada, Okawara, Fryer, Tomonaga, & Fukuda, 1994; Kumagai, Sarkar, & Ulthoff, 1994; Riley et al., 1994a). Like the rest of the body's tissues, rotator tendon cuff fibers become weaker with disuse and age, and require less force to disrupt them (Chung & Nissenbaum, 1975; Rathbun & Macnab, 1970). Aging has been described as "the single most important contributing factor in the pathogenesis of tears of the cuff tendons" (Matsen III, Fu, & Hawkins, 1992). Extrinsically, many mechanical exposures are

capable of modulating rotator cuff pathology. Different environmental exposures, such as posture, force and repetition all interact with musculoskeletal tissues to create internal exposures, consequently altering pathology risk (Wells, Van Eerd, & Hagg, 2004). Extrinsic factors in some sports can also increase injury risk, particularly in throwing. Rotator cuff tendon fibers are subjected to bending loads over the head of the humerus as it rotates with respect to the scapula (Matsen III, Sidles, Harrymann, & Lippert, 1994). With the arm positioned at the limit of range of motion, the glenoid rim can apply shear loads to the deep surface of the supraspinatus tendon, and may contribute to rotator cuff injury in throwing athletes (Ferrari, Ferrari, Coumas, & Pappas, 1994; Jobe, 1995; Sh Liu & Boynton, 1993; Rossi, Tenamian, Cerciello, & Walch, 1994; Tirman et al., 1994) (Figure 10). Extrinsic workplace exposures, including posture, repetition and hand force are outlined in detail in Section 2.2.1.

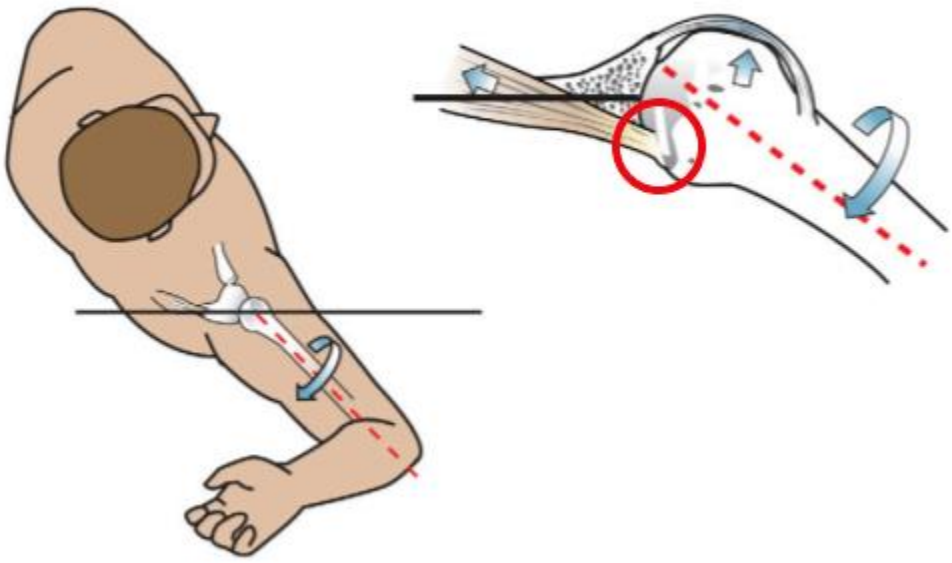

Figure 10. Humeral head rotation in throwing can generate impingement in the supraspinatus tendon. Adapted from Braun, Kokmeyer, & Millett (2009).

Rotator cuff pathologies follow a predictable injury cascade. The injuries often begin in the supraspinatus tendon before cascading anteriorly to the subscapularis or posteriorly to the

infraspinatus (Cofield, 1985; Reuther, Thomas, Tucker, Yannascoli, et al., 2014) (Figure 11). Rotator cuff failure through degenerative scenarios typically initiates with a partial-thickness defect on the deep surface near the attachment of the supraspinatus to the greater tuberosity (Davidson et al., 1995; Edelson & Teitz, 2000). Multiple research groups have described partial-thickness tears, and these observations suggest that the deep fibers of the cuff near the insertion are most vulnerable to failure due to three factors: exposure to high loads, relative lack of strength, and limited capacity for repair (Codman, 1934; Fukuda et al., 1987; Yamanaka et al., 1983). Injuries of the rotator cuff typically start where the stresses are presumably the greatest: at the deep surface of the anterior insertions of the supraspinatus, near the long head of the biceps (Edelson & Teitz, 2000). These tendon fibers fail when the applied load exceeds their strength, and can fail a few at a time, or *en masse* (Matsen III & Lippitt, 2004). These fibers retract after rupture, as the rotator cuff fibers are under tonic load, even with the arm at rest (Halder et al., 2002). Each instance of fiber failure increases the load on the neighbouring unruptured fibres, giving rise to the "zipper" phenomenon. This negatively affects the rotator cuff in multiple ways. Muscle detaches from bone, diminishing the amount of force the cuff muscles can deliver. Local anatomy becomes distorted, compromising the tendon's blood supply and contributing to local ischemia. Additionally, the tendon becomes exposed to joint fluid containing lytic enzymes, which remove any hematoma that could contribute to tendon healing (Marqueti, Parizotto, Chriguer, Perez, & Selistre-de-Araujo, 2006; Nakama, King, Abrahamsson, & Rempel, 2006; Sun et al., 2008). Without repair, degeneration continues through the supraspinatus tendon to produce a full-thickness defect in the anterior supraspinatus tendon. Once this defect is established, it typically propagates posteriorly into the infraspinatus (Cofield, 1985; Reuther, Thomas, Tucker, Sarver, et al., 2014). Progression increases the load on the biceps, often rupturing the tendon of the long head of the biceps in chronic

rotator cuff deficiencies (Ting, Jobe, & Barto, 1987). Further propagation crosses the bicipital groove and begins to involve the subscapularis, and can destabilize the tendon of the long head of the biceps, allowing subluxation of the tendon (Ting et al., 1987). Collectively, these defects decrease the ability of the rotator cuff to generate compression, which is important in providing glenohumeral stability (Lee, Kim, O'Driscol, Morrey, & An, 2000).

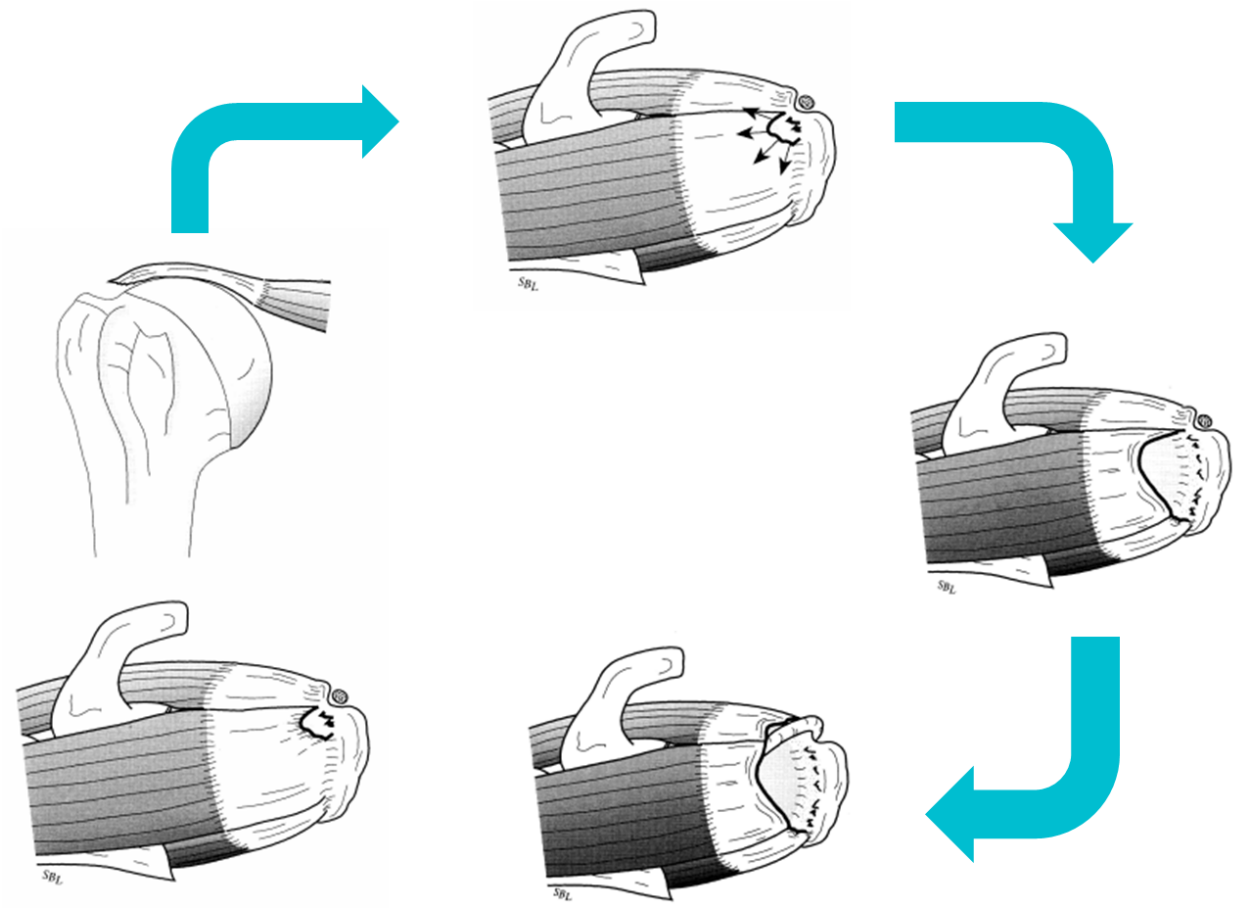

Figure 11. Rotator cuff defects often follow a predictable cascade of injury, typically originating in the supraspinatus tendon and expanding to the surrounding connective tissues. Adapted from Matsen III et al. (1994).

Rotator cuff injuries have multiple clinically meaningful manifestations. Patients commonly present to clinicians because they perceive a loss of shoulder comfort and function (van der Windt et al., 1995). A cohort study comparing rotator cuff injuries to 15 other common

shoulder conditions presented to clinicians indicated partial- and full thickness rotator cuff tears are the most common shoulder conditions presented (Largacha et al., 2006). Additionally, these individuals had a 34-49% reduction in range of motion, 41-61% decreases in strength, and over 80% of this group reported an inability to sleep on the affected side (Largacha et al., 2006). Despite similar injuries, clinical manifestations can vary substantially, and could include stiffness, weakness, or instability (Duckworth, Smith, Campbell, & Matsen III, 1999; Smith et al., 2000). Stiffness may be demonstrable as limitations in internal rotation with the arm in abduction, reaching from the back, cross-body abduction, flexion, or external rotation (Hegedus et al., 2012), and is most common in partial-thickness cuff lesions, but can also be associated with full-thickness cuff defects (Jackson, 1976). Some patients with full-thickness cuff defects may still be able to actively abduct the arm, but often demonstrate weakness on the affected side (Neviaser, 1971). Significant tendon fiber failure is usually manifested by weakness in manual muscle testing (Hawkins, Misamore, & Hobeika, 1985; Leroux et al., 1994; Leroux, Thomas, Bonnel, & Blotman, 1995). Clinical isometric tests are reasonably selective at isolating individual cuff muscles (Brookham, McLean, & Dickerson, 2010). These simple manual tests can be helpful in characterizing the size of the tendon defect, from single tears involving only the supraspinatus to two- or three-tendon tears, but tests must consider scapular position to prevent misdiagnosis (Kibler, 2006). An inability to keep the humeral head centred in the glenoid can result from cuff disease, and acute rotator cuff tears can contribute to recurrent anterior instability (Neviaser, Neviaser, & Neviaser, 1993; Sonnabend, 1994; Toolanen, Hildingssonl, Hedlund, Knibesto, & Oberg, 1993). Loss of the compressive effect of the rotator cuff paired with the loss of the stabilizing effect of the superior cuff tendon between the humeral head and the coracoacromial arch can contribute to superior glenohumeral instability (Flatow et al., 1994; Poppen & Walker,

1976). Clinical recommendations between operative and non-operative treatments are completed on a case-by-case basis (Neer, 1972). Early operative repair for complete rotator cuff tears were recommended by Codman, who may have carried out the first cuff repair in 1909 (Codman, 1911). Current views surrounding rotator cuff pathology, diagnosis, and treatment are similar to his original proposals. In both operative and nonoperative treatments, the goals are to avoid repeated injury and restore normal flexibility and strength (Ellman, Kay, & Wirth, 1993).

Rotator cuff defects do not tend to have strong healing responses without medical intervention. An examination of 17 rotator cuff specimens showed no natural closure of the rotator cuff defect, despite the evidence of granulation tissue and vessel proliferation near the intratendinous tears (Fukuda, Hamada, Nakajima, & Tomonaga, 1994). Further evidence of nonhealing cuff lesions has been highlighted through tracking of partial-thickness rotator cuff tears (Yamanaka & Matsumoto, 1994). After an initial arthrography, they monitored 40 rotator cuff tears (mean patient age 61 years, mean arthrography repeated at 412 days) that were managed without surgery. After an arthrography over a year later, only 10% of cases showed apparent healing, with another 10% indicating a reduction in size. Conversely, tear enlargement occurred in 50% of cases, with 25% of these cases progressing to full thickness lesions (Yamanaka & Matsumoto, 1994). Interestingly, clinical functional and pain scores improved at the follow-up visit (Yamanaka & Matsumoto, 1994). These observations mirror statements made by Codman 60 years prior – “It is my unproved opinion that many of these lesions never heal, although the symptoms caused by them usually disappear after a few months. Otherwise, how could we account for their frequent presence at autopsy?” (Codman, 1934). More critically, these studies indicate that reliance on clinical symptoms (such as function or pain) can be unreliable in determining rotator cuff integrity.

Undiagnosed or untreated rotator cuff injuries often generate chronic secondary effects. Atrophy, fatty degeneration, fibre retraction and loss of excursion are all commonly associated with chronic rotator cuff defects (Leivseth & Reikeras, 1994; Nakagaki et al., 1994). Earlier reattachment of the supraspinatus tendon (6 weeks) compared to later reattachment (12 weeks) prevented increases in fat accumulation within the muscle in an animal model (Uhthoff, Matsumoto, Trudel, & Himori, 2003). Atrophy in the muscle can occur within days to weeks following tendon detachment; animal models observed muscle volume reductions of 32% in detached rotator cuff muscle within the first six weeks (Safran, Derwin, Powell, & Ianotti, 2005). Beyond muscle changes, tendon changes occur. Collagen types I and XII were greatly increased initially after injury then decreased with time, suggesting a rationale for healing differences in chronic and acute tears (Yokota, Gimbel, Williams, & Soslowsky, 2005). These detachments should be repaired as early as possible, as it promotes a more rapid recovery of both muscle function and tendon elasticity (Coleman et al., 2003). However, once these secondary effects manifest, they increase with the duration of the tear, and are largely irreversible (Goutallier, Postel, Bernageau, Lavau, & Voisin, 1994; Goutallier, Postel, Bernageau, & Voisin, 1995).

2.2.1 Work Related Rotator Cuff Exposures

Occupational scenarios provide numerous opportunities for injury to the shoulder. Certain jobs seem to be problematic for the rotator cuff, including tree pruning, fruit picking, nursing, grocery clerking, longshoring, warehousing, carpentry, and painting (Luopajarvi, Kuorinka, Virolainen, & Holmberg, 1979). In 2015, the shoulder was the second most common site for allowed lost time claims behind the low back, with the most common claim being overexertion (WSIB, 2015). There is extensive research associating repetitive work and overexertion with increased shoulder injury risk (Bernard, 1997; Grieve & Dickerson, 2008; Punnett, Fine,

Keyserling, Herrin, & Chaffin, 2000; van Rijn, Huisstede, Koes, & Burdorf, 2010). Force, posture and repetition all interact with musculoskeletal tissues in the shoulder to create mechanical exposures that increase injury risk (Wells, Van Eerd, & Hagg, 2004).

2.2.1.1 Posture

Arm posture is linked to shoulder pain and injury. Strong associations exist between overhead work and pain or injury development (Bernard, 1997; Grieve & Dickerson, 2008; Herberts, Kadefors, Andersson, & Petersen, 1981; Punnett et al., 2000; van Rijn et al., 2010). These studies reported significant injury risk estimates (odds ratios 2.3-10.6), and was strongest in workplace tasks that had exposure to several risk factors, such as holding a tool while working overhead (Bernard, 1997; Grieve & Dickerson, 2008). Humeral elevation and axial rotation can both alter the size of the subacromial space, which could generate injury through impingement (Miranda, Viikari-Juntura, Heistaro, Heliovaara, & Riihimaki, 2005; Svendsen et al., 2004; van Rijn et al., 2010). The subacromial space may decrease when the arm is elevated, which is partly attributed to the greater humeral tuberosity which moves closer to the acromion process in elevation or when paired with external rotation (Graichen, Bonel, Stammberger, Englmeier, et al., 1999; Graichen, Bonel, Stammberger, Haubner, et al., 1999). Altering the work location relative to the individual has generated non-linear, spatially dependent characteristics in muscle activation at identical hand force requirements, both at individual and collective levels (McDonald, Brenneman, Cudlip, & Dickerson, 2014; McDonald, Picco, Belbeck, Chow, & Dickerson, 2012; Nadon et al., 2016). Several studies indicate that hand location modifies maximal arm strength (Chow & Dickerson, 2009; Cudlip & Dickerson, 2018a; Garg, Hegmann, & Kapellusch, 2005; La Delfa, Freeman, Petruzzi, & Potvin, 2014; Roman-Liu & Tokarski, 2005; Warwick, Novak,

Schultz, & Berkson, 1980), and the moment generating capability of muscles surrounding the shoulder are dependent on upper extremity posture (Kuechle, Newman, Itoi, & Morrey, 1997).

2.2.1.2 Repetition

Consensus exists with respect to increased shoulder injury risk due to exposure repetition, but little data documents its influence independently from other factors. Interactions between repetition and overhead postures revealed a higher prevalence of self-reported shoulder problems and impingement in individuals whose work entailed repetitive shoulder movements and sustained arm elevation (Frost & Andersen, 1999). The relationship between repetitive work and shoulder pain has been documented in a national representative sample of over 8000 participants (Miranda et al., 2005). Workers whose jobs require repetitive tasks are two to three times more likely to develop shoulder tendinitis (Frost et al., 2002). Positive associations between highly repetitive work and shoulder disorders have been determined, with odds ratios varying from 1.6-5.0 (Bernard, 1997). However, this evidence has limitations: three studies involved interactions between repetition and awkward postures, and the other studies with significant positive associations dealt primarily with symptoms rather than mechanisms.

Prolonged repetitive tasks can generate fatigue, and depend on several characteristics. Repetitive or sustained submaximal efforts can cause increases in perceived effort and inability to produce the required force (Enoka & Stuart, 1992). The processes and rate of fatigue differ between muscle groups, intensities, duration of effort (whether it be continuous or intermittent), and other subject-specific characteristics including age, sex, and motivation levels (Barry & Enoka, 2007). This fatigue alters kinematics, and numerous studies have examined kinematic changes of the shoulder following targeted fatigue of rotator cuff muscles (Borstad, Szucs, & Navalgund, 2009; Ebaugh, McClure, & Karduna, 2006a, 2006b; Tsai, McClure, & Karduna,

2003). These repetitive and fatiguing motions can alter upper extremity kinematics, which can increase risk of future shoulder pathology (Côté, Raymond, Mathieu, Feldman, & Levin, 2005; Fuller, Fung, & Côté, 2011; D. Gates & Dingwell, 2008; Lomond & Côté, 2011).

2.2.1.3 Hand Force

Conflicting research exists surrounding the link between manual forces and rotator cuff injury. Workers who have high force requirements (≥10% of their maximal voluntary contraction) were more likely to develop shoulder tendinitis compared to those with low force requirements, with odds ratios of 4.21 and 2.17, respectively (Frost et al., 2002). Similar results were observed in females exposed to heavy lifting more than 10 times per day and high hand force requirements for more than one hour/day for 3+ years, with an increased risk of shoulder disorder development (Miranda et al., 2005). Contradictorily, research involving machinists, car mechanics and house painters identified no significant relationship between low, medium and high hand force requirements and rotator cuff injuries (Svendsen et al., 2004). Additionally, the National Institute of Occupational Safety and Health (NIOSH) found insufficient evidence for a positive association between shoulder MSDs and force (Bernard, 1997).

2.3 Tendon Function & Mechanics

Tendon is a dense, durable connective tissue located at the ends of muscles. It consists of a portion external to muscle (the external tendon) and a portion internal to muscle (the aponeurosis of the muscle, called the internal tendon) (Zajac, 1989). Tendons are load bearing structures that transmit forces from muscle to bone (Andarawis-Puri, Flatow, & Soslowsky, 2015). They attach to bone by interlocking collagen with the surface of the bone or by continuation of the majority of collagen fibers into the periosteum (Benjamin et al., 2006). Many tendons approach their

attachment site obliquely, resulting in contact with the bone just before their attachment in certain positions of the joint in which they act, which can influence stress dissipation (Benjamin et al., 2006). Tendon is comprised of a fluid-saturated, hierarchically structured collagen network along the direction of loading. Tendon consists almost entirely of bundles of collagen fibres laying approximately parallel to its long axis, providing flexibility and tensile strength (Elliott, 1965). The smallest structural unit is the fibril, consisting largely of rod-like collagen molecules aligned end-to-end (Wang, 2006). Fibril diameters vary from 10-500nm, depending on species, age and location in the body (Wang, 2006). Young animals typically have uniformly small fibrils, whereas mature animals have large and small fibrils in a bimodal distribution (Moore & De Beaux, 1987; Parry, Flint, Gillard, & Craig, 1982). Fibers form the next level of tendon structure, and are composed of collagen fibrils bound by endotenons, a thin layer of connective tissue that contains blood vessels, lymphatics and nerves (Kastelic, Galeski, & Baer, 1978; Ochiai, Matsui, Miyaji, Merklin, & Hunter, 1979). Fiber bundles form fascicles, and bundles of these are wrapped by the epitenon; a fine, loose connective-tissue sheath which holds the vascular, lymphatic and nerve supplies to the tendon (Kastelic et al., 1978). Tendons are also surrounded by a third layer of connective tissue called the paratenon (synovial sheath in some locations), and when combined with the epitenon forms the peritendon, which reduces friction with the adjacent tissue (Schatzker & Branemark, 1969)(Figure 12).

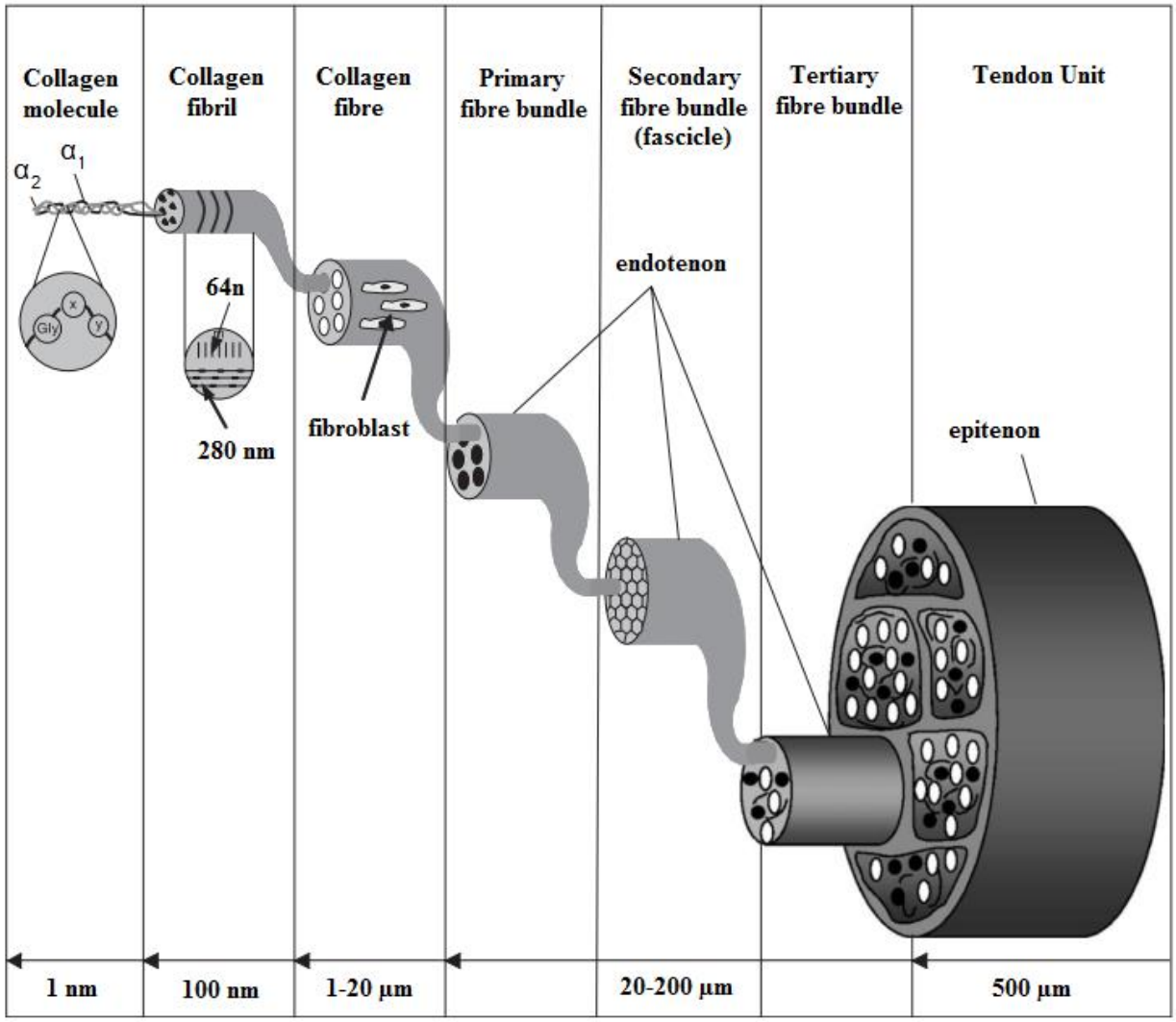

Figure 12. Hierarchy of tendon (modified from Wang, 2006).

Tendons have a complex composition, consisting of collagens, proteoglycans, glycoproteins, cells and water. Tendons are rich in collagen, with type I collagen representing ~60% of the dry mass of tendon and ~95% of the total collagen (Evans & Barbenel, 1975; Riley et al., 1994b). The remaining ~5% is made up of types III and V collagens. In normal tendons, type III collagen forms smaller, less organised fibrils, and is mainly located in the endotenon and epitenon (Duance, Restall, Beard, Bourne, & Bailey, 1977; Lapiere, Nusgens, & Pierard, 1977). However, it can also be observed in aging tendons or tendons that undergo high stresses, such as

the supraspinatus tendon (Fan, Sarkar, Franks, & Uhthoff, 1997). Type V collagen is located in the centre of type I collagen fibrils, and regulates fibril growth (Birk, Fitch, Babiarz, Doane, & Linsenmayer, 1990). Other collagens, including types II, VI, IX, X and XI are present in trace quantities mainly at the bone insertion site of fibrocartilage, strengthening the connection (Fukuta, Oyama, Kavalkovich, Fu, & Niyibizi, 1998; Waggett, Ralphs, Kwan, Woodnutt, & Benjamin, 1998). Tendons also contain proteoglycans in small quantities that vary with tendon location and mechanical exposure conditions (Berenson, Blevins, Plaas, & Vogel, 1996; Riley et al., 1994a). There are many proteoglycans, including aggrecan (holds water & resists compression) and decorin (facilitates fibrillary slippage during mechanical deformation) (Pins, Christiansen, Patel, & Silver, 1997; Vogel & Heinegard, 1985; Vogel & Koob, 1989). There are several proteins and glycoproteins present in the extracellular matrix, including elastin, which composes ~2% of the dry weight of the tendon (Jozsa, Lehto, Kvist, Balint, & Reffy, 1989). These elastic fibers may contribute to recovery of the crimp configuration following stretch (Butler, Goldstein, & Guilak, 2000). While many cell types are present in tendon, fibroblasts are the dominant type. Tendon fibroblasts align between collagen fiber bundles, and are responsible for protein synthesis and tendon remodeling during healing (Wang, 2006). Approximately 60% of the wet weight of tendon is water (Eichelberger & Brown, 1945).

Tendons are subject to dynamic forces *in vivo*, and have viscoelastic characteristics that contribute to its unique mechanical behaviour. Typically, the tendon stress-strain curve has an initial toe region, where the tendon is strained up to 2% (Wang, 2006). This toe region is thought to result from the gradual straightening of wavy or "crimped" collagen fibrils visible at the micron scale (Diamant, Keller, Baer, Litt, & Arridge, 1972; Kastelic et al., 1978). Crimp is present in all types of tendons (Dale, Baer, Keller, & Kohn, 1972). Evidence suggests that the crimp waveform

in tendon is planar (Elliott, 1965; Rigby, Hirai, Spikes, & Eyring, 1959). Measured crimp wavelengths in unloaded tendon range from ~30 μm in mouse supraspinatus tendon to ~120 μm in the rat tail (Hansen, Weiss, & Barton, 2002; Miller, Connizzo, Feeney, & Soslowsky, 2012; Miller, Connizzo, Feeney, Tucker, & Soslowsky, 2012). Under loading, crimp begins to disappear at strains corresponding to the low modulus (i.e. "toe") region of the stress strain curve, and observations of crimp are difficult to detect in the high modulus ("linear") region (Diamant et al., 1972; Rigby et al., 1959). Since many tendons operate mostly in the toe region *in vivo* (Maganaris & Paul, 1999), the process of uncrimping is of high relevance, and has recently been examined in prescribed loading conditions (Hansen et al., 2002; Miller, Connizzo, Feeney, & Soslowsky, 2012; Miller, Connizzo, Feeney, Tucker, et al., 2012). This hysteresis reflects a loss of viscoelastic dampening, likely due to changes in noncollagenous components in the interfibrillar space (Eliasson, Fahlgren, Pasternak, & Aspenberg, 2007) and loss of fibril crimp, leaving the elastic collagen to prominently respond to loading (Andarawis-Puri, Sereysky, Jepsen, & Flatow, 2012). This uncrimping in tendon is rate-dependent, with slower frequencies of loading/unloading demonstrating larger hysteresis (Buckley, Sarver, Freedman, & Soslowsky, 2013). At high strain rates, tendons become stiffer and are more effective in moving large loads (Josza & Kannus, 1997). In the linear region of the stress-strain curve where the tendon is stretched less than 4%, collagen fibers lose their crimp pattern. When the tendon is stretched beyond 4%, microscopic tearing begins, with failure beyond 8-10% strain (Butler, Grood, Noyes, & Zernicke, 1978) (Figure 13).

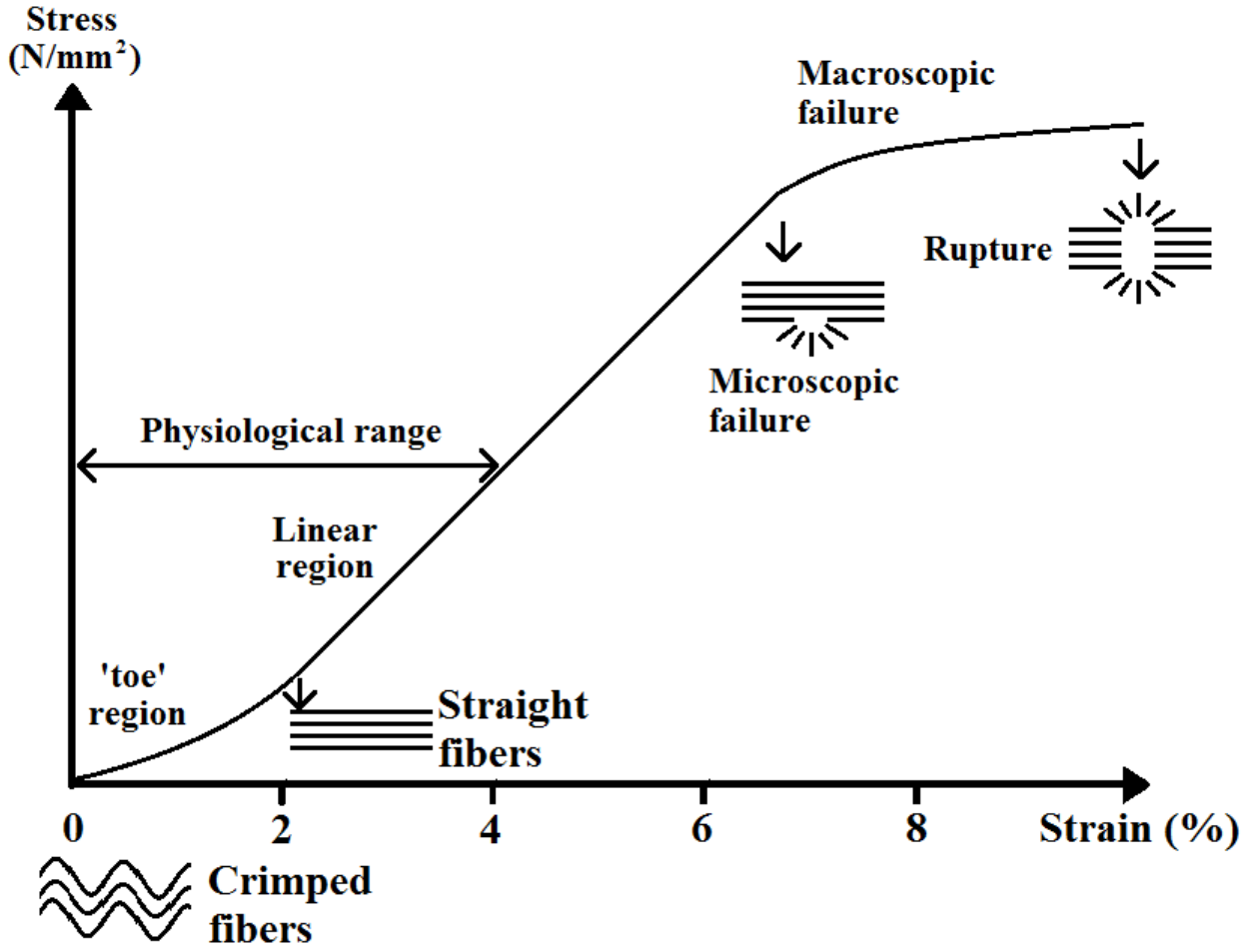

Figure 13. Representation of a typical tendon stress-strain curve.

Not all tendons share identical designs. While all tendons play a role in terms of positioning joints to facilitate movement, some also operate as energy stores to improve motion efficiency, such as locomotion (Thorpe et al., 2013). Energy-storing tendons experience high stresses and strains as they stretch during loading, ready to recoil and return energy to the system (Shepherd et al., 2014). These tendons often operate with low safety factors and have a high propensity for injury, such as the Achilles tendon (Batson et al., 2003; Hamner, Seth, & Delp, 2010). Within the tendon, the angle and length of the crimp pattern depends on the type of tendon and sample site within the tendon, and can affect its mechanical properties; for example, fibers with a small crimp angle fail before those with a larger crimp angle (Wilmink, Wilson, & Goodship, 1992).

Several contributing factors may lead to tendon remodeling or degeneration. Repetitive sub-injury loading with recovery, as in exercise, can promote tendon remodeling, leading to long-term structural and functional improvements (Andarawis-Puri et al., 2015). Animal model research indicates physiological exercise leads to enhanced cell proliferation, particularly tendon-derived progenitor cells and collagen production (Zhang, Pan, Liu, & Wang, 2010). This process involves a net degradation of collagen that begins immediately after exercise, then shifts to a net synthesis (Magnusson, Langberg, & Kjaer, 2010). Conversely, several factors may shift healthy remodeling to degeneration. Lack of recovery (Zhang et al., 2010), smoking (Ristolainen, Kettunen, Waller, Heinonen, & Kujala, 2014), obesity (Gumina et al., 2014), and high cholesterol (Beason et al., 2014) all promote degeneration instead of positive remodeling. Age and sex have also been correlated with higher incidences of degeneration, with females and aging individuals both exhibiting decreased collagen synthesis rates (Magnusson et al., 2007; Yu et al., 2013). While these correlations exist, the specific mechanisms by which these factors alter the biological environment of the responding cells remain unknown.

When tendon is overused, injuries can occur. Tendon overuse injuries are collectively referred to as tendinopathies (Khan, Cook, Kannus, Maffuli, & Bonar, 2002). While tendinopathies affect millions of individuals in occupational and athletic settings (Almekinders & Temple, 1998), few studies examine non-traumatic, overuse tendon injuries. Tendon overuse is defined as a repetitive stretching of a tendon and results in the inability of the tendon to endure further tension (Josza & Kannus, 1997). While tendinopathy is likely caused by intrinsic and extrinsic factors in combination, excessive mechanical loading is considered a major causative factor (Kjaer, 2004; Riley, 2004). It is believed that small, repetitive strains below the failure threshold of the tendon cause tendon microdamage and subsequent tendon inflammation (Wang, 2006). The tendon-bone

junction (i.e. enthesis) is susceptible to tendon overuse injury, or enthesopathy. The insertion site of tendons becomes metabolically active, the extracellular matrix composition is altered, collagen bundles loosen, lipids accumulate, and microcalcification may occur (Jarvinen et al., 1997; Thomopoulos et al., 2002; Thomopoulos, Williams, Gimbel, Favata, & Soslowsky, 2003). Trauma or excessive loading causes inflammation in the paratenon, resulting in paratenonitis or peritendinitis, causing edema, swelling, hyperemia of the tenosynovium, lymphocyte infiltration, and proliferation of blood cells (Jarvinen et al., 1997).

Tendon repair following injury is not always successful, but is associated with several modulating factors. Pre-tendinosis stages tend to heal, but the biochemical and mechanical properties never return to the pre-injury state (Leadbetter, 1992). Injury to the osteotendinous junction leads to bone loss and impaired function due to the weak tendon-bone interface (Devkota & Weinhold, 2003). This type of injury takes a long time to heal, with findings showing inflammation remaining beyond 6 weeks post-injury, and often results in inferior mechanical properties (Boyer et al., 2003; St Pierre et al., 1995; Thomopoulos et al., 2002). Non-pharmaceutical therapies, such as controlled immobilization, physical therapy, stretching and non-steroidal anti-inflammatory drugs (NSAIDs) are frequently used to treat tendinopathy, but only provide symptomatic relief (Wang, 2006). As much of cuff deterioration is irreversible (Goutallier et al., 1994), surgical interventions are a common treatment escalation in large rotator cuff defects. A primary indicator of prolonged surgical success is the size of the initial rotator cuff injury size. Surgical repairs of ruptured tendons have re-tear rates of up to 35% and 94% for small and large rotator cuff tears, respectively (Bishop et al., 2006; Galatz, Ball, Teefey, Middleton, & Yamaguchi, 2004). Differences between techniques chosen by individual surgeons can impact outcomes. Arthroscopic rotator cuff repairs have decreased biomechanical strength compared to open repairs,

despite good clinical results (Schneeberger, von Roll, Kalberer, Jacob, & Gerber, 2002). Repair integrity of the rotator cuff after open and mini-open techniques as assessed by MRI or ultrasound show more consistent results (Gerber, Fuchs, & Hodler, 2000; Harryman II et al., 1991; Liu & Baker, 1994), but are associated with increased post-surgical pain and discomfort (Bishop et al., 2006). Advanced patient age, large tear size, severe muscle atrophy and fatty infiltration, systemic diseases, and smoking are associated with surgical repair failure (Montgomery, Petrigliano, & Gamradt, 2012). Many studied treatments have led to mixed outcomes, likely due to differences in tendons, animals, and time course of evaluation between studies.

2.3.1 The Supraspinatus Tendon

The histology of the supraspinatus tendon has been examined in detail. Codman noted that transverse fibers existed on the upper portion of the tendon, and that "the insertion of the infraspinatus overlaps that of the supraspinatus to some extent. Each of the other tendons also interlaces its fibers to some extent with its neighbour's tendons." (Codman, 1934). The supraspinatus tendon splays out and interweaves with the infraspinatus tendon to form a common continuous insertion on the humerus (Clark, 1988; Clark & Harryman II, 1992; Clark, Sidles, & Matsen III, 1990). Blood vessels are present throughout the tendons, with no avascular regions (Clark, 1988; Clark & Harryman II, 1992; Clark et al., 1990). The supraspinatus attachment to the greater tuberosity can be divided into four zones: the tendon itself, uncalcified fibrocartilage, calcified fibrocartilage, and bone (Benjamin, Evans, & Copp, 1986). Blood vessels appear in three of the four zones, while the uncalcified fibrocartilage appears to be avascular (Benjamin et al., 1986). A tidemark is present between the calcified and uncalcified cartilage, similar to articular cartilage (Benjamin et al., 2002). The collagen often meets these tidemarks at approximately right angles (Benjamin et al., 2002). The tendon of the supraspinatus has sharp changes in fiber angles

just before the region of fibrocartilage, and only a slight change in angle within the fibrocartilagenous region (Benjamin et al., 1986). This is likely due to angle changes between the humerus and tendon during shoulder movement. While the muscle belly of the supraspinatus remains parallel to the scapular spine during motion, the tendon bends to reach its insertion on the humerus. This bending appears to take place above the fibrocartilage, so the collagen fibers meet the tidemark at right angles. The fibrocartilage generates a transitional region between the hard and soft tissues, protecting the fibers from sharp angulation at the bone-tendon interface (Benjamin et al., 2002).

Differences exist between the anterior and posterior supraspinatus tendon. Initial MRI examinations indicated a "fibrous frame" of tendon within the anterior region, while no such structure existed in the posterior region; additionally, the anterior tendon was described to be thicker and more robust compared to a small, short posterior tendon (Gagey, Gagey, Bastian, & Lassau, 1990; Gagey et al., 1995). Similar findings exist through MRI and anatomic correlations (Thomazeau, Duval, Darnault, & Dreano, 1996; Vahlensieck et al., 1994), sonography (Turrin & Cappello, 1997) and cadaveric dissection (Minagawa et al., 1996). An in-depth examination of supraspinatus cross-sections observed average PCSA of the anterior and posterior supraspinatus of $140 \pm 43 mm^2$ and $62 \pm 25 mm^2$, respectively; while their tendon cross sectional areas were $26.4 \pm 11.3 mm^2$ and $31.2 \pm 10.1 mm^2$ (Roh et al., 2000). These resulted in anterior-posterior ratios of 2.45 ± 0.82 for muscle and 0.87 ± 0.30 for tendon (Roh et al., 2000). These data suggest that the larger anterior region pulls through a smaller tendon area, and that anterior tendon stress near or at the osteotendinous junction can be greater than posterior tendon stress. This may be a reason for the increased thickness observed in the anterior tendon (Gagey et al., 1995; Gagey et al., 1990). While it is likely that tensile load is shared due to the interweaving fiber arrangement of the middle

region of the tendon (Clark & Harryman II, 1992; Nakajima & Fukuda, 1993), this may be an intrinsic risk factor for rotator cuff defects. Examinations of the shoulder, particularly the supraspinatus, should take into account its unique anatomy in biomechanical models and mechanical testing.

2.4 Experimental Techniques to Examine Tendon Mechanical Responses

Despite essential progress of research in the field, the factors and mechanisms that define the effect of loading as "healthy" versus overuse for particular tendons is largely unknown. Various methods have been used to determine mechanical properties of human and animal tissue, and have been outlined below.

2.4.1 Mechanical Testing and the Shoulder

In vitro testing can distinguish the mechanical behaviour of tissues to exposures. In experimental studies, it is important to distinguish between structural properties and material properties. Structural properties are derived from tests of entire structures, while material properties are determined from isolated tissue (Quapp & Weiss, 1998). Material properties tests do not describe the strength of insertion sites, but can provide information such as the tensile strength, ultimate strain and the shape of the stress-strain curve (Weiss & Gardiner, 2001). Depending on the specific goals, a variety of tests may be performed, such as uniaxial tensile testing (Gardiner, Cordaro, & Weiss, 2000; Quapp & Weiss, 1998; Weiss, 1994), biaxial tension (Kuznetsov, Pankow, Peteres, & Huang, 2019), or shear (Gardiner & Weiss, 2001). These testing configurations can be used to perform testing at a fixed strain rate, assess effects of cyclic loading, or examine viscoelastic creep or stress relaxation (Hughes, Kirby, Sikoryn, Apsden, & Cox, 1990; Kwan, Lin, & Woo, 1993; Yahia & Drouin, 1990). Typically, the elastic and viscoelastic properties

of soft tissues are determined using uniaxial tensile testing (Peltz, Perry, Getz, & Soslowsky, 2009). At present, little or no research exists that examines combination loading on tendon, such as simultaneous tension and torsion.

Mechanical testing using human tissue has been completed previously, but its feasibility is limited. For the shoulder, it would be extremely difficult to insert transducers for mechanical testing *in vivo*, as the tendons of the rotator cuff lie under more superficial muscles. Regions of tendon can be taken for tissue sampling (Fang & Lake, 2016), where various mechanical and histochemical tests can be completed. Some *in vivo* tendon force measurement methods do exist, but are used infrequently. A direct *in vivo* measurement system using a buckle transducer was published in 1990 (An, Berglund, Cooney, Chao, & Kovacevic, 1990), but this method focused on its potential use for the Achilles tendon, a region that does not possess the structural obstacles extant at the shoulder. In order to further understand rotator cuff exposure responses, researchers are often required to use means outside of human tissue testing.

An alternate method for examination of changes in tissue mechanical responses involves animal models, either *in vivo* or *in vitro*. Inherent limitations such as the feasibility of obtaining an adequate number of specimens, accessibility or ethical restrictions may prevent *in vivo* human or cadaveric testing, making an appropriate animal model important (Matsen III et al., 1992). Sheep infraspinatus has been used as a model for human supraspinatus tendon due to its interspecies similarity in size and anatomy (Andarawis-Puri, Ricchetti, & Soslowsky, 2009; Frisch, Marcu, Baer, Thelen, & Vanderby, 2014). However, it has been suggested that smaller mammals (such as mice, rats and dogs) provide a better representation of muscle architectural parameters than larger mammals such as sheep or cows due to their similarity in force production versus velocity trade-off and excursion ability, which are represented by fiber length-to-moment arm ratio and fiber

length-to-muscle length ratio, respectively (Mathewson, Kwan, Eng, Lieber, & Ward, 2014). The rat bony architecture emulates humans, and is considered to be the most appropriate animal model for human rotator cuff tendon pathology research (Soslowsky, Carpmenter, DeBano, Banerji, & Moalli, 1996). Other than some non-human primates, the rat is the only current animal model that possesses a supraspinatus tendon that passes below the coracoacromial arch, analogous to humans (Voleti, Buckley, & Soslowsky, 2012). Damage accumulation at the micro- and macroscale levels of the rat supraspinatus tendon has been achieved through mechanical testing and histology examinations, and coincided with those seen in human tendinopathies, providing evidence for a link between overuse and chronic supraspinatus injury (Soslowsky et al., 2000). The rat model has also been used to assess the efficacy of rotator cuff surgical repair techniques (Gimbel, Mehta, van Kleunen, Williams, & Soslowsky, 2004; Gimbel, van Kleunen, Williams, Thomopoulos, & Soslowsky, 2007; Thomopoulos et al., 2003), healing through administration of therapeutic agents (Bedi et al., 2010; Gulotta, Kovacevic, Packer, Deng, & Rodeo, 2011; Kovacevic et al., 2011; Rodeo et al., 2007), and fatigue loading *in vivo* (Andarawis-Puri & Flatow, 2011; Fung, Sereysky, et al., 2010; Fung, Wang, et al., 2010; Fung et al., 2008; Sun et al., 2008). These studies demonstrate the utility of the rat model for development and testing of research strategies surrounding rotator cuff pathology.

2.4.2 Imaging

Numerous imaging methods exist for examining histological changes in tissue. High-magnification optical microscopy has been used to examine crimp re-alignment following mechanical testing (Miller, Connizzo, Feeney, & Soslowsky, 2012; Miller, Connizzo, Feeney, Tucker, et al., 2012), and found decreased collagen fiber re-alignment, decreased crimp frequency and other mechanical properties from increasing preconditioning cycles. Another typical

visualization method for tendon examinations is polarized light microscopy (Rigby et al., 1959), a contrast enhancing-technique that has a high degree of sensitivity. This method has been used numerous times, often for ensuring alignment and examining crimp frequency (Lake, Miller, Elliott, & Soslowsky, 2009; Miller, Edelstein, Connizzo, & Soslowsky, 2012). However, other imaging methods including electron microscopy (Dlugosz, Gathercole, & Keller, 1978), optical coherence tomography (Hansen et al., 2002) and second-harmonic generation microscopy (Houssen, Gusachenko, Schanne-Klein, & Allain, 2011) have also been used to examine tendon. The imaging techniques used in these aforementioned studies may be costly, time consuming, or destructive to the tissue, precluding their widespread adoption (Fung, Sereysky, et al., 2010; Fung, Wang, et al., 2010; Thorpe, Riley, Birch, Clegg, & Screen, 2014). Finally, template matching algorithms have been used on high resolution images to describe localised tissue responses. This method involves the use of virtual source points in a user-definable region of interest, generating points that can be tracked on successive images captured during testing using a template matching algorithm (Horst & Veldhuis, 2008). This algorithm relies on naturally occurring changes in surface texture to track points on a tissue sample, but can be assisted through the use of contrast generating materials distributed over the surface of the specimen (Eilaghi, Flanagan, Brodland, & Ethier, 2009; Karakolis & Callaghan, 2014). This method has been effective in examining localised strain distributions in animal tissue, and can provide meaningful observations in reasonable processing times without destroying the tissue of interest.

2.4.3 Stress

Strong correlations have been observed between decreases in mechanical properties and increased supraspinatus tissue degeneration. Degenerative changes at the supraspinatus tendon insertion reduce the tensile strength of the tendon and constitute a primary pathogenic factor of

rotator cuff tear (Sano et al., 1997). Examinations of biomechanical properties using failure testing in rats with healthy or defective rotator cuffs observed significantly lower peak stress values at failure in defective shoulders (Kurdziel et al., 2019). The majority of tensile tendon testing involves loading to failure (Gimbel, Kleunen, et al., 2004; Reuther et al., 2015; Soslowsky et al., 2000; Tucker et al., 2016). However, failure testing provides little information about physiologically relevant exposures emulative of daily scenarios.

2.4.4 Hysteresis

Although some elastic energy can be stored in the tendon as stretch during a movement or postural perturbation, energy is also dissipated, the quantity of which is governed by hysteresis. This energy loss needs to be reinvested through muscle work, affecting the energetic cost. Hysteresis is defined as the differences between the area enclosed by the loading and unloading phases of the stress-strain curve, and is used to help describe the viscoeleastic properties of a tissue, changes have been used to denote differences in tissues between testing groups. Hysteresis has been used as a metric to denote differences in energy transfer capability between rat sexes in Achilles tendon research (Pardes et al., 2016) as well as comparisons between muscle groups (Gajdosik, Vander Linden, McNair, WIlliams, & Riggin, 2004). Examinations of hysteresis have often focused on changes in this energy absorption before and after a loading protocol. Examining hysteresis throughout a loading protocol has been completed in mouse patellar tendon (Freedman, Zuskov, Sarver, Buckley, & Soslowsky, 2015); this study observed a steep decrease in hysteresis within the first 25 cycles, then a slow decrease in hysteresis across the next 1000 cycles. Examining hysteresis across cycles with differing load intensities and elevation angles can provide insight into viscoelastic changes across these scenarios.

2.4.5 Stiffness

Tissue stiffness is a common metric examined in mechanical testing, particularly throughout a loading protocol. Materially, stiffness is defined as the length change evoked by a force of a given magnitude, as determined by the differences in force divided by the change in length. Material stiffness directly influences the force needed to stretch it, which in turn affects the metabolic (energy) cost of both movement and postural control (Blazevich, 2019). Stress-strain plots on linear axes can be used to directly determine stiffness (Gosline et al., 2002). Within the tendon, the collagen fibril structures along the length of the tendon stretch as the tendon is loaded. These fibrils provide tissues with extensibility at low stiffness by virtue of their crimp structure (Broom, 1978; Viidik, 1972) , allowing lengthening of the tissue. The cross-linking between these collagen molecules gives fibrils high tensile strength at higher extensions (Haut, 1985; Opsahl et al., 1982), allowing protection against hyperextension. These fibrils are capable of absorbing high strain energies, with energy absorptions ten times greater than steel wire by weight (Bhonsle & van Karsen, 1992; Shen, Dodge, Khan, Ballarini, & Eppell, 2010). This prevents the brittle fracture of overloaded tissues, instead generating subrupture events such as sprains and strains (Veres & Lee, 2012). Structurally, repeated overload cycles results in an increasing serial density of kinks along the length of the fibril (Veres, Harrison, & Lee, 2013b, 2013a; Veres & Lee, 2012). These kinks have been described as a mechanism that may toughen the collagen at a basic level by absorbing overload through sacrificial destruction (Baldwin, Kreplak, & Lee, 2016). The mechanical properties of these kinks have been modeled as a high density core surrounded by a low density shell (Baldwin et al., 2016). Alterations in tendon stiffness have been noted to be a marker of material alterations within the tendon and could be used as a marker for accumulation of fatigue damage (Freedman et al., 2015; Fung et al., 2008).

Stiffness is an important metric for the rotator cuff, and is used to examine pathology risk. Stiffness has been described in a kinesiology perspective both in terms of a material stiffness in surgical scenarios, as well as patient descriptions of their feelings surrounding a motion. For the purposes of this work, only material stiffness will be considered. Clinical examinations have observed increased rotator cuff tendon stiffness in individuals with pathologies in these tissues. Increases in tendon stiffness have been described as an early change in rotator cuff tendinopathy (Vasishta, Kelkar, Joshi, & Hapse, 2019). Hersche and Gerber (1998) reported increased passive tension and stiffness within the supraspinatus tendon following chronic tendon rupture using stepwise elongation and observing the tension force; passive stiffness was increased by 100% in comparison to individuals with no retraction. The authors posited that this increase in passive stiffness related to decreased capacity for generating muscle tension, and their clinical testing (which included manual and isokinetic testing) support these conclusions. Examinations of the supraspinatus tendon using shear-wave ultrasound elastography observed increased supraspinatus and infraspinatus tendon stiffness in individuals with adhesive capsulitis of the shoulder compared to healthy individuals, regardless of aging (Yun et al., 2019).

Rotator cuff repair uses stiffness as one of its metrics of surgical success. When completing rotator cuff repair surgically, passive stiffness of the tendon in the repair should be minimized and care should be taken to maximize repair strength through technical means (Burkhart, Johnson, Wirth, & Athanasiou, 1997). Davidson & Rivenburgh (2000) examined rotator cuff tendon passive stiffness at pre-operative and at 3, 6, 12 and 24-months post-operatively; increased repair stiffness was correlated with worse postoperative Constant scores (a metric associated with the ability to carry out normal daily activities (Constant & Murley, 1987)), decreased perceived improvement, decreased isokinetic strength, and increased pain. Increased tendon stiffness following

arthroscopic rotator cuff repair has been widely regarded as a factor associated with poor clinical outcomes (Brislin, Field, & Savoie III, 2007; Charousset et al., 2008; Huberty et al., 2009; Namdari & Green, 2010; Tauro, 2006). Rotator cuff repairs continue to be focused on minimizing post-operative stiffness to allow patients to maximize quality of life after surgery.

2.5 Summary

Research surrounding the rotator cuff is extensive, but critical knowledge gaps persist. Previous work has examined shoulder motion and the rotator cuff in both healthy and pathologic states, but minimal robust evidence exists for describing scenarios that increase the likelihood of transitioning from intact to compromised tissue states. New research surrounding regional differences in supraspinatus architecture provides novel insight into the rotator cuff (Kim et al., 2007; Kim, Ko, Dickerson, & Collins, 2017), but only a small amount of research exists surrounding these anterior and posterior regions and their implications for rotator cuff function. Improved data on regional differences, particularly in regional activations during a multitude of posture and work scenarios could highlight scenarios that predispose individuals to potentially harmful exposures. Tissue mechanics studies have quantified some tendon exposure tolerances (Ahmadzadeh, Connizzo, Freedman, Soslowsky, & Shenoy, 2013; Bey, Song, Wehrli, & Soslowsky, 2002), but mechanical tests are primarily loaded to specific strain percentages, which may not reflect tendon loading *in vivo*. It is unlikely that the complex *in vivo* supraspinatus tendon loading maintains an identical force vector throughout the range of motion of the shoulder, and work in this area needs to evolve with the goal of generating exposures that best reflect physiological *in vivo* loading. This thesis aimed to extend knowledge in each of these areas, and establish foundational data sets to enable future exploration of supraspinatus tendinopathy.

CHAPTER III – *IN VIVO* EXAMINATION OF REGIONAL SUPRASPINATUS ACTIVATION THROUGHOUT THE UPPER EXTREMITY RANGE OF MOTION

Published as: Cudlip AC, Dickerson CR. (2018) Regional activation of anterior and posterior supraspinatus differs by plane of elevation, hand load and elevation angle. Journal of Electromyography and Kinesiology, 43, 14-20.

Abstract

The supraspinatus is one of the muscles of the rotator cuff, and growing research on fibre type composition and mechanical advantages in specific postures suggest this muscle may have distinct anterior and posterior regions. Activation differences between these regions may identify important functional differences. This research quantified muscular activation of these regions throughout a range of motion with differing hand loads. Forty participants completed paced humeral elevations in 7 planes of elevation (0/15/30/40/60/75/90°) using 3 hand loads (unloaded arm/20%/40% maximal elevation force output). Indwelling electromyography collected muscle activity of the anterior and posterior supraspinatus. Hand load and elevation angle interacted to affect activity of the anterior supraspinatus in most planes of elevation - by up to 41 %MVC ($p<0.01$), but in few planes for the posterior region. Plane of elevation influenced anterior and posterior region activation by up to 17 %MVC and 13 %MVC, respectively ($p<0.01$). Increasing hand loads increased activation in both regions ($p<0.01$), but more so for the anterior region. These differences may indicate differences in function between the two regions. The sustained activation in the smaller posterior supraspinatus may indicate this region as primarily a glenohumeral stabilizer, while the larger anterior region acts to achieve glenohumeral motion.

3.1 Introduction

The supraspinatus is one of the four muscular elements of the rotator cuff and the most common site of initial rotator cuff pathology. Each rotator cuff muscle originates from the scapula and inserts into the humerus; they collectively act to maintain glenohumeral stability while contributing to humeral movement. The supraspinatus assists in abduction and external rotation of the shoulder (Malanga, Jenp, Growney, & An, 1996; Reinold et al., 2004), and is the component most associated with tendinopathies (Jobe & Moynes, 1982). The prevalence of partial- or full-thickness tears increases markedly after 40 years of age: research using 683 volunteers found 16.9% of asymptomatic volunteers had a rotator cuff tear, with prevalence rising from 6.7% from volunteers in their 30s to 45.8% of volunteers in their 60s (Wani, Abdulla, Habeebullah, & Kalogriantis, 2016). The shoulder represents the second most common site for allowed lost time claims behind the low back in 2015, with most shoulder claims relating to overexertion (WSIB, 2015).

Rotator cuff pathologies typically reduce upper extremity function, and often manifest as increased pain or decreased joint range of motion. Patients commonly present to clinicians due to perceived loss of shoulder comfort and function (van der Windt et al., 1995), and specific pathologies. Partial- and full thickness rotator cuff tears are the most common clinical shoulder presentations, and result in decreases in range of motion and strength for 30-50% and 40-60% of patients, respectively (Largacha et al., 2006). These changes can interfere with self-care ability and functional independence, particularly in older adults, decreasing quality of life (Harryman II et al., 1991; Lin, Weintraub, & Aragaki, 2008). Certain occupations are associated with rotator cuff pathology, including nursing, grocery clerking, warehousing, carpentry and painting (Luopajarvi et al., 1979).

The supraspinatus has a complex morphology that influences mechanical function. It consists of anterior and posterior regions, attaching to different sections of the supraspinatus tendon (Roh et al., 2000; Vahlensieck et al., 1994) (Figure 14). These regions have differing distributions of fibre types, with the middle portion of the anterior region having a higher proportion of Type I fibers than the posterior region (Kim et al., 2013). Musculotendinous architecture is an important determinant of muscle function (Lieber & Fridén, 2001). Cadaveric investigations have identified distinct regions of the supraspinatus with different mechanical functions depending on posture (Gates et al., 2010). However, as this work used cadaveric shoulders, it did not examine how these morphological differences influenced muscular activation patterns and potential consequent events.

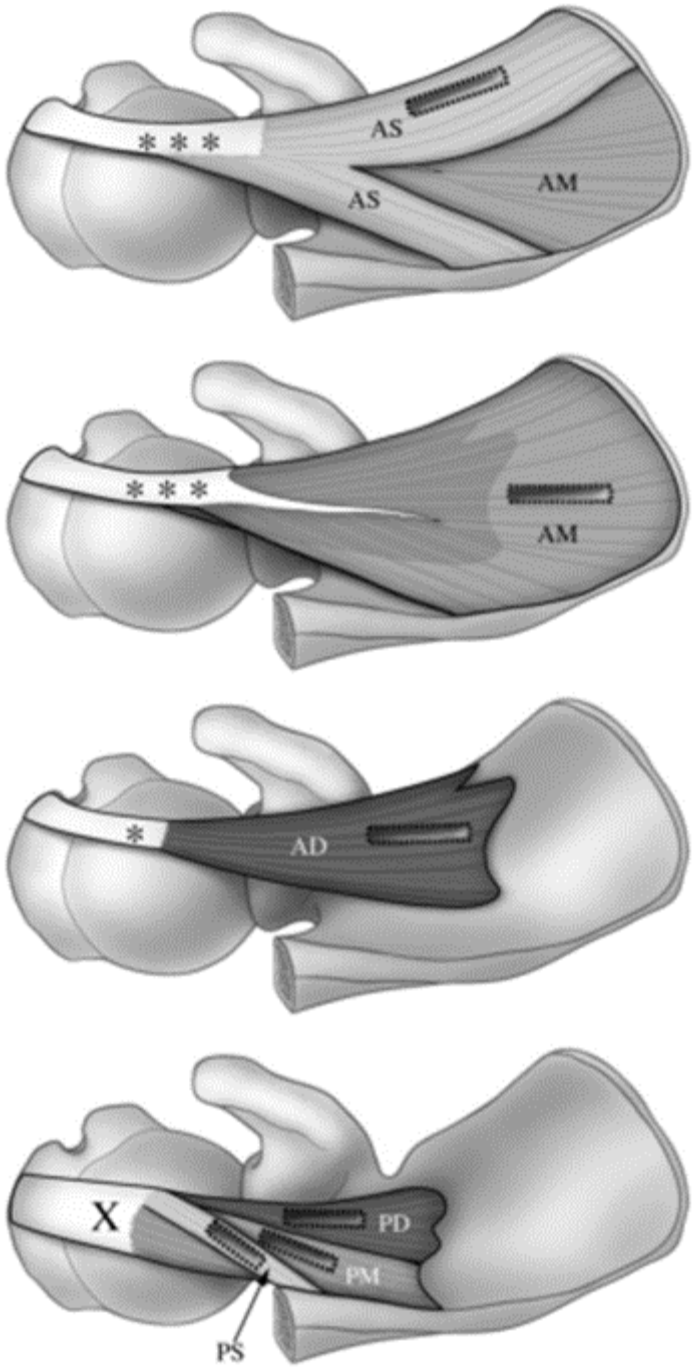

Figure 14. The superficial, middle and deep posterior supraspinatus (PS, PD, PM) lies deep to the superficial, middle and deep anterior region (AS, AM, AD), and has a smaller cross-sectional area but connects to a larger region of the tendon. The top image is the most superficial layer, with subsequent images indicating increasing depth. Adapted from Kim et al. (2010).

Differences in activation patterns within the supraspinatus are minimally described, but are crucial to injury pathogenesis. Previous research detailed differences in activation between the anterior and posterior regions as ratios in static arm postures of 30, 60 and 90º of humeral elevation in the scapular plane with a single hand load (Kim et al., 2016). When examining ratios of activation between these two regions in increasing abduction postures and between neutral and external rotation, these ratios shifted to increased relative posterior region activation with increasing abduction angle or increased external rotation, indicating that the posterior region may play a more pronounced role in postures with higher degrees of abduction and external rotation (Kim et al., 2017). To the author's knowledge, this is the only existing research to examine activation of the supraspinatus as separate regions during any humeral motion. Understanding of the interplay between the anterior and posterior regions is still in its infancy; development of normative posture-activation relationships will delineate the unexplored influence of postural differences and hand loads on concomitant anterior and posterior supraspinatus activations. Rotator cuff pathologies often affect the supraspinatus in initial stages, and often are paired with posterior region atrophy (Karas, Wang, Dhawan, & Cole, 2011; Kim et al., 2010, 2013). While research examining supraspinatus across a range of postures and tasks has been examined previously, quantification of the relative activations of both regions can help determine scenarios that increase activation and may increase future injury risk. This study quantified activation patterns of the anterior and posterior regions of the supraspinatus through different humeral ranges of motion and hand loads. Specific hypotheses were that regional activations would depend on both abduction angle and hand load, and that main effects of plane of elevation and hand load would be present in both supraspinatus regions.

3.2 Methods

This study employed electromyography (EMG) and motion capture on human participants. University-aged, right hand dominant individuals participated, and data collection occurred in one two-hour session. All participants were collected by the same researcher. Post-collection processing and analysis quantified differences between the two supraspinatus regions and activation patterns through humeral motion.

3.2.1 Participants

Forty right-handed participants [20 males – 25.0 ± 3.4 years, 1.78 ± 0.07m, 88.2 ± 13.2 kg; 20 females – 23.6 ± 3.9 years, 1.71 ± 0.07 m, 72.4 ± 12.1 kg] were recruited from a convenience sample. Exclusion criteria included self-reported upper limb or low back pain in the past 12 months, or allergies to rubbing alcohol and skin adhesives (Appendix A-E). This study was reviewed and received clearance through the institutional Office of Research Ethics.

Sample size was selected by conducting an *a priori* power analysis. This power analysis was completed using G*Power 3.1 (Universität Düsseldorf, Düsseldorf, Germany), and indicated that 32 participants was sufficient to obtain adequate power (Cohen, 1992; Faul, Erdfelder, & Lang, 2007) based on the primary outcomes of muscular activation in the anterior and posterior regions of supraspinatus. The effect size chosen (f^2 = 0.4) represented the lower range observed the in the literature for rotator cuff research, which has indicated variable effect sizes from 0.4-1.5 (Balke et al., 2013; Hughes et al., 2003; Tetreault, Krueger, Zurakowski, & Gerber, 2004).

3.2.2 Electromyography

EMG was collected from the supraspinatus using indwelling methods. Hypodermic needles, each containing two sterilized fine wire electrodes with barbed ends (Motion Lab Systems, Inc., Louisiana, USA) was inserted into the muscle belly of the anterior and posterior regions of the supraspinatus using previously published instructions (Kim et al., 2016) (Figure 15). Each indwelling electrode was guided throughout insertion using diagnostic ultrasound to ensure proper electrode placement. Ultrasound technique was used to determine the depth of these two regions, with the ultrasound probe placed laterally to the insertion site in order to track needle depth throughout the insertion. All EMG signals were sampled at 3000 Hz using a wireless telemetered system (Noraxon Telemyo 2400 T G2, Noraxon, Arizona, USA). Raw signals were band-pass filtered from 10-1000 Hz and differentially amplified with a common-mode rejection ratio >100 dB and an input impedance of 100 MΩ. Analog signals were converted to digital using a 16 bit A/D card with a ±3.5 V range.

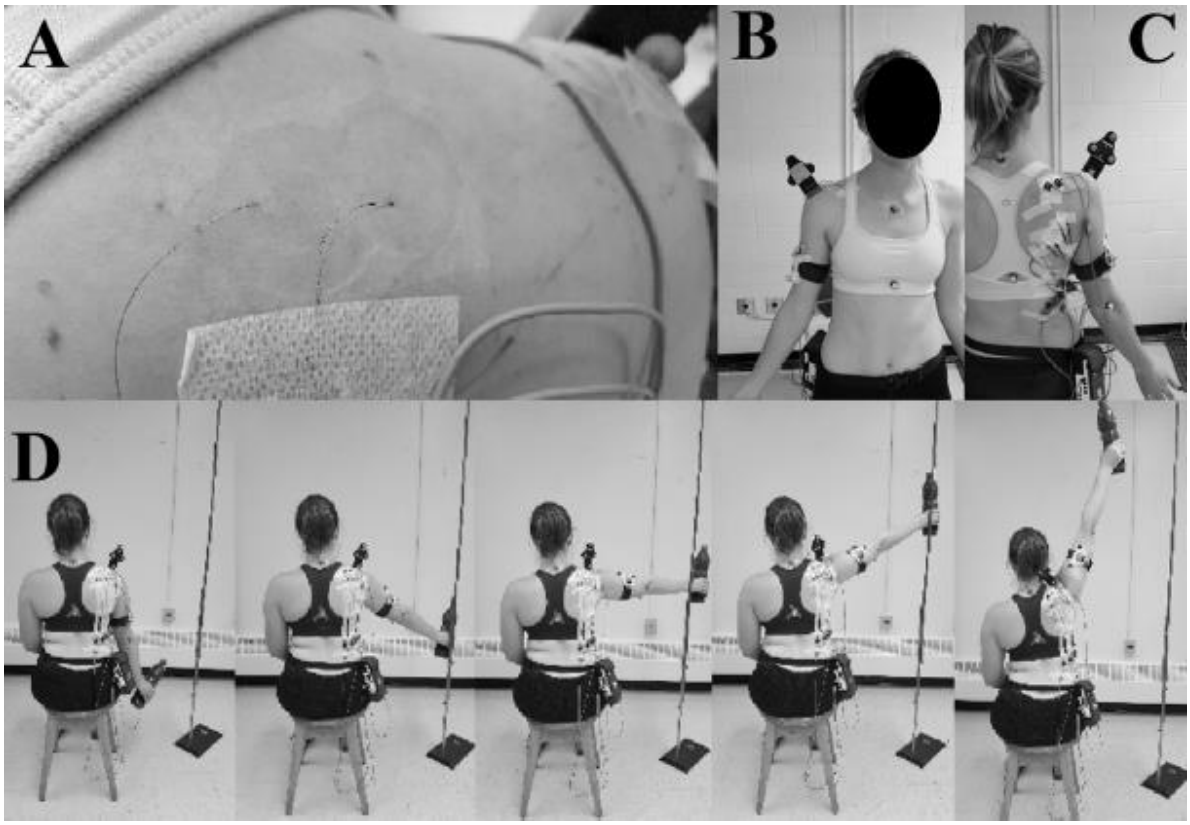

Figure 15. Experimental set-up. Two indwelling electrodes were placed into the anterior and posterior supraspinatus with ultrasound guidance (A). Motion capture markers were placed over bony landmarks of the torso and right upper extremity (B and C). Participants completed maximal arm elevations at a fixed cadence (2s to maximal elevation, 2s to return to zero elevation) in difference plane of elevation with differing hand loads. A guide rail was used to indicate plane of elevation for participants during experimental trials. Shown here is the ascending phase in the 40° plane of elevation with the 20% hand load (D).

3.2.3 Motion Capture

Three-dimensional motion was captured using thirteen VICON MX20 optoelectronic infrared cameras. These cameras tracked the position of reflective markers secured to the skin over anatomical landmarks. Three rigid clusters placed on the humerus, acromion and torso and 7 individual markers placed on the epicondyles of the right elbow, right acromion, suprasternal notch, xiphoid process, the 7^{th} cervical and 8^{th} thoracic vertebrae were tracked. Captured kinematic data was recorded with the VICON Nexus 1.8.5 software (VICON Motion Systems, Oxford, UK), and was sampled at 50 Hz. Following marker placement, calibration trials ensued. While the participant stood in the anatomical position, a stylus was used to palpate and record the position of the root of the scapular spine, the inferior angle, and the acromion angle (Grewal, Cudlip, & Dickerson, 2017). The relationship between the acromion cluster and these points allowed digital recreation of scapular orientation in post-processing.

3.2.4 Protocol

The protocol for each participant for each experimental session involved the sequential application of electromyography equipment, collection of maximal voluntary exertions, a 5-minute rest period, application of reflective markers for motion capture, then collection of experimental trials. Participants completed multiple repetitions of a maximal voluntary isometric exertion test under manual resistance. This maximal exertion is completed with the participant lying on their left side with their head resting on their left arm, with the right arm in 10° of abduction in the coronal plane. Participants were instructed to maximally abduct their arm, while a researcher prevented this motion by holding the participant's arm in place. This test was designed to elicit maximal activation from the supraspinatus, and was derived from the literature (Criswell, 2011). This is a standard posture for eliciting maximal supraspinatus electromyography recordings in

human testing (Cudlip et al., 2015; Maciukiewicz, Cudlip, Chopp-Hurley, & Dickerson, 2016; McDonald et al., 2014). This exertion was completed three times to improve reliability of the results (Fischer, Belbeck, & Dickerson, 2010). Exertions had a minimum of two minutes rest interposed (Chaffin, 1975). The highest post-processing electrical activity from these trials served as the reference to normalize subsequent electromyographic data for each respective supraspinatus region (Winter, 1991). These trials were filtered and processed using the same methods as experimental trials.

Following maximal voluntary isometric exertions, participants completed two maximal elevation force trials to establish individual hand force capacity by which to scale experimental hand loads. Participants sat in a backless chair identical to the one used in experimental trials, and raised their arm to 90° of humeral elevation in the frontal plane, with their thumb facing the ceiling. A hand dynamometer was placed on the wrist, and participants pushed upwards. Each trial lasted five seconds, and the maximal force from these two trials was used to determine the load of two bottles filled with lead shot representing 20% and 40% of this maximal force value.

Each experimental trial involved dynamic upper limb motion. Seven planes of elevation (0º/15º/30º/40º/60º/75º/90º) and three hand loads (unloaded/20%/40% of maximal elevation strength) were varied and each was completed twice, resulting in 42 testing scenarios. The shoulder elevation plane originated from the approximate glenohumeral joint centre. The 0º plane is humeral abduction, while the 90º plane coincides with humeral flexion. Planes of elevation were measured externally with a goniometer over the glenohumeral joint, coincident with the vertical y-axis of the thorax coordinate system (Wu et al., 2005). Humeral elevation angle was calculated with kinematic data after collection. Each participant had two seconds to raise their humerus to maximal humeral elevation starting from the anatomical position, then two seconds to return their arm to the starting

position while maintaining neutral humeral axial rotation. A metronome at 1 Hz was used to assist in this motion. A thin metal rail was placed just posterior to the current plane of elevation to act as a guide throughout the trial (Figure 15D). Participants were instructed to maintain contact with the metal rail throughout the arm elevation to ensure maintenance of plane of elevation. Two researchers (one seated behind the participant, one seated to the right of the participant) visually examined the motion of the participant to ensure participants stayed in the desired plane of elevation. If the participants did not maintain the desired plane of elevation, the trial was recollected. Participants were seated on a backless chair and experimental trials were completed in a randomized order.

3.2.5 Data Analysis

EMG was analysed with respect to amplitude. All signals were processed using custom MATLAB code (Matlab R2016, Mathworks Inc., Natick, MA). A high pass 4^{th} order Butterworth filter with a cut-off frequency of 30 Hz was applied to all signals in order to mitigate potential heart rate contamination (Drake & Callaghan, 2006). The signals were full-wave rectified and low-pass single pass filtered using a 2^{nd} order Butterworth filter with a 4 Hz cutoff frequency; this cutoff is commonly used for the low frequency motion of upper extremity musculature (Cudlip et al., 2015; Cudlip, Holmes, Callaghan, & Dickerson, 2018; Ho, Cudlip, Ribeiro, & Dickerson, 2019). Each trial was normalized to muscle specific maximum voluntary exertion data that were processed identically.

Kinematic analysis consisted of data filtering, marker reconstruction and local joint coordinate system construction, followed by conversion of marker data to joint center data and calculation of joint rotation sequences. All raw kinematic data was low pass filtered with a cut-off frequency of 6 Hz, and segment length and orthogonal coordinate systems were constructed using

ISB guidelines (Wu et al., 2005). Static scapular calibration trials were completed using the stylus to reconstruct the scapular coordinate system. Thoracohumeral rotations were calculated using ISB standards. These rotations used a Y-X-Y' sequence, representing plane of elevation, elevation angle, and humeral axial rotation (Wu et al., 2005).

3.2.6 Statistical Analysis

Statistical analysis focused on assessing activations of the anterior and posterior regions by posture. Normalized activation for both regions at seven thoracohumeral elevation angles (5/30/60/90/120/135/165°) in both the ascending and descending phases of motion were extracted for statistical analysis. A repeated measures ANOVA with 3 independent factors (plane of elevation, hand load, elevation angle) and each 2-way interaction examined muscle activity differences. Analyses were divided by phase of motion (ascending, descending). All statistical analyses were completed with JMP 14.0 software (SAS Institute, North Carolina, USA), with statistical significance considered at $\alpha = 0.05$. Initially males and females were separated into groups, but upon analysis no sex effects were observed, so these groups were placed together for analysis. Tukey HSD post-hoc analysis were conducted to identify levels of difference when warranted.

3.3 Results

Activation levels for both supraspinatus regions were influenced variously by hand load, plane of elevation and elevation angle. An interaction between hand load and elevation angle was observed in anterior supraspinatus during the ascending phase of movement in all planes but 30° ($p=0.01$-0.02), and in the descending phase of movement in the 0°, 15° and 40° planes of elevation ($p<0.01$ for each). The largest observed difference between elevation angles and loads occurred between the unloaded raise at 5° of elevation (4.7 +/- 3.2 %MVC) and the 40% load at 90° of

elevation in the 0° plane of elevation (46.1 +/- 6.1 %MVC), generating a 41.4 %MVC change (Figure 17, Appendix F). Interactions between hand load and abduction angle only affected posterior supraspinatus activation in the ascending phase in the 30° and 40° planes of elevation ($p=0.01$-0.02), and did not affect activation in any plane during the descending phase of movement. These activations included increases of 34.6 and 35.9 %MVC respectively with increased hand load, with activation peaking around 90° of elevation. While there was no statistically significant interaction between plane of elevation and hand load, both the anterior and posterior regions had near-significant differences in the descending phase of motion ($p = 0.05$-0.08), with higher activation in more sagittal planes and higher hand loads. There was no interaction effect on activation between plane of elevation and elevation angle ($p=0.13$-0.85).

Main effects of load, plane of elevation and abduction angle affected both regions of supraspinatus. These main effects altered activation at all planes of elevation in both phases of movement ($p<0.01$). Increasing hand loads resulted in increased muscle activation in both regions in all planes of elevation. In the anterior region, differences in loads altered muscle activation by up to 17 %MVC in the 0° plane during elevation, and by as little as 7 %MVC in the 90° plane during depression. The posterior region saw similar differences by hand load across planes, with the largest activation in the 0° plane during elevation (13.7 %MVC) and the smallest in the 75° plane (5.9 %MVC). Typically, differences between lighter loads and heavier loads were greater in planes closer to the sagittal plane. Plane of elevation affected both regions of supraspinatus ($p<0.01$), with more sagittal planes increasing supraspinatus activation (Figure 16). Differences in activation between planes increased when the load increased. Increasing humeral abduction increased muscular activation across all planes of elevation ($p<0.01$). Elevation angles of 60° and below always generated the lowest muscle activation, with elevation angles above 60° producing

increased activation, but activations at 90° and above were not always statistically different from one another. The largest range in activation was in the elevation phase of motion, of 30.7 %MVC in the anterior and 25.2 %MVC in the posterior region (30° plane of elevation, 5°-135°; 0° plane of elevation, 5° -165°, respectively) (Table 1).

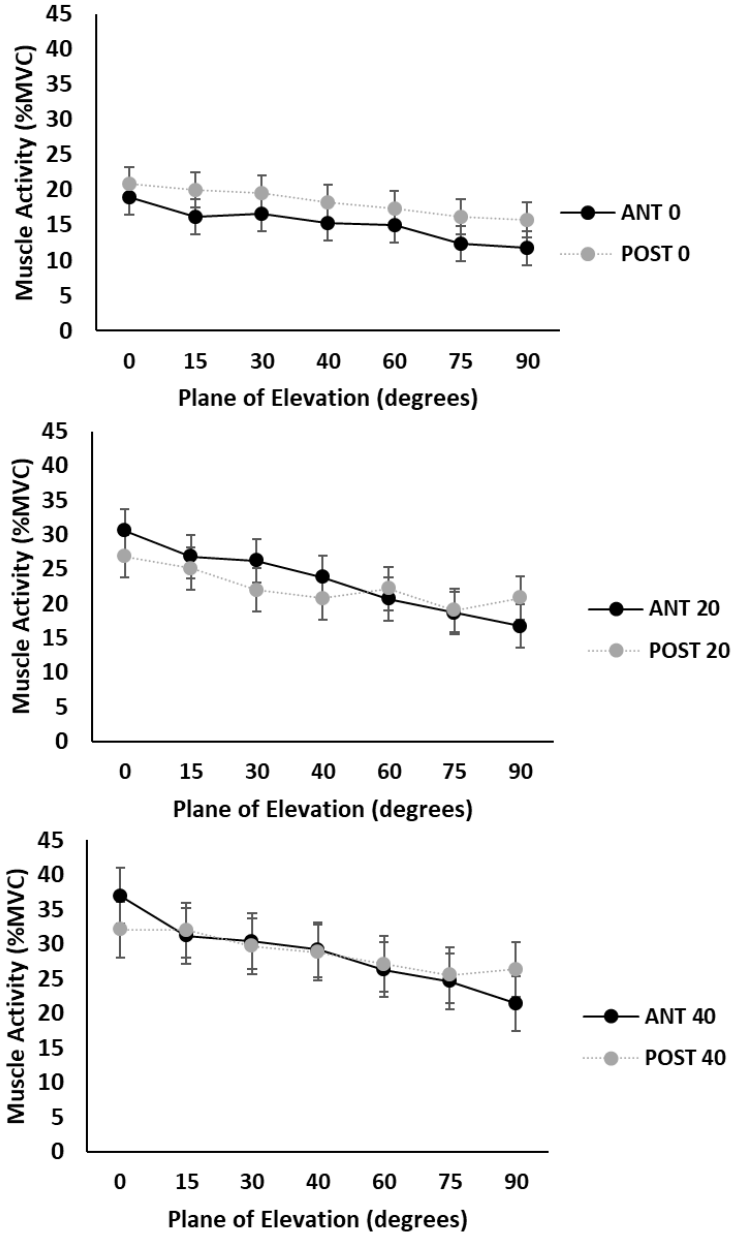

Figure 16. Differences in activation were observed in between supraspinatus regions across planes of elevation; activation decreased as the arm moved toward the sagittal plane.

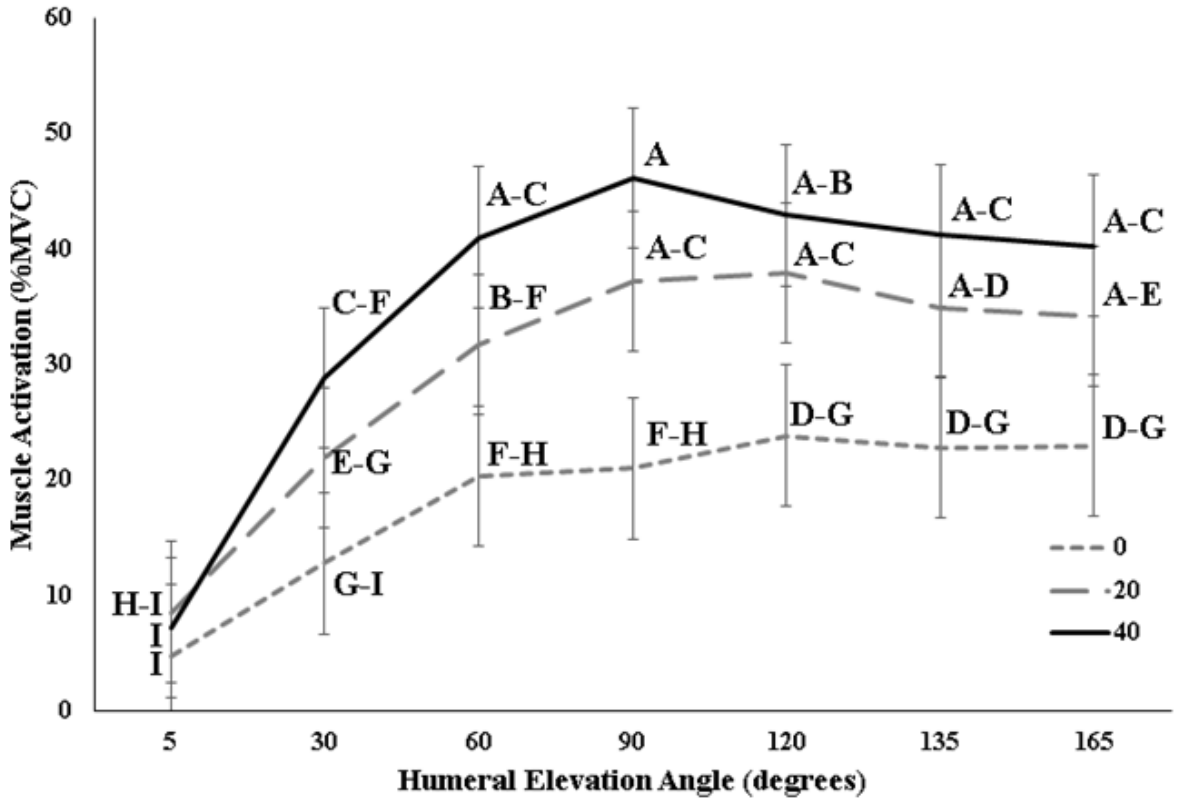

Figure 17. An interaction between load (unloaded/20%/40% of maximal elevation strength) and thoracohumeral elevation angle affected muscle activation. Shown above is the anterior supraspinatus in the 0° plane of elevation during the ascending phase of movement. Post-hoc differences are denoted by letters; points not sharing a letter are significantly different.

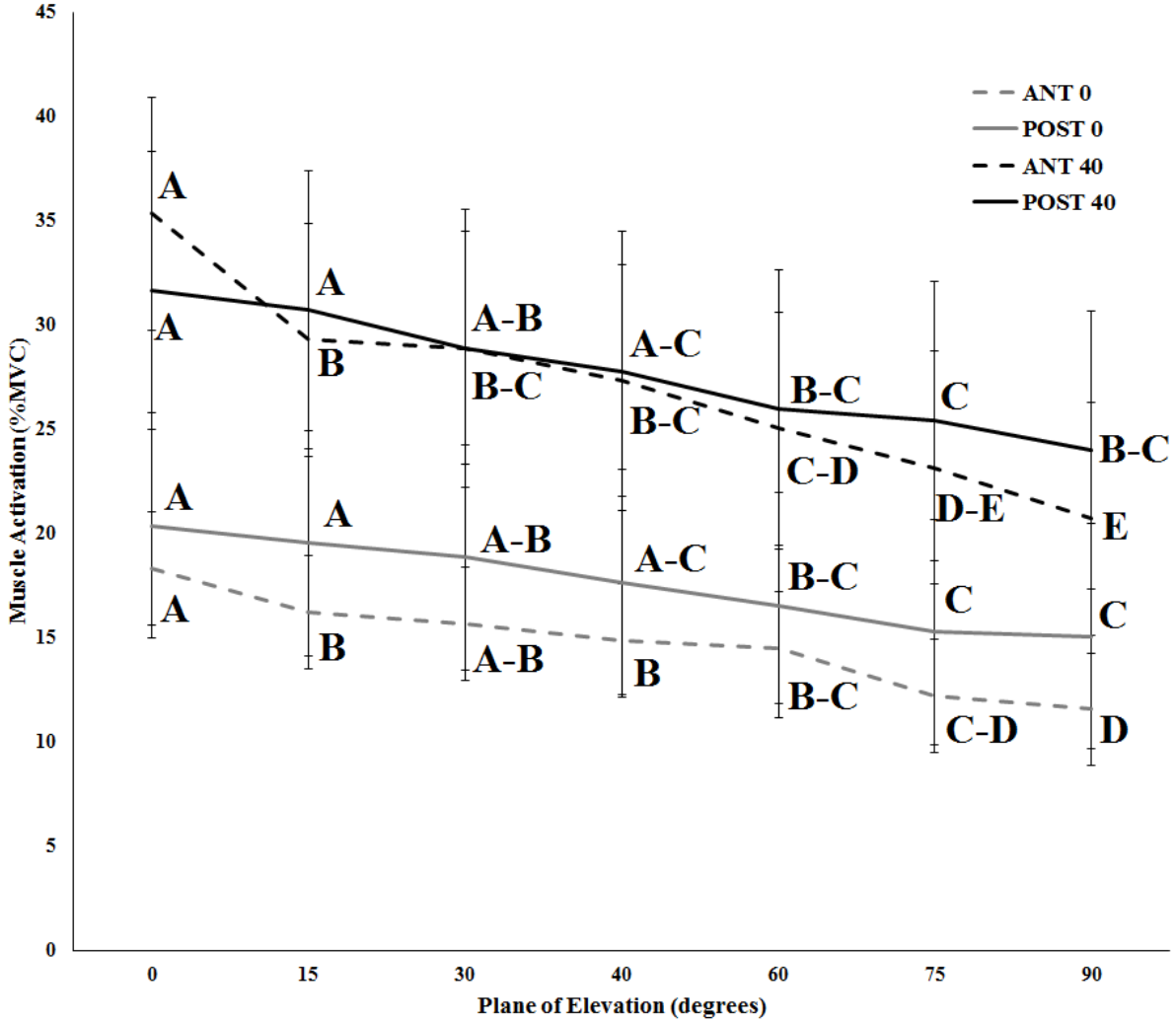

Figure 18. Normalized muscle activation of anterior (ANT) and posterior (POST) supraspinatus across loads (unloaded/40% maximal elevation strength) in ascending motion. Plane of elevation affected muscle activation, with more sagittal planes increasing activation in ascending motion. Post-hoc differences within muscle and load are denoted by letters; points within a load not sharing a letter are significantly different.

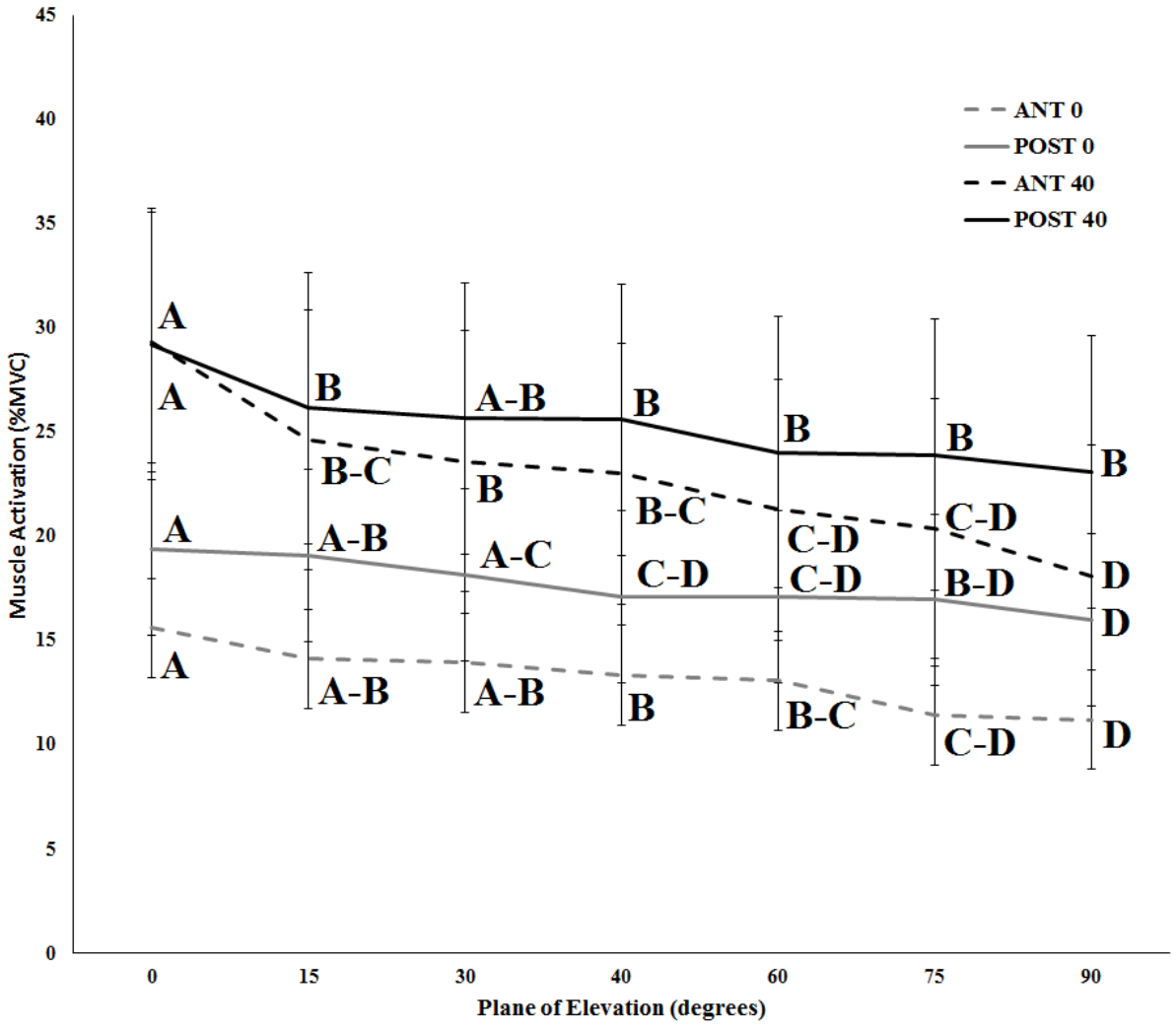

Figure 19. Normalized muscle activation of anterior (ANT) and posterior (POST) supraspinatus across loads (unloaded/40% maximal elevation strength) in descending motion. Plane of elevation affected muscle activation, with more sagittal planes increasing activation in descending motion. Post-hoc differences within muscle and load are denoted by letters; points within a load not sharing a letter are significantly different.

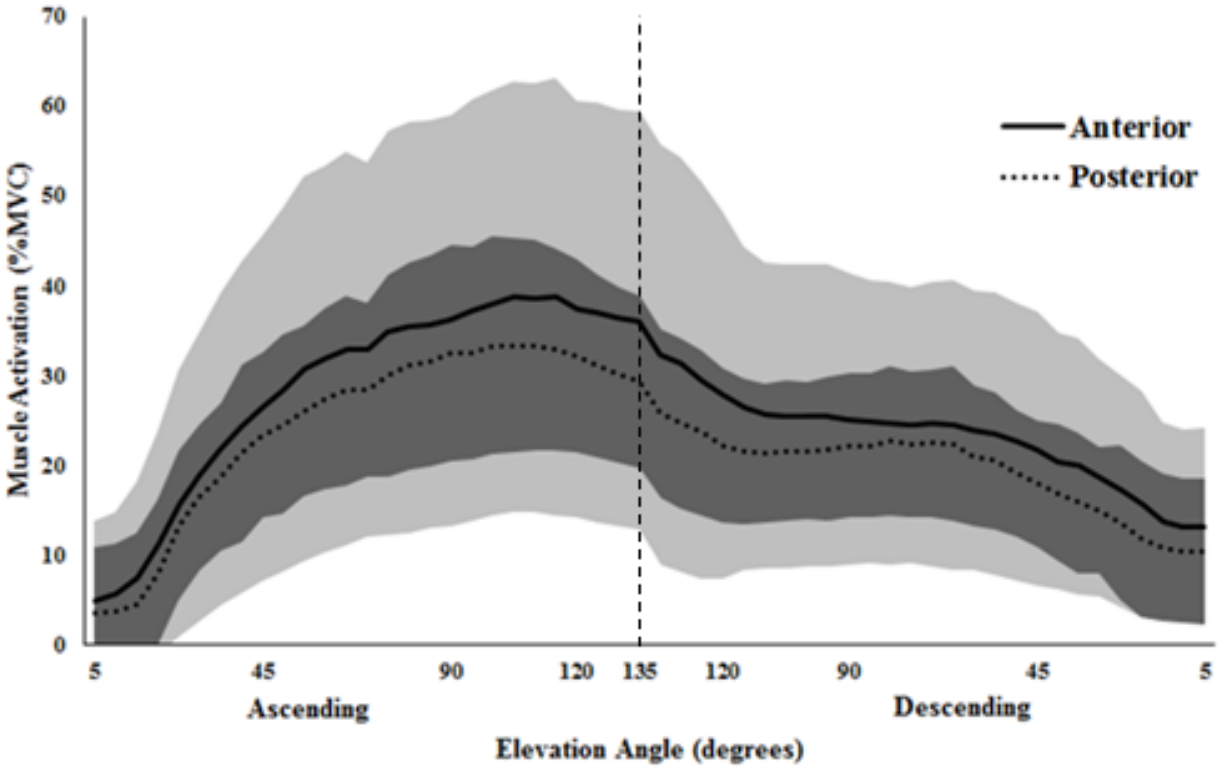

Figure 20. Means and standard deviations for the anterior and posterior supraspinatus throughout elevation angles. Standard deviations for the anterior region are in light grey, while standard deviations for the posterior region are in dark grey. The vertical dashed line represents moving from humeral elevation to depression.

Table 1. Statistical results for normalized activation (%MVE) of anterior and posterior supraspinatus by plane of elevation and elevation angle. Significant differences by plane are denoted by letters; values not sharing a letter are significantly different.

Phase of Movement	Muscle Region	Plane of Elevation	Elevation Angle (°)						
			5	30	60	90	120	135	165
Ascending	Anterior	0	6.7 (C)	21.1 (B)	30.9 (A)	34.7 (A)	34.8 (A)	32.9 (A)	32.4 (A)
		15	4.3 (C)	15.9 (B)	26.6 (A)	29.8 (A)	32.0 (A)	28.5 (A)	27.7 (A)
		30	3.6 (C)	13.8 (B-C)	24.9 (A-B)	28.2 (A-B)	29.1 (A-B)	34.3 (A)	33.7 (A)
		40	3.9 (C)	12.2 (B)	23.8 (A)	28.0 (A)	28.7 (A)	27.7 (A)	26.9 (A)
		60	4.5 (D)	10.4 (C)	20.8 (B)	27.5 (A)	27.1 (A)	24.3 (A-B)	24.0 (A-B)
		75	3.3 (D)	8.3 (C)	18.4 (B)	25.1 (A)	24.5 (A)	21.9 (A-B)	21.4 (A-B)
		90	3.6 (C)	7.5 (C)	15.1 (B)	20.8 (A)	23.3 (A)	21.6 (A)	21.3 (A)
	Posterior	0	7.6 (C)	20.1 (B)	28.6 (A)	30.1 (A)	32.8 (A)	32.5 (A)	32.8 (A)
		15	7.0 (C)	18.9 (B)	29.3 (A)	31.4 (A)	29.7 (A)	29.2 (A)	27.7 (A)
		30	5.6 (C)	16.6 (B)	26.8 (A)	28.3 (A)	27.8 (A)	27.7 (A)	27.1 (A)
		40	6.4 (C)	14.2 (B)	24.8 (A)	27.6 (A)	27.7 (A)	25.6 (A)	24.7 (A)
		60	7.4 (C)	13.5 (B)	25.1 (A)	27.6 (A)	25.2 (A)	25.0 (A)	24.6 (A)
		75	4.8 (C)	11.1 (B)	22.6 (A)	26.5 (A)	23.8 (A)	22.2 (A)	22.0 (A)
		90	7.1 (C)	14.3 (B)	23.3 (A)	26.2 (A)	24.7 (A)	24.1 (A)	23.6 (A)
Descending	Anterior	0	11.1 (D)	13.0 (D)	21.2 (C)	23.6 (B-C)	27.0 (A-B)	31.4 (A)	31.5 (A)
		15	9.8 (C)	13.1 (C)	18.6 (B)	18.8 (B)	24.8 (A)	26.4 (A)	26.6 (A)
		30	10.5 (B)	12.5 (B)	17.8 (A-B)	19.1 (A-B)	22.1 (A-B)	32.5 (A)	32.6 (A)
		40	9.2 (E)	12.7 (D-E)	17.0 (C-D)	19.4 (B-C)	21.9 (A-B)	26.0 (A)	26.1 (A)
		60	8.9 (D)	11.1 (D)	15.7 (C)	17.5 (C)	19.2 (B-C)	23.3 (A-B)	23.6 (A)
		75	9.2 (D)	10.7 (C-D)	14.6 (B-C)	17.2 (A-B)	18.1 (A-B)	20.3 (A)	20.5 (A)
		90	8.0 (D)	9.1 (D)	13.2 (C)	14.9 (B-C)	17.8 (A-B)	20.5 (A)	20.6 (A)
	Posterior	0	16.2 (C)	21.5 (B-C)	22.9 (B)	24.7 (A-B)	26.4 (A-B)	29.6 (A)	30.3 (A)
		15	15.1 (C)	18.0 (C)	23.1 (B)	22.7 (B)	23.3 (A-B)	26.7 (A-B)	27.2 (A)
		30	15.5 (D)	18.3 (C-D)	21.0 (B-C)	22.2 (B)	23.0 (A-B)	26.1 (A)	26.4 (A)
		40	14.9 (B)	17.5 (B)	21.5 (A)	22.6 (A)	23.0 (A)	23.8 (A)	24.3 (A)
		60	16.1 (C)	17.4 (B-C)	20.6 (A-B)	22.5 (A)	20.7 (A-B)	23.4 (A)	24.2 (A)
		75	15.2 (C)	17.1 (B-C)	20.9 (A)	19.3 (A-B)	20.4 (A)	21.7 (A)	21.8 (A)
		90	15.4 (C)	17.2 (B-C)	19.3 (A-C)	21.9 (A)	20.8 (A-B)	22.7 (A)	22.7 (A)

3.4 Discussion

The focus of this research was to examine regional activation changes in the anterior and posterior supraspinatus during arm elevations while altering planes of elevation and hand loads. Several activation differences within both supraspinatus regions were associated with altering these factors. Interactions between hand load and elevation angle existed, as well as main effects of hand load, plane of elevation and abduction angle on both anterior and posterior supraspinatus activation. These activation differences occurred across the range of motion, but influenced the anterior and posterior regions differently.

The anterior and posterior supraspinatus had activation differences throughout the range of motion that were likely due to functional differences between these regions. Mounting evidence suggests that the anterior and posterior regions of supraspinatus have functional distinctions (Hermenegildo et al., 2014; Kim et al., 2017, 2013; Roh et al., 2000). Three-dimensional computer modeling research of the suprascapular nerve has indicated that the anterior and posterior regions are innervated by different primary branches, allowing separate activation between these regions (Hermenegildo et al., 2014). The anterior region has an increase in Type I fibers compared to the posterior region, indicating a slower maximum shortening velocity and increased fatigue resistance (Kim et al., 2013). This anterior region also has an increased pennation angle, suggesting increased force capability at similar activation (Kim et al., 2007). These subregions have differences in their mechanical capability depending on posture; when altering glenohumeral elevation angle and axial humeral rotation, the anterior region acts as an internal and external rotator depending on humeral position, while the posterior region either acted as an external rotator or did not induce rotation (Gates et al., 2010). Activation patterns between these regions are minimally described; previous research detailed inter-regional variances in activation as ratios for static arm postures in the

scapular plane (Kim et al., 2017). When examining ratios of activation between these two regions in increasing abduction postures and between neutral and external rotation, these ratios shifted to increased relative posterior region activation with increasing abduction angle or increased external rotation, indicating that the posterior region may play a more pronounced role in postures with higher degrees of abduction and external rotation (Kim et al., 2017). The interaction between load and humeral abduction angle was far more evident in the anterior region, occurring in almost all planes of elevation in the ascending phase of movement and nearly half of the examined planes of elevation in the descending phase of motion. Greater loads and humeral elevation angles also increased anterior supraspinatus activation, peaking at 90° of thoracohumeral elevation, while peaks occurred above 90° in the posterior supraspinatus (Figure 20). Additionally, differences related to hand loads were far more pronounced in the anterior region. Above 90° of humeral elevation in both externally loaded scenarios, activation in the posterior region was within 1 %MVC, despite doubling hand load. The anterior region of the supraspinatus is larger and produces 71% of the total muscle force of the supraspinatus by PCSA (Gates et al., 2010). It attaches to a thicker, more tubular tendon that represents 47% of the total supraspinatus tendon cross-sectional area (Gates et al., 2010), and also has a larger flexor moment arm than the posterior supraspinatus, particularly between 18-54° of flexion (Ackland, Pak, Richardson, & Pandy, 2008). The smaller moment arm and force capability of the posterior region may indicate its primary role as a glenohumeral stabilizer, while the anterior region primarily assists in generating motion. Sustained loading of the posterior region to generate stability may lead to chronic injury and atrophy of the supraspinatus, as ~50% of cases observed with large retracted supraspinatus tendon tears had no distinguishable posterior region (Karas et al., 2011; Kim et al., 2010, 2013). It is undetermined whether atrophy of the posterior region leads to rotator cuff pathology or that the

inverse exists; however, is important to understand that these items are indelibly linked. Further research is required to further elucidate this relationship between the posterior region of the supraspinatus and injury pathology.

Plane of elevation affected supraspinatus capability for both regions. Activation for both regions decreased as the plane of elevation moved from the abduction plane to the flexion plane, despite identical hand loads. Similar decreases in activation have been observed in the anterior supraspinatus using fine wire EMG previously (Alenabi, Dal Maso, Tétreault, & Begon, 2016). The posterior supraspinatus activation similarly decreased across planes, but this difference in normalized activation was relatively smaller. Main effects of plane of elevation altered anterior region activation by up to 11.2 %MVC, but the posterior region by only up to 6.7 %MVC. The posterior region has been thought to quickly adjust tension on the rotator cuff, preventing buckling with dynamic motion (Hermenegildo et al., 2014; Kim et al., 2013). This sustained activation across planes supports the idea that the posterior region acts as a stabilizer, while the anterior region is responsible for assisting in shoulder motion.

There were some limitations inherent to this study. The participants were university-aged individuals with no self-reported history of upper extremity injury or pathology which limits the applicability of these results to an injured population. Additionally, only the supraspinatus was examined. Expanded interpretation of the results outside the context of the interplay between other muscles of the shoulder complex should be approached cautiously.

This study provides advanced knowledge surrounding activation of the supraspinatus, and further confirms that this muscle has distinct subregions with different functions related to upper extremity use. It represents the most comprehensive evaluation of the supraspinatus regions over a large set of planes of elevation and hand loads throughout the range of humeral elevation,

providing a more complete description of supraspinatus activation. Further, this research provides novel insights into the posterior region of supraspinatus, which is commonly associated with rotator cuff pathology. Further insights into the previously neglected complexity of the supraspinatus can improve understanding of rotator cuff pathology initiation and prevention. These findings can be leveraged to better simulate *in vivo* conditions more accurately, as well as determining biomechanically relevant loading scenarios for *in vitro* tissue testing.

CHAPTER IV – THE ABILITY OF SURFACE ELECTROMYOGRAPHY TO REPRESENT SUPRASPINATUS ANTERIOR AND POSTERIOR PARTITION ACTIVITY DEPENDS ON ELEVATION ANGLE, HAND LOAD AND PLANE OF ELEVATION

Published as: Cudlip AC, Kim SY, Dickerson CR. (2019) The ability of surface electromyography to represent supraspinatus anterior and posterior partition activity depends on elevation angle, hand load and plane of elevation. Journal of Biomechanics, 99, 109526.

Abstract

This study examined relationships between electromyography recorded from indwelling electrodes of the anterior and posterior supraspinatus and a bipolar surface supraspinatus electrode. Twenty male and twenty female participants completed full range humeral elevations in three planes of elevation (0/40/90°) with three hand loads (unloaded/20%/40% of maximal elevation strength). EMG activation was combined with motion capture to determine activation at instantaneous activation angles, and linear regressions of anterior and posterior indwelling electrodes relative to the bipolar surface electrode determined relationships between these signals. While no interactions between sex/plane/elevation angle/intensity existed for regressions, main effects for each of these factors individually affected regressions between surface and indwelling signals. Surface signals underestimated normalized indwelling activation at low elevation angles for both regions by up to 45% in the anterior supraspinatus ($p<0.01$), then overestimated activation at higher elevation angles. Surface EMG underestimated indwelling signals by up to 15% in unloaded conditions, while overestimating the posterior region by up to 17% in the 40% load condition ($p<0.01$). Sex effects showed increased overestimation by surface signals in the posterior region in males by 21% ($p<0.01$). Agreement between the surface and indwelling electrodes are

modulated by plane of elevation, elevation angle, load intensity and sex of the participant, and should be considered in future research design.

4.1 Introduction

The rotator cuff muscles collectively maintain glenohumeral stability while contributing to humeral movement, and the complex nature of the supraspinatus may demonstrate distinct regions within this muscle. The supraspinatus assists in abduction and external rotation of the shoulder (Malanga et al., 1996; Reinold et al., 2004), and is the component most commonly associated with tendinopathies (Jobe & Moynes, 1982). Its complex morphology has anterior and posterior regions which have differences in fibre type compositions, innervation and mechanical capability throughout postural ranges. Differences exist in fibre type between regions, with increased Type I fibers within the anterior region compared to the posterior region (Kim et al., 2013), indicating a slower maximum shortening velocity and is more resistant to fatigue. Pennation angle differences exist between the anterior and posterior regions, with an increased pennation angle in the anterior region compared to the posterior region (Kim et al., 2007), suggesting that the anterior region will generate greater force than the posterior region under similar activation conditions. More recently, a three-dimensional computer modeling study of the innervation pattern of the suprascapular nerve reported that the anterior and posterior regions of this muscle are innervated by different primary nerve branches (Hermenegildo et al., 2014). These subregions have differences in their mechanical capability depending on posture; when altering glenohumeral elevation angle and axial humeral rotation, the anterior region acts as an internal and external rotator depending on humeral position, while the posterior region either acted as an external rotator or did not induce rotation (Gates et al., 2010). Activation patterns between these regions are minimally described; previous research detailed inter-regional variances in activation as ratios in static arm postures in the scapular plane

(Kim et al., 2017). When examining ratios of activation between these two regions in increasing abduction postures and between neutral and external rotation, these ratios shifted to increased relative posterior region activation with increasing abduction angle or increased external rotation, indicating that the posterior region may play a more pronounced role in postures with higher degrees of abduction and external rotation (Kim et al., 2017). Inter-regional activations decrease as the plane of elevation rotates medially despite identical hand loads; differences also existed between regions, where sustained posterior region activation suggested a primary contribution as a glenohumeral stabilizer (Cudlip & Dickerson, 2018b).

Measurement of muscle activation using indwelling or surface electrodes during submaximal exertions is common. Recent studies used either surface (Maciukiewicz et al., 2016; McDonald et al., 2014) or indwelling (Alenabi, Whittaker, Kim, & Dickerson, 2019; Cudlip & Dickerson, 2018b) electrodes to measure supraspinatus activation. Researchers typically prefer surface electrodes for logistical reasons, as it does not require invasive methods, are faster to complete and can be done with less extensive training. Relationships were defined between surface and indwelling electrodes (Allen, Brookham, Cudlip, & Dickerson, 2013), but just one region of the supraspinatus was reported for a single plane of elevation. In light of technical requirements, method availability and experimental preferences, determining surface signal relative activations of the partitions of the supraspinatus would be beneficial, allowing more confident assessment of information content without using indwelling methods. The purpose of this study was to examine relationships between anterior and posterior supraspinatus indwelling electromyography and a surface supraspinatus signal across a range of arm postures. We hypothesized the anterior region would have better agreement with the surface signal than the posterior region.

4.2 Methods

Two bipolar indwelling electrodes and one bipolar surface electrode recorded supraspinatus activity as participants completed arm elevations using specific planes of elevation and hand loads. Bivariate analysis compared indwelling electrodes relative to the surface location across planes of elevation, elevation angles and hand loads.

4.2.1 Participants

Forty right-handed participants [20 males – 25.0 ± 3.4 years, 1.78 ± 0.07m, 88.2 ± 13.2 kg; 20 females – 23.6 ± 3.9 years, 1.71 ± 0.07 m, 72.4 ± 12.1 kg] participated. Exclusion criteria included self-reported previous upper limb or low back pain, history of bleeding disorders or rubbing alcohol and skin adhesive allergies. The sample for this study is the same sample of individuals as described in Chapter III.

Sample size was selected by conducting an *a priori* power analysis. This power analysis was completed using G*Power 3.1 (Universität Düsseldorf, Düsseldorf, Germany), and indicated that 32 participants was sufficient to obtain adequate power (Cohen, 1992; Faul et al., 2007) based on the primary outcomes of muscular activation in the anterior and posterior regions of supraspinatus. The effect size chosen (f^2 = 0.4) represented the lower range observed the in the literature for rotator cuff research, which has indicated variable effect sizes from 0.4-1.5 (Balke et al., 2013; Hughes et al., 2003; Tetreault, Krueger, Zurakowski, & Gerber, 2004).

4.2.2 Instrumentation

Electromyography (EMG) on the right supraspinatus and motion capture on the torso and right upper arm were collected. Hypodermic needles, each containing two sterilized Teflon-coated

stainless fine wire barbed electrodes (Motion Lab Systems, Inc., Louisiana, USA) with wire lengths of 50 and 75mm were inserted into the anterior and posterior supraspinatus respectively (Figure 14A) using previously published instructions (Kim et al., 2017) and were guided with ultrasound imaging. Ultrasound technique was used to determine the depth of these two regions, with the ultrasound probe placed laterally to the insertion site in order to track needle depth throughout electrode insertion. EMG was sampled at 3000 Hz using a wireless telemetered system (Noraxon Telemyo 2400 T G2, Noraxon, Arizona, USA). A single bipolar Ag-AgCl surface electrode with fixed 20mm inter-electrode spacing (Noraxon, Arizona, USA) was placed over the supraspinatus published electrode placements (Criswell, 2011), with a ground electrode on the clavicle. Raw signals were band-pass filtered from 10-1000 Hz and differentially amplified with a common-mode rejection ratio >100dB and input impedance of 100MΩ. Analog signals were converted to digital using a 16 bit A/D card with a ±3.5V range.

Three-dimensional motion was captured using a 13-camera optoelectronic infrared system (VICON, Oxford, UK). Rigid marker clusters placed on the humerus, acromion, and torso with seven individual markers placed on the epicondyles of the right elbow, right acromion, suprasternal notch, xiphoid process, C7 and T8 vertebrae were tracked (Figure 21B). Kinematics were recorded using VICON Nexus 1.8.5 software (VICON Motion Systems, Oxford, UK) at 50 Hz. During calibration, a stylus was used to record scapular landmarks (Grewal et al., 2017). Relationships between the acromion cluster and these points allowed post-processing digital recreation of scapular orientation.

4.2.3 Protocol

Following calibration, participants performed maximal exertions. Exertions were completed three times with two minutes rest interposed (Chaffin, 1975; Fischer, Belbeck, &

Dickerson, 2010) in postures designed to maximize supraspinatus activation (Criswell, 2011), and these data normalized subsequent experimental trials (Winter, 1991). Participants completed two maximal arm elevations seated in a backless chair with a straight arm at 90° humeral elevation in the frontal plane (Cudlip & Dickerson, 2018b). A hand dynamometer (Ergofet, Hoggan Scientific, Salt Lake City, UT, USA) placed at the wrist quantified force output; the average of these trials was used to normalize hand load during experimental trials.

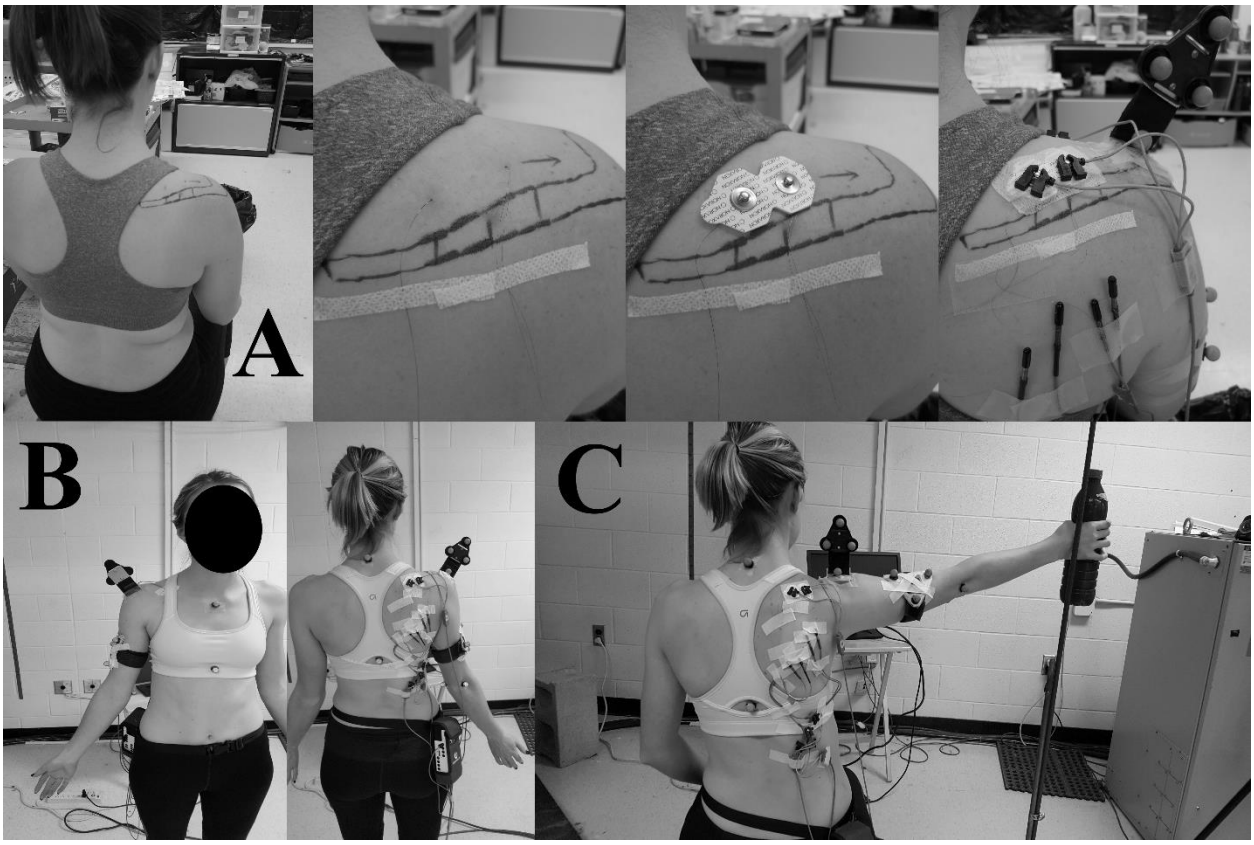

Figure 21. Experimental setup. Two indwelling electrodes were placed into the anterior and posterior supraspinatus with ultrasound guidance (A), then a bipolar surface electrode was placed on the supraspinatus muscle belly. Motion capture markers were placed over bony landmarks of the torso and right upper extremity (B). Participants completed arm elevations to maximal angle at a fixed cadence in differing planes of elevation with differing hand loads. A guide rail was used to indicate plane of elevation for participants during experimental trials (C).

Experimental trials consisted of arm elevation and depression combining planes of elevation (0/40/90°) and hand loads (unloaded/20%/40% of maximum elevation strength). Each

scenario was completed twice. Elevation planes were set using goniometric measurements over the glenohumeral joint coincident with the thorax coordinate system (Wu et al., 2005). Arm movements were completed at a fixed cadence using a metronome, with participants moving from zero to maximum elevation in two seconds, then two seconds to return to the starting position. A metal rail was placed to act as a guide throughout the trial. Participants were seated on a backless chair and experimental trials were completed in a fully randomized order.

4.2.4 Data and Statistical Analysis

EMG data were analysed with respect to amplitude. All signals were processed using custom MATLAB code (Matlab R2016, Mathworks Inc., Natick, MA). A high pass 4^{th} order Butterworth filter with a cut-off frequency of 30 Hz was applied to all signals to remove heart rate contamination (Drake & Callaghan, 2006). Signals were full-wave rectified and low-pass single pass filtered using a 2^{nd} order Butterworth filter at 4 Hz; this cut-off is commonly used for the low frequency motion of upper extremity musculature (Cudlip et al., 2015, 2018; Ho et al., 2019). then normalized with respect to region specific maximum voluntary exertions.

Kinematic analysis consisted of data filtering, coordinate system construction and calculation of joint rotation sequences. Raw kinematic data were low pass filtered at 6 Hz, and segment length and orthogonal coordinate systems were constructed using ISB guidelines (Wu et al., 2005). Static calibration trials for the scapula using the stylus were used to construct the scapular coordinate system. Thoracohumeral rotations were calculated using a Y-X-Y' rotation sequence (Wu et al., 2005).

EMG activation was paired with motion capture to determine activation at instantaneous elevation angles. Normalized activations for all electrodes were extracted at four elevation angles

(5/45/90/120° of thoracohumeral elevation) in each experimental scenario for the ascending and descending phases of motion. Linear bivariate fits of indwelling electrodes relative to the surface electrode were completed with lines of best fit using a fixed intercept of zero assessing each main effect (plane, intensity, angle) for each participant. Within each scenario, regression coefficients of each scenario were tabulated. These coefficients were examined using multiple 2-way repeated measures ANOVAs with combinations of five factors (sex, phase of motion, plane of elevation, elevation angle, and hand load) including each 2-way interaction to identify differences in coefficients of bivariate relationships of indwelling prediction based on surface electrode EMG. Statistical analyses were completed using JMP 14.0 (SAS Institute, North Carolina, USA), with significance considered at $\alpha = 0.05$, with post-hoc analyses conducted if differences emerged.

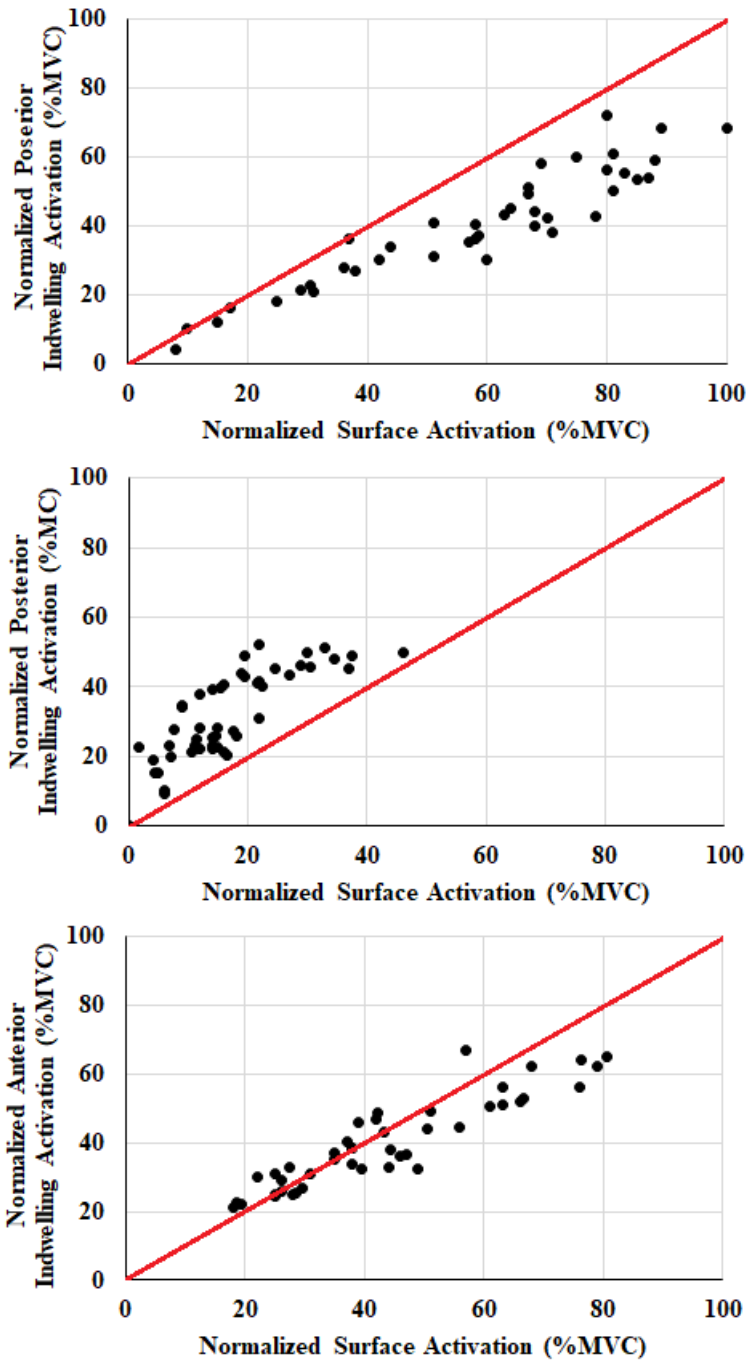

Figure 22. Bivariate regressions were completed between the bipolar surface electrode and the anterior and posterior indwelling electrodes. Each of these plots represent a different single trial for a different single participant. On each graph above a representation of unity where surface and indwelling normalized activation would be identical is represented by the solid line; points to the left of that line represent an underestimation of the bipolar surface electrode compared to indwelling EMG; points to the right represent an overestimation of surface EMG to indwelling EMG.

4.3 Results

Elevation angle, plane, load intensity and participant sex affected regression coefficients, but no interactions existed. Regression coefficients of 1.0 indicate perfect agreement between the indwelling and the surface EMG recording; values greater than 1.0 indicate underestimation of the bipolar surface electrode compared to the indwelling electrode, while values less than 1.0 indicate the opposite. Elevation angle effects existed for both regions ($p<0.01$), with surface EMG underestimating indwelling EMG at lower angles in both regions. The underestimation reached as high as 45% in the anterior region. Conversely, overestimation occurred at higher elevation angles (for example, 11% in the posterior region at 120°) (Figure 23). Regressions by elevation angle for anterior supraspinatus ($r^2 = 0.71$) and posterior supraspinatus ($r^2 = 0.71$) are as follows:

$$EMG_{IN,ANT,5DEG} = 1.53 \times EMG_{SRF,5DEG}$$

$$EMG_{IN,ANT,45DEG} = 1.26 \times EMG_{SRF,45DEG}$$

$$EMG_{IN,ANT,90DEG} = 0.99 \times EMG_{SRF,90DEG}$$

$$EMG_{IN,ANT,120DEG} = 0.89 \times EMG_{SRF,120DEG}$$

$$EMG_{IN,POST,5DEG} = 1.40 \times EMG_{SRF,5DEG}$$

$$EMG_{IN,POST,45DEG} = 1.16 \times EMG_{SRF,45DEG}$$

$$EMG_{IN,POST,90DEG} = 0.97 \times EMG_{SRF,90DEG}$$

$$EMG_{IN,POST,120DEG} = 0.89 \times EMG_{SRF,120DEG}$$

Where IN = indwelling electrode, SRF = bipolar surface electrode, ANT = anterior supraspinatus, POST = posterior supraspinatus, 5DEG = 5° arm elevation, 45DEG = 45° arm elevation, 90DEG = 90° arm elevation, 120DEG = 120° arm elevation.

Plane of elevation effects existed for the posterior supraspinatus ($p<0.01$), with surface EMG in the 0° plane overestimating posterior activation by up to 13%, while the 90° plane underestimated activation by 2%. Regressions by plane of elevation for anterior supraspinatus ($r^2 = 0.76$) and posterior supraspinatus ($r^2 = 0.78$) are as follows:

$$EMG_{IN,ANT,0PL} = 1.01 \times EMG_{SRF,0PL}$$

$$EMG_{IN,ANT,40PL} = 1.06 \times EMG_{SRF,40PL}$$

$$EMG_{IN,ANT,90PL} = 0.96 \times EMG_{SRF,90PL}$$

$$EMG_{IN,POST,0PL} = 0.87 \times EMG_{SRF,0PL}$$

$$EMG_{IN,POST,40PL} = 1.00 \times EMG_{SRF,40PL}$$

$$EMG_{IN,POST,90PL} = 1.02 \times EMG_{SRF,90PL}$$

Where IN = indwelling electrode, SRF = bipolar surface electrode, ANT = anterior supraspinatus, POST = posterior supraspinatus, 0PL = 0° plane of elevation, 40PL = 40° plane of elevation, 90PL = 90° plane of elevation.

Load effects occurred for both regions ($p<0.01$), with the unloaded condition significantly lower than the 20% or 40% conditions, but loaded conditions were not statistically different. Surface EMG underestimated indwelling signals in unloaded conditions in both regions by up to 15% while overestimating by up to 17% at the 40% load (Figure 24). Regressions by load intensity for anterior supraspinatus ($r^2 = 0.72$) and posterior supraspinatus ($r^2 = 0.76$) are as follows:

$$EMG_{IN,ANT,0L} = 1.15 \times EMG_{SRF,0L}$$

$$EMG_{IN,ANT,20L} = 0.93 \times EMG_{SRF,20L}$$

$$EMG_{IN,ANT,40L} = 0.88 \times EMG_{SRF,40L}$$

$$EMG_{IN,POST,0L} = 1.07 \times EMG_{SRF,0L}$$

$$EMG_{IN,POST,20L} = 0.86 \times EMG_{SRF,20L}$$

$$EMG_{IN,POST,40L} = 0.83 \times EMG_{SRF,40L}$$

Where IN = indwelling electrode, SRF = bipolar surface electrode, ANT = anterior supraspinatus, POST = posterior supraspinatus, 0L = zero hand load, 20L = 20% hand load, 40L = 40% hand load.

Participant sex affected the posterior region, but not the anterior region. Anterior indwelling signals were slightly underestimated compared to surface signals in both sexes (3% and 5% in males and females respectively), while the posterior region was overestimated in males by 21% and underestimated in females by 13% ($p<0.01$). Regressions by sex for anterior supraspinatus ($r^2 = 0.76$) and posterior supraspinatus ($r^2 = 0.72$) are as follows:

$$EMG_{IN,ANT,M} = 1.03 \times EMG_{SRF,M}$$

$$EMG_{IN,ANT,F} = 1.05 \times EMG_{SRF,F}$$

$$EMG_{IN,POST,M} = 0.79 \times EMG_{SRF,M}$$

$$EMG_{IN,POST,F} = 1.13 \times EMG_{SRF,F}$$

Where IN = indwelling electrode, SRF = bipolar surface electrode, ANT = anterior supraspinatus, POST = posterior supraspinatus, M = males, F = females.

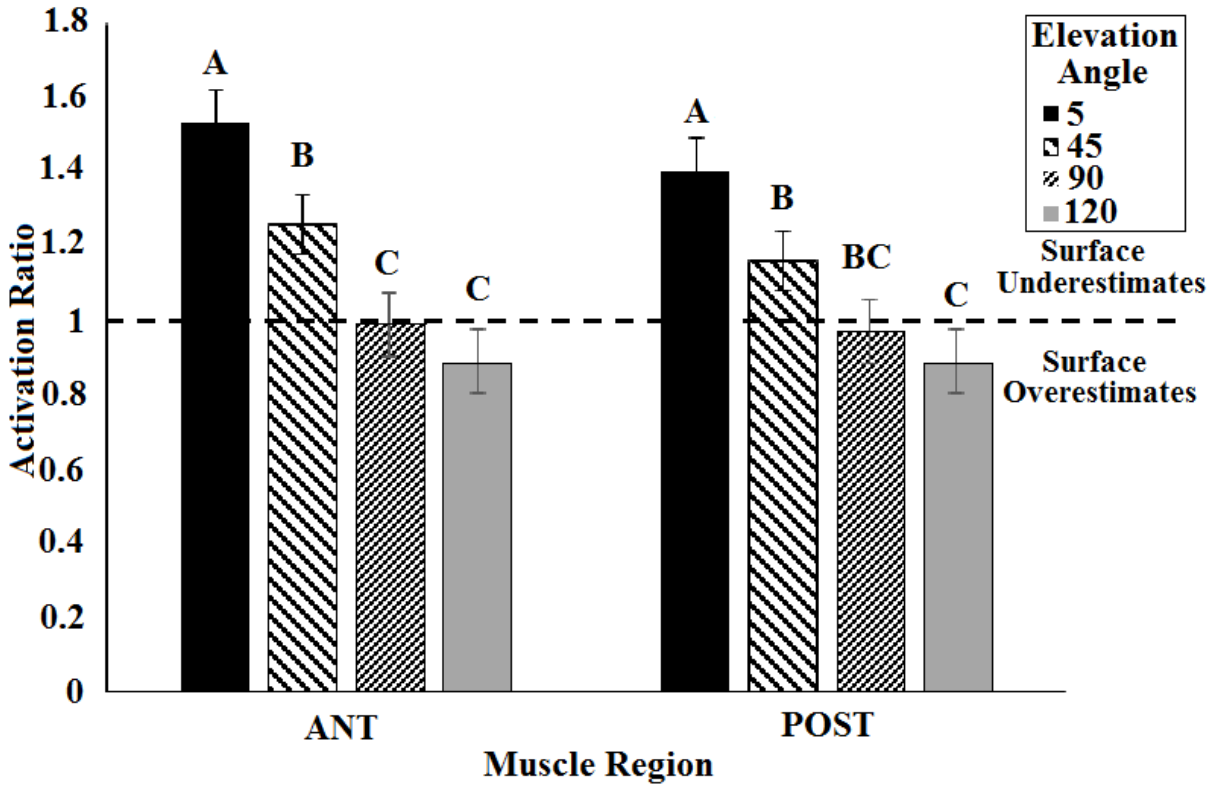

Figure 23. Humeral elevation angle affected EMG relationships in both anterior and posterior supraspinatus at 0, 45, 90 and 120° of elevation ($p<0.01$). Post-hoc differences are compared within a muscle region and are denoted by letters; bars within a muscle region not sharing a letter are significantly different.

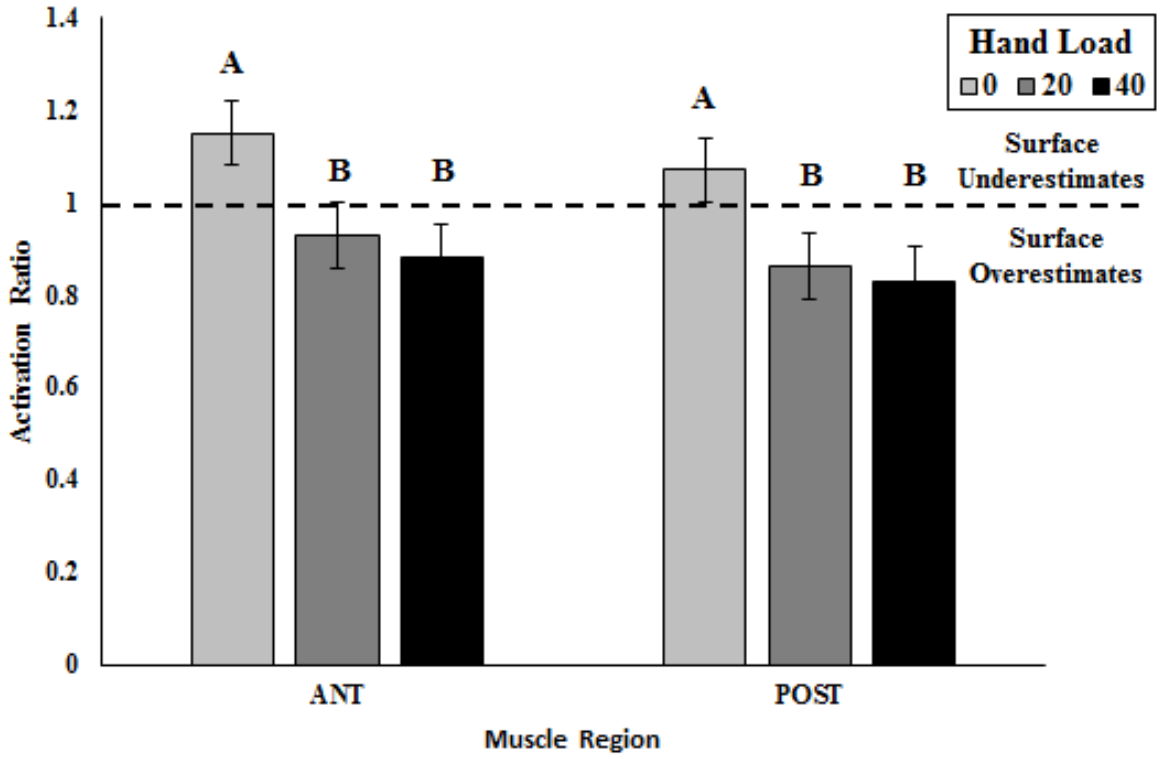

Figure 24. Normalized hand load affected EMG relationships in both supraspinatus regions at 0, 20% and 40% of normalized elevation strength ($p<0.01$). Post-hoc differences are compared within a muscle region and are denoted by letters; bars within a muscle region not sharing a letter are significantly different.

4.4 Discussion

Multiple relationships were defined between indwelling supraspinatus electrodes and the bipolar surface electrode across a range of tasks. Generally, predictions by surface signals were best near 90° of arm elevation and lower hand loads.

The largest prediction accuracy variations were associated with arm elevation changes and low absolute signal magnitudes. Surface EMG underestimated both indwelling region recordings at the lowest elevation angle, with underestimation decreasing as elevation increased (Figure 23). These differences in prediction accuracy at low angles were likely driven by the low EMG levels.

Normalized activation at these low angles was <10% MVC; similar to previous reports (Allen et al., 2013). The small absolute magnitude of these signals would result in larger misestimations with small differences in recording. The prediction of indwelling by surface EMG improved as elevation angle increased, having excellent agreement at 90° elevation with overestimations of 1-3%. Similar anterior supraspinatus agreement has been documented, with surface recordings overestimating by 12.3-31.6% (Allen et al., 2013; Waite, Brookham, & Dickerson, 2010). However, these relationships were quantified across the entire range of tasks completed in these studies, making individual posture inferences difficult.

EMG predictions from underestimation to overestimation from the bipolar surface electrode with increasing load may be related to the known nonlinearity of EMG signals (Figure 24). Conditions with higher loads generated overestimation of indwelling signals up to 17% in the posterior supraspinatus. Lower intensity exertions generate less overestimation; similar overestimations have been observed in maximal exertions compared to submaximal exertions (Waite et al., 2010), with overestimation decreasing by over 50%. Increased prediction bias in higher loads may relate to known nonlinearity of the EMG-force relationship (De Luca, 1997). Previous research comparing surface and indwelling EMG in leg musculature reported increasingly non-linear relationships at high intensities (Onishi et al., 2000) and high knee flexion (Kingston & Acker, 2018). These leg muscles have larger muscle volumes and motor unit groups than the supraspinatus; measurements in these muscles may have originated from different motor units, worsening these relationships. The smaller supraspinatus muscle volume appears to have muted a similar effect.

Differences in moment arm capability and muscle mass potentially altered EMG relationships for plane of elevation and participant sex. The holistic moment arm of supraspinatus

changes with plane of elevation and abduction angle (Kuechle et al., 1997; Liu, Hughes, Smutz, Niebur, & An, 1997). Shifts of the surface electrode in relation to the underlying muscle may alter innervation zone proximity. The innervation zone in the biceps shifts considerably with elbow angle (Martin & MacIsaac, 2006); a similar mechanism could potentially affect the supraspinatus in different planes of elevation, as the difference in these relationships in the posterior region moved from 11% overestimation in the 0° plane to 2% underestimation in the 90° plane. It is likely that an exposure of these subregions to the surface electrode changes with plane of elevation, particularly in the posterior region. Anthropometric differences may affect posterior region predictions between sexes. Males average ~60% more upper body muscle mass than females (Lassek & Gaulin, 2009); it is possible that this increase altered subcutaneous tissue volume between electrodes and their corresponding predictions. The estimated effective recording area of surface electrodes ranges between 10 and 20 mm from the skin surface (Barkhaus & Nandedkar, 1994; Fuglevand, Winter, Patla, & Stashuk, 1992), and the increased muscle bulk in males may have resulted in differences in the spatial volume of muscle fiber activations recorded by these two different electrodes. Large portions of the posterior supraspinatus are deep to the anterior region (Kim et al., 2007); activation of this deep region as observed by a surface electrode may be partially occluded by the anterior region.

Inherent limitations exist in this research. Only neutral arm elevations were examined, limiting the scope of application, as humeral rotations have been shown to alter the supraspinatus moment arm (Hik & Ackland, 2019), potentially altering activation characteristics. The use of university-aged participants makes population generalizations difficult. Finally, muscular cross-talk is commonly suspected for surface electrode recordings (Ounpuu, DeLuca, Bell, & Davis, 1997). No cross-correlation analysis between the bipolar surface electrode and surface electrodes

for other upper extremity muscles was completed for this work; however, cross-correlation analysis of cross-talk between shoulder region muscles has been completed previously (Waite et al., 2010), indicating modest cross-correlation levels of 4.4-17.3% that are at least partially due to shared functionality. Limited surface area exists for the bipolar electrode placement to ensure that muscular cross-talk is avoided, resulting in close proximity between the surface and indwelling electrodes. However, no interactions between these electrodes was observed. Additionally, the number of equations may limit the utility for future studies. However, the point of these equations was to allow researchers to understand the differences across planes of elevation, load intensities, elevation angles and participant sex. Future work should focus on development of a singular equation that includes all factors while adding additional factors such as axial humeral rotation.

This study provides insight into relationships between surface and indwelling EMG recordings of supraspinatus across a wide range of motions. While previous research has investigated parts of these relationships, none included the posterior supraspinatus nor the extensive range of arm elevations reported presently. Surface electrodes generate better agreement for the anterior region than the posterior region across the range of postures, but posterior region agreement with the bipolar surface electrode existed but may be sensitive to higher hand loads or individuals with larger upper extremity muscle bulk.

CHAPTER V – THE RESPONSE OF SUPRASPINATUS TENDON TO EXPOSURES EMULATIVE OF PHYSIOLOGICAL LEVELS IN AN ANIMAL MODEL

Abstract

Rotator cuff pathology typically originates in the supraspinatus tendon, but uncertainty exists on how combinations of posture and load intensity affect the intact, functional supraspinatus unit. The purpose of this study was expose the supraspinatus tendon to mechanical loading scenarios emulative of muscle activation and postural conditions measured *in vivo* and document its responses. Right shoulders from 48 Sprague-Dawley rats were placed into one of eight testing groups combining glenohumeral elevation angles (0/30/60/75°) and a high or low load intensity for 1500 cycles at 0.25 Hz using a custom mounting apparatus attached to a tensile testing system. Load intensities were determined from *in vivo* muscular activation levels measured in Chapter III and scaled to the animal model. Mechanical variables examined included maximum and minimum displacement, tangent stiffness and hysteresis. Localized surface stretch ratios were calculated based on virtual tracking points. A three-way interaction between elevation angle, load magnitude and cycle number occurred for tangent stiffness, with increasing angles, loads and cycles increasing stiffness by up to 49% in some scenarios. Longitudinal stretch ratios increased with increasing elevation angles, load intensities and cycle numbers, and differences existed between the articular and bursal sides of the tendon. Complex interactions between angle, load and cycle number suggest higher abduction angles, increased load magnitude and subsequent cycles increase mechanical responses within the tendon.

5.1 Introduction

The tendons of the rotator cuff help transfer force to bone for moment production and joint stabilization, but the inherent intricacy of this region exacerbates the complexity of these mechanics. Tendons incorporate important elastic and viscoelastic characteristics that may allow for dynamic interactions (Lieber, Leonard, & Brown-Maupin, 2000). This interaction can influence force transmission and energy storage and return (Alexander & Bennet-Clark, 1977; Maganaris & Paul, 1999; Reeves, Maganaris, & Narici, 2003). The supraspinatus tendon passes under the acromion, generating multiaxial loading due to its interactions with surrounding tissues (Bey et al., 2002). However, limited information exists to connect *in vitro* mechanical testing tendon responses to supposed *in vivo* tendon function. The importance of understanding the mechanical properties of the muscle-tendon unit is largely appreciated in locomotion, but has not extended to the upper extremity to the same degree (Magnusson, Narici, Maganaris, & Kjaer, 2008).

This complex architecture paired with issues of feasibility of human specimens for study has led researchers to seek alternative research methods using animal models. Limited availability of human specimens, cost of testing, and pathologies associated with cadaveric specimens limits yield of valuable results in human tissues. Previous research has identified the rat supraspinatus as a surrogate for the human supraspinatus, as it passes under an enclosed arch, comparable to the coracoacromial arch in humans (Soslowsky et al., 1996; Voleti et al., 2012).This animal model has demonstrated its utility for examining rotator cuff pathology and has been used to assess efficacy of rotator cuff surgical repair techniques (Gimbel, Kleunen, et al., 2004; Gimbel et al., 2007; Thomopoulos et al., 2003), tendon healing (Bedi et al., 2010; Gulotta et al., 2011; Kovacevic et

al., 2011; Rodeo et al., 2007) and fatigue loading (Andarawis-Puri & Flatow, 2011; Fung, Wang, et al., 2010; Fung et al., 2008; Sun et al., 2008).

In vitro research continues to focus on pathology locations within the rotator cuff and its potential causes. Instigation of rotator cuff tears are hypothesized to relate to tissue deformations (Fu, Harner, & Klein, 1991). Clinical observations and cadaveric studies indicate that the majority of rotator cuff tears begin in the supraspinatus tendon, occurring commonly in the mechanically stiffer anterior and middle thirds of the tendon (Kim et al., 2010; Loehr & Uhthoff, 1987). These tears may result from shearing between joint-side and bursal layers of the rotator cuff, which is supported by anatomical differences (Gohlke, Essigkrug, & Schmitz, 1994), histological evidence (Fukuda et al., 1994), and mechanical properties of the joint-side layer of the rotator cuff tendon (Nakajima, Rokuuma, Hamada, Tomatsu, & Fukuda, 1994). Alternatively, rotator cuff lesions have been postulated to arise from deformations in the coracohumeral ligament in external rotation, a ligament whose fibers blend with the supraspinatus tendon, resulting in adverse tendon loading via tensile loading during eccentric loading, particularly in throwing athletes (Kuhn, Bey, Huston, Blasier, & Soslowsky, 2000).

Critical knowledge gaps still exist in rotator cuff tendon function and changes in mechanical properties to loads. Current mechanical tensile testing is typically completed with the tendon completely excised from surrounding structures (Ahmadzadeh et al., 2013; Lake et al., 2009; Lake, Miller, Elliott, & Soslowsky, 2010), but MRI examination of a human cadaveric functional cuff unit has indicated that posture affects its mechanical behaviour (Bey et al., 2002). To the author's knowledge little present research exists connecting muscular activation profiles *in vivo* to *in vitro* measures utilizing these results to replicate physiologically relevant mechanical

testing scenarios. The purpose of this research was to expose specimens to scenarios emulative of activation and postural conditions measured in Chapter III and document tendon responses.

There were three hypotheses in this study:

1) *An interaction between posture and load intensity will alter tangent stiffness, hysteresis and stretch ratios, with statistically significant increases in the highest glenohumeral angle and the highest load.*

Previous research examining cadaveric supraspinatus tendons observed increased strain with increasing joint angles (Bey et al., 2002). Overhead postures are associated with several biomechanical consequences (Chopp, Fischer, & Dickerson, 2010; Chopp, O'Neill, Hurley, & Dickerson, 2010; Ebaugh et al., 2006a; Fischer, Chopp, & Dickerson, 2008; Grieve & Dickerson, 2008; Wiker, Chaffin, & Langolf, 1989) and require longer returns to work following injury (Ellman & Kay, 1991). While the increased loads at the same glenohumeral elevation angle are expected to generate increased results in dependent measures than lower intensities, this hypothesis expects an interaction between these two factors. This hypothesis will be supported if an interaction between glenohumeral elevation angle and load intensity is present in tangent stiffness, hysteresis and stretch ratios, with post-hoc testing indicating the highest responses in the 75° high load condition.

2) *Differences will exist between the stretch ratios on articular and bursal sides of the tendon, with increased stretch ratios on the articular side of the tendon.*

Strain analyses from MRI imaging have previously documented increased strain on the articular surface of the supraspinatus tendon with increasing abduction angles (Bey et al., 2002). Other findings have documented continuous high tensile loading on the articular surface

compared to the bursal side of the tendon (Huang et al., 2005). This hypothesis will be supported if differences exist between the articular stretch ratios are higher than bursal strain ratios, particularly at increased elevation angles.

3) *Increasing cycle numbers will alter mechanical outcome measures, with increases in stiffness, displacement and stretch ratios with increasing cycle numbers.*

Repetitive work is a consistent risk factor in ergonomics; workers whose jobs require repetitive motions are up to three times more likely to develop shoulder tendinitis (Frost et al., 2002). Positive associations between repetitive work and shoulder disorders have been previously documents, with odds ratios up to 5.0 (Bernard, 1997). This hypothesis will be supported if statistically significant differences are observed between the first and 1500th cycles in tangent stiffness, maximum and minimum cyclic displacement and stretch ratios, with increases in these metrics in the final cycle compared to the initial cycle.

5.2 Establishing System Capability and Rationale for Outcome Measures

In vitro examinations of tissue mechanics can be used to study changes in tendon mechanical behaviour in controlled settings. However, measurement of mechanical properties is mostly completed on specimens that are completely excised from surrounding tissues. Material property tests of an excised specimen do not describe the strength of insertion sites, but can provide information such as the tensile strength, ultimate strain and the shape of the stress-strain curve (Weiss & Gardiner, 2001). Despite MRI examinations indicating that the human rotator cuff mechanical behaviour is affected by glenohumeral posture (Bey et al., 2002), no research has incorporated a complete glenohumeral joint in its study design. The research described in this study has multiple novel contributions, particularly employing a complete functional supraspinatus

musculotendinous unit in set glenohumeral postures, and scaling applied loads to emulate muscular activation documented from human participants *in vivo*. As these methods are previously untested and direct comparisons for this method of testing are thus unavailable, an explicit description of these mechanical testing methods has been provided. First, suitability of the animal model was assessed. Subsequently, scaling of muscular activation from human *in vivo* research to *in vitro* supraspinatus tendon loading was assigned. Finally, methods for measuring mechanical tissue parameters were derived and selected for their relationship to future injury *in vivo*. These methodological steps are described below.

5.2.1 Use of an Animal Model

While it would be ideal to examine tendon properties of the human rotator cuff *in vivo*, feasibility of this methodology is limited. The difficulty of implanting force transducers into rotator cuff tendons *in vivo* is difficult due to the coverage of other overlying muscles and bony structures. Previous use of buckle transducers has been used to examine the Achilles tendon *in vivo* during walking and running (Komi, 1990; Komi, Salonen, Jarvninen, & Kokko, 1987), cycling (Gregor, Komi, & Jarvinen, 1987) and vertical jumping (Fukashiro, Komi, Järvinen, & Miyashita, 1993). Forces of the forearm flexor tendons have been examined *in vivo* using a buckle transducer during passive and active finger motion as well as pinch tasks in post-surgical carpal tunnel patients (Schuind, Garcia-Elias, Cooney III, & An, 1992), but neither the Achilles or forearm flexor tendons possess the structural obstacles endemic to the supraspinatus tendon. To best understand mechanical properties of these tissues, researchers are often required to use methods outside of *in vivo* examinations.

In vivo measurement of the human rotator cuff is difficult, requiring researchers to use other means. While the use of human cadavers to complete *in vitro* testing can provide tangible

benefits, inherent limitations including issues with specimen acquisition and accessibility or ethical restrictions may prevent this type of testing (Matsen III et al., 1992). Additionally, cadavers typically originate from older populations and generate specific tissue risks at the shoulder. Rotator cuff defects have been observed in ~15-25% of cadavers in previous studies (Fukuda et al., 1987; Lehman et al., 1995); these pathologies may interact with the testing protocol to obfuscate results. Alternatively, researchers can use animal models to assess rotator cuff tissue responses *in vivo* or *in vitro*. Multiple animal species have been used to examine rotator cuff responses. Sheep infraspinatus has been used as a surrogate for human supraspinatus due to its similarity in size and anatomy between the two species (Andarawis-Puri et al., 2009; Frisch et al., 2014). However, analyses of fiber length-to-moment arm ratio and fiber length-to-muscle length ratio have identified smaller mammals such as mice, rats and dogs as better representatives of muscle architecture parameters than larger mammals such as sheep or cows (Mathewson et al., 2014).

Of these animal models, the Sprague-Dawley rat serves as the best current surrogate for human supraspinatus testing. The bony architecture in the Sprague-Dawley rat is similar to humans (Soslowsky et al., 1996), and is the only non-primate animal model that possesses a supraspinatus that passes below the coracoacromial arch, similar to humans (Voleti et al., 2012). Mechanical testing and histology examinations of the rat supraspinatus have micro- and macroscale damage accumulations similar to those seen in the human supraspinatus, providing evidence for a link between overuse and chronic supraspinatus injury (Soslowsky et al., 2000).

Sprague-Dawley rat investigations have examined fatigue loading responses, surgical repair techniques, and healing through therapeutic agents. An *in vivo* model of the rat patellar tendon examined fatigue loading at differing load levels; morphological assessment showed progression from mild collagen kinks at low load intensity to fiber disruption at high loading

levels; increases in MMP-13 were upregulated for moderate loading, but not low level loading (Andarawis-Puri & Flatow, 2011). This suggests that mechanisms for fatigue loading are distinct from acute laceration. Rat tendon microstructure has been characterized *in vivo* using multiphoton microscopy to assess frequency-based properties of damage; results showed 3D microstructure changes with load changes, characterized by kinked deformation at low intensity, fiber dissociation at moderate intensity, and fiber thinning and discontinuities at high intensity levels (Fung, Sereysky, et al., 2010). Continued research using the same methods as Fung et al. (2010) observed that histological changes indicating structural repair may not be initiated until end-stage fatigue life, indicating the repair response may be unable to restore the damaged tendon to its pre-fatigue architecture (Fung, Wang, et al., 2010). Surgical repair techniques have been widely examined in the rat model. Examining tendon mechanical properties at extended time points after detachment revealed a dramatic decrease in mechanical properties immediately after detachment; some mechanical properties, such as stiffness, continued to increase relative to normal after longer periods of injury (Gimbel, Kleunen, et al., 2004). This stiffness increase is associated with increased tension required at repair to reappose the tendon to its original insertion site (Gimbel, Mehta, et al., 2004). This repair tension rapidly increases initially after injury, followed by an progressive increase over time (Gimbel, Mehta, et al., 2004). Therapeutic agents have also been assessed in this animal model, particularly in tendon-to-bone healing. Regulating MMP-13 or application of mesenchymal stem cells transforming growth factor-beta 3 (TGF-β(3)) have been associated with improved tissue regeneration and tendon-to-bone healing after detachment (Bedi et al., 2010; Gulotta et al., 2011; Kovacevic et al., 2011; Rodeo et al., 2007). Collectively, these studies demonstrate the utility of the Sprague-Dawley rat model for development and testing of rotator cuff pathology.

5.2.2 Scaling EMG Activation to In Vitro Tendon Loading

Typically, tensile testing on tendon is completed using displacement control, where the specimen is loaded in tension to a specified strain rate, or loaded to failure with increasing strain levels at a fixed rate. However, the current study chose loading levels driven by muscle activation observed in humans *in vivo*, and required determining tendon load force magnitudes that utilized these EMG values, as well as scaling from a human supraspinatus tendon to a Sprague-Dawley rat tendon.

Activation for the two human supraspinatus regions *in vivo* were extracted from Chapter III, and these activation levels were used with regional cross-sectional area to calculate a total muscle force value for scaling. Anterior and posterior supraspinatus subregions have been calculated at 15.4 ± 5.7 and 2.5 ± 0.7 cm^3, respectively (Kim et al., 2007). Maximal force transmitted through the supraspinatus tendon in humans during maximum contraction has been calculated to be 196 N (Bassett, Browne, Morrey, & An, 1990), while peak force observed through tetanic stimulation in rat supraspinatus is documented to be 5.4 N in 12 month old animals (Plate et al., 2014). The supraspinatus is a highly pennate muscle, and previous research has quantified the predictive coefficient of determination (r^2) between the muscle line of action and the tendon line to be 0.98 (Lee et al., 2015), and for this research it was assumed that no force vector outside the line of action of the tendon exists. The magnitude of the force vector was determined as follows:

$$||FV|| = [(a_{AR} * PCSA_{AR}) + (a_{PR} * PCSA_{PR})] * F_{max} \quad (1)$$

Where FV is the magnitude of force vector of the combined supraspinatus regions; a_{AR} and a_{PR} are the activation of the anterior and posterior regions of the supraspinatus respectively as

described by the outcomes of the study in Chapter III and normalized to values between 0 and 1, where 1 represents maximal activation, while $PCSA_{AR}$ and $PCSA_{PR}$ is the percentage of the entire supraspinatus muscle represented by the anterior and posterior regions in humans (described as the PSCA of that region divided by the PSCA of the entire supraspinatus muscle) and F_{max} is the maximal force capability of the supraspinatus, as detailed above. The direction of this force vector is directly in line with the centre of the tendon. A force-length relationship modifier has not been included as previous research has estimated the operating range of the fascicles to be at or near optimal (within +/-2% of optimal length) across all regions of the supraspinatus in different arm postures (Langenderfer, Patthanacharoenphon, Carpenter, & Hughes, 2006), and so was assumed to be at optimal length for force generation. The magnitude of this force vector was determined as a percentage of the force described by Bassett et al (1990) and this same percentage was used to determine force magnitude as a percentage of the maximal tetanic force described by Plate et al. (2014). This activation was treated as a static exertion at these fixed glenohumeral elevation angles (as opposed to moving through glenohumeral elevation angles) to accommodate testing system capability.

5.2.3 Specimen Preparation and Creation of Glenohumeral Postures

Developing the novel mechanical testing method included design and fabrication of specialized mounting pots to establish glenohumeral angles, dissection of surrounding shoulder tissues, and affixation of the specimen to the testing unit. Each of these specimens was placed into one of four glenohumeral postures and loaded at one of two loading levels.

All specimens were harvested from the right shoulder of female Sprague-Dawley rats aged between 9 weeks and 12 months of age at harvesting. The age of these specimens aligns with ages

of specimens from previous research of 9-1l2 weeks (Fox et al., 2014), 14 weeks (Kurdziel et al., 2019; Newton et al., 2016) and 12 months (Plate et al., 2014; Soslowsky et al., 2000). However, many studies involving Sprague-Dawley rats do not explicitly describe the age of the specimens, only describing them as "adult" rats or not describing the age of the specimens at all (Gimbel, Kleunen, et al., 2004; Miller, Connizzo, & Soslowsky, 2012; Peltz, Dourte, et al., 2009; Reuther, Thomas, Tucker, Yannascoli, et al., 2014; Rooney et al., 2017; Sun et al., 2008; Tucker et al., 2016). However, the weights of the rats in these papers were described at 400-450 grams, which aligns with rat ages from 14-50 weeks (Charles River Laboratories International, 2011). The age of maturity in rats is well documented, with rats becoming sexually mature at about the sixth week (Sengupta, 2013). Following sexual maturity, every day is approximately equivalent to 34.8 human days, and a 12 month old rat is considered equivalent in age to a 30 year old human (Sengupta, 2013).

Specimen dissection was completed identically for all tests. The right arm and scapula was amputated from the rat body, and skin and fur was removed over the entire scapula, rotator cuff, humerus and forearm. All muscles except for the supraspinatus were excised. The acromioclavicular ligament was dissected and the clavicle was removed. The coracoid process was removed at the height of the glenoid to accommodate camera imaging. The joint capsule was excised starting from the subscapular edge of the glenoid, then moving around the circumference starting inferiorly to minimize risk of lacerating the supraspinatus tendon. Upon excising the capsule, only the supraspinatus muscle and tendon remained; this was the only tissue connecting the humerus and scapula.

Following dissection, cross-sectional area of the supraspinatus tendon was calculated. Tendon cross-sectional area was calculated using a laser measurement system (LJ-V7080,

Keyence Corporation, Osaka, Japan). The manufacturer's specifications indicated that the laser displacement sensor had an accuracy of 46 μm in the transverse direction (transverse to the primary tendon fiber axis) and resolution of 20 μm in the vertical direction (primary height axis). The tendon was laid flat onto a surface below the laser, the infraspinatus fossa and lateral epicondyle of the humerus laying on the flat surface. This posture was identical to the testing postures within the mechanical testing system, and the laser was placed in a transverse direction across the midpoint of the tendon, orthogonal to the direction of the fiber orientation of the tendon. The software of the laser system calculated the cross-sectional area by integrating the area under the laser that had displacement. This area was calculated to the nearest 0.01 mm^2. This method of laser displacement to calculate cross-sectional area has been used previously to measure dimensional changes non-destructively in porcine cervical spine disc specimens (Gooyers & Callaghan, 2015) and rat supraspinatus tendon (Peltz, Perry, et al., 2009; Peltz et al., 2010). Cross-section area for specimens used in this study was 3.86 ± 0.19 mm^2; this cross-sectional area is similar to the cross sectional area of approximately 3.75 mm^2 observed in previous research including supraspinatus tendon cross sectional area for Sprague Dawley rats younger than 12 months who had normal cage activity (Peltz et al., 2010).

Each specimen was placed in a glenohumeral posture that corresponded to postures examined *in vivo* (Chapters III-IV). The normalized supraspinatus activation observed at 0º, 45º, 90º and 120º of abduction within the coronal plane in work completed in Chapter III was used to set activation characteristics for the *in vitro* testing. These ranges of thoracohumeral activation represent postures across the range of motion typically observed in human motion. These ranges of motions are similar within the Sprague-Dawley rat forelimb; range of forelimb motion in these animals has been observed to be approximately 170° (Peltz, Dourte, et al., 2009). These *in vivo*

angles are thoracohumeral angles; corresponding glenohumeral angles for these postures are 0º, 30º, 60º and 75º of glenohumeral elevation (Itoi et al., 1996).

Specimens were placed into custom mounting fixtures designed to enforce specific glenohumeral postures. Four custom mounting pots were developed using Rhino 6 3D Print Design (Robert McNeel & Associates, Seattle, WA, USA). Mounting pots were designed and stereolithography (.stl) files were exported for 3D printing. 3D printing was completed using ABS plastic with a 50% infill. This infill level was determined during pilot testing; a 50% infill prevented flexion of the mounting pot while minimizing weight on the loading arm of the testing system. Each mounting pot was printed multiple times to facilitate successive specimens within a testing angle on the same day. The pot was designed to encase the scapula, and the orientation of this pot was altered relative to the arm of the testing system. Mounting pot design involved a cylindrical tube with a secant removed at the side wall of the pot oriented at the inferior angle of the scapula. This was designed through pilot testing to ensure orientation of the scapula to prevent anterior/posterior scapular tilt. The mounting pot had two sets of circular holes 1.2mm in diameter 90° clockwise and counter clockwise to this flat section of the pot; these holes were designed to fit 18 gauge wire (1.02mm diameter) for secure fixation of the scapula. This mounting pot had an attachment designed to connect to the base of the pot and affix to the arms of the testing system (Cellscale, Waterloo, ON). The dimensions of the testing arm were measured, and a negative of these dimensions were created in this attachment, allowing mechanical coupling with minimal backlash. The orientation of the mounting pot relative to the testing arm was altered in each of the four mounting pots, generating glenohumeral angles of 0º, 30º, 60º and 75º (Figure 25).

Figure 25. Mounting pots generated differing glenohumeral angles. The rectangular portion attached to the displacement arm of the testing system, while the cylindrical portion housed the scapula.

5.2.4 Selection and Definition of Tissue Exposure Measures

Multiple tissue exposure metrics were examined in this study. Each of these metrics were selected to provide insight into changes in tendon mechanical properties. These exposure measures included tangent stiffness, hysteresis, and optical tendon stretch measures. Each of these measures is detailed below.

5.2.4.1 Tangent Stiffness

Tangent stiffness was analyzed throughout the testing protocol at different cycles. Within a cycle, tangent stiffness was calculated using the slope between the maximum and minimum force and displacements as described by the testing actuators for that cycle (Figure 26). Testing actuator force and displacement values have been used previously to calculate tendon stiffness (Freedman

et al., 2015; Fung et al., 2008). This calculation was completed in the 1st, 10th, 100th, 250th, and every 250 cycles until 1500 cycles were completed. These cycles were selected to manage data volume while providing sufficient resolution throughout the testing session.

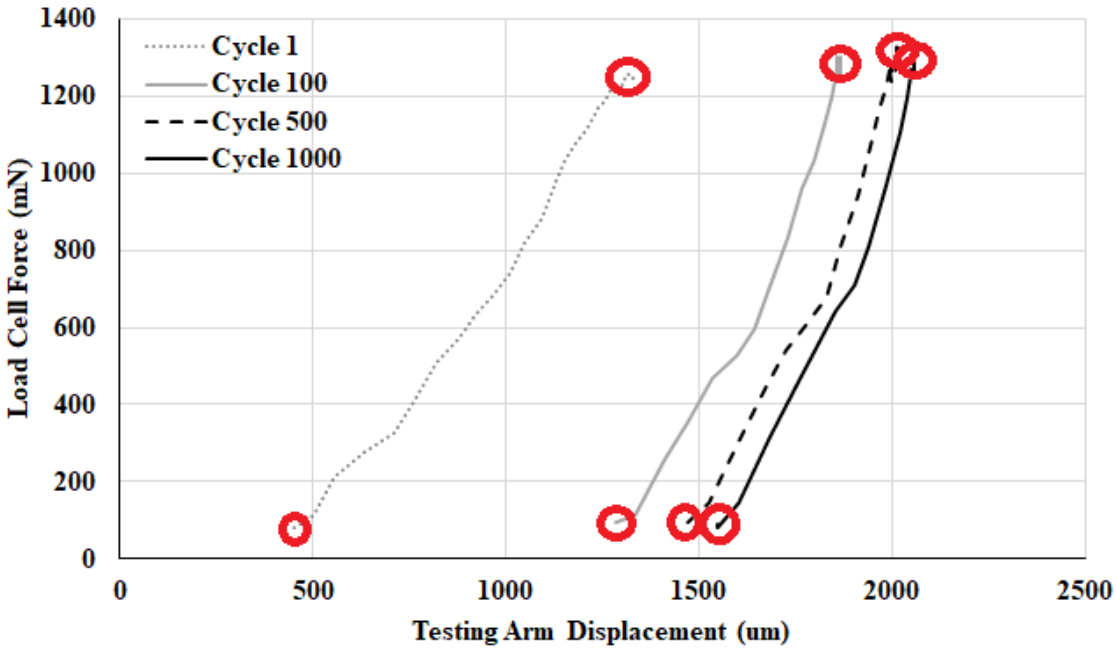

Figure 26. Tangent stiffness was calculated at varying cycles within the testing protocol. Depicted are representative cycles within a specimen; tangent stiffness was calculated using maximum and minimum force and displacement values from the mechanical testing system.

Changes in tendon stiffness have been linked to rotator cuff pathology. Stiffness increases during the secondary phase of fatigue loading, followed by a sharp decrease in stiffness in the tertiary phase of loading immediately prior to tendon failure (Fung et al., 2008). Fung et al (2008) applied a multi-stage *ex vivo* loading protocol; first, tendons were loaded to a sub-failure endpoint based on stiffness loss, then two fatigue loading protocols were applied, separated with an 80 minute recovery period where the tendon was completely unloaded in a slightly slackened state. Return to initial stiffness did not occur following this recovery period, in contrast to loading

induced changes in bone (Jepsen & Davy, 1997; Joo, Jepsen, & Davy, 2007). This reflects the plastic nature of microstructure changes in cyclic loading involving formation of damage patterns of various types, including those that do not involve fiber rupture and are not reversible following the recovery period. Increases in stiffness have been described as an early marker in rotator cuff pathology (Vasishta et al., 2019). Increased stiffness has been observed *in vitro* in individuals via shear wave elastography in the supraspinatus tendon in individuals with idiopathic adhesive capsulitis (Yun et al., 2019). Increased passive stiffness occurred following tendon rupture, with a 100% increase in stiffness compared to individuals without tendon rupture (Hersche & Gerber, 1998). These links between stiffness changes and pathology merits their examination throughout the testing protocol.

5.2.4.2 Hysteresis

Hysteresis was calculated within cycles at multiple points throughout the testing protocol. Hysteresis was defined as the differences in the areas enclosed by the load-displacement curve within a testing cycle (Figure 27). Data was collected at 10 Hz from the mechanical testing system, and all points within this cycle were used for integration of these curves. Hysteresis was calculated such that loss is reported as a positive value; integration of the unloading phase of the curve that resulted in a 15% smaller value is thus deemed a hysteresis value of +15% hysteresis loss. Hysteresis was calculated within a cycle for the 1^{st}, 10^{th}, 100^{th}, 250^{th}, and every 250 cycles until the 1500^{th} cycle. These cycles were selected to provide resolution throughout the loading protocol, particularly at the beginning of loading when changes in hysteresis were predicted to alter the most.

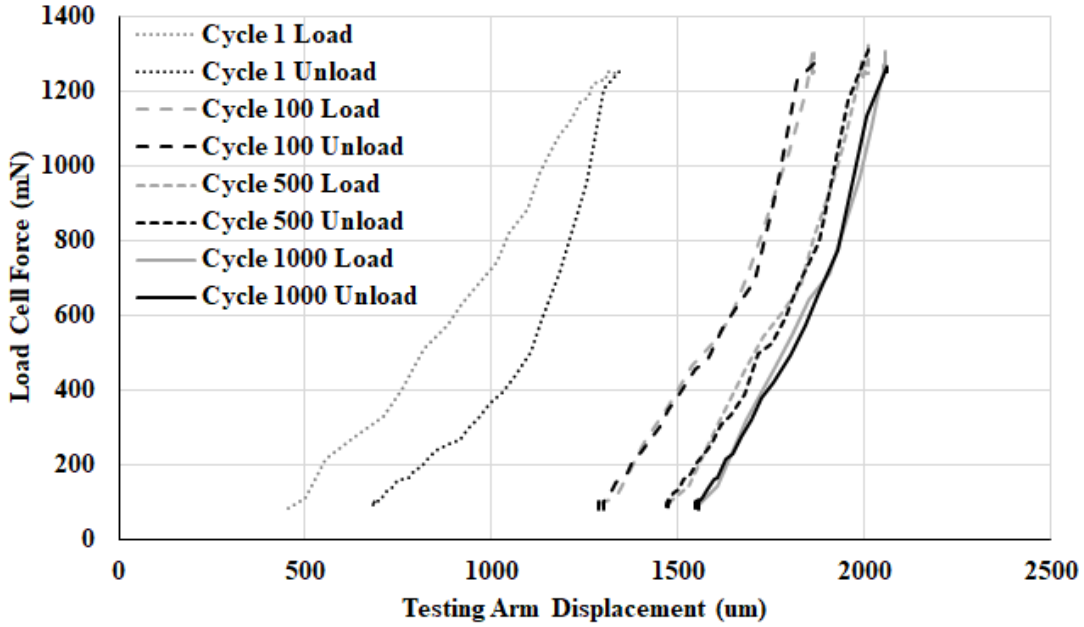

Figure 27. Hysteresis was calculated using load and displacement values from the mechanical testing system. Hysteresis was calculated as the difference between the integrated curves of the loading and unloading phases within a cycle. Loading phases for each cycle are in grey; unloading phases are in black, with different dash types representing different cycles.

Hysteresis was measured throughout the protocol to examine temporal viscoelastic changes. In rat supraspinatus, increased hysteresis occurred in males (Bonilla, Pardes, Freedman, & Soslowsky, 2019), as well as in rat Achilles tendons, where similar results were observed (Pardes et al., 2016). When comparing loading to fatigue at different load intensities, hysteresis loss was not different between low or moderate intensities, but increased hysteresis loss was observed at high load intensities (Fung et al., 2008). Freedman et al (2015) examined a cyclic loading protocol in mouse patellar tendons and observed a steep decrease in hysteresis loss within the first 25 cycles, then a slow decrease in hysteresis across the next 1000 cycles. Examining this change in energy loss throughout the loading protocol provides insight in viscoelastic changes between groups and across these cycles of loading.

Examining this hysteresis can provide insight into changes within the tendon. It has been suggested that changes in the hysteresis of the musculotendinous unit may result from changes in viscosity or friction, particularly in the rearrangement or slipping of collagen fibers (Nordez, McNair, Casari, & Cornu, 2008, 2009). Increased hysteresis may have a detrimental effect on the utilization of elastic energy, particularly within activities using the stretch-shortening cycle, such as walking, running or jumping (Kubo, Kanehisa, Miyatani, Tachi, & Fukunaga, 2003). Increased hysteresis was observed in individuals with peripheral arterial disease, and was described as a significant contributor to decreased walking endurance (King, Vanicek, & O'Brien, 2016). Determining scenarios with increased energy loss could be indicative of increased changes within the tendon, notably at the level of collagen rearrangement.

5.2.4.3 Tendon Stretch

Tendon stretch has been associated with supraspinatus tendon pathology, and is not homogeneous throughout the tendon. Short term cyclic loading *ex* vivo identified that elongation increased at successive loading cycles prior to the occurrence of microscopic failure of fibers (Thornton, Shrive, & Frank, 2002). During fatigue loading tendon peak clamp-to-clamp strain has been shown to increase continuously, following a repeated pattern marked by inflection points at secondary and tertiary fatigue phases (Fung et al., 2008). The authors postulated that tendon clamp-to-clamp strain is a useful and accurate marker of damage accumulation in the progression of tendon fatigue (Fung et al., 2008). When loaded *ex vivo* in fatigue loading with an 80 minute period for recovery, peak strain was found to be nonrecoverable; this observation reflects that the damage which is manifested by the strain increase is structural and not associated with a transient response resulting from fatigue loading (Fung et al., 2008). Using texture correlation analyses from MRI images of cadaveric shoulders, Bey et al (2002) reported significant alterations in supraspinatus

tendon strain with joint position, with increased strains at higher abduction angles. At lower angles, they found that the superior surface sustained increased strains than the inferior surface (Bey et al., 2002). These differences in strain gradients across the surfaces of the supraspinatus tendon suggest differential propensities for tear initiation, particularly on the articular side due to the continuous presence of high tensile loading on this surface (Huang et al., 2005).

Optical tendon stretch was calculated at different cycles throughout the loading protocol. Tendon stretch was calculated by tracking visual tendon features throughout the loading protocol and measuring positional displacements relative to other features. After specimen potting but prior to affixing the specimen within the mechanical testing system, contrast was created on the tendon using powdered graphite applied in a random pattern. A fibre-optic indirect light source was used to improve contrast for imaging while minimizing reflective glare in imaging. Mechanical testing was recorded at 10 Hz using a camera with an image resolution of 1280x690 pixels (Sony XCD-910, Sony Electronics, Inc., Tokyo, Japan). For each specimen, a source image was extracted prior to the first testing cycle but after preload cycles, and displacement of points within the tendon were compared to this source image.

Features were tracked at varying points throughout the loading protocol using a template matching algorithm. Virtual source points were placed over a user-definable region of interest on the source image using high contrast features generated by the powdered graphite. These virtual points were exclusively placed onto the supraspinatus tendon, and differed between specimens. Points were selected by examining the image files and determining the region of the image that contained only the supraspinatus tendon while excluding features that were located on the humerus or the glenoid. These features located on the tendon were selected and processed for subsequent image frames. Movement of each source point was tracked on successive images captured during

the tensile testing using a template matching algorithm (Horst & Veldhuis, 2008). This algorithm relies on changes in surface texture to track points on a tissue sample. The algorithm tracks movement by defining a template of pixels around each virtual point on the source image then searching for a searching for a matching template on subsequent images. Application of powdered graphite in a random fashion increased contrast of these surface features to ensure fidelity of the surface tracking technique. Parametric variations to the tracking algorithm were examined in pilot testing to determine optimal tracking efficiency via altering template size surrounding tracking points from ranges of 5-20 pixels; however, there was no systematic trend in tracking improvement when altering template algorithm range. Similar issues have been encountered by Karakolis et al. (2014) when using an identical setup. As such, each specimen was examined using multiple tracking template parameters, and the range that provided tracking on visual features with minimal error was selected for virtual point processing. These virtual points were exported as XY coordinates following tracking.

Localized tendon stretch was calculated by using coordinates of virtual points and tracking displacement and length changes between these points. The application of powdered graphite prior to mechanical testing provided sufficient contrast to visually estimate the primary fibril direction. In each tracked image, the longitudinal axis of the primary fibril direction of the tendon on this 2D image was determined manually using the same methods as those used to track virtual points above. Localized stretch values were calculated using this fibril direction as a reference system to generate longitudinal and transverse stretch ratio values to correspond to the direction of the tendon. Stretch ratio calculations were completed between these tracked points using Equation 2:

$$\lambda = \frac{l_f}{l_i} \qquad (2)$$

Where λ is the stretch ratio, l_f is the final length between the two tracked points, and l_i is the initial length between the two tracked points. Stretch ratios were chosen over engineering strain to accommodate regional differences within this system. Engineering strain has been described as a small strain measure which loses validity once the strain in a model exceeds ~5%; beyond this value, stretch ratios should be applied (Wu, 2004). Multiple stretch ratios were calculated, including best approximation of complete tendon stretch by selecting the most proximal and distal points, as well as selection of points that were located only on the articular or bursal sides of the tendon. The number of points within each image allowed for multiple stretch ratio calculations along both the bursal and articular sides, but the random location of these points relative to the insertion precluded examination of regional stretch ratio calculation beyond articular or bursal differences.

Displacement of tracked points within the tendon were used to compare tendon displacement to displacement of the arms of the mechanical testing system. Displacement of the mechanical arms of the testing system were exported, and relative displacement of the most proximal and distal tracked points in the direction of the testing arms was calculated. A pixel-to-distance conversion was calculated by placing a measuring tape under the camera at the height of the specimen; 1 pixel was equal to 11 μm. As the camera height was fixed across specimens and the relative distance from the specimen to the camera was equivalent across specimens, this pixel-to-distance ratio was maintained across specimens. This intra-tendon displacement was compared to the mechanical testing arm displacement. Displacement of the tracked points in the same direction of the mechanical testing arms was 88.62 ± 1.73 % of the distance described across all specimens tested. This value is lower than the 92% clamp-to-clamp displacement translated to tendon deformation as described by Fung et al (2008); however, the tracked points did not

encompass the entirety of the tendon; it is likely that possessing points closer to the osteotendinous and musculotendinous junctions would have resulted in calculation values that were greater than the present outcomes. The purpose of this examination was to demonstrate a similarity between the optical and testing system displacements; as all other tissues had been excised and affixed, the only tissue for loading was this tendon and was indicated by these displacement values.

5.2.5 Development of the Cyclic Loading Protocol

Following dissection and testing setup, each specimen completed a testing protocol which consisted of preconditioning cycles followed by a 1500 cycle testing protocol. Each specimen was loaded using one of two load protocols in one of four postures, resulting in eight testing groups. Each load corresponded to the normalized activation observed at that angle using loading scenarios from Chapter III (low load = unloaded hand, high load = bottle in hand equivalent to 40% maximal arm elevation strength), in an attempt to emulate physiological exposures. Prior to experimental testing, sampled were preconditioned using an identical protocol for all specimens. The preconditioning was performed prior to tensile testing to provide all samples with a consistent loading history to allow for more consistent and simplified mathematical interpretation of mechanical properties (Miller, Connizzo, & Soslowsky, 2012). Preconditioning involved 10 cycles of loading from zero to 0.5 N as measured by the load cell at 0.25 Hz. This loading value was chosen to correspond with previous examinations of supraspinatus tendon in Sprague-Dawley rats; Gimbel et al. (2004) completed 10 preconditioning cycles from 0.1 to 0.5 N; Miller et al. (2012) completed 10 preconditioning cycles in Sprague-Dawley supraspinatus tendons at 0.25 Hz at loads between 0.1 and 0.5 N.

Immediately following preconditioning, experimental trials were completed. All specimens were loaded for 1500 cycles at a frequency of 0.25 Hz. This frequency was chosen for

two reasons: to mimic the loading rate used in the preconditioning section, and to provide sufficient time for the testing system to reach the required force loads while minimizing both overshoot of the force levels of the system and static loading of the tendon. This frequency was determined in pilot testing; choosing faster loading frequencies or increased load arm speed resulted in failure to successfully obtain loading levels within 50 mN without overshoot. 1500 cycles was selected to represent the peak number of repetitive cycles that may be completed in an 8 hour work day in an industrial setting (Potvin, 2012). The goal of this testing protocol was not explicitly to generate tendon failure; instead, the goal was to have test specimens with loading emulative of that encountered over the course of a work day. Pilot testing indicated that even after 4000 cycles of loading the intensities used in this study did not result in failure of the tendon. At the end of 1500 cycles each specimen was in the secondary phase of fatigue based on rake displacement within cycles; previous testing of 1000 cycles at 1 Hz showed an initial rapid strain increase within 100 cycles, followed by a much slower steady increase in strain (Fung, Wang, et al., 2010; Fung et al., 2008); a similar outcome was observed in the current specimens (Figure 28).

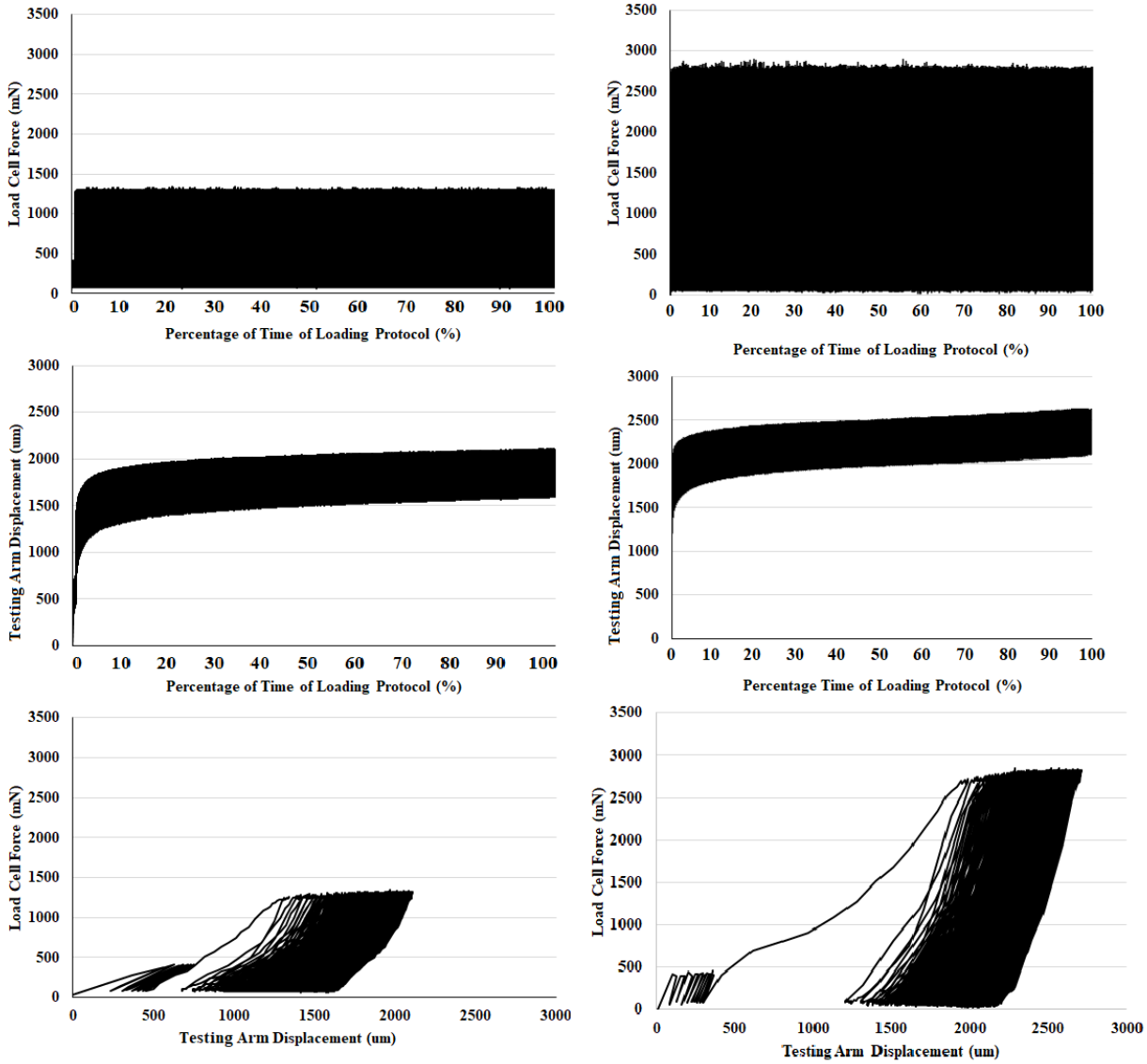

Figure 28. Representative specimen loading responses, as described by the testing system. The graphs on the left are from a specimen in the 30° low loading protocol; specimens on the right are from a 75° high load protocol. These graphs include 10 cycles of preload to 0.5 N (visible in bottom row of graphs), then 1500 cycles of loading at the specified load level. Load cell force over time (top), rake displacement over time (middle) and load over displacement (bottom) are depicted.

5.3 Methods

This study centered on *in vitro* mechanical testing of the supraspinatus in an animal model to characterize scenarios that may modulate changes in tendon mechanical behaviour. Two independent variables (applied tendon load and glenohumeral elevation angle) were modulated to simulate human upper extremity postures and load intensities (Figure 29).

5.3.1 Materials

A total of 48 shoulders were harvested from healthy rats. All specimens were right shoulders of healthy Sprague-Dawley rats aged between 9 weeks and 12 months; the age of these specimens aligns with previous animal model rotator cuff examinations (Soslowsky et al., 2000). Only the right shoulder was used to ensure that differences observed were not confounded by bilateral differences. The rats acted as control animals in a previous research study, and experienced normal cage activity. Sample size was selected via an a priori power analysis completed using G*Power 3.1 (Universität Düsseldorf, Düsseldorf, Germany). It indicated that 40 specimens was sufficient to obtain adequate power (Cohen, 1992; Faul et al., 2007). The effect size chosen ($f^2 = 0.5$) represented a conservative effect size compared to prior *in vitro* studies using Sprague-Dawley rats, which had effect sizes from 0.81-5.2 for tangent stiffness (Fung et al., 2008; Reuther, Thomas, Tucker, Yannascoli, et al., 2014), 0.7–4.02 for strain (Fung et al., 2008; Thornton et al., 2002), and 0.5-3.5 for hysteresis (Sereysky, Andarawis-Puri, Jepsen, & Flatow, 2012; Veres et al., 2013b).

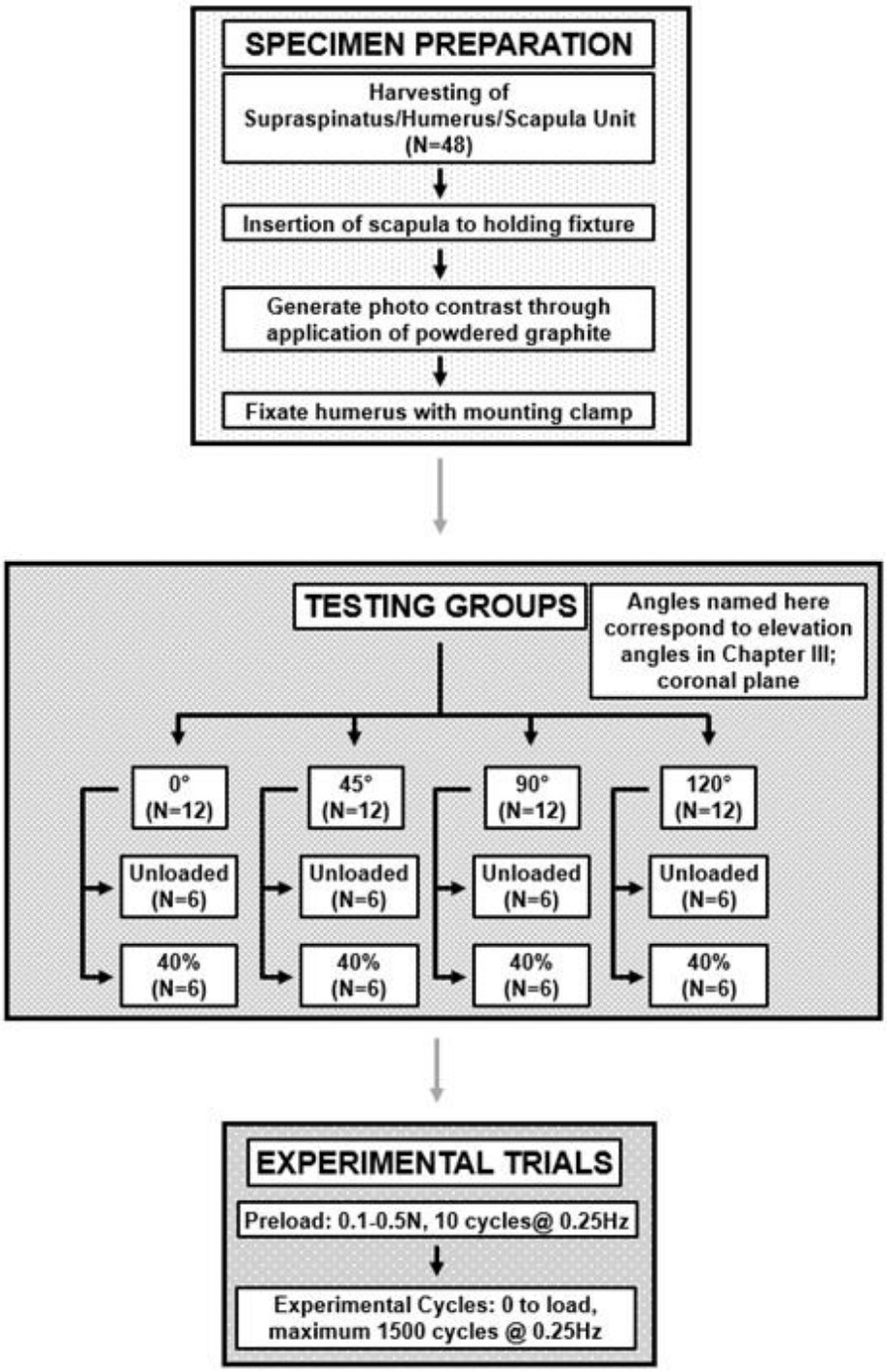

Figure 29. Graphic interpretation of Chapter V experimental protocol. Study collection consisted of specimen preparation and mounting, then experimental trials. Specimens were placed in one of eight testing groups.

5.3.2 Specimen Preparation

Specimen preparation consisted of supraspinatus harvesting and mounting. Rat shoulders were dissected free of excess soft tissue, retaining the humerus, scapula, supraspinatus muscle and tendon. Specimen dissection was completed identically for all tests. Specimens were affixed into custom 3D printed mounting pots made of ABS plastic, which had different orientations depending on angle testing group (Figure 30). The specimen was fixed in the pot using 18-gauge stainless steel wire threaded through the scapula at 1/3 and 2/3 of the proximal distance of the scapula, and was then fixated with dental plaster (Denstone, Miles, South Bend, IN, USA). The specimen was affixed in the dental plaster so that the entirety of the scapula was inserted up to immediately beneath the glenoid rim. This mounting pot was placed onto one arm of a biaxial tissue testing system (BioTester 5000, Waterloo Instruments Inc., Waterloo, ON), while the humerus was clamped onto another end of the biaxial testing system using a mounting clamp and affixed with self-adhesive grip tape (Figure 30D). The epicondyles of the humerus were removed prior to testing to prevent axial humeral rotation when securing the clamp. One 5-N load cell with an accuracy of 0.2% of rated full scale and two stepper motor actuators with a resolution equivalent to 1 μm and maximum movement frequency of 100Hz was sampled at 10 Hz and was used to track force and displacement throughout mechanical testing.

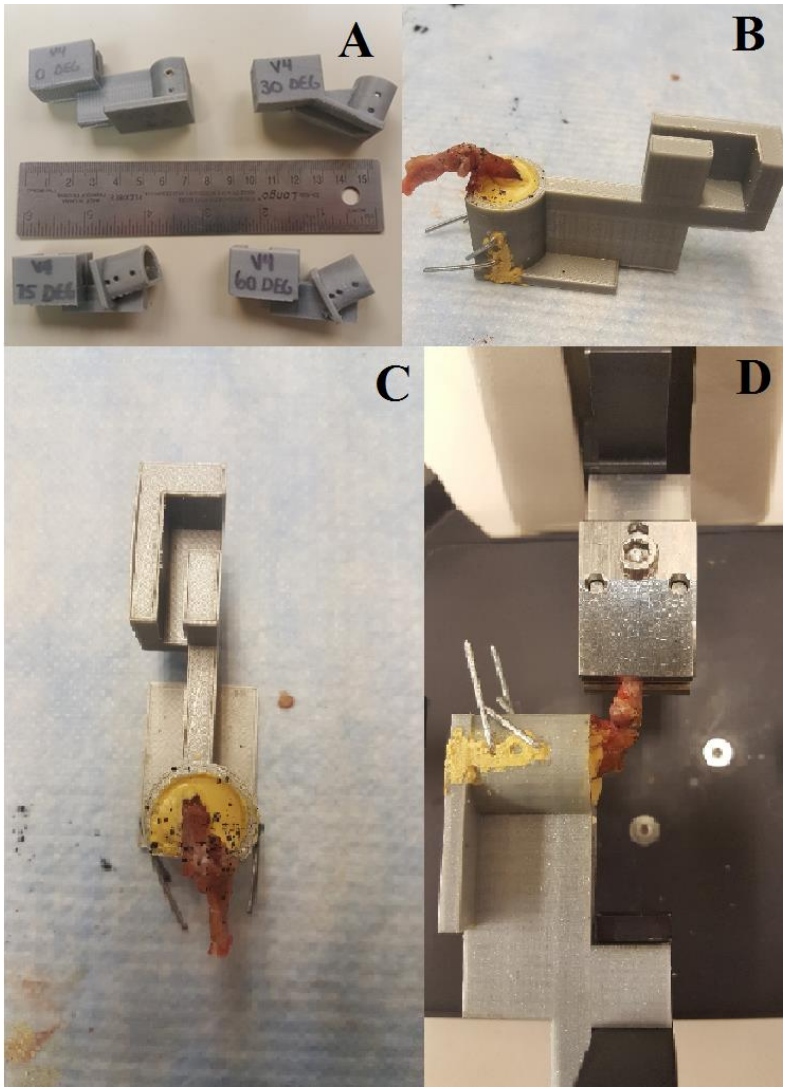

Figure 30. Each specimen was placed in one of four mounting pots with differing scapular orientations (A), and affixed with 18-gauge wire and dental plaster (B, C). This unit was mounted on one end to the neck of one arm of the testing apparatus, and the humerus was clamped on the other end (D).

To avoid dehydration during testing, the tissue samples were kept in a controlled relative humidity chamber. A partially enclosed polyethylene dome was placed around the tissue sample and connected to an ultrasonic humidifier (Repti Fogger, Zoo Med, San Luis Obispo, CA). This humidifier delivered constant humidity using distilled water (Gruevski, Gooyers, Karakolis, & Callaghan, 2016).

Image capture was conducted during trials to enable local strain derivation in post-processing. Tissue samples were marked with graphite powder to track displacement of features for stretch ratio calculations. Tests were recorded with a camera at a rate of 10 Hz, and image resolution of 1280x690 pixels (Sony XCD-910, Sony Electronics, Inc., Tokyo, Japan). A source image was taken from the sample at zero load after the final preload cycle and prior to the first experimental testing cycle, and virtual points were generated from the contrast created by the applied powdered graphite. The movement of these virtual points was tracked in successive images using a template-matching algorithm used previously for tissue testing (Eilaghi et al., 2009; Horst & Veldhuis, 2008). A fibre-optic indirect light source was used to provide adequate contrast without generating reflective glare in imaging.

5.3.3 Postural Selection

Four glenohumeral postures were examined. The scapula was constrained in position, and the glenohumeral joint was positioned at 0º, 30º, 60º and 75º of glenohumeral elevation in the sagittal plane. These glenohumeral angles correspond to arm postures of approximately 0º, 45º, 90º and 120º abduction (Itoi et al., 1996).

5.3.4 Specimen Loading Procedures

The viscoelastic properties of the supraspinatus tendon were examined through tensile testing. This loading protocol consisted of applying a preload, then a cyclic loading protocol. Each specimen only underwent one cyclic loading protocols described below.

5.3.4.1 Translation of Human EMG to Loading Levels for Tissue Testing

Activations from the two human supraspinatus regions were used to determine *in vitro* load levels. These values from human anatomy were used to specify the loading in the rat supraspinatus

using activations of the normalized anterior and posterior regions of the supraspinatus respectively as described by the outcomes of the study in Chapter III , and cross-sectional area of the anterior and posterior human supraspinatus as described by the literature (Kim et al., 2007) and scaled to the maximal force capability between human and rat supraspinatus tendon, as detailed in Section 5.2.2 (Figure 31). The direction of this force vector was parallel to the centre line of the tendon. The normalized supraspinatus activation observed at 0º, 45º, 90º and 120º of abduction within the coronal plane in work completed in Chapter III was used to set activation characteristics for the *in vitro* testing.

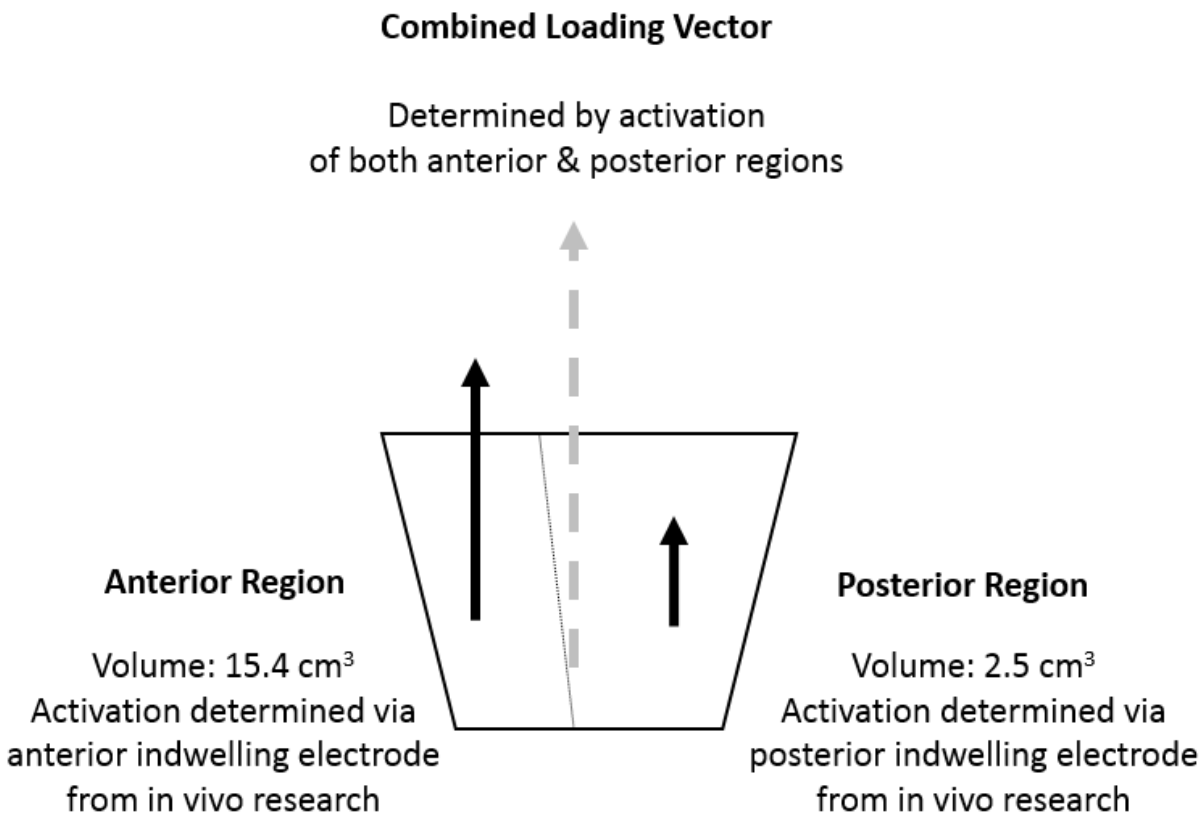

Figure 31. Representative load vector in supraspinatus testing. The vector was determined by relative contributions of both supraspinatus regions, incorporating cross sectional area and activation from Chapter III.

5.3.4.2 Preconditioning

Each specimen underwent preconditioning prior to experimental testing. This preload consisted of 10 cycles of uniaxial tension from zero to 0.5 N at a rate of 0.25 Hz. The force magnitude used in this preload regimen is consistent with previous research using rat supraspinatus tissue for mechanical testing (Freedman, Zuskov, Sarver, Buckley, & Soslowsky, 2015; Soslowsky et al., 2000).

5.3.4.3 Loading Protocol

Each specimen was loaded using one of two load protocols in one of four postures, resulting in eight testing groups. Each load corresponded to the normalized activation observed at that angle using loading scenarios from Chapter III (low load = unloaded hand, high load = bottle in hand equivalent to 40% maximal arm elevation strength). These tendons were fatigue tested at 0.25 Hz between an unloaded state and the force level described by activation from Chapter III and conversion to force values through Eq. 1 (Table 2).

Table 2. Force load levels for each of the 8 testing groups, as determined by *in vivo* EMG results and conversion to force values for *in vitro* animal testing

		Load (percentage of maximal elevation strength from *in vivo* work; loads are in N)	
		Low Load (LL)	**High Load (HL)**
Glenohumeral Angle (Degrees)	**0**	0.4	0.5
	30	1.3	2.4
	60	1.5	2.6
	75	1.6	2.7

Previous fatigue load magnitudes for rat supraspinatus were between 2-4 N, representing 25-75% of its ultimate failure load (Freedman et al., 2015). The tendons were repetitively loaded

for 1500 cycles (Figure 32). During loading, force and displacement data were collected at 10 Hz using LabJoy (Cellscale, Waterloo, ON). Upon completion of testing, all samples were retained and returned to the institution Central Animal Facility for incineration.

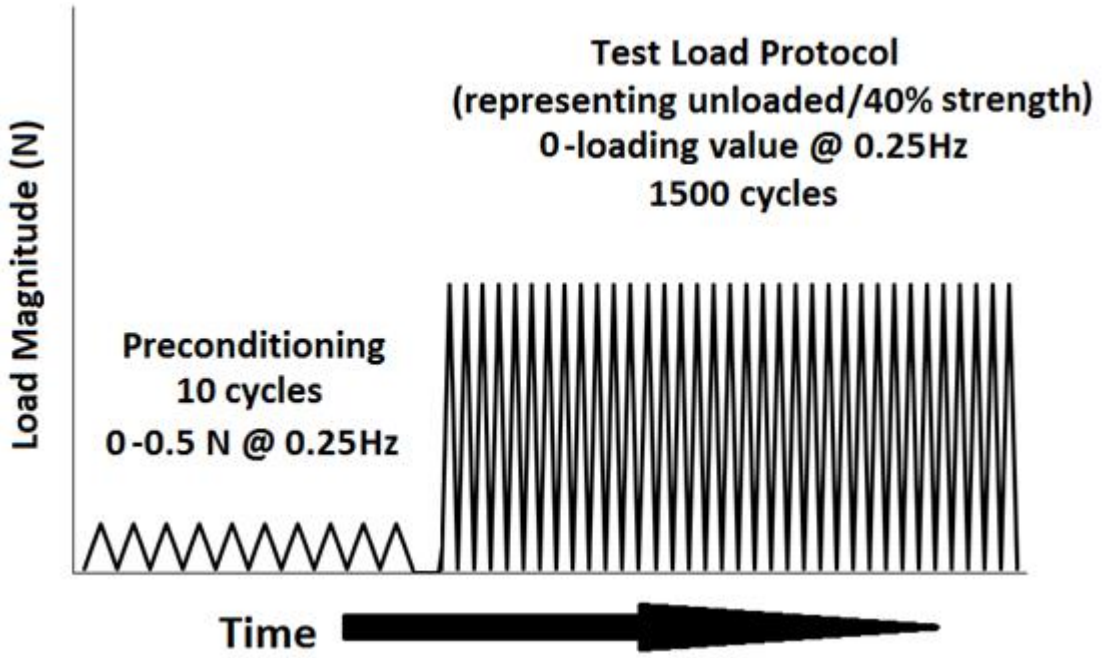

Figure 32. Representative *in vitro* load protocol of each rat supraspinatus specimen.

5.4 Data Analysis

Several post processing tissue parameters were computed for each test specimen at specific time points. These mechanical parameters were extracted from the first testing cycle, as well as the 10^{th}, 100^{th}, 250^{th}, and then every 250 cycles until the 1500^{th} cycle. The selection for every 250 cycles was to provide insight into tissue parameter changes throughout the loading protocol while balancing sufficient resolution and data management. Mechanical parameters included maximum and minimum cyclic displacement, tangent stiffness, and hysteresis, as described in Section 5.2.4.

Stretch ratios as determined by image processing were extracted at defined time points. Stretch ratios were calculated for the supraspinatus tendon by comparing displacement of tracked points from specimen images in the first, 10^{th}, 100^{th} and 1500^{th} testing cycles to the unloaded specimen at the end of the final preload cycle (Figure 33). These points were generated through the use of powdered graphite applied in a random fashion; points were not identical between specimens. Points on the tendon were selected for their high visual contrast and ability to be reliably identified tracked throughout successive images; the tracking algorithm relies on the surface texture being visible to the camera. The longitudinal fiber direction was tracked in each frame; this fiber direction was used to define the longitudinal and transverse stretch ratio dimensions in subsequent frames. The unloaded frame immediately prior to the first loading cycle was used to normalize stretch ratios for each subsequent tracking frame. The imaging frame associated with the peak loading within the cycle as described by the mechanical testing system was selected for tracking within each desired testing cycle. The most proximal and distal tracked points within the tendon were used to calculate a stretch ratio for the overall tendon; in addition, stretch ratios were calculated using adjacent points on the articular and bursal sides of the tendon to provide insight into differences in stretch ratios between these two sides of the tendon. As multiple points were available on the articular or bursal portions of the tendon, multiple stretch ratios could be calculated for the articular or bursal sides of the tendon; however, the location of these points and the number of available comparisons varied across specimens.

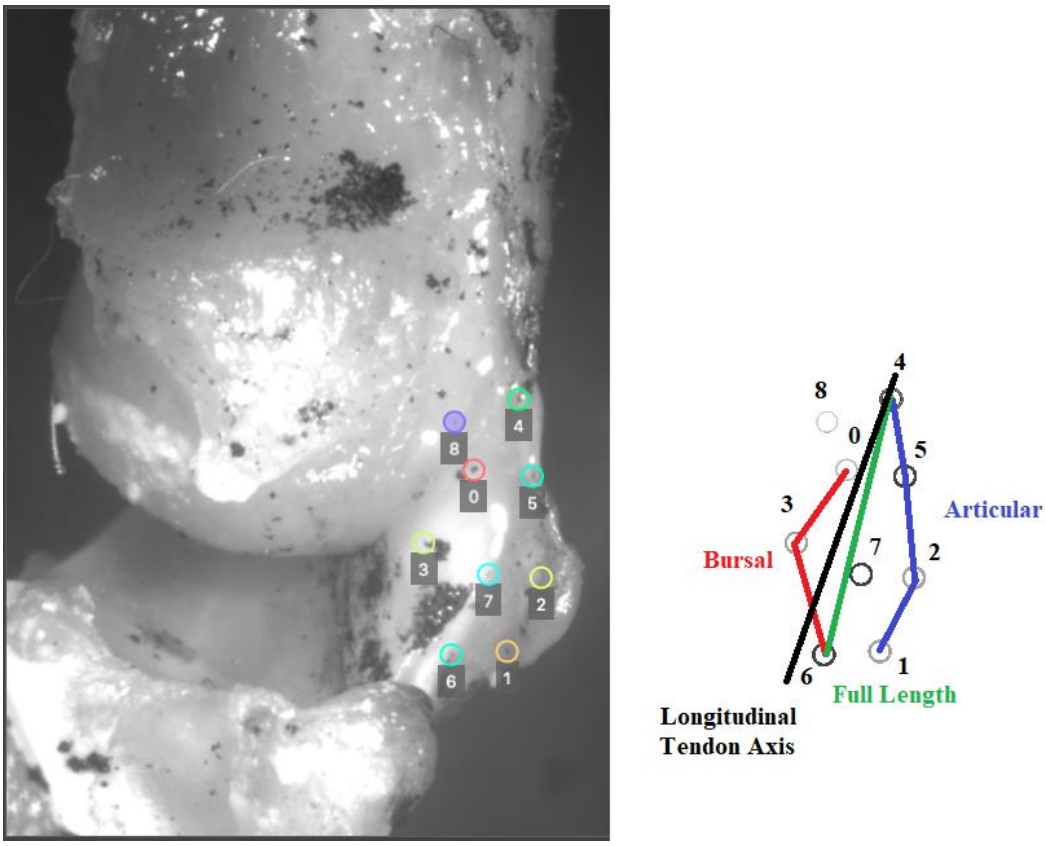

Figure 33. Virtual points were tracked across the supraspinatus tendon to be used to generate stretch ratios in post-processing. Shown above is a specimen in the 30° elevation condition at the low load. A full length stretch ratio was calculated using the points connected in green; individual stretch ratios were calculated on the articular (blue) and bursal (red) sides of the tendon. These ratios were calculated relative to a coordinate system aligned with the primary fibre direction of the tendon (black).

Statistical analyses examined the effects of position and load intensity on supraspinatus tendon responses. To examine interactions between elevation angle and the magnitude of loading on changes in tendon mechanical properties, a two-factor mixed general linear model (load, elevation angle, load*elevation angle) was applied to the dependent variables of maximum and minimum displacement, tangent stiffness, hysteresis and stretch ratios, with cycle number as a repeated measure. Simple effects were used to analyse all significant interactions. These analyses were completed using JMP 14.0 software (SAS Institute, North Carolina, USA), with post-hoc analysis as indicated by the general linear model.

5.5 Results

Outcome measures for tangent stiffness, hysteresis, maximum and minimum displacement and stretch ratios were influenced variously by glenohumeral elevation angle, loading level and cycle number, as well as interactions between these variables. No specimens experienced complete rupture or failure of the tendon throughout the loading protocol. Each of the dependent variables are discussed separately below.

5.5.1 Tangent Stiffness

A significant three-way interaction ($p=0.0009$) between elevation angle, load magnitude and cycle number existed for tangent stiffness (Figure 34). Subsequent analysis of interactions between elevation angle and load magnitude at each observed load cycle revealed significant main effects of elevation angle at all cycles except the first and 10^{th} cycles ($p=0.0015$ to 0.0289) (Table 3). Specifically, specimens assigned to the 75° elevation group were significantly different than the 0° group in all significant cycles, as well as significantly different than all specimens in the 30° group except at the 100^{th} cycle, when they were not significantly different from one another. The 60° specimen group was not significantly different from any other angles at the same cycle except in the 750^{th} cycle, when greater tangent stiffness was observed in the 60° group (3.46 mN/μm) than the 0° group (2.42 mN/μm). The greatest stiffness was observed in the high load intensity group at 75° of glenohumeral elevation (4.64 mN/μm); this group also experienced a 49% increase in stiffness throughout the loading protocol. The smallest changes between the first and final cycles were in the low load at 0° and high load at 30° groups; stiffness in both of these groups increased by less than 6.2% (Figure 34). Significant main effects of load magnitude were present at each

observed cycle (p=0.011 to 0.0267), with increased stiffness in the high load magnitude for all cycles.

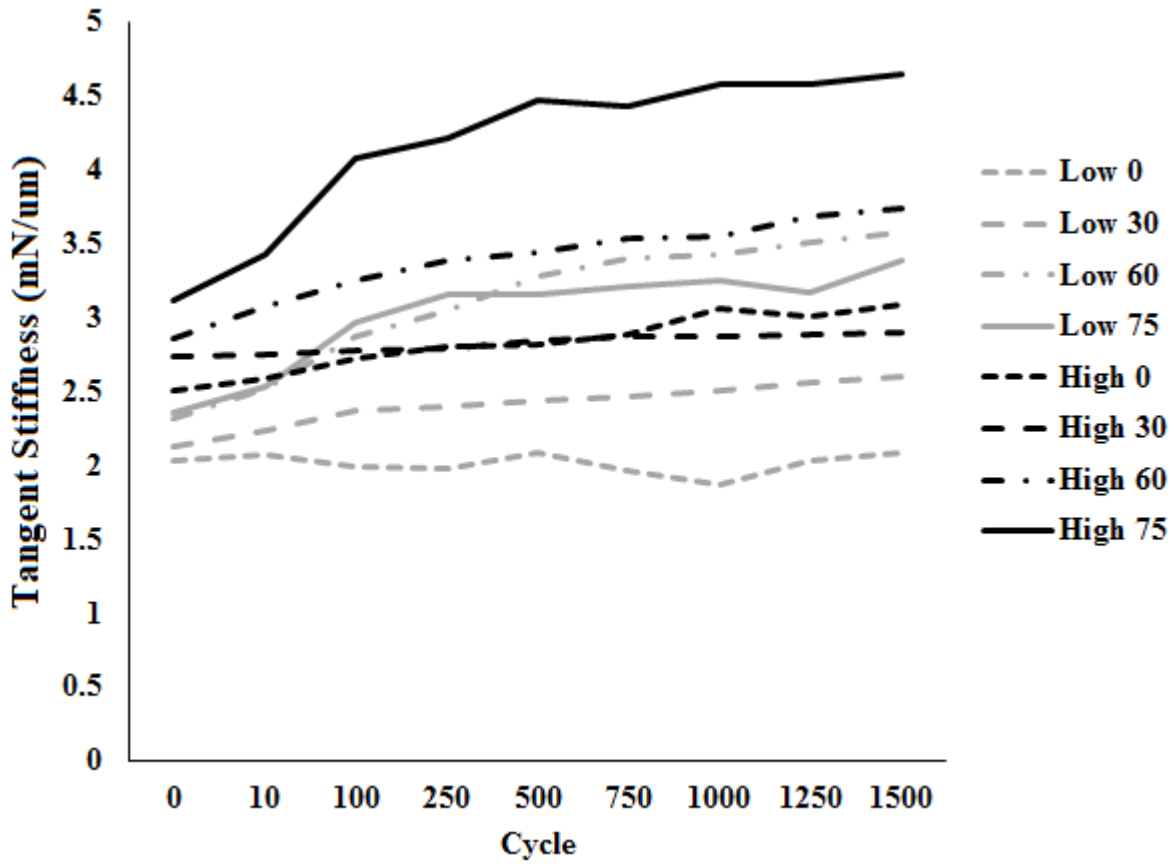

Figure 34. A three-way interaction affected tangent stiffness (p=0.0007). Specimen groups with the same elevation angle have common dash types, with high load intensities in black and low load intensities in grey. Typically, higher elevation angles had increased stiffness compared to lower elevation angles, higher load intensities had increased stiffness compared to low load intensities, and stiffness increased within a specimen with subsequent cycles.

Table 3. Tangent stiffness measurements by elevation angle, load magnitude and cycle number, in mN/μm. Shaded p values indicate significant differences. Significant differences within elevation angle and load magnitude by cycle number are denoted by letters; values not sharing a letter are significantly different.

		Elevation Angle					Load Magnitude	
Cycle	P value	0	30	60	75	P value	High	Low
1	0.642	2.27	2.43	2.58	2.73	0.0305	2.8 (A)	2.2 (B)
10	0.3657	2.33	2.49	2.79	2.98	0.0315	2.96 (A)	2.34 (B)
100	0.0289	2.36 (B)	2.58 (AB)	3.06 (AB)	3.52 (A)	0.0267	3.21 (A)	2.55 (B)
250	0.0078	2.39 (B)	2.59 (B)	3.21 (AB)	3.69 (A)	0.024	3.3 (A)	2.65 (B)
500	0.0042	2.45 (B)	2.64 (B)	3.36 (AB)	3.81 (A)	0.0254	3.39 (A)	2.74 (B)
750	0.0015	2.42 (C)	2.66 (BC)	3.46 (AB)	3.82 (A)	0.0145	3.43 (A)	2.76 (B)
1000	0.0023	2.47 (B)	2.69 (B)	3.48 (AB)	3.92 (A)	0.011	3.51 (A)	2.76 (B)
1250	0.0039	2.52 (B)	2.72 (B)	3.59 (AB)	3.87 (A)	0.0163	3.53 (A)	2.82 (B)
1500	0.0026	2.58 (B)	2.75 (B)	3.66 (AB)	4.02 (A)	0.0256	3.59 (A)	2.91 (B)

5.5.2 Hysteresis

A three-way interaction between elevation angle, load magnitude and cycle number influenced hysteresis measures (p=0.0002, Figure 35). Examining interactions of elevation and load at each observed load cycle indicated increased hysteresis in the 75° conditions in the first cycle (p=0.0444) and increased hysteresis at high loads at the 10^{th} and 100^{th} cycles (p=0.228 and 0.028, respectively) (Table 4). In the first cycle, hysteresis was significantly increased for specimens in the 75° arm elevation condition (17.72% hysteresis loss) than any other condition. In the 10^{th} and 100^{th} cycles, hysteresis loss was increased in the high load conditions than low load conditions, with 6.58% and 5.79% in the high loads and 3.88% and 3.49% in the low loads for the 10^{th} and 100^{th} cycles, respectively.

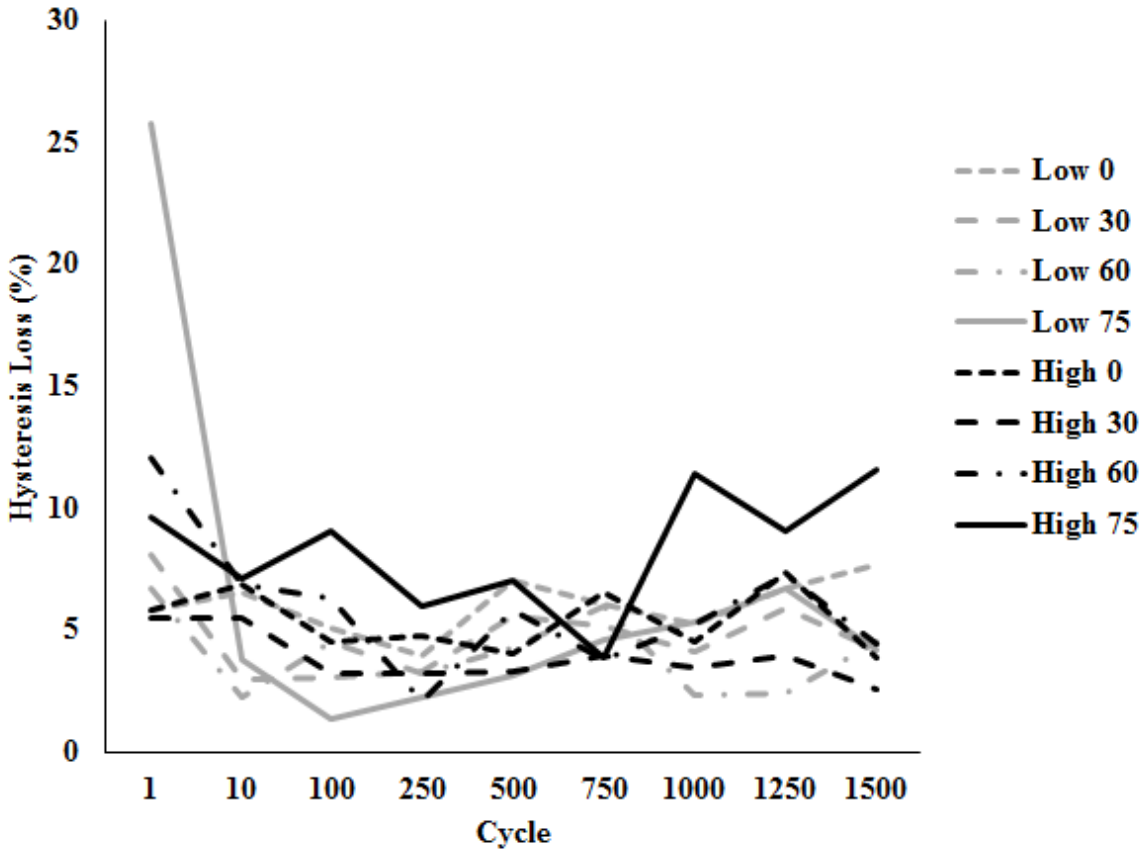

Figure 35. A three-way interaction affected hysteresis (p=0.0002), with the greatest hysteresis in the highest elevation angle and load magnitude in the first load cycle.

Table 4. Hysteresis loss measurements by elevation angle, load magnitude and cycle number, in % hysteresis loss. Shaded p values indicate significant differences. Significant differences within elevation angle and load magnitude by cycle number are denoted by letters; values not sharing a letter are significantly different.

		Elevation Angle					Load Magnitude	
Cycle	P value	0	30	60	75	P value	High	Low
1	0.0444	5.79 (B)	6.79 (B)	9.39 (B)	17.72 (A)	0.2977	8.25	11.59
10	0.4308	6.71	4.2	4.54	5.47	0.0228	6.58 (A)	3.88 (B)
100	0.3704	4.78	3.15	5.43	5.2	0.028	5.79 (A)	3.49 (B)
250	0.5797	4.37	3.28	2.66	4.13	0.3935	4.03	3.2
500	0.9354	5.56	4.43	5.07	5.08	0.9805	5.05	5.02
750	0.6762	6.32	4.56	4.85	4.23	0.4786	4.54	5.44
1000	0.0544	4.88	3.8	3.78	8.3	0.156	6.15	4.25
1250	0.3485	7.07	4.93	4.86	7.9	0.3164	6.93	5.45
1500	0.2861	5.82	3.39	7.96	7.87	0.4972	5.61	6.91

5.5.3 Maximum and Minimum Cyclic Displacement

Elevation angle and cycle number influenced maximum and minimum displacement, while load did not. An interaction between elevation angle and cycle number affected minimum displacement ($p=0.0482$, Figure 36). Minimum displacement increased within each elevation angle as cycle number increased, but this increased displacement affected higher elevation angles more than lower elevation angles. Minimum displacement ranged from 215.7 ± 104.6 μm in the first cycle at the 0° elevation angle to 2550.3 ± 424.7 μm in the 1500th cycle at the 75° elevation angle. Main effects of cycle and elevation angle affected maximum displacement ($p<0.0001$ and $p=0.0087$), respectively. Increasing cycles resulted in increased maximum displacement; significant increases in displacement were observed for the 1500th cycle compared to the 1st, 10th, 100th and 250th cycles (Figure 37). This main effect of cycle on maximum displacement was significantly lower in the 0° elevation (611.0 ± 200.2 μm) than all other elevation angles, but the 30°/60°/75° elevation angles were not significantly different from one another (2337.6 ± 381.6 μm, 2238.3 ± 396.5 μm and 2265.7 ± 348.2 μm, respectively).

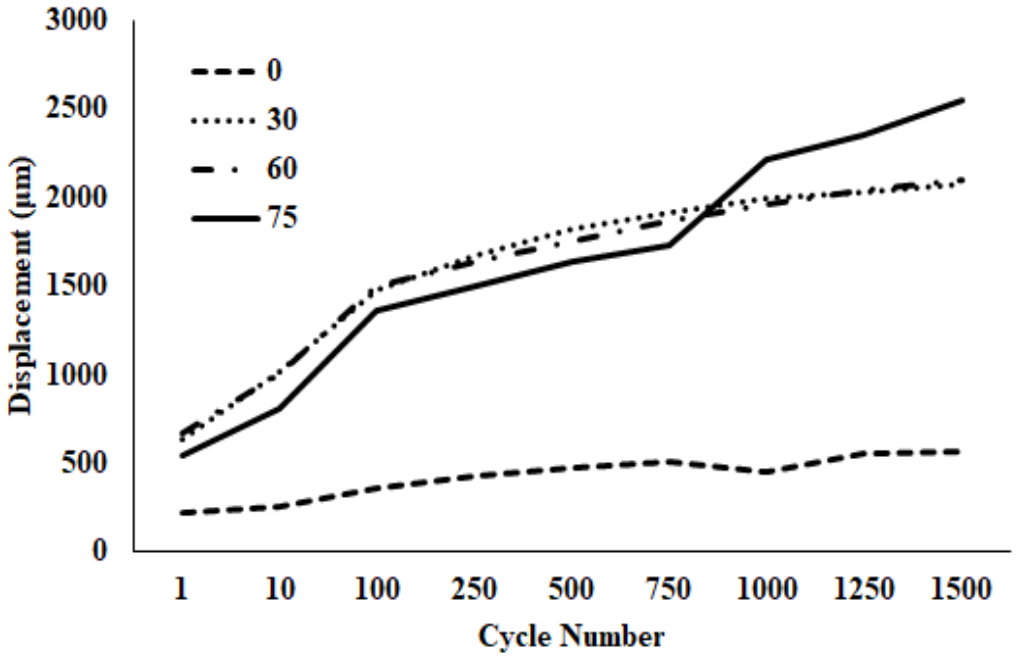

Figure 36. Minimum displacement was affected by an interaction between elevation angle and cycle number (p = 0.482), with the greatest displacement occurring in increased elevation angles and later cycle numbers.

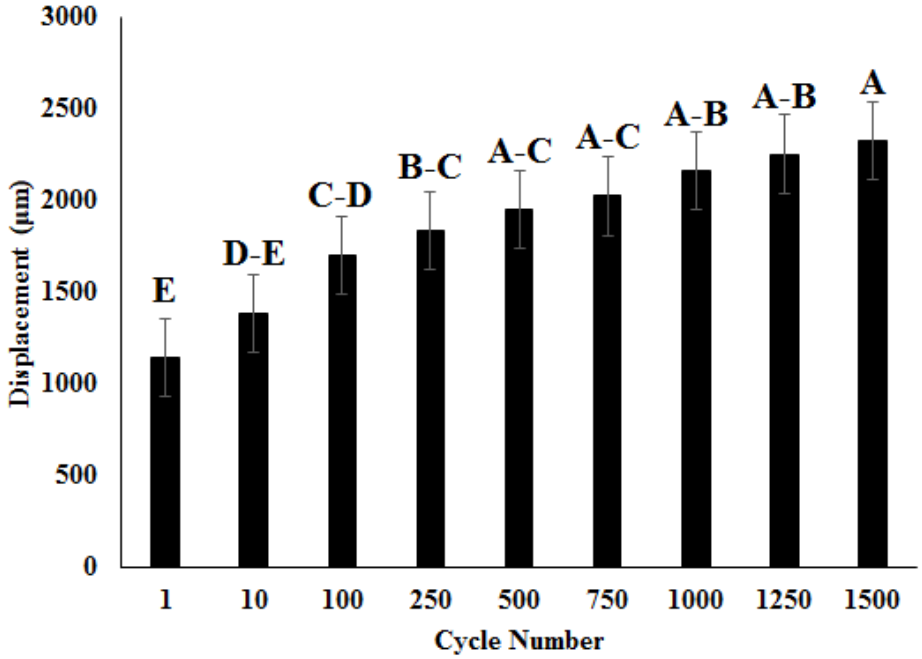

Figure 37. Maximum displacement was affected by a main effect of cycle number (p<0.0001), with increasing cycles resulting in increased maximum displacement. Significant post-hoc differences are denoted by letters; bars not sharing a letter are significantly different.

5.5.4 Stretch Ratios

Elevation angle, load intensity and cycle number affected longitudinal and transverse stretch ratios, with some interactions. A three-way interaction between elevation angle, load intensity and cycle number affected longitudinal stretch ratios ($p = 0.0396$), while an interaction between elevation angle and cycle number ($p = 0.0141$) influenced transverse stretch ratios. While load intensity affected longitudinal stretch ratios, it did not affect transverse stretch ratios ($p = 0.2581$). Generally, increased elevation angles, load intensities and cycle numbers resulted in increased longitudinal and decreased transverse stretch ratios. When examining articular and bursal stretch ratios, higher longitudinal stretch ratios were observed on the bursal side at low elevation angles, but higher stretch ratios on the articular side at high elevation angles.

A significant three-way interaction ($p = 0.0396$) between elevation angle, load magnitude and cycle number existed for longitudinal stretch ratios (Figure 38), while an interaction between elevation angle and cycle number altered transverse stretch ratios ($p = 0.0141$), but load intensity did not affect transverse stretch ratios ($p = 0.6729$). Subsequent analysis of longitudinal interactions between elevation angle and load magnitude at each observed load cycle revealed significant main effects of both factors at the 1^{st} and 10^{th} cycles ($p<0.0001$), but no interaction ($p = 0.0576$ and 0.10, respectively), and interactions between elevation angle and load intensity at the 100^{th} and 1500^{th} cycles ($p = 0.0014$ to 0.0032). Specifically, the high intensity generated larger stretch ratios than the low intensity in the 1^{st} (1.0230 and 1.0137, respectively) and 10^{th} (1.0292 and 1.0182, respectively) cycles. In these 1^{st} and 10^{th} cycles, specimens in the 75° and 60° elevation angles had larger stretch ratios than specimens in the 30° or 0° conditions (1.0253, 1.0306, 1.0089, and 1.0086 for the 10^{th} cycle; 1.0346, 1.0348, 1.0149, and 1.0104 for the 10^{th} cycle, respectively), but the 75° and 60° specimens were not different from one another, and the 30° and 0° specimens

were not different from one another. Interactions between elevation angle and intensity in the 100th and 1500th cycles observed the greatest increase in stretch ratios in specimens assigned to the high load intensity and 75° elevation angle, with stretch ratios of 1.0545 in the 100th cycle and 1.0643 in the 1500th cycle (Figure 37). An interaction between elevation angle and cycle number affected transverse stretch ratios ($p = 0.0141$), with higher cycle elevation angles and cycle numbers resulting in more compressive stretch ratios.

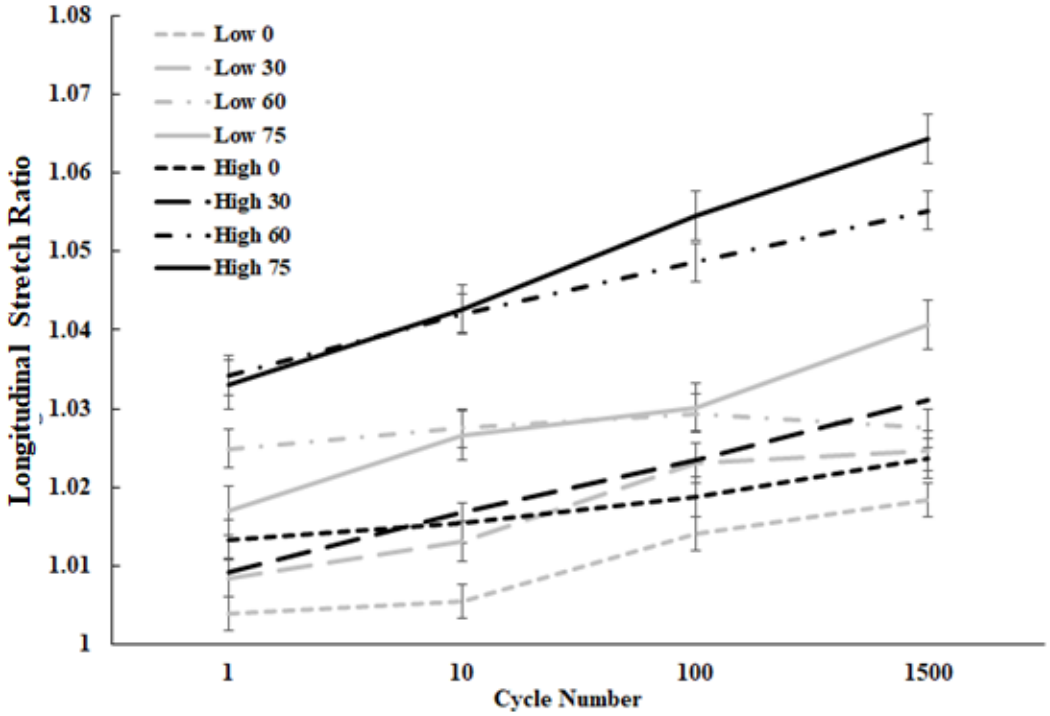

Figure 38. Longitudinal stretch ratios were altered by a three-way interaction between elevation angle, load intensity and cycle number. Generally, increased elevation angles, load intensities and cycle numbers increased longitudinal stretch ratios.

Articular and bursal stretch ratios had similar responses to one another, with alterations in longitudinal stretch ratios for both sides of the tendon changing with each main effect ($p<0.0001$), as well as an interaction between elevation angle and load intensity ($p = 0.0014$ and 0.0209 for articular and bursal, respectively). Articular longitudinal stretch ratios were greatest in the high

load condition at 75° of glenohumeral elevation, which was significantly different than all conditions except the 60° high load condition (Figure 39). An identical trend was observed in bursal longitudal stretch ratios ($p = 0.0209$), although articular stretch ratios had lower absolute magnitudes high glenohumeral elevation angles and higher absolute magnitudes at lower elevation angles.

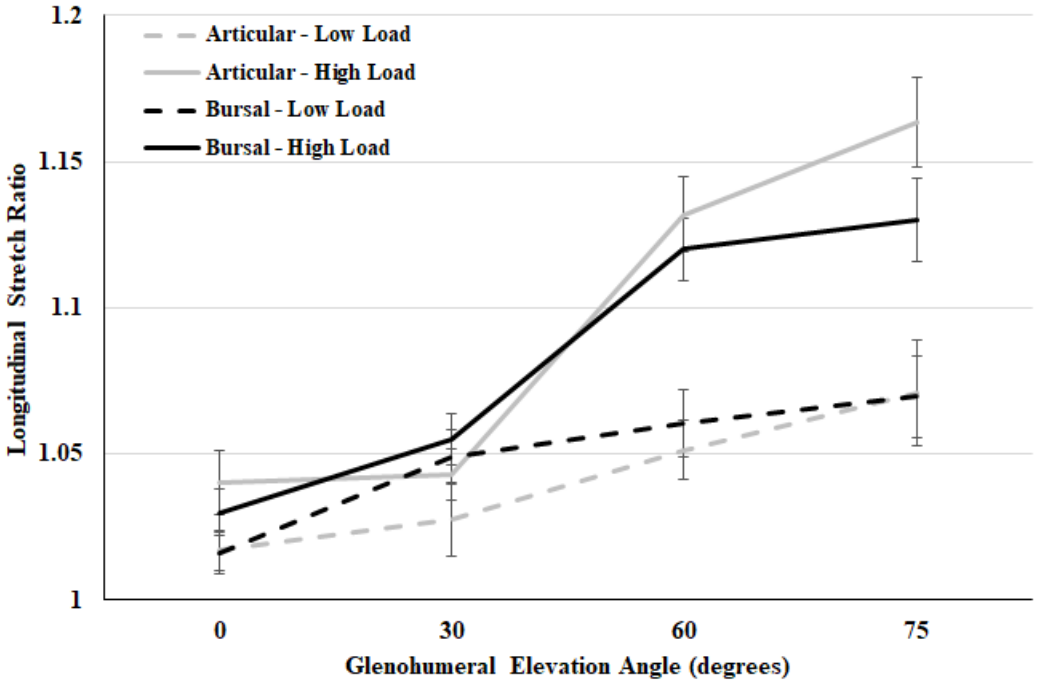

Figure 39. Articular and bursal longitudinal stretch ratios were altered by an interaction between glenohumeral elevation angle and load intensity; increasing load intensities and elevation angles resulted in increased longitudinal stretch ratios.

5.6 Discussion

The purpose of this research was to examine mechanical changes in the rat supraspinatus tendon when exposing these specimens to loading scenarios emulative of the activation and postural conditions seen *in vivo*. Observed differences between these scenarios indicated increased mechanical loading in the highest elevation angle, as well as interactions between posture, load and repetition. These differences occurred across most of the examined mechanical variables, while 3-way interactions in both tangent stiffness and hysteresis indicated complex relationships between load, posture and repetition. The three hypotheses outlined in the introduction were supported; hypotheses 1 described an interaction between glenohumeral elevation angle and load intensity on tangent stiffness, hysteresis and stretch ratios, with the highest responses in the highest elevation angle and highest load. Differences between the articular and bursal stretch existed in the high load condition but were less evident in the low load conditions, resulting in partial support of this hypothesis. The final hypothesis described elevated responses in tangent stiffness, maximum and minimum cyclic displacement and stretch ratios with increased cycle numbers; this was observed in each of these metrics, supporting this hypothesis.

This primary objective of this loading protocol was to leverage muscular activation observed *in vivo* and scale this loading in humans to an animal model to detail how these postures and load intensities might alter mechanical properties of the supraspinatus tendon. This necessitated the development of a novel testing approach as described in Section 5.2 that retained a complete supraspinatus unit to generate glenohumeral elevation postures while loading the tendon. While current knowledge describes how glenohumeral posture affects mechanical behaviour of the supraspinatus tendon (Bey et al., 2002), this facet is typically ignored when completing mechanical testing of the supraspinatus tendon. Often, this involves complete excision

of the supraspinatus tendon from the humerus and supraspinatus muscle (Ahmadzadeh et al., 2013; Lake et al., 2009, 2010), despite extant understanding that these postures potentially alter the mechanical responses of these tissues. Thus, the focus was on generating loading intended to emulate *in vivo* scenarios, not to specifically generate failure of the supraspinatus tendon through sustained destructive testing.

Increases in tangent stiffness as elevation angles, load intensities and tensile cycles increased indicate differential exposures. Trends of increasing stiffness were observed in all loading scenarios, but the greatest increases were at high elevation angles and high cycle numbers, with specimens in the 60° and 75° elevation angles having stiffness values 30-49% higher. This was the result of smaller differences in displacement between the maximal and minimal displacements of the system through successive cycles. Initially, the differences between maximum and minimum displacement were larger; both the absolute maximum and minimum displacement values increased over time, but the minimum values increased at a faster rate, resulting in smaller differences in displacement and greater stiffness values. Research by Newton et al. (2016) evaluated effects of elevation angle on rat supraspinatus tendon, and observed increased stiffness with increasing elevation angle, similar to current results. Despite both works observing increasing stiffness, comparison of these values is difficult, as the previous work employed displacement control for stress-relaxation and load-to-failure tests, compared to force-controlled cyclic loading used in the present study. Cyclic loading has increased stiffness in rat supraspinatus tendon, as well as patellar and Achilles tendons (Fouré, Nordez, & Cornu, 2010; Heinemeier et al., 2012; Rooney et al., 2017; Seynnes et al., 2009). Elevated stiffness followed the typical stiffness pattern in fatigue loading, with an increase in stiffness throughout the secondary phase of loading (Fung et al., 2008). This stiffness increases until the tertiary phase where a steep

decline in stiffness occurs during tendon failure. Although the current research did not generate the tertiary phase of tendon loading, increases in stiffness throughout the loading protocol occurred. Previous research indicated that these stiffness changes do not recover over time; a multi-stage *ex vivo* loading protocol that included an 80 minute recovery period between loading protocols showed an immediate return to the tendon stiffness from the last cycle of the previous stage, instead of a return to the initial stiffness (Fung et al., 2008). This represents a contrast to loading induced changes in bone, where a recovery toward initial stiffness has been documented (Jepsen & Davy, 1997; Joo et al., 2007).

This increase in stiffness is likely an indication of microstructure changes occurring during cyclic loading of tendon. In prior work employing repeated overload cycles while using scanning electron microscopy, damage was characterized by serial disruption (kinking) of the collagen fibril structures along their length (Veres & Lee, 2012). Subsequent studies identified that this fibril disruption, termed "discrete plasticity", also occurred at individual and repeated subrupture loads (Veres et al., 2013a, 2013b). These successive overload cycles resulted in an increasing serial density of kinks along the length of the fibril (Veres et al., 2013b; Veres & Lee, 2012). These kinks may be a part of a structural mechanism which absorbs overload energy via sacrificial destruction of certain subfibrils, toughening collagen at a very basic level (Baldwin et al., 2016). Mechanical properties of these kinked collagen fibrils can be modeled as a high-density core surrounded by a low-density shell (Baldwin et al., 2016); it is possible that these higher density kinks in the collagen fibrils result in an increased stiffness of the tendon, and that the stiffest tendons in the current study occurred in tendons with higher elevation angles and increased load intensities. Overhead work and repetitive submaximal loading as risk factors are well described as occupational shoulder injury mechanisms (Chopp, O'Neill, et al., 2010; Ebaugh et al., 2006a; van der Windt et al., 1995);

the findings from this research support the notion that higher elevation angles and repetitive loading can raise likelihood of rotator cuff injury.

Increased tendon stiffness has been linked to rotator cuff pathology. Clinically, increases in tendon stiffness have been described as an early change in rotator cuff tendinopathy (Vasishta et al., 2019). Stiffness has also been documented after supraspinatus tendon rupture, with a doubling of passive tendon stiffness compared to non-ruptured individuals (Hersche & Gerber, 1998). Increases in stiffness in the supraspinatus and infraspinatus have also been have been observed in individuals with adhesive capsulitis of the shoulder using shear wave elastography (Yun et al., 2019). This increase in passive stiffness has been proposed to relate to a decreased capacity for muscle tension generation, and decreased outcomes in manual and isokinetic testing (Hersche & Gerber, 1998). Tendon stiffness is also a metric for repair efficacy, with increased tendon stiffness following arthroscopic repair widely regarded as a marker for poor clinical outcomes (Brislin et al., 2007; Charousset et al., 2008; Huberty et al., 2009; Namdari & Green, 2010; Tauro, 2006). Additionally, increased post-operative tendon stiffness was correlated with decreased isokinetic strength and increased pain reports (Davidson & Rivenburgh, 2000). The increases in tissue stiffness observed in this research support the notion that changes are occurring within the tendon that may be a marker for future rotator cuff pathology risk.

Differences in stretch ratios across mechanical loading factors indicate differential responses to combinations of glenohumeral elevation angle, load intensity and cycle number; additionally, differences existed between the articular and bursal sides of the tendon. A three-way interaction between each of these factors affected longitudinal stretch ratios, with the greatest stretch ratios in the final cycles at the 60° and 75° glenohumeral angles at high load intensities. Previous cyclic loading of tendon has highlighted increases in peak clamp-to-clamp strain with

inflection points at the secondary and tertiary phases of loading (Fung et al., 2008). These differences within the tendon are likely due to the complex loading environment which includes tensile forces as well as compression and shear due to neighbouring anatomy and the large range of motion of the glenohumeral joint (Lake et al., 2009; Miller, Connizzo, Feeney, Tucker, et al., 2012; Miller, Connizzo, & Soslowsky, 2012; Thomopoulos et al., 2003). A main effect of glenohumeral elevation angle also existed, with increasing strain at higher glenohumeral angles. Analogous results were reported previously in a narrower range of 15-60° glenohumeral elevation in human cadaveric shoulders (Bey et al., 2002). Differences existed between stretch ratios for the entire length of the tendon compared to smaller, regional stretch ratio calculations; often, these regional stretch ratios described were higher compared to the tendon as a whole. Peak regional stretch ratios were documented as high as 1.16 on the articular surface in the high load scenarios at 75° of glenohumeral elevation. Similar increases have been observed previously (Andarawis-Puri et al., 2009); regional strain reports have been documented to differ by as much as 10%, depending on the region examined within the tendon, and stretch ratios differed by up to 11.2% in the current research. A possible factor for these regional stretch ratio differences is the form of the calculation; as stretch ratio is calculated based on the change in relative displacement of two points in the final condition compared to the initial condition, absolute changes of similar magnitudes when examining a smaller portion compared to the tendon as a whole would result in larger stretch ratios. However, examination of these points and differences in these regional stretch ratios was limited, as the random nature of the features for tracking made separation of these line segments difficult to partition for the purposes of statistical analysis. Additional research is required to elucidate regional differences in stretch ratios within this tendon beyond comparisons of articular and bursal measures.

Tendon strain has been associated with supraspinatus tendon pathology, and is not homogeneous throughout the tendon. Short term cyclic loading *ex* vivo showed that elongation increased at successive loading cycles prior to the occurrence of microscopic failure of fibers (Thornton et al., 2002). During fatigue loading tendon peak clamp-to-clamp strain increased continuously, following a repeated pattern marked by inflection points at secondary and tertiary fatigue phases (Fung et al., 2008). The authors postulated that tendon clamp-to-clamp strain is a useful and accurate marker of damage accumulation in the progression of tendon fatigue (Fung et al., 2008). When loaded *ex vivo* in fatigue loading with an 80 minute period for recovery, peak strain was nonrecoverable; this observation reflects that the damage which is manifested by the strain in crease is structural and not associated with a transient response resulting from fatigue loading (Fung et al., 2008). Using texture correlation analyses from MRI images of cadaveric shoulders, Bey et al (2002) reported significant alterations in supraspinatus tendon strain with joint position, with up to 12% higher strain when moving from 15° to 60° of glenohumeral elevation . At lower angles, the superior surface sustained higher strains than the inferior surface (Bey et al., 2002). Differences in local stretch ratios within the supraspinatus tendon suggest an inhomogeneous structure which may modulate its ability to respond in repetitive loading or when the glenohumeral angle is altered. These differences across the surfaces of the supraspinatus tendon suggest that the potential for tear initiation is not homogenous across tendon regions, particularly on the articular side due to the continuous presence of high tensile loading on this surface (Huang et al., 2005). The current research identified elevated stretch ratios on the articular side when high elevation angles were paired with high loads, but differences in the magnitude of these stretch ratios existed throughout the range of elevation angles and loads. At high elevation angles and high loads, stretch ratios on the articular side were greater, but at lower loads or

elevation angles, stretch ratios were higher on the bursal side of the tendon, although differences involved stretch ratios differences that were less than 1.2% between the two regions. Differences between the articular and bursal sides of the tendon have been identified in cadaveric human shoulders (Gohlke et al., 1994), as the articular side of this tendon crosses the coracohumeral ligament at a right angle. The decrease of supraspinatus fibers identified at this junction may result in an area of lower mechanical resistance (Gohlke et al., 1994).

Cyclic loading was an important factor influencing stretch ratios. A primary cause of tendon degeneration is overuse or fatigue loading, which produces repeated microscale damage of the load-bearing collagen fibrils (Cook & Purdam, 2009; Fung, Wang, et al., 2010; Gibbon, Cooper, & Radcliffe, 1999; Kujala, Sarna, & Kaprio, 2005; Nakama et al., 2006; Soslowsky et al., 2000; Szczesny, Aeppli, David, & Mauck, 2018). Injury due to mechanical overload of a tendon results in the disruption of its ordered hierarchical structure, long term alteration in its mechanical properties, and loss of function (Baldwin et al., 2016; Sharma & Maffuli, 2005; Spiesz et al., 2015). Increases in stretch ratios may result in prolonged changes within the tendon; previous research involving *ex vivo* fatigue loading that included an 80 minute period for recovery between testing bouts observed no recovery in peak tendon strain (Fung et al., 2008). This supports the idea that this strain increase reflects changes within the tendon that are structural, and not a transient response (Fung et al., 2008).

Hysteresis changes with increasing cycles found initial increased hysteresis loss, followed by a flattening of this curve with consecutive loading cycles. Similar changes in hysteresis have been observed in the literature (Freedman et al., 2015; Fung et al., 2008). The greatest hysteresis loss was observed in the highest glenohumeral elevation angle and at the highest load. A similar response was documented where the highest loading group had hysteresis values that were

significantly larger, but low and moderate loading groups did not differ from one another (Fung et al., 2008). Decreases in hysteresis have been observed in a long term resistive loading protocol, and have been postulated to be an increase in capability of returning stored strain energy (Reeves, Maganaris, et al., 2003; Reeves, Narici, & Maganaris, 2003). Hysteresis decreases in the current study may be linked to increasing displacements throughout the loading protocol; initial hysteresis loss may have been generated through the rearrangement or slipping of collagen fibers within the tendon (Nordez et al., 2008, 2009). As the displacement of the tendon increased, less slipping of the collagen fibrils occurred, and energy loss was through breakage of hydrogen bonds in the collagen structure, which has been identified as a potential mechanism of dissipating overload energy while maintaining the collagen scaffolding (Veres et al., 2013a; Veres & Lee, 2012). Hysteresis loss has been previously found to be nonrecoverable (Andarawis-Puri et al., 2012), in contrast to loading-induced changes in bone (Jepsen & Davy, 1997; Joo et al., 2007), and have been described to reflect the plastic nature of induced microstructural changes, particularly in the formation of damage patterns of various types including those that do not involve fiber rupture (Freedman et al., 2015; Fung et al., 2008). These findings support the notion that this loading protocol generated changes within the tendon that were not simply transient responses.

5.7 Limitations

There are some inherent limitations that should be considered in the context of these findings; these can be loosely separated into limitations surrounding the use of an *in vitro* animal model and limitations of the mechanical system used to complete this research.

Limitations exist in the use of non-human tissue samples. The use of Sprague-Dawley rat shoulders as a surrogate for the human shoulder does not exactly replicate the human condition. However, the rat shoulder has a similar bony architecture, with an enclosed arch through which

the supraspinatus tendon must pass, comparable to the coracoacromial arch found in humans (Soslowsky et al., 2000). This similar architecture and soft tissue anatomy has identified it as a viable proxy for the human shoulder (Soslowsky et al., 1996). Rotator cuff stress concentration in tendon samples have shown to be highly conserved across species in up to a three order of magnitude range of body mass (Saadat, Deymier, Birman, Thomopoulos, & Genin, 2016), meaning these results can be viably extrapolated to humans. Secondly, the continuous testing did not account for possible effects of physiological tissue repair that may occur during rest periods from repeated loading exposures. Chronic rotator cuff tears in humans typically develop over a long period of time as a result of intrinsic and extrinsic factors (Gimbel, Kleunen, et al., 2004), and the effects measured in this study may be exacerbated or mitigated in the presence of physiological repair. As the tissues used were dead animal tissues, the findings from this study may not completely represent human rotator cuff loading, as living human tissue would have the potential to undergo recovery and repair. However, previous research including recovery periods in an animal model has indicated that some mechanical outcome measures (including those examined in the current study) are non-recoverable even after seven days (Andarawis-Puri et al., 2012; Fung et al., 2008).

There are also limitations regarding the methodology employed. Applied force levels were not synonymous across testing groups; as the purpose of this work was to link *in vivo* and *in* vitro methods to understand how posture and load affect the supraspinatus and its tendon, applying an identical load across all postures would not have represented the differences observed *in vivo.* The novel methodology involving inclusion of a complete glenohumeral joint to examine supraspinatus loading has never before been completed to the author's knowledge, and the use of load control (as opposed to controlling clamp-to-clamp displacement) results in a very limited number of

comparable studies. However, best efforts were made to provide context to the current research findings with respect to current findings using similar tissues. Cross sectional area was measured in the same posture prior to affixing the tendon within the mounting system; it was not possible to measure tendon cross-sectional area once the specimen was placed within the mechanical testing system. As these postures differed across testing groups, it is plausible that the differences in posture may have altered the cross sectional area of the tendon, which could have affected outcome measures. Only one plane of elevation was selected for testing of these specimens. As these load intensities were driven by electromyography recordings from Chapter III, external factors (such as muscle co-contraction, passive stretch or moment arm changes) beyond this activation were not included in determining mechanical load levels for this tendon. Altering humeral postures both in plane of elevation and axial rotation have been shown to alter rotator cuff activation and tissue responses *in vivo*, particularly in subacromial impingement (Graichen, Bonel, Stammberger, Englmeier, et al., 1999; Graichen, Bonel, Stammberger, Haubner, et al., 1999; Miranda et al., 2005; Svendsen et al., 2004; van Rijn et al., 2010). It is unlikely that the supraspinatus would have identical responses across these different planes of elevation. While the current study examined multiple loading levels, only one frequency of loading was examined, which meant that different absolute magnitudes would have resulted in different loading rates. The focus of this work was to examine different loading intensities at a fixed cycle rate; completing these tasks in identical loading rates would have resulted in different lengths of loading protocol, which may have confounded results. It is likely that the supraspinatus tendon is a 'positional' tendon, which accumulate more discrete plasticity at slower strain rates than 'energy storing' tendons, such as the Achilles tendon (Chambers, Herod, & Veres, 2018). Examining at additional loading rates *in vitro* could provide important information.

The mechanical testing devices used also generated limitations. One optical camera was used for calculating stretch ratios on tracked points of the tendon. As the tendon was a 3D structure and the focal length of the camera was a fixed distance, differences in displacement closer or beyond the focal length may not have been accurately represented, and may have altered tracking displacements and therefore calculations. The primary fibril direction was estimated on this 2D plane using the contours provided by the powdered graphite, and potential changes in the primary direction outside of this plane image was not accounted for in this work. In addition, the use of 2D imaging to characterize changes throughout a cyclic loading protocol likely underestimates the actual amount of change within the tissues (Fung, Sereysky, et al., 2010). However, the setup of the system and the equipment available precluded the use of a second camera setup or the use of other imaging techniques. As the system was acting in load control, a tolerance value was placed around the target load to prevent force oscillation. This force tolerance was 50 mN; as such, it is possible that the loads placed on the tendon may not be identical to the prescribed loads, but these loads are within 50 mN of the desired load. Finally, the method of loading the tendon may not completely represent loading observed *in vivo*. The method used produced an exertion where the glenohumeral posture did not change throughout the load. As an muscle contraction infers some degree of muscle shortening and the tensile testing created tendon stretching, it is possible that the direction of the force of the tendon was not precisely recreated. As the *in vivo* muscular activations used to scale this loading were extracted from isokinetic tasks, the lack of change in glenohumeral posture may have affected the outcomes. The testing system was designed to generate axial loading in one or two orthogonal directions, and moving a specimen through glenohumeral elevation angles while applying loads was not feasible. Finally, as all surrounding tissues were excised except for the supraspinatus tendon, the loading may not identically reproduce that observed *in*

vivo. The uniaxial loading resulted in the head of the humerus being pulled away from the centre of the glenoid as loading was applied to the tendon; this loading *in vivo* would be supported by surrounding structures, including other rotator cuff tendons, the deltoid, and joint capsule. As all of these supporting tissues were removed, it is possible that tendon stretch observed in this study exceeds that seen *in vivo*. However, if these structures were to remain intact for testing, it would be unclear whether the loading of the system was being applied to the supraspinatus tendon or to other structures.

5.8 Conclusions

This study was successful in demonstrating that glenohumeral elevation angle, load intensity and cyclic loading affect mechanical responses of the supraspinatus tendon through changes in tangent stiffness, hysteresis and optical stretch ratios. Increased tangent stiffness and optical stretch ratios occurred when higher glenohumeral elevation angles, increased load intensity and successive number of cycles were applied to the supraspinatus tendon. While posture, force and repetition have all been described as occupational risk factors *in vivo*, the mechanistic changes observed in these specimens support these consensus guidelines for shoulder exposures, particularly in tangent stiffness and local strain results.

These data advocate continued *in vitro* research into rotator cuff loading while attempting to replicate physiologically relevant exposure scenarios. While the scenarios examined are limited relative to the range of shoulder postures and loads examined *in vivo*, they represent positive growth in our understanding of rotator cuff loading. Future research should expand the use of physiologically relevant exposure levels to additional planes of glenohumeral elevation, as these were documented to alter muscular activation *in vivo*, which would alter the load intensities as

described in these methods. Expanded interconnection between *in vivo* and *in vitro* methods would be fundamentally useful assist in description of rotator cuff function.

CHAPTER VI – CONTRIBUTIONS

This work has identified the potential for quantifiable links between *in vivo* and *in vitro* through the use of combined methodologies to move toward a better understanding of rotator cuff mechanics. This dissertation demonstrates that supraspinatus loading is not homogeneous throughout the range of motion, and that these differences have profound effects on the rotator cuff. The series of *in vivo* and *in vitro* experimental efforts detailed in this document supported the global objective of this work: to evaluate how postural differences and external load magnitudes alter supraspinatus and its tissue-level muscular and tendinous responses. This section presents novel contributions and novel findings in summarized formats.

6.1 Novel Contributions

1) **Establishment of the quantitative relationship between the anterior and posterior supraspinatus activation throughout the humeral range of motion.** Activation of the anterior and posterior regions of the supraspinatus were collected from the largest sample of arm postures to date (Chapter III). Previously, concomitant activation level recordings for both regions was limited to four arm elevation angles within a single plane of elevation. Activations were collected using indwelling electromyography in both regions and provide orders of magnitude more information surrounding these two regions compared to previous efforts (Kim et al., 2017). The present work examined seven planes of elevation with over 30 angles examined across two phases of motion and three hand load intensities, resulting in activations measured over more than 1250 postures. Collecting these time series EMG data in conjunction with motion capture of the torso and upper extremity enabled the first

experimentally collected activation profiles of both regions of the supraspinatus across a range of arm postures.

2) **Bridging of *in vivo* muscular activation to *in vitro* mechanical testing to generate physiologically relevant tensile loads.** The EMG activations observed in the anterior and posterior regions of supraspinatus from the *in vivo* study (Chapter III) were used to determine applied force load levels for force-controlled tensile testing (Chapter V). Typical mechanical tendon testing was previously completed using continued tensile stretch until failure or cyclic tensile loading to specified strain levels. To date, this is the first known attempt to generate physiologically relevant force-controlled tensile loading based on corresponding electromyographic activations.

3) **A methodology for examining rotator cuff loading as a complete glenohumeral unit.** Typically, mechanical testing is completed on an excised portion of tendon, but changing humeral posture alters supraspinatus tendon mechanical behaviour. Only one other study has considered humeral posture when examining changes in mechanical properties of the supraspinatus tendon (Newton et al., 2016), but this work only had the supraspinatus connected to the humerus while excising the scapula. This work is the first known attempt to retain the complete glenohumeral unit for mechanical testing of the supraspinatus tendon. Maintaining the functional humerus-supraspinatus-scapula unit allowed orientation of the glenohumeral joint to postures observed *in vivo* (Chapter V).

6.2 Novel Findings

1) **Regional activation of the anterior and posterior supraspinatus was influenced by plane of elevation, hand load and elevation angle.** Hand load and elevation angle interacted to affect activity of the anterior supraspinatus in most planes of elevation, by up to 41 %MVC; this interaction only affected activity in the posterior supraspinatus in a few planes. The differences between these two regions indicate functional distinctions between these two regions. Based on these findings, it can be posited that the primary role of the posterior region is to act as a glenohumeral stabilizer, while the anterior region primarily assists in generating motion.
2) **The ability of a bipolar surface electrode to predict both anterior and posterior supraspinatus indwelling activation throughout the humeral range of motion is dependent on plane of elevation, elevation angle, load intensity and participant sex, and should be considered when collecting electromyography for this muscle.** For the first time, comparison between surface and indwelling signals for the posterior supraspinatus was collected and analysed. Typically, these surface signals underestimated activation at low elevation angles and low hand load intensities, but overestimated supraspinatus activation as humeral elevation angles and hand loads increased. Excellent agreement was observed across the range of motion, with less than 5 %MVC difference between signals in the scapular plane or when humeral elevation was at 90°. The results from this work expand our understanding of the relationship between surface and indwelling electromyography for this muscle, both in the number of postures examined and the inclusion of the posterior region of supraspinatus.

3) **Posture and load intensity modulate supraspinatus tendon responses and highlight the heterogeneous nature of this tendon.** Increasing glenohumeral elevation angles, load magnitude and number of cycles increased tangent stiffness by up to 49%, while stretch ratios were altered by glenohumeral elevation angle, load intensity and cycle number, with some differences existing between the articular and bursal sides of the tendon. These findings highlight the complex nature of this tendon while indicating key factors that modulate mechanical properties.

6.3 Future Work

Considerable work is still required to holistically define supraspinatus regional activation and quantify changes in tendon mechanical behaviour from physiologically relevant tendon loading. This dissertation combined both *in vivo* and *in vitro* examinations of the rotator cuff, and generated meaningful directions for potential future work.

The assessment of *in vivo* regional supraspinatus activation provided an unprecedented level of information on a wide range of arm postures; however, the paucity of available data for comparison to these findings requires continued effort. Expansion of the body of knowledge surrounding these two regions in a wider range of tasks and postures will continue to improve our understanding of functional differences between these two subregions and its implications for rotator cuff function and dysfunction. Axial humeral rotation modulates relative regional supraspinatus activation (Kim et al., 2017), but existing data is limited to two postures. Comparisons between the healthy control participants, such as those used in this research, and individuals with varieties of rotator cuff pathologies could elucidate how these regional activations change with pathology and help to improve rehabilitative responses. In addition, consideration of

regional structural and activation characteristics, such as moment arms of the subregions, potential differences between activation onsets, examination of activation and joint stiffness, and co-contraction with other rotator cuff musculature could provide additional insight.

The mechanical testing completed *in vitro* represented physiologically relevant force controlled loading and provides a new approach to mechanical testing for the supraspinatus in an animal model. The majority of the work in tensile tendon testing historically used displacement control, examining changes in dependent measures such as tangent stiffness or hysteresis at focused strain rates. Bridging the knowledge gap between strain-focused tensile loading in previous work and the force-loading based on EMG activation in this work is paramount to further this research direction. This dissertation examined multiple glenohumeral elevation angles and load magnitudes, but examined a single plane of elevation. The precedent *in vivo* measurements highlighted that plane of elevation influenced muscular recruitment; thus, expanding the range of tested postures to additional planes is critical. Altering the rate of loading could also provide additional insight; previous research quantified that altering strain rate affected tendon mechanical behaviours (Chambers et al., 2018; Willett, Labow, Avery, & Lee, 2007; Willett, Labow, & Lee, 2008). The current work was not designed to load the tendon to failure; developing additional loading protocols that would result in failure of the tendon would provide additional important details into the sequence of events that lead to rotator cuff rupture.

REFERENCES

Ackland, D., Pak, P., Richardson, M., & Pandy, M. (2008). Moment arms of the muscles crossing the anatomical shoulder. *Journal of Anatomy*, *213*(4), 383–390.

Ahmadzadeh, H., Connizzo, B., Freedman, B., Soslowsky, L., & Shenoy, V. (2013). Determining the contribution of glycosaminoglycans to tendon mechanical properties with a modified shear-lag model. *Journal of Biomechanics*, *46*, 2497–2503.

Alenabi, T., Dal Maso, F., Tétreault, P., & Begon, M. (2016). The effects of plane and arc of elevation on electromyography of shoulder musculature in patients with rotator cuff tears. *Clinical Biomechanics*, *32*, 194–200.

Alenabi, T., Whittaker, R., Kim, S., & Dickerson, C. (2019). Arm posture influences on regional supraspinatus and infraspinatus activation in isometric arm elevation efforts. *Journal of Electromyography and Kinesiology*, *44*, 108–116.

Alexander, R., & Bennet-Clark, H. (1977). Storage of elastic strain energy inmuscle and other tissues. *Nature*, *265*, 114–117.

Allen, T., Brookham, R., Cudlip, A., & Dickerson, C. (2013). Comparing surface and indwelling electromyographic signals of the supraspinatus and infraspinatus muscles during submaximal axial humeral rotation. *Journal of Electromyography and Kinesiology*, *23*(6), 1343–1349.

Almekinders, L., & Temple, J. (1998). Etiology, diagnosis, and treatment of tendonitis: an analysis of the literature. *Medicine and Science in Sports and Exercise*, *30*, 1183–1190.

An, K.-N., Berglund, L., Cooney, W., Chao, E., & Kovacevic, N. (1990). Direct in vivo tendon force measurement system. *Journal of Biomechanics*, *23*(12), 1269–1271.

Andarawis-Puri, N, & Flatow, E. (2011). Tendon fatigue in response to mechanical loading. *Journal of Musculoskeletal and Neuronal Interactions*, *11*(2), 106–114.

Andarawis-Puri, N, Flatow, E., & Soslowsky, L. (2015). Tendon basic science: Development, repair, regeneration, and healing. *Journal of Orthopaedic Research*, *33*(6), 780–784.

Andarawis-Puri, N, Sereysky, J., Jepsen, K., & Flatow, E. (2012). The relationship between cyclic fatigue loading, changes in initial mechanical properties, and the in vivo temporal mechanical response of the rat patellar tendon. *Journal of Biomechanics*, *45*, 59–65.

Andarawis-Puri, Nelly, Ricchetti, E. T., & Soslowsky, L. J. (2009). Rotator cuff tendon strain correlates with tear propagation. *Journal of Biomechanics*, *42*(2), 158–163.

Baldwin, S., Kreplak, L., & Lee, J. (2016). Characterization via atomic force microscopy of discrete plasticity in collagen fibrils from mechanically overloaded tendons: Nano-scale structural changes mimic rope failure. *Journal of the Mechanical Behaviour of Biomedical Materials*, *60*, 356–366.

Balke, M., Schmidt, C., Dedy, N., Banerjee, M., Bouillon, B., & Liem, D. (2013). Correlation of acromial morphology with impingement syndrome and rotator cuff tears. *Acta*

Orthopaedica, *84*(2), 178–183.

Barkhaus, P., & Nandedkar, S. (1994). Recording characteristics of the surface EMG electrodes. *Muscle & Nerve*, *17*, 1317–1323.

Barry, B., & Enoka, R. (2007). The neurobiology of muscle fatigue: 15 years later. *Integrative and Comparative Biology*, *47*(4), 465–473.

Basmajian, J., & Bazant, F. (1959). Factors preventing downward dislocation of the adducted shoulder joint in an electromyographic and morphological study. *Journal of Bone & Joint Surgery*, *41*, 1182–1186.

Bassett, R., Browne, A., Morrey, B., & An, K.-N. (1990). Glenohumeral muscle force and moment mechanics in a position of shoulder instability. *Journal of Biomechanics*, *23*(5), 405–415.

Batson, E., Paramour, R., Smith, T., Birch, H., Patterson-Kane, J., & Goodship, A. (2003). Are the material properties and matrix composition of equine flexor and extensor tendons determined by their functions? *Equine Veterinary Journal*, *35*(3), 314–318.

Beason, D., Tucker, J., Lee, C., Edelstein, L., Abboud, J., & Soslowsky, L. (2014). Rat rotator cuff tendon-to-bone healing properties are adversely affected by hypercholesterolemia. *Journal of Shoulder and Elbow Surgery*, *23*(6), 867–872.

Bedi, A., Kovacevic, D., Hettrich, C., Gulotta, L., Ehteshami, J., Warren, R., & Rodeo, S. (2010). The effect of matrix metalloproteinase inhibition on tendon-to-bone healing in a rotator cuff repair model. *Journal of Shoulder and Elbow Surgery*, *19*(3), 384–391.

Benjamin, M., Evans, E., & Copp, L. (1986). The histology of tendon attachments to bone in man. *Journal of Anatomy*, *149*, 89–100.

Benjamin, M., Kumai, T., Milz, S., Boszczyk, B., Boszczyk, A., & Ralphs, J. (2002). The skeletal attachment of tendons - tendon "entheses." *Comparative Biochemistry and Physiology - A Molecular and Integrative Physiology*, *133*(4), 931–945.

Benjamin, M., Toumi, H., Ralphs, J., Bydder, G., Best, T., & Milz, S. (2006). Where tendons and ligaments meet bone: Attachment sites ('entheses') in relation to exercise and/or mechanical load. *Journal of Anatomy*, *208*(4), 471–490.

Berenson, M., Blevins, F., Plaas, A., & Vogel, K. (1996). Proteoglycans of human rotator cuff tendons. *Journal of Orthopaedic Research*, *14*, 518–525.

Bernard, B. (1997). *Musculoskeletal Disorders and Workplace Factors: A Critical Review of Epidemiologic Evidence for Work-Related Musculoskeletal Disorders of the Neck, Upper Extremity and Low Back*. Washington, DC.

Bey, M., Brock, S., Beierwaltes, W., Zauel, R., Kolowich, P., & Lock, T. (2007). In vivo measurement of subacromial space width during shoulder elevation: Technique and preliminary results in patients following unilateral rotator cuff repair. *Clinical Biomechanics*, *22*(7), 767–773.

Bey, M., Song, H., Wehrli, F., & Soslowsky, L. (2002). Intratendinous strain fields of the intact

supraspinatus tendon: the effect of glenohumeral joint position and tendon region. *Journal of Orthopaedic Research*, *20*, 869–874.

Bhonsle, S., & van Karsen, C. (1992). Mechanical and fatigue properties of stress relieved type 302 stainless steel wire. *Journal of Materials Engineering and Performance*, *1*(3), 363–369.

Bickelhaupt, B., Eckmann, M., Brennick, C., & Rahimi, O. (2019). Quantitative analysis of the distal, lateral and posterior articular branches of the axillary nerve to the shoulder: Implications for intervention. *Regional Anesthesia and Pain Medicine*, *44*(9), 875–880.

Bigliani, L., Morrison, D., & April, E. (1986). The morphology of the acromion and its relationship to rotator cuff tears. *Orthopaedic Transactions*, *10*, 228.

Birk, D., Fitch, J., Babiarz, J., Doane, K., & Linsenmayer, T. (1990). Collagen fibrillogenesis in vitro: interaction of types I and V collagen regulates fibril diameter. *Journal of Cell Science*, *95*(4), 649–657.

Bishop, J., Klepps, S., Lo, I., Bird, J., Gladstone, J., & Flatow, E. (2006). Cuff integrity after arthroscopic versus open rotator cuff repair: A prospective study. *Journal of Shoulder and Elbow Surgery*, *15*(3), 290–299.

Bjelle, A., Hagberg, M., & Michaelson, G. (1981). Occupational and individual factors in acute shoulder-neck disorders among industrial worker. *British Journal of Industrial Medicine*, (38), 356–363.

Blasier, R., Guldberg, R., & Rothman, E. (1992). Anterior shoulder stability: contributions of rotator cuff forces and the capsular ligaments in a cadaver model. *Journal of Shoulder and Elbow Surgery*, *1*(3), 140–150.

Blazevich, A. (2019). Adaptations in the passive mechanical properties of skeletal muscle to altered patterns of use. *Journal of Applied Physiology*, *126*, 1483–1491.

Bonilla, K., Pardes, A., Freedman, B., & Soslowsky, L. (2019). Supraspinatus tendons have different mechanical properties across sex. *Journal of Biomechanical Engineering*, *141*(1), 0110021.

Borstad, J., Szucs, K., & Navalgund, A. (2009). Scapula kinematic alterations following a modified push-up plus task. *Human Movement Science*, *28*(6), 738–751.

Bost, F., & Inman, V. (1942). The pathological changes in recurrent dislocation of the shoulder. *The Journal of Bone and Joint Surgery*, *24*(3), 595–613.

Boyer, M., Harwood, F., Ditsios, K., Amiel, D., Gelberman, R., & Silva, M. (2003). Two-portal repair of canine flexor tendon insertion site injuries: histologic and immunohistochemical char- acterization of healing during the early postoperative period. *The Journal of Hand Surgery*, *28*, 469–474.

Braun, S., Kokmeyer, D., & Millett, P. (2009). Shoulder injuries in the throwing athlete. *Journal of Bone and Joint Surgery*, *91*, 966–978.

Brislin, K., Field, L., & Savoie III, F. (2007). Complications after arthroscopic rotator cuff repair. *Arthroscopy*, *23*, 124–128.

Brookham, R., McLean, L., & Dickerson, C. (2010). Construct validity of muscle force tests of the rotator cuff muscles: an electromyographic investigation. *Physical Therapy*, *90*(4), 572–580.

Broom, N. (1978). Simultaneous morphological and stress-strain studies of the fibrous components in wet heart valve leaflet tissue. *Connective Tissue Research*, *6*, 37–50.

Browne, A., Hoffmeyer, P., Tanaka, S., An, K.-N., & Morrey, B. (1990). Glenohumeral elevation studied in three dimensions. *The Journal of Bone and Joint Surgery*, *72*(5), 843–845.

Buckley, M., Sarver, J., Freedman, B., & Soslowsky, L. (2013). The dynamics of collagen uncrimping and lateral contraction in tendon and the effect of ionic concentration. *Journal of Biomechanics*, *46*(13), 2242–2249.

Burkhart, S., Johnson, T., Wirth, M., & Athanasiou, K. (1997). Cyclic loading of transosseous rotator cuff repairs: tension overload as a possible cause of failure. *Arthroscopy*, *13*, 172–176.

Butler, D., Goldstein, S., & Guilak, F. (2000). Functional tissue engineering: the role of biomechanics. *Journal of Biomechanical Engineering*, *122*, 570–575.

Butler, D., Grood, E., Noyes, F., & Zernicke, R. (1978). Biomechanics of ligaments and tendons. *Exercise and Sport Sciences Reviews*, *6*, 125–181.

Chaffin, D. (1975). Ergonomics guide for the assessment of human static strength. *American Industrial Hygeine Association Journal*, *36*(7), 505–511.

Chambers, N., Herod, T., & Veres, S. (2018). Ultrastructure of tendon rupture depends on strain rate and tendon type. *Journal of Orthopaedic Research*, *36*(11), 2842–2850.

Chard, M., Hazelman, R., Hazelman, B., King, R., & Reiss, B. (1991). Shoulder disorders in the elderly : a community survey. *Arthritis and Rheumatism*, *34*(6), 766–769.

Charles River Laboratories International, I. (2011). *Research models: CD® IGS Rats*.

Charousset, C., Grimberg, J., Duranthon, L., Bellaïche, L., Petrover, D., & Kalra, K. (2008). The time for functional recovery after arthroscopic rotator cuff repair: correlation with tendon healing controlled by computed tomography arthrography. *Arthroscopy*, *24*, 25–33.

Chiang, H., Chen, S., Yu, H., & Ko, Y. (1990). The occurrence of carpal tunnel syndrome in frozen food factory employees. *The Kaohsiung Journal of Medical Sciences*, *6*(2), 73–80.

Chiang, H., Ko, Y., Chen, S., Yu, H., Wu, T., & Chang, P. (1993). Prevalence of shoulder and upper limb disorders among workers in the fish processing industry. *Scandinavian Journal of Work, Environment & Health*, *19*(2), 126–131.

Chopp-Hurley, J. (2015). *Development of a probabilistic population model for the prediction of subacromial geometric variability*. 237.

Chopp, J., Fischer, S., & Dickerson, C. (2010). The impact of work configuration, target angle and hand force direction on upper extremity muscle activity during sub-maximal overhead work. *Ergonomics*, *53*(1), 83–91.

Chopp, J., O'Neill, J., Hurley, K., & Dickerson, C. (2010). Superior humeral head migration occurs after a protocol designed to fatigue the rotator cuff: a radiographic analysis. *Journal of Shoulder and Elbow Surgery, 19*, 1137–1144.

Chow, A., & Dickerson, C. (2009). Shoulder strength of females while sitting and standing as a function of hand location and force direction. *Applied Ergonomics*, *40*(3), 303–308.

Chung, S., & Nissenbaum, M. (1975). Congential and developmental defects of the shoulder. *The Orthopaedic Clinics of North America*, *6*(2), 381–392.

Clark, JC. (1988). Fibrous anatomy of the rotator cuff. *American Academy of Orthopaedic Surgeons*.

Clark, JM, & Harryman II, D. (1992). Tendons, ligaments, and capsule of the rotator cuff. *Journal of Bone & Joint Surgery, 74*(5), 713–725.

Clark, JM, Sidles, J., & Matsen III, F. (1990). The relationship of the glenohumeral joint capsule to the rotator cuff. *Clinical Orthopaedics and Related Research, 254*, 29–34.

Codman, E. (1911). Complete rupture of the supraspinatus tendon. Operative treatment with report of two successful cases. *Boston Medical and Surgical Journal*, *164*(20), 708–710.

Codman, E. (1934). *The Shoulder*. Boston: Thomas Todd.

Codman, E. (1937). Rupture of the supraspinatus - 1834 to 1934. *Journal of Bone & Joint Surgery, 19*(3), 643–652.

Cofield, R. (1985). Rotator cuff disease of the shoulder. *Journal of Bone & Joint Surgery*, *67*(6), 974–979.

Cohen, J. (1992). Statistical power analysis. *Current Directions in Psychological Science*, *1*(3), 98–101.

Colachis Jr, S., & Strohm, B. (1971). Effect of suprascapular and axillary nerve blocks on muscle force in upper extremity. *Archives of Physical Medicine and Rehabilitation*, *52*(1), 22–29.

Colachis Jr, S., Strohm, B., & Brechner, V. (1969). Effects of axillary nerve block on muscle force in the upper extremity. *Archives of Physical Medicine and Rehabilitation*, *50*(11), 647–654.

Coleman, S., Fealy, S., JR, E., MacGillivray, J., Altchek, D., Warren, R., & Turner, S. (2003). Chronic rotator cuff injury and repair model in sheep. *The Journal of Bone and Joint Surgery, 85*(12), 2391–2402.

Constant, C., & Murley, A. (1987). A clinical method of functional assessment of the shoulder. *Clinical Orthopaedics and Related Research*, *214*(1), 160–164.

Cook, J., & Purdam, C. (2009). Is tendon pathology a continuum? A pathology model to explain the clinical presentation of load-induced tendinopathy. *British Journal of Sports Medicine*, *43*, 409–416.

Côté, J., Raymond, D., Mathieu, P., Feldman, A., & Levin, M. (2005). Differences in multi-joint

kinematic patterns of repetitive hammering in healthy, fatigued and shoulder-injured individuals. *Clinical Biomechanics*, *20*(6), 581–590.

Criswell, E. (2011). *Cram's Introduction to Surface Electromyography, Second Edition*. Sudbury, ON: Jones & Bartlett Learning.

Cudlip, A., Callaghan, J., & Dickerson, C. (2015). Effects of sitting and standing on upper extremity physical exposures in materials handling tasks. *Ergonomics*, *0139*(December), 1–10.

Cudlip, A., & Dickerson, C. (2018a). Female maximal push/pull strength capabilities by humeral abduction angle in bilateral exertions. *Applied Ergonomics*, *70*.

Cudlip, A., & Dickerson, C. (2018b). Regional activation of anterior and posterior supraspinatus differs by plane of elevation, hand load and elevation angle. *Journal of Electromyography and Kinesiology*, *43*(June), 14–20.

Cudlip, A., Holmes, M., Callaghan, J., & Dickerson, C. (2018). The effects of shoulder abduction angle and wrist angle on upper extremity muscle activity in unilateral right handed push/pull tasks. *International Journal of Industrial Ergonomics*, *64*, 102–107.

Cudlip, A., Meszaros, K., & Dickerson, C. (2016). The influence of hand location and force direction on shoulder muscular activity in females during nonsagittal multidirectional overhead exertions. *Human Factors: The Journal of the Human Factors and Ergonomics Society*, *58*(1), 120–139.

Dale, W., Baer, E., Keller, A., & Kohn, R. (1972). Ultrastructure of mammalian tendon. *Experientia*, *28*, 1293–1297.

Dalton, S., Cawston, T., Riley, G., Bayley, I., & Hazleman, B. (1995). Human shoulder tendon biopsy samples in organ culture produce procollagenase and tissue inhibitor of metalloproteinases. *Annals of the Rheumatic Diseases*, *54*(7), 571–577.

Das, S., Ray, G., & Saka, A. (1966). Observation of the tilt of the glenoid cavity of the scapula. *Journal of the Anatomical Society of India*, *15*, 114–118.

Davidson, P., Elattrache, N., Jobe, C., & Jobe, F. (1995). Rotator cuff and posterior– superior glenoid labrum injury associated with increased glenohumeral motion: a new site of impingement. *Journal of Shoulder and Elbow Surgery*, *4*, 384–390.

Davidson, P., & Rivenburgh, D. (2000). Rotator cuff repair tension as a determinant of functional outcome. *Journal of Shoulder and Elbow Surgery*, *9*(6), 502–506.

De Luca, C. (1997). *The Use of Surface Electromyography in Biomechanics*. 135–163.

DePalma, A., Cooke, A., & Probhaker, M. (1969). The role of the supraspinatus in recurrent anterior dislocation of the shoulder. *Clinical Orthopaedics and Related Research*, *54*, 35–49.

Devkota, A., & Weinhold, P. (2003). Mechanical response of tendon subsequent to ramp loading to varying strain limits. *Clinical Biomechanics*, *18*, 969–974.

Diamant, J., Keller, A., Baer, E., Litt, M., & Arridge, R. (1972). Collagen; ultrastructure and its

relation to mechanical properties as a function of ageing. *Proceedings of the Royal Society of London. Series B, Biological Sciences*, *180*, 293–315.

Dlugosz, J., Gathercole, L., & Keller, A. (1978). Transmission electron-microscope studies and their relation to polarizing optical microscopy in rat tail tendon. *Micron*, *9*, 71–82.

Doody, S., Freedman, L., & Waterland, J. (1970). Shoulder movements during abduction in the scapular plane. *Archives of Physical Medicine and Rehabilitation*, *51*(10), 595–604.

Drake, J., & Callaghan, J. (2006). Elimination of electrocardiogram contamination from electromyogram signals: an evaluation of currently used removal techniques. *Journal of Electromyography and Kinesiology*, *16*, 175–187.

Duance, V., Restall, D., Beard, H., Bourne, F., & Bailey, A. (1977). The location of three collagen types in skeletal muscle. *FEBS Letters*, *79*, 248–252.

Duckworth, D., Smith, K., Campbell, B., & Matsen III, F. (1999). Self-assessment questionnaires document substantial variability in the clinical expression of rotator cuff tears. *Journal of Shoulder and Elbow Surgery*, *8*(4), 330–333.

Dunkman, A., Buckley, M., Mienaltowski, M., Adams, S., Thomas, S., Kumar, A., … Soslowsky, L. (2014). The injury response of aged tendons in the abscence of biglycan and decorin. *Matrix Biology*, *35*(4), 232–238.

Ebaugh, D., McClure, P., & Karduna, A. (2006a). Effects of shoulder muscle fatigue caused by repetitive overhead activities on scapulothoracic and glenohumeral kinematics. *Journal of Electromyography and Kinesiology*, *16*(3), 224–235.

Ebaugh, D., McClure, P., & Karduna, A. (2006b). Scapulothoracic and glenohumeral kinematics following an external rotation fatigue protocol. *Journal of Orthopaedic Sports Physical Therapy*, *36*(8), 557–571.

Edelson, G., & Teitz, C. (2000). Internal impingement in the shoulder. *Journal of Shoulder and Elbow Surgery*, *9*, 308–315.

Eichelberger, L., & Brown, J. (1945). The fat, water, chloride, total nitrogen, and collagen nitrogen content in the tendons of the dog. *Journal of Biological Chemistry*, *158*, 283–289.

Eilaghi, A., Flanagan, J., Brodland, G., & Ethier, C. (2009). Strain uniformity in biaxial specimens is highly sensitive to attachment details. *Journal of Biomechanical Engineering*, *131*(9), 091003.

Eliasson, P., Fahlgren, A., Pasternak, B., & Aspenberg, P. (2007). Unloaded rat achilles tendons continue to grow, but lose viscoelasticity. *Journal of Applied Physiology*, *103*(2), 459–463.

Elliott, D. (1965). Structure and function of mammalian tendon. *Biological Reviews*, *40*(3), 392–421.

Ellman, H., & Kay, S. (1991). Arthroscopic subacromial decompression forchronic impingement. *The Bone & Joint Journal*, *73*(3), 395–398.

Ellman, H., Kay, S., & Wirth, M. (1993). Arthroscopic treatment of full-thickness rotator cuff tears: 2- to 7-year follow up study. *Arthroscopy*, *9*(2), 195–200.

Engelhardt, C., Ingram, D., Müllhaupt, P., Farron, A., Pioletti, D., & Terrier, A. (2016). Effect of partial-thickness tear on loading capacities of the supraspinatus tendon: a finite element analysis. *Computer Methods in Biomechanics and Biomedical Engineering*, *19*(8), 875–882.

Enoka, R., & Stuart, D. (1992). Neurobiology of muscle fatigue. *Journal of Applied Physiology*, *72*(5), 1631–1648.

Evans, J., & Barbenel, J. (1975). Structural and mechanical properties of tendon related to function. *Equine Veterinary Journal*, *7*, 1–8.

Fan, L., Sarkar, K., Franks, D., & Uhthoff, H. (1997). Estimation of total collagen and types I and III collagen in canine rotator cuff tendons. *Calcified Tissue International*, *61*, 223–229.

Fang, F., & Lake, S. (2016). Multiscale mechanical integrity of human supraspinatus tendon in shear after elastin depletion. *Journal of the Mechanical Behaviour of Biomedical Materials*, *63*, 443–455.

Faul, F., Erdfelder, E., & Lang, A.-G. (2007). G*Power3: A Flexible Statistical Power Analysis Program for the Social, Behavioral, and Biomedical Sciences. *Behavioral Research Methods*, *39*(2), 175–191.

Ferrari, J., Ferrari, D., Coumas, J., & Pappas, A. (1994). Posterior ossification of the shoulder: the Bennett lesion. Etiology, diagnosis, and treatment. *American Journal of Sports Medicine*, *22*(2), 171–175.

Fischer, S., Belbeck, A., & Dickerson, C. (2010). The influence on providing feedback on force production and within-participant reproducibility during voluntary exertions for the anterior deltoid, middle deltoid, and infraspinatus. *Journal of Electromyography and Kinesiology*, *20*(1), 68–75.

Fischer, S., Chopp, J., & Dickerson, C. (2008). Overhead work: evidence-driven job design and evaluation. *Position Paper for the Center of Research Expertise for the Prevention of Musculoskeletal Disorders (CRE-MSD).*

Fischer, S. L., Belbeck, A. L., & Dickerson, C. R. (2010). The influence of providing feedback on force production and within-participant reproducibility during maximal voluntary exertions for the anterior deltoid, middle deltoid, and infraspinatus. *Journal of Electromyography and Kinesiology*, *20*(1), 68–75.

Flatow, E., Soslowsky, L., Ticker, J., Pawluk, R., Hepler, M., Ark, J., … Bigliani, L. (1994). Excursion of the rotator cuff under the acromion. Patterns of subacromial contact. *American Journal of Sports Medicine*, *22*(6), 779–788.

Fouré, A., Nordez, A., & Cornu, C. (2010). Plyometric training effects on Achilles tendon stiffness and dissipative properties. *Journal of Applied Physiology*, *109*(3), 849–854.

Fox, A., Schar, M., Wanivenhaus, F., Chen, T., Attia, E., Binder, N., … Rodeo, S. (2014). Fluoroquinolones Impair Tendon Healing in a Rat Rotator Cuff Repair Model: A Preliminary Study. *The American Journal of Sports Medicine*, *42*(12), 2851–2859.

Freedman, B., Zuskov, A., Sarver, J., Buckley, M., & Soslowsky, L. (2015). Evaluating changes in tendon crimp with fatigue loading as an ex vivo structural assessment of tendon damage.

Journal of Orthopaedic Research, *33*(6), 904–910.

Freedman, L., & Munro, R. (1966). Abduction of the arm in the scapular plane: scapular and glenohumeral movements. A roentgenographic study. *Journal of Bone & Joint Surgery*, *48*(8), 1503–1510.

Frisch, K., Marcu, D., Baer, G., Thelen, D., & Vanderby, R. (2014). The influence of partial and full thickness tears on infraspinatus tendon strain patterns. *Journal of Biomechanical Engineering*, *136*(5), 05100.

Frost, P., & Andersen, J. (1999). Shoulder impingement syndrome in relation to shoulder intensive work. *Occupational and Environmental Medicine*, *56*(7), 494–498.

Frost, P., Bonde, J., Mikkelsen, S., Andersen, J., Fallentin, N., Kaergaard, A., & Thomsen, J. (2002). Risk of shoulder tendinitis in relation to shoulder loads in monotonous repetitive work. *American Journal of Industrial Medicine*, *41*(1), 11–18.

Fu, F., Harner, C., & Klein, A. (1991). Shoulder impingement syndome. A critical review. *Clinical Orthopaedics and Related Research*, *269*, 162-173.

Fuglevand, A. J., Winter, D. A., Patla, A. E., & Stashuk, D. (1992). Detection of motor unit action potentials with surface electrodes: influence of electrode size and spacing. *Biological Cybernetics*, *153*, 143–153.

Fukashiro, S., Komi, P., Järvinen, M., & Miyashita, M. (1993). Comparison between the directly measured achilles tendon force and the tendon force calculated from the ankle joint moment during vertical jumps. *Clinical Biomechanics*, *8*(1), 25–30.

Fukuda, H., Hamada, K., Nakajima, T., & Tomonaga, A. (1994). Pathology and pathogenesis of the intratendinous tearing of the rotator cuff viewed from en block histologic sessions. *Clinical Orthopaedics and Related Research*, *304*, 60–67.

Fukuda, H., Mikasa, M., & Yamanaka, K. (1987). Incomplete thickness rotator cuff tears diagnosed by subacromial bursography. *Clinical Orthopaedics and Related Research*, *223*, 51–58.

Fukuta, S., Oyama, M., Kavalkovich, K., Fu, F., & Niyibizi, C. (1998). Identification of types II, IX and X collagens at the insertion site of the bovine achilles tendon. *Matrix Biology*, *17*, 65–73.

Fuller, J., Fung, J., & Côté, J. (2011). Time-dependent adaptations to posture and movement characteristics during the development of repetitive reaching induced fatigue. *Experimental Brain Research*, *211*(1), 133–143.

Fung, D., Sereysky, J., Basta-Pljakic, J., Laudier, D., Huq, R., Jepsen, K., … Flatow, E. (2010). Second harmonic generation imaging and Fourier transform spectral analysis reveal damage in fatigue-loaded tendons. *Annals of Biomedical Engineering*, *38*(5), 1741–1751.

Fung, D., Wang, V., Andarawis-Puri, N., Basta-Pljakic, J., Li, Y., Laudier, D., … Flatow, E. (2010). Early response to tendon fatigue damage accumulation in a novel in vivo model. *Journal of Biomechanics*, *43*(2), 274–279.

Fung, D., Wang, V., Laudier, D., Shine, J., Basta-Pljakic, J., Jepsen, K., … Flatow, E. (2008). Subrupture tendon fatigue damage. *Journal of Orthopaedic Research*, *27*(2), 264–273.

Gagey, N., Gagey, O., Bastian, G., & Lassau, J. (1990). The fibrous frame of the supraspinatus muscle—correlations between anatomy and MRI findings. *Surgical and Radiologic Anatomy*, *12*(8), 291–292.

Gagey, N., Quillard, J., Gagey, O., Meduri, G., Bittoun, J., & Lassau, J. (1995). Tendon of the normal supraspinatus muscle: correlations between MR imaging and histology. *Surgical and Radiologic Anatomy*, *17*, 329–334.

Gajdosik, R., Vander Linden, D., McNair, P., WIlliams, A., & Riggin, T. (2004). Effects of an eight-week stretching program on the passive-elastic properties and function of the calf muscles of older women. *Clinical Biomechanics*, *20*, 973–983.

Galatz, L., Ball, C., Teefey, S., Middleton, W., & Yamaguchi, K. (2004). The outcome and repair integrity of completely arthroscopically repaired large and massive rotator cuff tears. *Journal of Bone & Joint Surgery*, *86*(2), 219–224.

Gardiner, J., Cordaro, N., & Weiss, J. (2000). Elastic and viscoelastic shear properties of the medial collateral ligament. Trans 46th Meeting Orthop Res Soc 2000;25:63. *Transactions of the 46th Meeting of the Orthopaedic Research Society*, *25*(63), 63.

Gardiner, J., & Weiss, J. (2001). Simple shear testing of parallel-fibered plana soft tissues. *Journal of Biomechanical Engineering*, *123*(2), 170–175.

Garg, A., Hegmann, K., & Kapellusch, J. (2005). Maximum one-handed shoulder strength for overhead work as a function of shoulder posture in females 5: 131–140. *Occupational Ergonomics*, *5*, 131–140.

Gates, D., & Dingwell, J. (2008). Gates, Deanna H., & Dingwell, Jonathan B. (2008). The effects of neuromuscular fatigue on task performance during repetitive goal-directed movements. Experimental Brain Research, 187(4), 573–585. *Experimental Brain Research*, *187*(4), 573–585.

Gates, J., Gilliland, J., McGarry, M., Park, M., Acevedo, D., Fitzpatrick, M., & Lee, T. (2010). Influence of distinct anatomic subregions of the supraspinatus on humeral rotation. *Journal of Orthopaedic Research*, *28*(1), 12–17.

Gerber, C., Fuchs, B., & Hodler, J. (2000). The results of repair of massive tears of the rotator cuff. *Journal of Bone & Joint Surgery*, *82*, 505–515.

Gibbon, W., Cooper, J., & Radcliffe, G. (1999). Sonographic incidence of tendon microtears in athletes with chronic Achilles tendinosis. *British Journal of Sports Medicine*, *33*, 129–130.

Gimbel, J., Kleunen, J., Mehta, S., Perry, S., Williams, G., & Soslowsky, L. (2004). Supraspinatus tendon organizational and mechanical properties in a chronic rotator cuff tear animal model. *Journal of Biomechanics*, *37*(5), 739–749.

Gimbel, J., Mehta, S., van Kleunen, J., Williams, G., & Soslowsky, L. (2004). The tension required at repair to reappose the supraspinatus tendon to bone rapidly increases after injury. *Clinical Orthopaedics and Related Research*, *426*, 258–265.

Gimbel, J., van Kleunen, J., Williams, G., Thomopoulos, S., & Soslowsky, L. (2007). Long durations of immobilization in the rat result in enhanced mechanical properties of the healing supraspinatus tendon insertion site. *Journal of Biomechanical Engineering*, *129*, 400–404.

Gohlke, F., Essigkrug, B., & Schmitz, F. (1994). The pattern of the collagen fiber bundles of the capsule of the glenohumeral joint. *Journal of Shoulder and Elbow Surgery*, *3*(3), 111–128.

Gooyers, C., & Callaghan, J. (2015). Exploring interactions between force, repetition and posture on intervertebral disc height loss and bulging in isolated porcine cervical functional spinal units from sub-acute-faulre magnitudes of cyclic compressive loading. *Journal of Biomechanics*, *48*, 3701–3708.

Gosline, J., Lillie, M., Carrington, E., Guerette, P., Ortlepp, C., & Savage, K. (2002). Elastic proteins: Biological roles and mechanical properties. *Philosophical Transactions of the Royal Society B: Biological Sciences*, *357*(1418), 121–132.

Goutallier, D., Postel, J., Bernageau, J., Lavau, L., & Voisin, M. (1994). Fatty muscle degeneration in cuff ruptures. Pre- and postoperative evaluation by CT scan. *Clinical Orthopaedics and Related Research*, *304*, 78–83.

Goutallier, D., Postel, J., Bernageau, J., & Voisin, M. (1995). Fatty infiltration of disrupted rotator cuff muscles. *Revue Du Rhumatisme (English Ed)*, *62*(6), 415–422.

Graichen, H., Bonel, H., Stammberger, T., Englmeier, K., Reiser, M., & Eckstein, F. (1999). Subacromial space width changes during abduction and rotation – a 3-D MR imaging study. *Surgical and Radiologic Anatomy*, *21*(1), 59–64.

Graichen, H., Bonel, H., Stammberger, T., Haubner, M., Rohrer, H., Englmeier, K., … Eckstein, F. (1999). Three-dimensional analysis of the width of the subacromial space in healthy subjects and patients with impingement syndrome. *American Journal of Roentgenology*, *172*(4), 1081–1086.

Gregor, R., Komi, P., & Jarvinen, M. (1987). Achilles tendon forces during cycling. *International Journal of Sports Medicine*, *8*(1), 9–14.

Grewal, T.-J., Cudlip, A., & Dickerson, C. (2017). Comparing non-invasive scapular tracking methods across elevation angles, planes of elevation and humeral axial rotations. *Journal of Electromyography and Kinesiology*, *37*.

Grieve, J., & Dickerson, C. (2008). Overhead work: Identification of evidence-based exposure guidelines. *Ocupational Ergonomics*, *8*(1), 53–66.

Gruevski, K., Gooyers, C., Karakolis, T., & Callaghan, J. (2016). The effect of local hydration environment on the mechanical properties and unloaded temporal changes of isolated porcine annular samples. *Journal of Biomechanical Engineering*, *138*(10), 104502.

Gulotta, L., Kovacevic, D., Packer, J., Deng, X., & Rodeo, S. (2011). Bone marrow–derived mesenchymal stem cells transduced with scleraxis improve rotator cuff healing in a rat model. *American Journal of Sports Medicine*, *39*, 1282–1289.

Gumina, S., Candela, V., Passaretti, D., Latino, G., Venditto, T., Mariani, L., & Santilli, V.

(2014). The association between body fat and rotator cuff tear: the influence on rotator cuff tear sizes. *Journal of Shoulder and Elbow Surgery*, *23*(11), 1669–1674.

Hagberg, M. (1981). Work load and fatigue in repetitive arm elevations. *Ergonomics*, *24*(7), 543–555.

Halder, A., O'Driscoll, S., Heers, G., Mura, N., Zobitz, M., An, K., & Kreusch-Brinker, R. (2002). Biomechanical comparison of effects of supraspinatus tendon detachments, tendon defects, and muscle retractions. *Journal of Bone and Joint Surgery*, *84*(5), 780–785.

Hamada, K., Okawara, Y., Fryer, J., Tomonaga, A., & Fukuda, H. (1994). Localization of mRNA of procollagen alpha 1 type I in torn supraspinatus tendons. In situ hybridization using digoxigenin labeled oligonucleotide probe. *Clinical Orthopaedics and Related Research*, *304*, 18–21.

Hamner, S., Seth, A., & Delp, S. (2010). Muscle contributions to propulsion and support during running. *Journal of Biomechanics*, *43*, 2709–2916.

Hansen, K., Weiss, J., & Barton, J. (2002). Recruitment of tendon crimp with applied tensile strain. *Journal of Biomedical Engineering*, *124*, 72–77.

Harryman II, D., Mack, L., Wang, K., Jackins, S., Richardson, M., & Matsen III, F. (1991). Repairs of the rotator cuff. Correlation of functional results with integrity of the cuff. *Journal of Bone & Joint Surgery*, *73*, 982–989.

Haut, R. (1985). The effect of a lathyritic diet on the sensitivity of tendon to strain rate. *Journal of Biomechanical Engineering*, *107*, 166–174.

Hawkins, R., Misamore, G., & Hobeika, P. (1985). Surgery for full-thickness rotator-cuff tears. *Journal of Bone & Joint Surgery*, *67*(9), 1349–1355.

Hegedus, E., Goode, A., Cook, C., Michener, L., Myer, C., Myer, D., & Wright, A. (2012). Which physical examination tests provide clinicians with the most value when examining the shoulder? Update of a systematic review with meta-analysis of individual tests. *British Journal of Sports Medicine*, *46*(14), 964–978.

Heinemeier, K., Skovgaard, D., Bayer, M., Qvortrup, K., Kjaer, A., Kjaer, M., … Kongsgaard, M. (2012). Uphill running improves rat Achilles tendon tissue mechanical properties and alters gene expression without inducing pathological changes. *Journal of Applied Physiology*, *113*(5), 827–836.

Herberts, P., Kadefors, R., Andersson, G., & Petersen, I. (1981). Shoulder pain in industry: An epidemiological study on welders. *Acta Orthop Scand*, *52*(2), 299–306.

Herberts, P., Kadefors, R., Högfors, C., & Sigholm, G. (1984). Shoulder pain and heavy manual labor. *Clinical Orthopaedics and Related Research*, *191*, 166–178.

Hermenegildo, J., Roberts, S., & Kim, S. (2014). Innervation pattern of the suprascapular nerve within supraspinatus: A three-dimensional computer modeling study. *Clinical Anatomy*, *27*(4), 622–630.

Hersche, O., & Gerber, C. (1998). Passive tension in the supraspinatus musculotendinous unit

after long-standing rupture of its tendon: a preliminary report. *Journal of Shoulder and Elbow Surgery*, *7*(4), 393–396.

Hik, F., & Ackland, D. (2019). The moment arms of the muscles spanning the glenohumeral joint : a systematic review. *Journal of Anatomy*, *234*, 1–15.

Ho, A., Cudlip, A., Ribeiro, D., & Dickerson, C. (2019). Examining upper extremity muscle demand during selected push-up variants. *Journal of Electromyography and Kinesiology*, *44*(November 2018), 165–172.

Holzbaur, K., Murray, W., & Delp, S. (2005). A model of the upper extremity for simulating musculoskeletal surgery and analyzing neuromuscular control. *Annals of Biomedical Engineering*, *33*(6), 829–840.

Horst, C., & Veldhuis, J. (2008). *Biotester 5000 - User manual*. Waterloo, ON: Waterloo Instruments Inc.

Houssen, Y., Gusachenko, I., Schanne-Klein, M., & Allain, J. (2011). Monitoring micrometer-scale collagen organization in rat-tail tendon upon mechanical strain using second harmonic microscopy. *Journal of Biomechanics*, *44*, 2047–2052.

Howell, S., & Galinat, B. (1989). The glenoid-labral socket. A constrained articular surface. *Clinical & Orthopaedic Related Research*, *243*, 122–125.

Howell, S., & Kraft, T. (1991). The role of supraspinatus and ifnraspinatus muscles in glenohumeral kinematics of anterior shoulder instability. *Clinical Orthopaedics and Related Research*, *263*, 128–134.

Huang, C., Wang, V., Pawluk, R., Bucchieri, J., Levine, W., Bigliani, L., … Flatow, E. (2005). Inhomogeneous mechanical behavior of the human supraspinatus tendon under uniaxial loading. *Journal of Orthopaedic Research*, *23*(4), 924–930.

Huberty, D., Schoolfield, J., Brady, P., Vadala, A., Arrigoni, P., & Burkhart, S. (2009). Incidence and treatment of postoperative stiffness following arthroscopic rotator cuff repair. *Arthroscopy*, *25*, 880–890.

Hughes, D., Kirby, M., Sikoryn, T., Apsden, R., & Cox, A. (1990). Comparison of structure, mechanical properties, and functions of lumbar spinal ligaments. *Spine*, *15*(8), 787–795.

Hughes, R., Bryant, C., Hall, J., Wening, J., Huston, L., Kuhn, J., … Blasier, R. (2003). Glenoid inclination is associated with full-thickness rotator cuff tears. *Clinical Orthopaedics and Related Research*, *407*, 86–91.

Inman, V., Saunders, J., & Abbott, L. (1944). Observations on the function of the shoulder joint. *Journal of Bone & Joint Surgery*, *26*, 1–30.

Itoi, E., Hsu, H.-C., & An, K.-N. (1996). Biomechanical investigation of the glenohumeral joint. *Journal of Shoulder and Elbow Surgery*, *5*(5), 407–424.

Jackson, D. (1976). Chronic rotator cuff impingement in the throwing athlete. *American Journal of Sports Medicine*, *4*(6), 231–240.

Jarvinen, M., Jozsa, L., Kannus, P., Jarvinen, T., Kvist, M., & Leadbetter, W. (1997).

Histopathological findings in chronic tendon disorders. *Scandinavian Journal of Medicine and Science in Sports*, *7*, 86–95.

Jepsen, K., & Davy, D. (1997). Comparison of damage accumulation measures in human cortical bone. *Journal of Biomechanics*, *30*, 891–894.

Jobe, C. (1995). Posterior superior glenoid impingement: expanded spectrum. *Arthroscopy*, *11*(5), 530–536.

Jobe, F., & Moynes, D. (1982). Delineation of diagnostic criteria and a rehabilitation program for rotator cuff injuries. *American Journal of Sports Medicine*, *10*(6), 336–339.

Jonsson, B. (1988). The static load component in muscle work. *European Journal of Applied Physiology*, *57*(3), 305–310.

Joo, W., Jepsen, K., & Davy, D. (2007). The effect of recovery time and test conditions on viscoelastic measures of tensile damage in cortical bone. *Journal of Biomechanics*, *40*, 2731–2737.

Josza, L., & Kannus, P. (1997). *Human tendons: anatomy, physiology, and pathology*. Human Kinetics.

Jozsa, L., Lehto, M., Kvist, M., Balint, J., & Reffy, A. (1989). Alterations in dry mass content of collagen fibers in degenerative tendinopathy and tendon-rupture. *Matrix Biology*, *9*, 140–146.

Karakolis, T., & Callaghan, J. (2014). Localized strain measurements of the intervertebral disc annulus during biaxial tensile testing. *Computer Methods in Biomechanics and Biomedical Engineering*, *18*(16), 1737–1743.

Karas, V., Wang, M., Dhawan, A., & Cole, B. (2011). Biomechanical factors in rotator cuff pathology. *Sports Medicine and Arthroscopy Review*, *19*(3), 202–206.

Kastelic, J., Galeski, A., & Baer, E. (1978). The multicomposite structure of tendon. *Connective Tissue Research*, *6*, 11–23.

Keyes, E. (1952). Anatomical observations on senile changes in the shoulder. *Journal of Bone & Joint Surgery*, *19*, 953–960.

Khan, K., Cook, J., Kannus, P., Maffuli, N., & Bonar, S. (2002). Time to abandon the ‘“tendinitis”’ myth. *British Medical Journal*, *324*(738), 626–627.

Kibler, W. (2006). Evaluation of apparent and absolute supraspinatus strength in patients with shoulder injury using the scapular retraction test. *American Journal of Sports Medicine*, *34*(10), 1643–1647.

Kim, H., Dahiya, N., Teefey, S., Middleton, W., Stobbs, G., Steger-May, K., … Keener, J. (2010). Location and initiation of degenerative rotator cuff tears: an analysis of three hundred and sixty shoulders. *Journal of Bone & Joint Surgery*, *92*(5), 1088–1096.

Kim, S., Bleakney, R., Boynton, E., Ravichandiran, K., Rindlisbacher, T., Mckee, N., & Agur, A. (2010). Investigation of the static and dynamic musculotendinous architecture of supraspinatus. *Clinical Anatomy*, *23*(1), 48–55.

Kim, S., Boynton, E., Ravichandiran, K., Fung, L., Bleakney, R., & Agur, A. (2007). Three-dimensional study of the musculotendinous architecture of supraspinatus and its functional implications. *Clinical Anatomy*, *20*, 648–655.

Kim, S., Collins, D., & Dickerson, C. (2016). Electromyographic investigation of anterior and posterior regions of supraspinatus: a novel protocol based on anatomical insights. *Proceedings of the 11th Meeting of the International Shoulder Group*, *1*, 75–76.

Kim, S., Ko, J., Dickerson, C., & Collins, D. (2017). Electromyographic investigation of anterior and posterior regions of supraspinatus: a novel approach based on anatomical insights. *International Biomechanics*, *4*(2), 60–67.

Kim, S., Lunn, D., Dyck, R., Kirkpatrick, L., & Rosser, B. (2013). Fiber type composition of the architecturally distinct regions of human supraspinatus muscle: A cadaveric study. *Histology and Histopathology*, *28*(8), 1021–1028.

King, S., Vanicek, N., & O'Brien, T. (2016). Gastrocnemius muscle architecture and Achilles tendon properties influence walking distance in claudicants with peripheral arterial disease. *Muscle & Nerve*, *53*(5), 733–741.

Kingston, D., & Acker, S. (2018). Representing fine-wire EMG with surface EMG in three thigh muscles during high knee flexion movements. *Journal of Electromyography and Kinesiology*, *43*, 55–61.

Kjaer, M. (2004). Role of extracellular matrix in adaptation of tendon and skeletal muscle to mechanical loading. *Physiological Reviews*, (84), 649–698.

Komi, P. (1990). Relevance of in vivo force measurements to human biomechanics. *Journal of Biomechanics*, *23*(1), 23–34.

Komi, P., Salonen, M., Jarvninen, M., & Kokko, O. (1987). In vivo registration of Achilles tendon forces in man. *International Journal of Sports Medicine*, *8*(1), 3–8.

Kovacevic, D., Fox, A., Bedi, A., Ying, L., Deng, X., Warren, R., & Rodeo, S. (2011). Calcium-phosphatematrix with or without TGF-β3 improves tendon-bone healing after rotator cuff repair. *American Journal of Sports Medicine*, *39*(4), 811–819.

Kubo, K., Kanehisa, H., Miyatani, M., Tachi, M., & Fukunaga, T. (2003). Effect of low-load resistance training on the tendon properties in middle-aged and elderly women. *Acta Physiologica Scandinavica*, *178*(1), 25–32.

Kuechle, D. K., Newman, S. R., Itoi, E., & Morrey, B. F. (1997). Shoulder muscle moment arms during horizontal flexion and elevation. *Journal of Shoulder and Elbow Surgery*, *6*(5), 429–439.

Kuhn, J., Bey, M., Huston, L., Blasier, R., & Soslowsky, L. (2000). Ligamentous restraints to external rotation of the humerus in the late-cocking phase of throwing. A cadaveric biomechanical investigation. *American Journal of Sports Medicine*, *28*(2), 200–205.

Kujala, U., Sarna, S., & Kaprio, J. (2005). Cumulative incidence of achilles tendon rupture and tendinopathy in male former elite athletes. *Clinical Journal of Sport Medicine*, *15*, 133–135.

Kumagai, J., Sarkar, K., & Ulthoff, H. (1994). The collagen types in the attachment zone of rotator cuff tendons in the elderly: an immunohistochemical study. *Journal of Rheumatology*, *21*(11), 2096–2100.

Kumar, V., & Balasubramaniam, P. (1985). The role of atmospheric pressure in stabilising the shoulder. An experimental study. *Journal of Bone and Joint Surgery*, *67*(5), 719–721.

Kuorinka, I., & Forcier, L. (1995). *Work-related musculoskeletal disorders (WMSDs): a reference book for prevention*. London, England: Taylor & Francis.

Kurdziel, M., Davidson, A., Ross, D., Seta, J., Doshi, S., Baker, K., & Maerz, T. (2019). Biomechanical properties of the repaired and non-repaired rat supraspinatus tendon in the acute postoperative period. *Connective Tissue Research*, *60*(3), 254–264.

Kuznetsov, S., Pankow, M., Peteres, K., & Huang, H.-S. S. (2019). Strain state dependent anisotropic viscoelasticity of tendon-to-bone insertion. *Mathematical Biosciences*, *308*(2), 1–7.

Kwan, M., Lin, T., & Woo, S.-Y. (1993). On the viscoelastic properties of the anteromedial bundle of the anterior cruciate ligament. *Journal of Biomechanics*, *26*(4–5), 447–452.

La Delfa, N., Freeman, C., Petruzzi, C., & Potvin, J. (2014). Equations to predict female manual arm strength based on hand location relative to the shoulder. *Ergonomics*, *57*(2), 254–261.

Lake, S., Miller, K., Elliott, D., & Soslowsky, L. (2009). Effect of fiber distribution and realignment on the nonlinear and inhomogeneous mechanical properties of human supraspinatus tendon under longitudinal tensile loading. *Journal of Orthopaedic Research*, *27*, 1596–1602.

Lake, S., Miller, K., Elliott, D., & Soslowsky, L. (2010). Tensile properties and fiber alignment of human supraspinatus tendon in the transverse direction demonstrate inhomogeneity, nonlinearity, and regional isotropy. *Journal of Biomechanics*, *43*, 727–732.

Langenderfer, J., Patthanacharoenphon, C., Carpenter, J., & Hughes, R. (2006). Variability in isometric force and moment generating capacity of glenohumeral external rotator muscles. *Clinical Biomechanics*, *21*, 701–709.

Lapiere, C., Nusgens, B., & Pierard, G. (1977). Interaction between collagen type I and type III in conditioning bundles organization. *Connective Tissue Research*, *5*, 21–29.

Largacha, M., Parsons IV, I., Campbell, B., Titelman, R., Smith, K., & Matsen III, F. (2006). Deficits in shoulder function and general health associated with sixteen common shoulder diagnoses: A study of 2674 patients. *Journal of Shoulder and Elbow Surgery*, *15*(1), 30–39.

Lassek, W., & Gaulin, S. (2009). Costs and benefits of fat-free muscle mass in men: relationship to mating success, dietary requirements, and native immunity. *Evolution and Human Behaviour*, *30*(5), 322–328.

Leadbetter, W. (1992). Cell-matrix response in tendon injury. *Clinics in Sport Medicine*, *11*, 533–578.

Lee, D., Li, Z., Sohail, Q., Jackson, K., Fiume, E., & Agur, A. (2015). A three-dimensional

approach to pennation angle estimation for human skeletal muscle. *Computer Methods in Biomechanics and Biomedical Engineering*, Vol. 18, pp. 1474–1484. Taylor & Francis.

Lee, S.-B., Kim, K.-J., O'Driscol, S., Morrey, B., & An, K.-N. (2000). Dynamic glenohumeral stability provided by the rotator cuff muscles in the mid-range and end-range of motion. A study in cadavera. *The Journal of Bone and Joint Surgery*, *82*(6), 849–857.

Lehman, C., Cuomo, F., Kummer, F., & Zuckerman, J. (1995). The incidence of full thickness rotator cuff tears in a large cadaveric population. *Bulletin for Hospital Joint Diseases*, *54*(1), 30–31.

Leivseth, G., & Reikeras, O. (1994). Changes in muscle fiber cross-sectional area and concentrations of Na,K-ATPase in deltoid muscle in patients with impingement syndrome of the shoulder. *Journal of Orthopaedic Sports Physical Therapy*, *19*(3), 146–149.

Leroux, J., Codine, P., Thomas, E., Pocholle, M., Mailhe, D., & Blotman, F. (1994). Isokinetic evaluation of rotational strength in normal shoulders and shoulders with impingement syndrome. *Clinical Orthopaedics and Related Research*, *304*, 108–115.

Leroux, J., Thomas, E., Bonnel, F., & Blotman, F. (1995). Diagnostic value of clinical tests for shoulder impingement syndrome. *Revue Du Rhumatisme (English Ed)*, *62*(6), 423–428.

Lieber, R., & Fridén, J. (2001). Clinical significance of skeletal muscle architecture. *Clinical Orthopaedics and Related Research*, *383*, 140–151.

Lieber, R., Leonard, M., & Brown-Maupin, C. (2000). Effects of muscle contraction on the load-strain properties of frog aponeurosis and tendon. *Cells Tissues Organs*, *166*, 48–54.

Lin, JC, Weintraub, N., & Aragaki, D. (2008). Nonsurgical treatment for rotator cuff injury in the elderly. *Journal of the Americal Medical Directors Association*, *9*(9), 626–632.

Lin, JJ, Lim, H., & Yang, J. (2006). Effect of shoulder tightness on glenohumeral translation, scapular kinematics, and scapulohumeral rhuthm in subjects with stiff shoulders. *Journal of Orthopaedic Research*, *24*(5), 1044–1051.

Lindblom, K., & Palmer, I. (1939). Ruptures of the tendon aponeurosis of the shoulder joint - the so-called supraspinatus ruptures. *Acta Radiologica*, *20*(6), 563–577.

Liu, J., Hughes, R., Smutz, W., Niebur, G., & An, K.-N. (1997). Roles of deltoid and rotator cuff muscles in shoulder elevation. *Clinical Biomechanics*, *12*(1), 32–38.

Liu, SH, & Baker, C. (1994). Arthroscopically assisted rotator cuff repair: correlation of functional results with integrity of the cuff. *Arthroscopy*, *10*, 54–60.

Liu, Sh, & Boynton, E. (1993). Posterior superior impingement of the rotator cuff on the glenoid rim as a cause of shoulder pain in the overhead athlete. *Arthroscopy*, *9*(6), 697–699.

Loehr, J., & Uhthoff, H. (1987). The pathogenesis of degenerative rotator cuff tears," Orthop. Trans. *Orthopaedic Transactions*, *11*, 237.

Lomond, K., & Côté, J. (2011). Differences in posture–movement changes induced by repetitive arm motion in healthy and shoulder-injured individuals. *Clinical Biomechanics*, *26*(2), 123–129.

Lujan, T., Underwood, C., Jacobs, N., & Weiss, J. (2009). Contribution of glycosaminoglycans to viscoelastic tensile behavior of human ligament. *Journal of Applied Physiology (Bethesda, Md. : 1985), 106*(2), 423–431.

Luopajarvi, T., Kuorinka, I., Virolainen, M., & Holmberg, M. (1979). Prevalence of tenosynovitis and other injuries of the upper extremities in repetitive work. *Scandinavian Journal of Work, Environment & Health*, *5*(3), 48–55.

Maciukiewicz, J., Cudlip, A., Chopp-Hurley, J., & Dickerson, C. (2016). Effects of overhead work configuration on muscle activity during a simulated drilling task. *Applied Ergonomics*, *53*, 10–16.

Maganaris, C., & Paul, J. (1999). In vivo human tendon mechanical properties. *Journal of Physiology*, *521*(1), 307–313.

Magnusson, S., Hansen, M., Langberg, H., Miller, B., Haraldsson, B., Westh, E., … Kjaer, M. (2007). The adaptability of tendon to loading differs in men and women. *International Journal of Experimental Pathology*, *88*(4), 237–240.

Magnusson, S., Langberg, H., & Kjaer, M. (2010). The pathogenesis of tendinopathy: balancing the response to loading. *National Reviews in Rheumatology*, *6*, 262–268.

Magnusson, S., Narici, M., Maganaris, C., & Kjaer, M. (2008). Human tendon behaviour and adaptation, in vivo. *Journal of Physiology*, *1*, 71–81.

Makela, M., Heliovaara, M., Sainio, P., Knekt, P., Impivaara, O., & Aromaa, A. (1999). Shoulder joint impairment among Finns aged 30 years or over: Prevalence, risk factors and co-morbidity. *Rheumatology*, *38*(7), 656–662.

Malanga, G., Jenp, Y.-N., Growney, E., & An, K.-N. (1996). EMG analysis of shoulder positioning in testing and strengthening the supraspinatus. *Medicine and Science in Sports and Exercise*, *28*(6), 661–664.

Malicky, D., Soslowsky, L., & Blasier, R. (1996). Anterior glenohumeral stabilization factors: Progressive effects in a biomechanical model. *Journal of Orthopaedic Research*, *14*, 282–286.

Marqueti, R., Parizotto, N., Chriguer, R., Perez, S., & Selistre-de-Araujo, H. (2006). Androgenic-anabolic steroids associated with mechanical loading inhibit matrix metallopeptidase activity and affect the remodeling of the achilles tendon in rats. *American Journal of Sports Medicine*, *34*(8), 1274–1280.

Martin, S., & MacIsaac, D. (2006). Innervation zone shift with changes in joint angle in the brachial biceps. *Journal of Electromyography and Kinesiology*, *16*(2), 144–148. https://doi.org/10.1016/j.jelekin.2005.06.010

Mathewson, M., Kwan, A., Eng, C., Lieber, R., & Ward, S. (2014). Comparison of rotator cuff muscle architecture between humans and other selected vertebrate species. *Journal of Experimental Biology*, *217*(2), 261–273.

Matias, R., & Pascoal, A. (2006). The unstable shoulder in arm elevation: A three-dimensional and electromyographic study in subjects with glenohumeral instability. *Clinical*

Biomechanics, *21*(1), 52–58.

Matsen III, F., Fu, F., & Hawkins, R. (1992). *The Shoulder: A Balance of Mobility and Stability*.

Matsen III, F., & Lippitt, S. (2004). *Shoulder Surgery: Principles and Procedures*. Philadelphia, PA: WB Saunders.

Matsen III, F., Sidles, J., Harrymann, D., & Lippert, S. (1994). *Practical Evaluation and Management of the Shoulder* (p. 256). p. 256. Philadelphia: WB Saunders.

McDonald, A, Picco, B., Belbeck, A., Chow, A., & Dickerson, C. (2012). Spatial dependency of shoulder muscle demands in horizontal pushing and pulling. *Applied Ergonomics*, *43*(6), 971–978.

McDonald, AC, Brenneman, E., Cudlip, A., & Dickerson, C. (2014). The spatial dependency of shoulder muscle demands for seated lateral hand force exertions. *Journal of Applied Biomechanics*, *30*(1), 1–11.

Meskers, C., Fraterman, H., Van der Helm, F., Vermeulen, H., & Rozing, P. (1998). In vivo estimation of the glenohumeral joint rotation center from scpular bony landmarks by linear regression. *Journal of Biomechanics*, *31*, 93–96.

Meyer, A. (1924). Further evidences of attrition in the human body. *American Journal of Anatomy*, *34*, 241–267.

Milgrom, C., Schaffler, M., Gilbert, S., & van Holsbeeck, M. (1995). Rotator-cuff changes in asymptomatic adults. The effect of age, hand dominance and gender. *The Journal of Bone and Joint Surgery*, *77*(2), 296–298.

Miller, K., Connizzo, B., Feeney, E., & Soslowsky, L. (2012). Characterizing local collagen fiber re-alignment and crimp behavior throughout mechanical testing in a mature mouse supraspinatus tendon model. *Journal of Biomechanics*, *45*(12), 2061–2065.

Miller, K., Connizzo, B., Feeney, E., Tucker, J., & Soslowsky, L. (2012). Examining differences in local collagen fiber crimp frequency throughout mechanical testing in a developmental mouse supraspinatus tendon model. *Journal of Biomechanical Engineering*, *134*(4), 1–7.

Miller, K., Connizzo, B., & Soslowsky, L. (2012). Effect of preconditioning and stress relaxation on local collagen fiber re-alignment: inhomogeneous properties of rat supraspinatus tendon. *Journal of Biomechanical Engineering*, *134*(3), 031007.

Miller, K., Edelstein, K., Connizzo, B., & Soslowsky, L. (2012). Effect of preconditioning and stress relaxation on local collagen fiber re-alignment: inhomogeneous properties of rat supraspinatus tendon. *Journal of Biomechanical Engineering*, *134*(3), 031007.

Minagawa, H., Itoi, E., Sato, T., Konno, N., Hongo, M., & Sato, K. (1996). Morphology of the transitional zone of intramuscular to extramuscular tendons of the rotator cuff. *Katakansetsu*, *20*, 103–110.

Miranda, H., Viikari-Juntura, E., Heistaro, S., Heliovaara, M., & Riihimaki, H. (2005). A population study on differences in the determinants of a specific shoulder disorder versus nonspecific shoulder pain without clinical findings. *American Journal of Epidemiology*,

161(9), 847–855.

Montgomery, S., Petrigliano, F., & Gamradt, S. (2012). Failed rotator cuff surgery, evaluation and decision making. *Clinical Journal of Sport Medicine*, *31*, 693–712.

Moore, M., & De Beaux, A. (1987). A quantitative ultrastructural study of rat tendon from birth to maturity. *Journal of Anatomy*, *153*, 163–169.

Moseley, H. (1952). *Ruptures to the Rotator Cuff*. Springfield, Ill: Charles C Thomas.

Moseley, H., & Goldie, I. (1963). The arterial pattern of the rotator cuff of the shoulder. *Journal of Bone & Joint Surgery*, *45*(4), 780–789.

Moseley, H., & Overgaard, B. (1962). The anterior capsular mechanism in recurrent anterior disocation of the shoulder. *The Journal of Bone and Joint Surgery*, *44*(4), 913–927.

Motzkin, N., Itoi, E., Morrey, B., & An, K.-N. (1998). Contribution of capsuloligamentous structures to passive static inferior glenohumeral stability. *Clinical Biomechanics*, *13*(1), 54–61.

Nadon, A., Vidt, M., Chow, A., & Dickerson, C. (2016). The spatial dependency of shoulder muscular demands during upward and downward exertions. *Ergonomics*, *59*(10), 1294–1306.

Nakagaki, K., Tomita, T., Sakurai, G., Oshiro, O., Tamai, S., & Ozaki, J. (1994). Anatomical study on the atrophy of supraspinatus muscle belly with cuff tear. *Nihon Seikeigaka Gakkai Zasshi*, *68*(7), 516–521.

Nakajima, T., & Fukuda, H. (1993). Fiber arrangements of the supraspinatus tendon. *Journal of Shoulder and Elbow Surgery*, *3*, 49.

Nakajima, T., Rokuuma, N., Hamada, K., Tomatsu, T., & Fukuda, H. (1994). Histologic and biomechanical characteristics of the supraspinatus tendon: reference to rotator cuff tearing. J Shoulder Elbow Surg 1 W4;3:79-87. *Journal of Shoulder and Elbow Surgery*, *3*(2), 79–87.

Nakama, L., King, K., Abrahamsson, S., & Rempel, D. (2006). VEGF, VEGFR-1 and CTGF cell densities in tendon are increased with cyclical loading: an in vivo tendinopathy model. *Journal of Orthopaedic Research*, *24*, 393–400.

Namdari, S., & Green, A. (2010). Range of motion limitation after rotator cuff repair. *Journal of Shoulder and Elbow Surgery*, *19*, 290–296.

Neer, C. (1972). Anterior acromioplasty for the chronic impingement syndrome in the shoulder: a preliminary report. *Journal of Bone & Joint Surgery*, *54*(1), 41–50.

Neer, C. (1983). Impingement lesions. *Clinical Orthopaedics and Related Research*, *173*, 70–77.

Neviaser, J. (1971). Ruptures of the rotator cuff of the shoulder: new concepts in the diagnosis and operative treatment of chronic ruptures. *Archives of Surgery*, *102*, 483–485.

Neviaser, R., Neviaser, T., & Neviaser, J. (1993). Anterior dislocation of the shoulder and rotator cuff rupture. *Clinical Orthopaedics and Related Research*, *291*, 103–106.

Newton, M. D., Davidson, A. A., Pomajzl, R., Seta, J., Kurdziel, M. D., & Maerz, T. (2016). *The*

influence of testing angle on the biomechanical properties of the rat supraspinatus tendon. *49*, 4159–4163.

Newton, M., Davidson, A., Pomajzl, R., Seta, J., Kurdziel, M., & Maerz, T. (2016). The influence of testing angle on the biomechanical properties of the rat supraspinatus tendon. *Journal of Biomechanics*, *49*(16), 4159–4163.

Nordez, A., McNair, P., Casari, P., & Cornu, C. (2008). Acute changes in hamstrings musculo-articular dissipative properties induced by cyclic and static stretching. *International Journal of Sports Medicine*, *29*, 414–422.

Nordez, A., McNair, P., Casari, P., & Cornu, C. (2009). The effect of angular velocity and cycle on the dissipative properties of the knee during passive cyclic stretching: a matter of viscosity or solid friction. *Clinical Biomechanics*, *24*(77–81).

Nyffeler, R., Sheikh, R., Atkinson, T., Jacob, H., Favre, P., & Gerber, C. (2006). Effects of glenoid component version on humeral head displacement and joint reaction forces: An experimental study. *Journal of Shoulder and Elbow Surgery*, *15*(5), 625–629.

Ochiai, N., Matsui, T., Miyaji, N., Merklin, R., & Hunter, J. (1979). Vascular anatomy of flexor tendons. I. Vincular system and blood supply of the profundus tendon in the digital sheath. *The Journal of Hand Surgery*, *4*, 321–330.

Ohlsson, K., Attewell, R., Palsson, B., Karlsson, B., Balogh, I., Johnsson, B., … Skerfving, S. (1995). Repetitive industrial work and neck and upper limb disorders in females. *American Journal of Industrial Medicine*, *27*(5), 731–747.

Onishi, H., Yagi, R., Akasaka, K., Momose, K., Ihashi, K., & Handa, Y. (2000). *Relationship between EMG signals and force in human vastus lateralis muscle using multiple bipolar wire electrodes*. *10*, 59–67.

Opsahl, W., Zernian, H., Ellison, M., Lewis, D., Ruckers, R., & Riggins, R. (1982). Role of copper in collagen cross-linking and its influence on selected mechanical properties of chick bone and tendon. *The Journal of Nutrition*, *112*(4), 708–716.

Ounpuu, S., DeLuca, P., Bell, K., & Davis, R. (1997). Using surface electrodes for the evaluation of the rectus femoris, vastus medialis and vastus lateralis muscles in children with cerebral palsy. *Gait & Posture*, *5*, 211–216.

Pardes, A., Freedman, B., Fryhoffer, G., Salka, N., Bhatt, P., & Soslowsky, L. (2016). Males have inferior achilles tendon material properties compared to females in a rodent model. *Annals of Biomedical Engineering*, *44*(10), 2901–2910.

Parry, D., Flint, M., Gillard, G., & Craig, A. (1982). A role for glycosaminoglycans in the development of collagen fibril. *FEBS Letters*, *149*, 1–7.

Peltz, C., Dourte, L., Kuntz, A., Sarver, J., Kim, S.-Y., Williams, G., & Soslowsky, L. (2009). The effect of postoperative passive motion on rotator cuff healing in a rat model. *The Journal of Bone and Joint Surgery*, *91*(10), 2421–2429.

Peltz, C., Perry, S., Getz, C., & Soslowsky, L. (2009). Mechanical properties of the long-head of the biceps tendon are altered in the presence of rotator cuff tears in a rat model. *Journal of*

Orthopaedic Research, *27*(3), 416–420.

Peltz, C., Sarver, J., Dourte, L., Wurgler-Hauri, C., Williams, G., & Soslowsky, L. (2010). Exercise following a short immobilization period is detrimental to tendon properties and joint mechanics in a rat rotator cuff injury model. *Journal of Orthopaedic Research*, *28*, 841–845.

Pins, G., Christiansen, D., Patel, R., & Silver, F. (1997). Self- assembly of collagen fibers. Influence of fibrillar alignment and decorin on mechanical properties. *Biophysical Journal*, *73*, 2164–2172.

Plate, J., Pace, L., Seyler, T., Moreno, R., Smith, T., & Tuohy, C. (2014). Age-related changes affect rat rotator cuff muscle function. *Journal of Shoul*, *23*, 91–98.

Pope, D., Croft, P., Pritchard, C., & Silman, A. (1997). Prevalence of shoulder pain in the community: the influence of case definition. *Annals of the Rheumatic Diseases*, *56*(5), 308–312.

Poppen, N., & Walker, P. (1976). Normal and abnormal motion of the shoulder. *The Journal of Bone and Joint Surgery*, *58*, 195–201.

Potvin, J. (2012). Predicting maximum acceptable efforts for repetitive tasks: an equation based on duty cycle. *Human Factors: The Journal of the Human Factors and Ergonomics Society*, *54*(2), 175–188.

Punnett, L., Fine, L., Keyserling, W., Herrin, G., & Chaffin, D. (2000). Shoulder disorders and postural stress in automobile assembly work. *Scandinavian Journal of Work, Environment & Health*, *26*(4), 283–291.

Quapp, K., & Weiss, J. (1998). Material characterization of human medial collateral ligament. *Journal of Biomechanics*, *120*, 757–763.

Rathbun, J., & Macnab, I. (1970). The microvascular pattern of the rotator cuff. *The Journal of Bone and Joint Surgery*, *52*(3), 540–553.

Reeves, N., Maganaris, C., & Narici, M. (2003). Effect of strength training on human patella tendon mechanical properties of older individuals. *Journal of Physiology*, *548*, 971–981.

Reeves, N., Narici, M., & Maganaris, C. (2003). Strength training alters the viscoelastic properties of tendons in elderly humans. *Muscle & Nerve*, *28*, 74–81.

Reinold, M., Wilk, K., Fleisig, G., Zheng, N., Barrentine, S., Chmielewski, T., … Andrews, J. (2004). Electromyographic analysis of the rotator cuff and deltoid musculature during common shoulder external rotation exercises. *Journal of Orthopaedic Sports Physical Therapy*, *34*(7), 385–394.

Reuther, K., Thomas, S., Tucker, J., Sarver, J., Gray, C., Rooney, S., … Soslowsky, L. (2014). Disruption of the anterior-posterior rotator cuff force balance alters joint function and leads to joint damage in a rat model. *Journal of Orthopaedic Research*, *32*(5), 638–644.

Reuther, K., Thomas, S., Tucker, J., Vafa, R., Gordon, J., Liu, S., … Soslowsky, L. (2015). Overuse Activity in the Presence of Scapular Dyskinesis Leads to Shoulder Tendon

Damage in a Rat Model. *Annals of Biomedical Engineering*, *43*(4), 917–928.

Reuther, K., Thomas, S., Tucker, J., Yannascoli, S., Caro, A., Vafa, R., … Soslowsky, L. (2014). Scapular dyskinesis is detrimental to shoulder tendon properties and joint mechanics in a rat model. *Journal of Orthopaedic Research*, (11), 1436–1443.

Rigby, B. J., Hirai, N., Spikes, J. D., & Eyring, H. (1959). The Mechanical Properties of Rat Tail Tendon. *The Journal of General Physiology*, *43*(2), 265–283.

Riley, G. (2004). The pathogenesis of tendinopathy. A molecular perspective. *Rheumatology*, *43*, 131–142.

Riley, G., Harrall, R., Constant, C., Chard, M., Cawston, T., & Hazleman, B. (1994a). Glycosaminoglycans of human rotator cuff tendons: changes with age and in chronic rotator cuff tendinitis. *Annals of the Rheumatic Diseases*, *53*, 367–376.

Riley, G., Harrall, R., Constant, C., Chard, M., Cawston, T., & Hazleman, B. (1994b). Tendon degeneration and chronic shoulder pain: changes in the collagen composition of the human rotator cuff tendons in rotator cuff tendinitis. *Annals of the Rheumatic Diseases*, *53*, 359–366.

Ristolainen, L., Kettunen, J., Waller, B., Heinonen, A., & Kujala, U. (2014). Training- related risk factors in the etiology of overuse injuries in endurance sports. *Journal of Sports Medicine and Physical Fitness*, *54*(1), 78–87.

Rodeo, S., Potter, H., Kawamura, S., Turner, A., Kim, H., & Atkinson, B. (2007). Biologic augmentation of rotator cuff tendon-healing with use of a mixture of osteoinductive growth factors. *Journal of Bone & Joint Surgery*, *89*, 2485–2497.

Roh, M., Wang, V., April, E., Pollock, R., Bigliani, L., & Flatow, E. (2000). Anterior and posterior musculotendinous anatomy of the supraspinatus. *Journal of Shoulder and Elbow Surgery*, *9*(5), 436–440.

Roman-Liu, D., & Tokarski, T. (2005). Upper limb strength in relation to upper limb posture. *International Journal of Industrial Ergonomics*, *35*, 19–31.

Rooney, S., Torino, D., Baskin, R., Vafa, R., Kuntz, A., & Soslowsky, L. (2017). Rat supraspinatus tendon responds acutely and chronically to exercise. *Journal of Applied Physiology*, *123*, 757–763.

Rossi, F., Tenamian, P., Cerciello, G., & Walch, G. (1994). Posterosuperior glenoid rim impingement in athletes: the diagnostic value of traditional radiology and magnetic resonance. *La Radiologica Medica*, *87*(1–2), 22–27.

Rothman, R., & Parke, W. (1965). The vascular anatomy of the rotator cuff. *Clinical Orthopaedics and Related Research*, *41*, 176–188.

Saadat, F., Deymier, A., Birman, V., Thomopoulos, S., & Genin, G. (2016). The concentration of stress at the rotator cuff tendon-to-bone attachment site is conserved across species. *Journal of the Mechanical Behaviour of Biomedical Materials*, *62*, 24–32.

Safran, O., Derwin, K., Powell, K., & Ianotti, J. (2005). Changes in rotator cuff muscle volume,

fat content, and passive mechanics after chronic detachment in a canine model. *The Journal of Bone and Joint Surgery*, *87*(12), 2662–2670.

Saha, A. K. (1971). Dynamic Stability of the Glenohumeral Joint. *Acta Orthopaedica*, *42*(6), 491–505.

Sano, H., Ishii, H., Yeadon, A., Backman, D., Brunet, J., & Uhthoff, H. (1997). Degeneration at the insertion weakens the tensile strength. *Journal of Orthopaedic Research*, *15*, 719–726.

Schatzker, J., & Branemark, P. (1969). Intravital observations on the microvascular anatomy and microcirculation of the tendon. *Acta Orthopaedica*, *126*, 1–23.

Schneeberger, A., von Roll, A., Kalberer, F., Jacob, H., & Gerber, C. (2002). Mechanical strength of arthroscopic rotator cuff repair techniques: an in vitro study. *Journal of Bone & Joint Surgery*, *84*(12), 2152–2160.

Schuind, F., Garcia-Elias, M., Cooney III, W., & An, K.-N. K. (1992). Flexor tendon forces: in vivo measurements. *Journal of Hand Surgery*, *17*(2), 291–298.

Sengupta, P. (2013). The laboratory rat: relating its age with human's. *International Journal of Preventative Medicine*, *4*(6), 624–630.

Sereysky, J., Andarawis-Puri, N., Jepsen, K., & Flatow, E. (2012). Structural and mechanical effects of in vivo fatigue damage induction on murine tendon. *Journal of Orthopaedic Research*, *30*(6), 965–972.

Seynnes, O., Erskine, R., Magnaris, C., Longo, S., Simoneau, E., Grosset, J., & Narici, M. (2009). Training-induced changes in structural and mechanical properties of the patellar tendon are related to muscle hypertrophy but not to strength gains. *Journal of Applied Physiology*, *107*(2), 523–530.

Sharkey, N., Marder, R., & Hanson, P. (1994). The entire rotator cuff contributes to elevation of the arm. *Journal of Orthopaedic Research*, *12*(5), 699–708.

Sharma, P., & Maffuli, N. (2005). Tendon injury and tendinopathy: healing and repair. *Journal of Bone & Joint Surgery*, *87*(1), 187–202.

Shen, Z., Dodge, M., Khan, H., Ballarini, R., & Eppell, S. (2010). In vitro fracture testing of submicron diameter collagen fibril specimens. *Biophysical Journal*, *99*(6), 1986–1995.

Shepherd, J., Legerlotz, K., Demirci, T., Klemt, C., Riley, G., & Screen, H. (2014). Functionally distinct tendon fascicles exhibit different creep and stress relaxation behaviour. *Proceedings of the Institution of Mechanical Engineers. Part H, Journal of Engineering in Medicine*, *228*(0), 49–59.

Smith, K., Harryman II, D., Antoniou, J., Campbell, B., Sidles, J., & Matsen III, F. (2000). A prospective, multipractice study of shoulder function and health status in patients with documented rotator cuff tears. *Journal of Shoulder and Elbow Surgery*, *9*(5), 395–402.

Sonnabend, D. (1994). Treatment of primary anterior shoulder dislocation in patients older than 40 years of age. Conservative versus operative. *Clinical Orthopaedics and Related Research*, *304*, 74–77.

Soslowsky, L., Carpmenter, J., DeBano, C., Banerji, I., & Moalli, M. (1996). Development and use of an animal model for investigations on rotator cuff disease. *Journal of Shoulder and Elbow Surgery*, *5*, 383–392.

Soslowsky, L., Thomopoulos, S., Tun, S., Flanagan, L., Keefer, C., Mastaw, J., & Carpenter, J. (2000). Overuse activity injures the supraspinatus tendon in an animal model : A histologic and biomechanical study. *Journal of Shoulder and Elbow Surgery*, *9*(2), 79–84.

Spiesz, E., Thorpe, C., Chaudhry, S., Riley, G., Birch, H., Clegg, P., & Screen, H. (2015). Tendon extracellular matrix damage, degradation and inflammation in response to in vitro overload exercise. *Journal of Orthopaedic Research*, *33*(6), 889–897.

St Pierre, P., Olson, E., Elliott, J., O'Hair, K., McKinney, L., & Ryan, J. (1995). Tendon-healing to cortical bone compared with healing to a cancellous trough. A biomechanical and histological evaluation in goats. *Journal of Bone & Joint Surgery*, *77*, 1858–1866.

Stenlund, B., Goldie, I., Hagberg, M., Hogstedt, C., & Marions, O. (1992). Radiographic osteoarthrosis in the acromioclavicular joint resulting from manual work or exposure to vibration. *British Journal of Industrial Medicine*, *49*, 588–593.

Struyf, F., Nijs, J., Baeyens, J., Mottram, S., & Meeusen, R. (2011). Scapular positioning and movement in unimpaired shoulders, shoulder impingement syndrome, and glenohumeral instability. *Scandinavian Journal of Medicine and Science in Sports*, *21*(3), 352–358.

Sun, H., Li, Y., Fung, D., Majeska, R., Schaffler, M., & Flatow, E. (2008). Coordinate regulation of IL-1β and MMP-13 in rat tendons following subrupture fatigue damage. *Clinical Orthopaedics and Related Research*, *466*, 1555–1561.

Svendsen, S., Gelineck, J., Mathiassen, S., Bonde, J., Frich, L., Stengaard-Pedersen, K., & Egund, N. (2004). Work above shoulder level and degenerative alterations of the rotator cuff tendons: A magnetic resonance imaging study. *Arthritis and Rheumatism*, *50*(10), 3314–3322.

Szczesny, S., Aeppli, C., David, A., & Mauck, R. (2018). Fatigue loading of tendon results in collagen kinking and denaturation but does not change local tissue mechanics. *Journal of Biomechanics*, *71*, 251–256.

Tauro, J. (2006). Stiffness and rotator cuff tears: incidence, arthroscopic findings, and treatment results. *Arthroscopy*, *22*, 581–586.

Terry, G., Hammon, D., France, P., & Norwood, L. (1991). The stabilizing function of passive shoulder restraints. *The American Journal of Sports Medicine*, *19*(1), 26–34.

Tetreault, P., Krueger, A., Zurakowski, D., & Gerber, C. (2004). Glenoid version and rotator cuff tears. *Journal of Orthopaedic Research*, *22*(1), 202–207.

Thomazeau, H., Duval, J., Darnault, P., & Dreano, T. (1996). Anatomical relationship and capsular attachments of the supraspinatus muscle. *Surgical and Radiologic Anatomy*, *18*, 221–225.

Thomopoulos, S., Hattersley, G., Rosen, V., Mertens, M., Galatz, L., Williams, G., & Soslowsky, L. (2002). The localized expression of extracellular matrix components in

healing tendon insertion sites: an in situ hybridization study. *Journal of Orthopaedic Research*, *20*, 454–463.

Thomopoulos, S., Williams, G., Gimbel, J., Favata, M., & Soslowsky, L. (2003). Variation of biomechanical, structural, and compositional properties along the tendon to bone insertion site. *Journal of Orthopaedic Research*, *21*, 413–419.

Thornton, G., Shrive, N., & Frank, C. (2002). Ligament creep recruits fibres at low stresses and can lead to modulus- reducing fibre damage at higher creep stresses: a study in rabbit medial collateral ligament model. *Journal of Orthopaedic Research*, *20*, 967–974.

Thorpe, C., Klemt, C., Riley, G., Birch, H., Clegg, P., & Screen, H. (2013). Helical substructures in energy-storing tendons provide a possible mechanism for efficient energy storage and return. *Acta Biomater*, *9*(8), 7498–7956.

Thorpe, C., Riley, G., Birch, H., Clegg, P., & Screen, H. (2014). Effect of fatigue loading on structure and functional behaviour of fascicles from energy-storing tendons. *Acta Biomaterialia*, *10*(7), 3217–3224.

Thunes, J., Miller, R., Pal, S., Damle, S., Debski, R., & Maiti, S. (2015). The effect of size and location of tears in the supraspinatus tendon on potential tear propagation. *Journal of Biomechanical Engineering*, *137*(07), 081012.

Ting, A., Jobe, F., & Barto, P. (1987). An EMPG analysis of the lateral biceps in shoulders with rotator cuff tears. *Paper Presented at the American Shoulder and Elbow Surgeons 3rd Open Meeting*. San Fransisco.

Tirman, P., Bost, F., Garvin, G., Peterfy, C., Mall, J., Steinbach, L., … Crues III, J. (1994). Posterosuperior glenoid impingement of the shoulder: findings at MR imaging and MR arthrography with arthroscopic correlation. *Radiology*, *193*(2), 431–436.

Toolanen, G., Hildingssonl, C., Hedlund, T., Knibesto, M., & Oberg, L. (1993). Early complications after anterior dislocation of the shoulder in patients over 40 years. *Acta Orthop Scand*, *64*(5), 549–552.

Townley, C. (1950). The capsular mechanism in recurrent dislocation of the shoulder. *Journal of Bone & Joint Surgery*, *32*(2), 370–380.

Tsai, N.-T., McClure, P., & Karduna, A. (2003). Effects of muscle fatigue on 3-dimensional scapular kinematics. *Archives of Physical Medicine and Rehabilitation*, *84*(7), 1000–1005.

Tubbs, R., Loukas, M., Shahid, K., Judge, T., Pinyard, J., Shoja, M., … Oakes, W. (2007). Anatomy and quantitation of the subscapular nerves. *Clinical Anatomy*, *20*(6), 656–659.

Tucker, J. J., Riggin, C. N., Connizzo, B. K., Mauck, R. L., Steinberg, D. R., Kuntz, A. F., … Bernstein, J. (2016). *Effect of Overuse-Induced Tendinopathy on Tendon Healing in a Rat Supraspinatus Repair Model*. (January), 161–166.

Turkel, S., Panio, M., Marshall, J., & Girgis, F. (1981). Stabilizing mechanisms preventing anterior dislocation of the glenohumeral joint. *Journal of Bone & Joint Surgery*, *63*(8), 1208–1217.

Turrin, A., & Cappello, A. (1997). Sonographic anatomy of the supraspinatus tendon and adjacent structures. *Skeletal Radiology*, *26*, 89–93.

Uhthoff, H., Matsumoto, F., Trudel, G., & Himori, K. (2003). Early reattachment does not reverse atrophy and fat accumulation of the supraspinatus - an experimental study in rabbits. *Journal of Orthopaedic Research*, *21*(3), 386–392.

Vahlensieck, M., an Haack, K., & Schmidt, H.-M. (1994). Two portions of the supraspinatus muscle: a new finding about the muscles macroscopy by dissection and megnetic resonance imaging. *Surgical and Radiologic Anatomy*, *16*, 101–104.

Van der Helm, F. (1994). a Finite Element Musculoskeletal the Shoulder Mechanism. *Journal of Biomechanics*, *27*(5), 551–559.

van der Windt, D., Koes, B., de Jong, B., & Bouter, L. (1995). Shoulder disorders in general practice: incidence, patient characteristics, and management. *Annual Rheumatoid Disorders*, *54*, 959–964.

van Rijn, R., Huisstede, B., Koes, B., & Burdorf, A. (2010). Associations between work-related factors and specific disorders of the shoulder – systematic review of literature. *Scandinavian Journal of Work, Environment & Health*, *36*(3), 189–201.

Vasishta, A., Kelkar, A., Joshi, P., & Hapse, R. (2019). The value of sonoelastography in the diagnosis of supraspinatus tendinopathy - A comparison study. *British Journal of Radiology*, *92*(1096), 20180951.

Veeger, H., Yu, B., & An, K. (1996). Orientation of axes in the elbow and forearm for biomechanical modeling. *Proceedings of the First Conference of the International Shoulder Group*, 83–87.

Veres, S., Harrison, J., & Lee, J. (2013a). *Cross-Link Stabilization Does Not Affect the Response of Collagen Molecules , Fibrils , or Tendons to Tensile Overload*. (December), 1907–1913.

Veres, S., Harrison, J., & Lee, J. (2013b). *Repeated Subrupture Overload Causes Progression of Nanoscaled Discrete Plasticity Damage in Tendon Collagen Fibrils*. (May), 731–737.

Veres, S., & Lee, J. (2012). Designed to fail: A novel mode of collagen fibril disruption and its relevance to tissue toughness. *Biophysical Journal*, *102*(12), 2876–2884.

Viidik, A. (1972). Simultaneous mechanical and light microscopic studies of collagen fibers. *Zeitschrift Für Anatomie Und Entwicklungsgeschichte*, *136*, 204–212.

Vogel, K., & Heinegard, D. (1985). Characterization of proteoglycans from adult bovine tendon. *Journal of Biological Chemistry*, *260*, 9298–9306.

Vogel, K., & Koob, T. (1989). Structural specialization in tendons under compression. *International Review of Cytology*, *115*, 267–293.

Voleti, P., Buckley, M., & Soslowsky, L. (2012). Tendon healing: repair and regeneration. *Annual Review of Biomedical Engineering*, *14*, 47–71.

Waggett, A., Ralphs, J., Kwan, A., Woodnutt, D., & Benjamin, M. (1998). Characterization of collagens and proteoglycans at the insertion of the human Achilles tendon. *Matrix Biology*,

16, 457–470.

Waite, D., Brookham, R., & Dickerson, C. (2010). On this suitability of using surface electrode placements to estimate muscle activity of the rotator cuff as recorded by intramuscular electrodes. *Journal of Electromyography and Kinesiology*, *20*(5), 903–911.

Walker, P. (1977). *Human Joints and their Artificial Replacements*. Springfield, Ill: Charles C Thomas.

Wang, J. (2006). Mechanobiology of tendon. *Journal of Biomechanics*, *39*(9), 1563–1582.

Wani, Z., Abdulla, M., Habeebullah, A., & Kalogriantis, S. (2016). Rotator cuff tears: Review of epidemiology, clinical assessment and operative treatment. *Trauma*, *18*(3), 190–204.

Ward, S. R., Hentzen, E. R., Smallwood, L. H., Eastlack, R. K., Burns, K. a, Fithian, D. C., … Lieber, R. L. (2006). *Rotator Cuff Muscle Architecture*. (0), 1–7.

Warwick, D., Novak, G., Schultz, A., & Berkson, M. (1980). Maximum voluntary strengths of male adults in some lifting, pushing and pulling activities. *Ergonomics*, *23*(1), 49–54.

Watson-Jones, R. (1960). *Fractures and Joint Injuries*. Baltimore: Williams & Williams.

Weiss, J. (1994). *A constitutive model and finite element representation for transversely isotropic soft tissues*. University of Utah.

Weiss, J., & Gardiner, J. (2001). Computational Modeling of Ligament Mechanics. *Critical Reviews in Biomedical Engineering*, *29*(4), 1–70.

Wells, J., Zipp, J., Schuette, P., & McEleney, J. (1983). Musculoskeletal disorders among letter carriers. *Journal of Occupational Medicine*, *25*(11), 814–820.

Wells, R., Van Eerd, D., & Hagg, G. (2004). Mechanical exposure concepts using force as the agent. *Scandinavian Journal of Work, Environment & Health*, *30*(3), 179–190.

Wiker, S. F., Chaffin, D. B., & Langolf, G. D. (1989). Shoulder posture and localized muscle fatigue and discomfort. *Ergonomics*, *32*(2), 211–237.

Willett, T., Labow, R., Avery, N., & Lee, J. (2007). Increased proteolysis of collagen in an in vitro tensile overload tendon model. *Annals of Biomedical Engineering*, *35*(11), 1961–1972.

Willett, T., Labow, R., & Lee, J. (2008). *Mechanical Overload Decreases the Thermal Stability of Collagen in an In Vitro Tensile Overload Tendon Model*. (December), 1605–1610.

Wilmink, J., Wilson, A., & Goodship, A. (1992). Functional significance of the morphology and micromechanics of collagen fibres in relation to partial rupture of the superficial digital flexor tendon in racehorses. *Research in Veterinary Science*, *53*, 354–359.

Wilson, C., & Duff, G. (1943). Pathologic study of degeneration and rupture of the supraspinatus tendon. *Archives of Surgery*, *47*, 121–135.

Winter, D. (1991). Electromyogram recording, processing, and normalization: Procedures and considerations. *Journal of Human Muscle Performance*, *1*(2), 5–15.

WSIB. (2015). *2015 Statistical Report*.

Wu, G., van Der Halm, F., Veeger, H., Maksous, M., Van Roy, P., Anglin, C., … Buchholz, B. (2005). ISB recommendation on definitions for the reporting of human joint motion - Part II: shoulder, elbow, wrist and hand. *Journal of Biomechanics*, *38*, 981–992.

Wu, H.-C. (2004). *Continuum Mechanics and Plasticity*. Boca Raton, Florida, USA: Chapman & Hall/CRC Press.

Wuelker, N., Roetman, B., Plitz, W., & Knop, C. (1994). Function of the supraspinatus muscle in a dynamic shoulder model. *Unfallichirug*, *97*(6), 308–313.

Yahia, L., & Drouin, G. (1990). Study of the hysteresis phenomenon in canine anterior cruciate ligaments. *Journal of Biomechanical Engineering*, *12*, 57–62.

Yamanaka, K., Fukuda, H., Hamada, K., & Mikasa, M. (1983). Incomplete thickness tears of the rotator cuff. *European Journal of Orthopaedic Surgery & Traumatology*, *26*, 713.

Yamanaka, K., & Matsumoto, T. (1994). The joint side tear of the rotator cuff. A followup study by arthrography. *Clinical Orthopaedics and Related Research*, *304*, 68–73.

Yokota, A., Gimbel, J., Williams, G., & Soslowsky, L. (2005). Supraspinatus tendon composition remains altered long after tendon detachment. *Journal of Shoulder and Elbow Surgery*, *14*(1(Suppl S)), 72S-78S.

Yu, T.-Y., Pang, J.-H., Wu, K.-H., Chen, M.-L., Chen, C.-H., & Tsai, W.-C. (2013). Aging is associated with increased activities of matrix metalloproteinase-2 and -9 in tenocytes. *BMC Musculoskeletal Disorders*, *14*(2), 1–7.

Yun, S., Jim, W., Cho, N., Ryu, K.-N., Yoon, Y., Cha, J., … CHoi, N. (2019). Shear-wave and strain ultrasound elastography of the supraspinatus and infraspinatus tendons in patients with idiopathic adhesive capsulitis of the shoulder: A prospective case-control study. *Korean Journal of Radiology*, *20*(7), 1176–1185.

Zajac, F. (1989). Muscle and tendon: properties, models, scaling, and application to biomechanics and motor control. *Critical Reviews in Biomedical Engineering*, Vol. 17, pp. 359–411.

Zhang, J., Pan, T., Liu, Y., & Wang, J. (2010). Mouse treadmill running enhances tendons by expanding the pool of tendon stem cells (TSCs) and TSC-related cellular production of collagen. *Journal of Orthopaedic Research*, *28*(9), 1178–1183.

APPENDIX A – EMG INFORMATION PACKET

INFORMATION CONSENT FORM

Study Title

Examining Regional Supraspinatus Activation using Indwelling Electromyography

Research Team

Student Investigator	*Faculty Supervisor*
Alan Cudlip	Clark Dickerson, PhD
Department of Kinesiology University of Waterloo 519-888-4567 x37495 accudlip@uwaterloo.ca	Department of Kinesiology University of Waterloo 519-888-4567 x37844 clark.dickerson@uwaterloo.ca

---

Purpose of the Study

The goal of this investigation is to determine regional changes in supraspinatus activation through the shoulder reach envelope. Recent research has indicated that the supraspinatus muscle is comprised of two sections, which may respond differently from one another throughout the range of motion of the shoulder. Our aim is to define the activation level of these two regions and indicate changes between these two regions in simple arm elevation tasks. Results from this investigation may provide insight into rotator cuff injury risk.

Procedures Involved in this Study and Time Commitment

As a participant in this research study, you will be asked to attend one session of approximately 2 hours in duration. During this session, you will be asked to move your arm from resting at your side to maximal elevation with a straight arm. Some of these trials will have an empty hand, others will have a weight in a bottle held in the hand.

The testing session procedures are as follows.

Instrumentation:

- Upon arrival, the skin overlying the supraspinatus on the right supraspinatus will be shaved and cleansed with rubbing alcohol by a research investigator of the same gender as you, the participant. This shaving and cleansing is so that the surface electromyography (EMG) electrodes can be adhered to a surface with minimal interference through dead skin cells or hair. These electrodes are coated with an adhesive similar to a disposable bandage. A disposable razor will be used and discarded after

shaving. EMG will be collected throughout each session using this bipolar electrode, with a ground electrode placed on the clavicle.

- The placement of these electrodes can be seen on the diagram below (filled circle).
- Two indwelling needles will be placed in the anterior and posterior regions of the supraspinatus. These electrodes are approximately half the width of a human hair. You will be asked to lay face down on the therapy table during insertion. You will be notified before insertion of the electrode. This insertion will feel like a small poke with a toothpick, and will only be momentary discomfort. You will not feel the electrodes while they are in the supraspinatus muscle. The placement of these electrodes will be verified using ultrasound, and the needle will be removed as soon as placement is correct. The electrode wires will be removed at the end of the collection.
- Reflective markers will also be placed on bony landmarks on the right arm and the torso. These locations are indicated on the diagram below.

Procedures:

- Following application of the needle and surface electrodes, you will be asked to perform three exertions where you push as hard as you can This exertion involves you lying on your left side, with your head supported by your left hand. This exertion is designed to determine your maximal output of the supraspinatus, allowing comparison between participants. A two minute rest period will be given in between each exertion.
- Following these maximal exertions, reflective markers will be place on your body on bony landmarks. These will be used to capture your movements during the task protocol. A total of 7 individual markers and 3 clusters will be placed on your body. Locations of these placements can be seen in the diagram to the right.

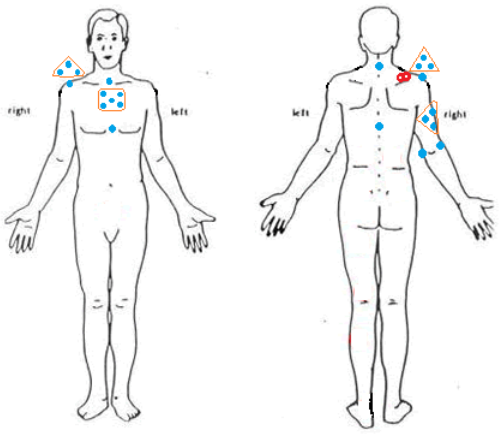

- After initial measures, collection of the task protocol will begin. You will be asked to sit on a backless chair, and tape marks will be placed on the floor around you to mark planes of elevation.
- Each position will involves moving your arm straight up and down at a pace of 2 seconds up and 2 seconds down, totalling 4 seconds per trial. Some of these trials will have no hand weight; others will have a weight held in your hand. These weights will be scaled to your strength.
- With your permission, photographs may be taken throughout the collection to demonstrate postures during each task and document the experimental setup. If these photographs would be used in publications or presentations, your face would be blackened in the picture, ensuring your anonymity in the photo.

Inclusion / Exclusion Criteria

Only university aged (18-40 years), right-handed males and females will be included in this study. Individuals who have had pain and/or injury in arm or shoulder, or the back within the past year will be excluded in this study. This will be asked by the research investigators prior to collection, and participants who have any of these criteria will not be able to participate in this study. Rubbing alcohol must be used to cleanse the skin prior to electrode placement. As this is a mandatory step in the procedure, anyone with an allergy or sensitivity to rubbing alcohol will not be able to participate in this study.

Potential Risks and Associated Safeguards

- The insertion of the needle electrodes is a sterile procedure. Some participants have a fear of needles. These needles are very tiny, and generate very little discomfort on the onset of insertion, and no pain while the needle is guiding the electrodes to their destination. The needle will be withdrawn as soon as the location has been met. Individuals who have a fear of needles can remove themselves from the study at any point in time.
- Some participants may experience skin irritation or redness from the adhesives used to adhere the electrodes to the skin. This is similar to irritation that may be caused by a disposable bandage and typically fades within 1-3 days. The occurrence of irritation is rare in participants.
- The portable parts of electrical recording systems are battery operated and isolate you from the main power lines. There is no risk of electrical shock.
- Some participants may experience fatigue or mild discomfort from the submaximal contractions. This discomfort should disappear in 1-3 days. If you feel fatigued at any time, simply notify one of the research investigators and we will be happy to provide you with a rest period.

Changing Your Mind about Participation

At any point in the study, you may withdraw from participating without penalty. To do so, indicate this to the investigators by saying, “I no longer wish to participate in this study.”

Potential Benefits of Participation

By participating in this study, you will have the opportunity to gain or further your knowledge and understanding of experimental procedures and theories of human movement research. Results from this investigation will provide insight into activity patterns of the supraspinatus across the range of shoulder mobility. The knowledge gained from this research may assist in the reduction of upper extremity injury risk in the workplace, as well as more comprehensive treatment methods and rehabilitation approaches. Significant findings will be summarized to provide biomechanics researchers insight into this new area of research.

Remuneration

After completion of the testing session, you will receive $40 cash in appreciation for your help. This money is taxable, and should be included in future tax considerations. If you choose to withdraw before the completion of the study, you will be prorated for $20/hour for your time completed, rounding up to the next complete hour.

Confidentiality and Data Security

Each participant will be assigned a 3 letter identification code instead of using your name for the purposes of this study. This code will begin with the letter M or F (depending on if you are male or female) and then a number between 1 and 20, indicating your number (so the first male participant would be M01, and the fifteenth female participant will be F15). Your name or initials will not be used or linked to this data, and only the investigators will have this code. All data will be stored indefinitely on password protected computer hard drives and/ or digital storage media (which will remain in the investigator's locked filing cabinet when not in use). Separate consent will be requested in order to use photographs for teaching, scientific presentations, or in publications of this work.

Concerns about Participation

We would like to assure you that this study has been reviewed by, and received ethics through the University of Waterloo's Office of Research Ethics (ORE). However, the final decision about participation is yours. In the event that you have any comments or concerns resulting from your participation in this study, please contact the Director of the ORE (Dr. Maureen Nummelin) at 519-888-4567 ext. 36005 or at maureen.nummelin@uwaterloo.ca .

Questions about the Study

If you have any further questions, or want any other information about this study, please feel free to contact Alan Cudlip or Dr. Clark Dickerson.

Sincerely yours,

Alan Cudlip
Department of Kinesiology
University of Waterloo
519-888-4567 x37495
accudlip@uwaterloo.ca

Clark Dickerson, PhD
Department of Kinesiology
University of Waterloo
519-888-4567 x37844
clark.dickerson@uwaterloo.ca

APPENDIX B – EMG CONSENT FORM

CONSENT OF PARTICIPATION

Project Title: **Examining Regional Supraspinatus Activation Using Indwelling Electromyography**

Principal Investigator: **Alan Cudlip**

Faculty Supervisor: **Dr. Clark Dickerson**

I have read the information presented in the information letter about a study being conducted by Alan Cudlip (Principal Investigator) and Dr. Clark Dickerson (Faculty Supervisor) of the Department of Kinesiology at the University of Waterloo. I have had the opportunity to ask any questions related to this study, to receive satisfactory answers to my questions, and any additional details I wanted. I am aware that I may withdraw without penalty at any time by advising the researchers of this decision.

This project has been reviewed by, and received ethics clearance through a University of Waterloo Research Ethics Committee. I was informed that if I have any comments or concerns resulting from my participation in this study, I may contact the Director of the ORE at 519-888-4567 ext. 36005.

With full knowledge of all foregoing, I agree, or my own free will, to participate in this study. I understand that I am NOT waiving my legal rights or releasing the investigator(s) or involved institution(s) from their legal and professional responsibilities by signing this document.

Participant's Name (Please Print): _____

Participant's Signature: _____

Date: _____

Witnessed: _____

APPENDIX C – EMG CONSENT TO PHOTOGRAPHS

CONSENT TO USE PHOTOGRAPHS IN TEACHING, PRESENTATIONS, and/or PUBLICATIONS

Project Title: **Examining Regional Supraspinatus Activation Using Indwelling Electromyography**

Student Investigator: **Alan Cudlip**

Faculty Supervisor: **Dr. Clark Dickerson**

Sometimes a certain photograph clearly demonstrates a particular feature or detail that would be helpful in teaching or when presenting the study results at a scientific conference or in a publication.

I agree to allow photographs in which I appear to be used in teaching, scientific presentations and/or publications with the understanding that I will not be identified by name. I am aware that I may withdraw this consent at any time without penalty, and the photograph will be confidentially shredded. I understand that if my face should appear in any\ photograph, it will be blackened out in any publication to maintain my anonymity.

I was informed that if I have any comments or concerns resulting from my participation in this study I may contact the Director of the ORE (Dr. Maureen Nummelin) at 519-888-4567 ext. 36005 or at maureen.nummelin@uwaterloo.ca , and I understand that this study has received ethics clearance through a University of Waterloo Research Ethics Committee.

Participant's Name (Please Print): _____

Participant's Signature: _____

Date: _____

Witnessed: _____

APPENDIX D – EMG FEEDBACK FORM

Feedback Letter

Dear Participant,

We would like to thank you for your participation in this study. As a reminder, the purpose of the study was to examine the regional changes in supraspinatus activation within the shoulder reach envelope.

Please remember that any data pertaining to you as an individual participant will be kept confidential. Once all the data is collected and analysed for this study, it is our intent to share this information with the research community through seminars, conferences, presentations, and journal articles. If you are interested in receiving more information regarding the results of this study, or if you have questions or concerns, please contact us via or e-mail (details listed at the bottom of this page). If you would like a summary of the results, please let us know by providing us with your contact information. When the study is completed, we will send it to you. The expected date for the study findings to be available is December 31, 2017.

As with all University of Waterloo projects involving human participants, this project was reviewed by, and received ethics clearance through a University of Waterloo Research Ethics Committee. Should you have any comments or concerns resulting from your participation in this study, please contact the Director of the ORE (Dr. Maureen Nummelin) at 519-888-4567 ext. 36005 or at maureen.nummelin@uwaterloo.ca .

Thank you again for your participation in this study. As a reminder, the $40 you have received as remuneration is taxable, and should be included in future tax considerations.

Sincerely yours,

Alan Cudlip
Department of Kinesiology
University of Waterloo
519-888-4567 x37495
accudlip@uwaterloo.ca

Clark Dickerson, PhD
Department of Kinesiology
University of Waterloo
519-888-4567 x37844
clark.dickerson@uwaterloo.ca

I have participated in the study:

Examining Regional Supraspinatus Activation Using Indwelling Electromyography
I would like a summary of the results.

Name: _____

E-mail: _____

APPENDIX E – EMG REMUNERATION

REMUNERATION FOR PARTICIPATION

Project Title: **Examining Regional Supraspinatus Activation Using Indwelling Electromyography**

Student Investigator: **Alan Cudlip**

Faculty Supervisor: **Dr. Clark Dickerson**

We thank you for your participation in this research. We hope that the findings from this work can be used to further illuminate rotator cuff injury research.

Enclosed is **$__** for participating in this study. As a reminder, this remuneration is taxable, and shoulder be included in future tax considerations.

Sincerely yours,

Alan Cudlip

Department of Kinesiology
University of Waterloo
519-888-4567 x37495
accudlip@uwaterloo.ca

Clark Dickerson, PhD

Department of Kinesiology
University of Waterloo
519-888-4567 x37844
clark.dickerson@uwaterloo.ca

I have received remuneration for participating in the study:

Examining Regional Supraspinatus Activation Using Indwelling Electromyography

Name: _____

Remuneration Received: $_____

Witnessed: _____

APPENDIX F – *IN VIVO* SUPRASPINATUS ACTIVATION TABLES

Table 5. Statistical results for plane of elevation and load. Post-hoc differences within a plane of elevation are denoted by letters.

Muscle Region	Phase of Movement	Plane of Elevation	Load 0	20	40
Anterior	Ascending	0	18.3 (C)	29.4 (B)	35.3 (A)
		15	15.6 (C)	25.8 (B)	29.3 (A)
		30	16.2 (B)	26.8 (A)	28.8 (A)
		40	14.8 (C)	22.7 (B)	27.3 (A)
		60	14.5 (C)	19.9 (B)	25.0 (A)
		75	12.2 (C)	17.4 (B)	23.1 (A)
		90	11.5 (C)	16.4 (B)	20.7 (A)
	Descending	0	15.6 (C)	23.5 (B)	29.3 (A)
		15	13.9 (C)	21.7 (B)	23.6 (A)
		30	14.1 (B)	24.3 (A)	24.6 (A)
		40	13.3 (C)	20.4 (B)	23.0 (A)
		60	13.0 (C)	16.8 (B)	21.2 (A)
		75	11.4 (C)	15.5 (B)	20.4 (A)
		90	11.1 (C)	15.4 (B)	18.1 (A)
Posterior	Ascending	0	20.3 (C)	26.3 (B)	31.6 (A)
		15	19.5 (C)	24.0 (B)	30.7 (A)
		30	18.8 (B)	20.9 (B)	28.8 (A)
		40	17.6 (B)	19.4 (B)	27.7 (A)
		60	16.5 (C)	21.2 (B)	25.9 (A)
		75	15.0 (C)	18.0 (B)	24.0 (A)
		90	15.2 (C)	20.8 (B)	25.3 (A)
	Descending	0	19.3 (C)	25.0 (B)	29.2 (A)
		15	19.0 (C)	22.4 (B)	25.6 (A)
		30	18.1 (C)	21.1 (B)	26.1 (A)
		40	16.9 (C)	20.8 (B)	25.6 (A)
		60	17.0 (C)	21.6 (B)	23.9 (A)
		75	17.1 (B)	18.3 (B)	23.0 (A)
		90	16.0 (C)	20.0 (B)	24.0 (A)

Table 6. Load*Angle interaction results for anterior supraspinatus in ascending phase. Post-hoc differences by plane of elevation are denoted by letters.

Plane of Elevation	Load	Angle						
		5	**30**	**60**	**90**	**120**	**135**	**165**
0° (p=0.02)	**0**	4.7 I	12.7 G-I	20.2 F-H	20.9 F-H	23.7 D-G	22.7 D-G	22.9 D-G
	20	8.4 H-I	21.8 E-G	31.6 B-F	37.2 A-C	37.8 A-C	34.9 A-D	34.1 A-E
	40	7.1 I	28.8 C-F	40.9 A-C	46.1 A	42.8 A-B	41.1 A-C	40.2 A-C
15° (p<0.01)	**0**	3.2 G	9.5 E-G	16.4 D-F	17.8 D-E	23.2 C-D	19.9 D-E	19.5 D-E
	20	4.0 G	16.4 D-F	26.4 B-D	32.6 A-C	37.0 A-B	32.4 A-C	31.8 A-C
	40	5.7 F-G	21.8 C-D	37.0 A-B	39.1 A	35.9 A-B	33.4 A-C	32.1 A-C
30° (p=0.33)	**0**	4.3	11.5	17.3	18.8	21.0	20.3	20.0
	20	3.1	11.1	22.0	27.4	29.4	47.6	46.7
	40	3.3	18.9	35.4	38.4	36.8	34.9	34.2
40° (p<0.01)	**0**	5.3 I-K	9.5 H-K	14.9 G-J	17.3 F-H	19.5 D-H	18.8 E-H	18.5 F-H
	20	2.1 K	10.3 H-K	23.4 C-G	27.5 B-F	30.7 A-D	33.1 A-C	32.2 A-C
	40	4.4 J-K	16.8 F-I	33.2 A-C	39.4 A	36.1 A-B	31.2 A-C	30.2 A-E
60° (p<0.01)	**0**	4.4 H	9.3 G-H	14.2 E-H	16.7 D-G	19.4 C-G	18.5 C-G	18.7 C-G
	20	3.8 H	9.7 F-H	20.6 C-F	28.6 A-C	27.2 A-D	25.0 B-E	24.6 B-E
	40	5.2 H	12.1 F-H	27.7 A-D	37.2 A	34.6 A-B	29.4 A-C	28.7 A-C
75° (p<0.01)	**0**	2.9 I	6.2 H-I	11.7 F-I	15.0 E-H	17.9 C-G	16.2 D-H	15.3 E-H
	20	2.9 I	7.8 G-I	17.6 C-G	25.0 A-E	24.1 B-E	22.4 B-E	22.0 B-F
	40	4.0 I	10.9 G-H	25.9 A-D	35.3 A	31.5 A-B	27.2 A-C	26.9 A-C
90° (p=0.01)	**0**	2.8 J	6.7 G-J	9.5 F-J	12.9 E-I	17.7 B-F	15.5 C-G	15.5 C-G
	20	3.8 I-J	6.4 G-J	13.8 D-H	20.0 A-E	23.8 A-C	23.7 A-D	23.1 A-D
	40	4.2 H-J	9.5 F-J	22.0 A-E	29.4 A	28.4 A	25.7 A-B	25.4 A-C

Table 7. Load*Angle interaction results for anterior supraspinatus in descending phase. Post-hoc differences by plane of elevation are denoted by letters.

Plane of Elevation	Load	Angle						
		5	**30**	**60**	**90**	**120**	**135**	**165**
0° (p=0.01)	**0**	9.9 F	10.6 F	14.2 E-F	14.9 E-F	17.1 E-F	21.0 C-F	21.5 C-F
	20	10.2 F	13.4 E-F	19.4 D-F	23.9 B-E	29.5 A-D	34.2 A-B	33.9 A-B
	40	13.5 E-F	16.8 E-F	30.2 A-D	32.1 A-C	34.5 A-B	39.0 A	39.2 A
15° (p<0.01)	**0**	9.0 G	10.5 F-G	12.4 E-G	12.5 E-G	16.6 C-G	17.9 C-G	18.6 C-F
	20	9.9 F-G	14.0 E-G	18.2 C-G	20.1 B-E	28.9 A-B	30.6 A	30.5 A
	40	10.5 F-G	15.1 D-G	25.2 A-C	23.9 A-D	29.0 A-B	30.7 A	30.9 A
30° (p=0.44)	**0**	9.6	11.1	11.8	12.9	15.5	18.8	18.8
	20	9.9	11.7	16.7	17.2	22.7	45.9	46.2
	40	11.8	14.6	25.0	27.2	28.0	32.6	32.9
40° (p<0.01)	**0**	8.0 F	11.1 E-F	10.8 E-F	13.9 E-F	14.2 D-F	17.6 B-F	17.8 B-F
	20	9.7 E-F	11.7 E-F	16.5 C-F	17.9 B-E	25.1 A-C	31.1 A	31.3 A
	40	9.9 E-F	15.5 C-F	23.9 A-D	26.6 A-B	26.6 A-B	29.3 A	29.2 A
60° (p=0.17)	**0**	8.4	9.2	1.0	14.0	13.4	17.8	18.2
	20	8.8	9.7	15.0	15.9	20.1	24.0	24.1
	40	9.4	14.2	21.6	22.6	24.0	28.2	28.5
75° (p=0.13)	**0**	7.9	8.6	9.7	12.0	12.0	14.6	14.9
	20	8.4	10.1	13.6	15.9	18.6	21.1	21.2
	40	10.7	13.3	20.3	23.7	23.8	25.1	25.3
90° (p=0.15)	**0**	7.6	8.0	8.9	10.9	12.9	15.0	15.0
	20	7.7	9.0	13.6	14.6	18.6	22.1	22.3
	40	8.8	10.5	17.3	19.3	21.9	24.5	24.5

Table 8. Load*Angle interaction results for posterior supraspinatus in ascending phase. Post-hoc differences by plane of elevation are denoted by letters

Plane of Elevation	Load	Angle						
		5	**30**	**60**	**90**	**120**	**135**	**165**
0° (p=0.06)	**0**	7.2	15.4	20.4	21.8	25.5	26.0	25.9
	20	10.3	20.2	27.3	30.7	32.5	32.2	31.1
	40	5.2	24.8	38.2	37.9	40.3	39.3	35.6
15° (p=0.07)	**0**	6.6	12.5	22.0	23.1	23.5	24.8	24.2
	20	7.1	19.0	26.7	30.4	29.0	28.7	27.7
	40	7.2	25.5	39.5	40.8	36.6	34.2	31.4
30° (p=0.01)	**0**	7.3	14.0	20.7	20.1	22.7	23.4	23.7
		G	F-G	F-G	F-G	D-F	D-F	C-F
	20	4.1	13.7	24.5	26.4	26.1	26.3	25.7
		G	F-G	B-F	B-E	B-E	B-E	B-E
	40	5.5	22.4	35.2	38.7	34.8	33.5	32.0
		G	D-F	A-B	A	A-C	A-D	A-D
40° (p=0.02)	**0**	8.8	12.6	18.9	20.5	21.1	20.4	20.9
		G-H	E-H	D-G	C-F	C-F	C-F	C-F
	20	2.0	11.0	23.8	24.5	26.2	25.0	23.6
		H	F-H	C-E	B-D	B-D	B-D	C-E
	40	8.6	19.0	31.8	37.9	35.9	31.3	29.7
		G-H	D-G	A-C	A	A-B	A-C	A-D
60° (p=0.11)	**0**	6.5	10.9	18.5	18.9	20.0	19.7	21.0
	20	6.4	14.6	25.5	27.1	24.2	25.8	25.4
	40	9.2	15.2	31.5	36.9	31.6	29.5	27.6
75° (p=0.63)	**0**	3.7	7.1	17.1	19.8	18.8	18.7	20.1
	20	3.2	10.2	21.7	25.2	23.0	22.2	20.9
	40	7.5	16.2	29.1	34.7	29.6	25.8	25.0
90° (p=0.84)	**0**	4.9	9.6	16.1	18.8	19.1	19.0	19.5
	20	8.0	11.8	23.8	26.3	25.8	25.7	24.5
	40	8.3	21.6	30.1	33.8	29.3	27.6	27.0

Table 9. Load*Angle interaction results for posterior supraspinatus in descending phase. Post-hoc differences by plane of elevation are denoted by letters

Plane of Elevation	Load	Angle						
		5	30	60	90	120	135	165
0° (p=0.61)	0	13.7	15.1	17.0	18.7	20.9	24.8	25.4
	20	15.7	26.3	20.9	24.5	27.6	29.7	30.4
	40	19.2	23.2	30.8	30.9	30.8	34.5	35.1
15° (p=0.81)	0	13.1	16.1	18.3	20.1	18.9	23.1	24.0
	20	15.9	18.2	23.2	21.1	23.4	26.7	27.2
	40	16.4	19.9	27.8	27.0	27.7	30.3	30.7
30° (p=0.32)	0	14.5	14.9	15.7	17.2	18.8	22.8	23.2
	20	15.0	18.6	21.6	20.8	22.0	24.8	25.1
	40	16.9	21.3	26.2	28.6	28.3	30.5	30.9
40° (p=0.09)	0	13.5	14.3	16.7	16.2	17.8	19.7	20.7
	20	15.7	20.2	27.0	30.1	28.7	28.7	28.9
	40	15.7	20.2	27.0	30.1	28.7	28.7	28.9
60° (p=0.94)	0	13.9	15.2	15.8	18.6	16.7	18.7	20.7
	20	15.4	17.1	20.9	24.3	21.1	24.5	24.8
	40	19.1	20.1	25.1	24.7	23.9	27.0	27.3
75° (p=0.23)	0	14.4	15.7	16.6	16.5	17.5	19.0	20.0
	20	15.0	15.6	18.3	17.8	19.5	21.1	20.7
	40	16.2	20.0	27.9	23.6	24.1	24.9	24.6
90° (p=0.31)	0	14.3	14.9	15.0	16.0	14.8	18.3	18.8
	20	14.3	16.9	18.2	22.2	21.8	23.8	23.6
	40	17.8	20.0	24.7	27.8	25.9	26.1	26.0

Table 10. Statistical results for plane of elevation and elevation angle. Significant differences by plane are denoted by letters; values not sharing a letter are significantly different.

Muscle Region	Phase of Movement	Plane of Elevation	Abduction Angle						
			5	30	60	90	120	135	165
Anterior	Ascending	0	6.7 (C)	21.1 (B)	30.9 (A)	34.7 (A)	34.8 (A)	32.9 (A)	32.4 (A)
		15	4.3 (C)	15.9 (B)	26.6 (A)	29.8 (A)	32.0 (A)	28.5 (A)	27.7 (A)
		30	3.6 (C)	13.8 (B-C)	24.9 (A-B)	28.2 (A-B)	29.1 (A-B)	34.3 (A)	33.7 (A)
		40	3.9 (C)	12.2 (B)	23.8 (A)	28.0 (A)	28.7 (A)	27.7 (A)	26.9 (A)
		60	4.5 (D)	10.4 (C)	20.8 (B)	27.5 (A)	27.1 (A)	24.3 (A-B)	24.0 (A-B)
		75	3.3 (D)	8.3 (C)	18.4 (B)	25.1 (A)	24.5 (A)	21.9 (A-B)	21.4 (A-B)
		90	3.6 (C)	7.5 (C)	15.1 (B)	20.8 (A)	23.3 (A)	21.6 (A)	21.3 (A)
	Descending	0	11.1 (D)	13.0 (D)	21.2 (C)	23.6 (B-C)	27.0 (A-B)	31.4 (A)	31.5 (A)
		15	9.8 (C)	13.1 (C)	18.6 (B)	18.8 (B)	24.8 (A)	26.4 (A)	26.6 (A)
		30	10.5 (B)	12.5 (B)	17.8 (A-B)	19.1 (A-B)	22.1 (A-B)	32.5 (A)	32.6 (A)
		40	9.2 (E)	12.7 (D-E)	17.0 (C-D)	19.4 (B-C)	21.9 (A-B)	26.0 (A)	26.1 (A)
		60	8.9 (D)	11.1 (D)	15.7 (C)	17.5 (C)	19.2 (B-C)	23.3 (A-B)	23.6 (A)
		75	9.2 (D)	10.7 (C-D)	14.6 (B-C)	17.2 (A-B)	18.1 (A-B)	20.3 (A)	20.5 (A)
		90	8.0 (D)	9.1 (D)	13.2 (C)	14.9 (B-C)	17.8 (A-B)	20.5 (A)	20.6 (A)
Posterior	Ascending	0	7.6 (C)	20.1 (B)	28.6 (A)	30.1 (A)	32.8 (A)	32.5 (A)	32.8 (A)
		15	7.0 (C)	18.9 (B)	29.3 (A)	31.4 (A)	29.7 (A)	29.2 (A)	27.7 (A)
		30	5.6 (C)	16.6 (B)	26.8 (A)	28.3 (A)	27.8 (A)	27.7 (A)	27.1 (A)
		40	6.4 (C)	14.2 (B)	24.8 (A)	27.6 (A)	27.7 (A)	25.6 (A)	24.7 (A)
		60	7.4 (C)	13.5 (B)	25.1 (A)	27.6 (A)	25.2 (A)	25.0 (A)	24.6 (A)
		75	4.8 (C)	11.1 (B)	22.6 (A)	26.5 (A)	23.8 (A)	22.2 (A)	22.0 (A)
		90	7.1 (C)	14.3 (B)	23.3 (A)	26.2 (A)	24.7 (A)	24.1 (A)	23.6 (A)
	Descending	0	16.2 (C)	21.5 (B-C)	22.9 (B)	24.7 (A-B)	26.4 (A-B)	29.6 (A)	30.3 (A)
		15	15.1 (C)	18.0 (C)	23.1 (B)	22.7 (B)	23.3 (A-B)	26.7 (A-B)	27.2 (A)
		30	15.5 (D)	18.3 (C-D)	21.0 (B-C)	22.2 (B)	23.0 (A-B)	26.1 (A)	26.4 (A)
		40	14.9 (B)	17.5 (B)	21.5 (A)	22.6 (A)	23.0 (A)	23.8 (A)	24.3 (A)
		60	16.1 (C)	17.4 (B-C)	20.6 (A-B)	22.5 (A)	20.7 (A-B)	23.4 (A)	24.2 (A)
		75	15.2 (C)	17.1 (B-C)	20.9 (A)	19.3 (A-B)	20.4 (A)	21.7 (A)	21.8 (A)
		90	15.4 (C)	17.2 (B-C)	19.3 (A-C)	21.9 (A)	20.8 (A-B)	22.7 (A)	22.7 (A)